Frameworks for Assessing and Improving Urban Water Supply Security Planning under Climate Change

by

Fiona Laura Paton

BE (Hons); BSc

Thesis submitted to The University of Adelaide

School of Civil, Environmental & Mining Engineering in

fulfilment of the requirements for the degree of

Doctor of Philosophy

Submitted December 2013

Table of Contents

Abstract

There exist large uncertainties in projecting future climate and understanding how climate change projections relate to water supply. Non-traditional water sources (e.g., stormwater harvesting), which are emerging as adaptation options to augment stressed water supply systems, further complicate the simulation of these systems. However, in assessing a city's water supply security, there is no framework explicitly acknowledging and accounting for both the additional complexities and uncertainties associated with non-traditional water sources and climate change impacts. Furthermore, mitigation and adaptation measures to climate change should be considered. However, minimising GHG emissions (and thus considering mitigation) is likely to conflict with other objectives of water supply system planning. Hence, a multi-objective evolutionary algorithm (MOEA) approach is necessary to balance multiple objectives, as well as to efficiently search many feasible alternatives to find Pareto-optimal solutions. However, for cities, MOEA studies incorporating GHG emissions and thus focussing on both mitigating and adapting to climate change do not exist.

The main aim of this thesis is to develop methods for assessing and improving urban water supply security planning under climate change to better understand: (1) the relative magnitudes of uncertainty sources in assessing climate change impacts; (2) enhanced simulation complexity of non-traditional water sources and increased uncertainty of climate change impacts; and (3) adaptation and mitigation responses to climate change. Consequently, major contributions of this research include: (1) developing a scenario-based sensitivity analysis to understand the relative magnitudes of uncertainty sources in assessing the impacts of climate change on water supply systems; (2) developing a generalised framework for a city's water supply system that outlines the additional complexities due to the incorporation of non-traditional water sources and the additional uncertainties due to climate change impacts; and (3) incorporating GHG emissions as an objective function within a MOEA framework to take into consideration both adaptation and mitigation responses to climate change. Furthermore, while these frameworks could readily be applied to any

city, Adelaide's southern water supply system is used as a real-life case study to illustrate the practical management implications.

The methods developed in the thesis were found to be effective when applied to Adelaide's southern water supply system. Results indicate that studies analysing the impact of climate change on water supply security should consider uncertainties other than those associated with climate change and hydrological modelling, as these could have as great, if not greater, impacts on water supply security projections. Furthermore, trade-offs exist between cost and supply security for solutions that use desalination and harvested stormwater to augment water supply; however, use of rainwater tanks is undesirable, as they are an expensive source. In terms of the trade-off between economic cost and GHG emissions, the main drivers are the presence of rainwater tanks and the desalination plant – rainwater tanks are an expensive option, while desalination is a GHG emission intensive option. Consequently, while desalination may be a good adaptation option, other water sources may be better mitigation measures. Accounting for GHG emissions is thus important to ensure mitigation measures are considered.

Statement of Originality

I certify that this work contains no material which has been accepted for the award of any other degree or diploma in my name, in any university or other tertiary institution and, to the best of my knowledge and belief, contains no material previously published or written by another person, except where due reference has been made in the text. In addition, I certify that no part of this work will, in the future, be used in a submission in my name, for any other degree or diploma in any university or other tertiary institution without the prior approval of the University of Adelaide and where applicable, any partner institution responsible for the joint-award of this degree.

I give consent to this copy of my thesis when deposited in the University Library, being made available for loan and photocopying, subject to the provisions of the Copyright Act 1968.

The author acknowledges that copyright of published works contained within this thesis resides with the copyright holder(s) of those works.

I also give permission for the digital version of my thesis to be made available on the web, via the University's digital research repository, the Library Search and also through web search engines, unless permission has been granted by the University to restrict access for a period of time.

Signed: . . . . . Date: . . . . . .

Acknowledgements

Foremost, I wish to thank my supervisors, Professor Holger Maier and Professor Graeme Dandy for their support, encouragement and guidance. Thank you for giving me the freedom to determine the direction this research project should take; for forcing me to grapple with problems and to challenge myself; for the flexibility in and understanding of my working hours and other commitments and interests; and, most importantly, for your effort, energy and dedication to this research.

Many people deserve thanks for their assistance in developing the computer programs for this thesis, none less than David Cresswell, who modified *WaterCress* on a number of occasions to suit the requirements of my research. Thank you also to Jeffrey Newman, a fellow postgraduate student and friend, who was always willing to help me with computer programming and Sri Srikanthan, who offered wonderful support for the *Stochastic Climate Library*. I would also like to thank Matthew Gibbs, Mark Thyer, Michael Leonard, Joanna Szemis and Leanne Webb for their input and support.

This research was made possible and enhanced by the financial support of the eWater CRC, which allowed me to purchase data, publish the papers presented herein and present my research at *MODSIM* (Cairns, 2009) and the *10th International Conference on Hydroinformatics* (Hamburg, 2012). I also acknowledge the G08 Universities Consortium for giving me the opportunity to partake at the *Climate Change: Science + Humanities* conference (Boston, 2010); and the Australia Korea Foundation, Australian Government, for giving me the opportunity to take part in the *Australia-Korea Next Generation Leaders Program: Sustainable Water Resource Management* (Korea, 2011). These conference experiences have influenced and contributed to the ideas developed in this thesis.

Finally, thank you to my family and friends, particularly Will, who have understood my study commitments and who have been compassionate and encouraging when I have doubted myself. Your continual support has enabled me to focus on finishing my doctoral studies.

List of Figures

List of Tables

List of Acronyms

AIC	Akaike Information Criterion
ASR	Aquifer Storage and Recovery
BoM	Bureau of Meteorology
Cdf	Cumulative distribution function
CFF	Climate Futures Framework
CMIP	Coupled Model Intercomparison Project
CRC	Cooperative Research Centre
CSIRO	(Australian) Commonwealth Scientific and Industrial Research Organisation
ENSO	El Niño Southern Oscillation
FFCEF	Full Fuel Cycle Emissions Factor
GA	Genetic Algorithm
GCM	General Circulation Model
GHG	Greenhouse Gas Emissions
HDPE	High Density Polyethylene
IPCC	Intergovernmental Panel on Climate Change
Lcd	Litres per capita per day
LOS	Level Of Service
MBO	Murray Bridge-Onkaparinga
MOEA	Multi-Objective Evolutionary Algorithm
MOGA	Multi-Objective Genetic Algorithm
MOO	Multi-Objective Optimisation
MSCL	Mild Steel Cement Lined
NS	Nash-Sutcliffe
NSGA-II	Non-Sorted Genetic Algorithm 2
PPD	Patched Point Dataset
PSHV	Port Stanvac Happy Valley
PV	Present Value
RCF	Representative Climate Future
RDM	Robust Decision Making
RMSE	Root Mean Squared Error
RRO	Rainfall-Runoff Model
SCL	Stochastic Climate Library
SD	Standard Deviation
SRES	Special Report on Emissions Scenarios
UWOT	Urban Water Optioneering Tool
UWSS	Urban Water Supply System
WaterCress	Water – Community Resource Evaluation and Simulation System
WSMGA	Water System Multi-objective Genetic Algorithm
WTP	Water Treatment Plant

Chapter 1

1 Introduction

Over half of the world's population now lives in urban areas, with urbanisation an even greater phenomenon for some countries, such as Australia, which has an urban population close to 90% [*Martine*, 2007]. Consequently, there is an ongoing challenge for urban water authorities to ensure they can supply the large, concentrated, and growing water demands of urban areas, both now and in the future. Assessing urban water supply security can help water authorities to meet this challenge. However, this is becoming increasingly more complex, due to: (1) climate change projections, including associated uncertainties; (2) uptake of non-traditional water sources; and (3) an appreciation of the need to mitigate, as well as adapt to, climate change pressures.

Traditionally, water supply system planning and management in the developed world has been founded on the concept of stationarity, which assumes that, while exhibiting fluctuations, water supply systems operate in an unchanging envelope of variability [*Milly et al*., 2008]. However, this assumption is now no longer valid due to the impacts of substantial anthropogenic climate change on the hydrological cycle [*Milly et al*., 2008]. Consequently, planning approaches must evolve to accommodate non-stationarity [*Towler et al.,* 2012]. Furthermore, there still exist large uncertainties in projecting future climate on hydrology, which, as *Chen et al.* [2011b] explain, cascade down from:

(1) greenhouse gas (GHG) emissions scenarios, (2) general circulation model (GCM) structures and parameters, (3) GCM initial conditions, (4) downscaling methods, (5) hydrological model structures, and (6) hydrological model parameters. In terms of the impact of climate change on future runoff, there has been increasing attention given to uncertainties in GHG emissions scenarios, GCM models, GCM initial conditions, downscaling techniques, and hydrological models and parameters [*Boe et al.*, 2009; *Chen et al.*, 2011a, 2011b; *Chiew and McMahon*, 2002; *Chiew et al.*, 2009b, 2009c, 2010; *Diaz-Nieto and Wilby*, 2005; *Dibike and Coulibaly*, 2005; *Forbes et al.*, 2011; Majone et al., 2012; *Manning et al.*, 2009; *Mpelasoka and Chiew*, 2009; *Wilby and Harris*, 2006; *Wilby et al.*, 2006]. Furthermore, *Boe et al.* [2009], *Chen et al.* [2011a, 2011b], *Chiew et al.* [2009c], *Mpelasoka and Chiew* [2009] and *Wilby and Harris* [2006] also explicitly compared the magnitude of runoff changes caused by the different sources of uncertainty associated with climate change and hydrological modelling. This is valuable because water authorities must understand the greatest sources of uncertainties for water supply system security and whether these are epistemic (systematic) or aleatoric (statistical). Systematic uncertainties, such as model inadequacy or data measurement inaccuracies, are potentially reducible (by the water authority's action or others); while statistical uncertainties, such as natural rainfall variability, are inherent and will always exist. If major sources of uncertainty are reducible by the water authority, then effort can be directed toward reducing this uncertainty, while if irreducible uncertainties dominate impacts on water supply security, then adaptation responses must be developed to cope with this uncertainty.

However, while runoff may be a good indicator of water availability, it cannot be used as a surrogate for water supply security, because the impacts of climate change on runoff do not necessarily correlate with those on water supply due to additional complexities and uncertainties. For example, water simulation models not only incorporate demand, but also model (1) water storages, (2) transmission systems, (3) treatment systems, and (4) user-specified operating rules [*Traynham et al.*, 2011]. Additional uncertainty also exists when moving from runoff estimated by hydrological models to water supply security, associated with uncertainties in future population, per capita water

demand, regulatory requirements, water law, consumer preferences, and environmental standards [*Wiley and Palmer*, 2008]. Consequently, while a number of studies have investigated the impact of climate change on water supply systems, including sources of uncertainty [*Fowler et al*., 2003; *Gober et al.*, 2010; *Groves et al.*, 2008c; *Kaczmarek et al.*, 1996; *Lopez et al.*, 2009; *O'Hara and Georgakakos*, 2008; *Traynham et al.*, 2011; *Vicuna et al.*, 2010; *Wiley and Palmer*, 2008; *Zhu et al.*, 2005], no studies exist that compare the uncertainty sources in terms of their relative magnitudes.

Furthermore, in the case of water supply security, the additional consideration of demand means a ''failure" of supply to meet demand can be identified at a critical point in time, while there are no such critical points when only examining runoff. It is important to identify these critical points in time, so that plans to avoid failures can be implemented well in advance. This is necessary because large-scale infrastructure associated with water supply systems can result in potentially long lead times for their expansion. Furthermore, understanding how uncertainties interact through the development of ''best'' and ''worst'' cases will help water authorities establish likely bounds of future water supply security, which is imperative for them to understand the degree to which water supply may need to be supplemented, or demand reduced, in the future.

Understanding the characteristics of projected system failures will enable water authorities to adapt their water supply systems most appropriately to prevent, or at least reduce, projected system failures. However, regardless of the additional uncertainties of climate change impacts, water supply system adaptation is not a straightforward task. In recent years, to accommodate growth, there has been a reduced reliance on traditional water supplies, accompanied by a move towards combinations of large, engineering water projects, water reuse, and conservation measures [Chung et al., 2009]. This integration of non-traditional water sources increases the complexity of simulating a city's water system because their inclusion requires additional considerations in terms of: (a) levels of usability (e.g., potable and non-potable); (b) degree of climate dependence; (c) spatial and temporal scales; and (d) source integration and priority. For example, for some water supplies (such

as stormwater harvesting), water may not be treated to a level suitable for human consumption, which in turn would require water supply to be targeted toward non-potable end uses and delivered via a third-pipe network. Alternatively, in terms of scale, instead of using monthly time-steps to simulate reservoir supply, a daily time-step may be necessary to accurately calculate the yield of smaller, decentralised sources (such as household rainwater tanks), resulting in the need for more precise input data (e.g. daily climate data) and increased computational effort.

A number of studies in the context of urban water supply planning have considered incorporating non-traditional water sources. *Chung et al.* [2008] developed an integrated water supply system model in an object-orientated system dynamics simulation environment, to evaluate decentralised treatment options, allowing for multiple sources, users, and transportation and treatment systems. A decision-support tool (Urban Water Optioneering Tool (UWOT)) for the development (or cluster) scale, which has the functionality to supply water from rainwater harvesting and greywater recycling, has also been developed by *Makropoulos et al.* [2008]. However, the focus of these papers is on the model for simulating the urban water supply system, rather than an integrated assessment framework for urban water supply system planning that not only incorporates a simulation model that can model non-traditional water sources, but also the impacts, and associated uncertainties, of climate change.

From the perspective of climate change impact assessment studies at the city scale, only a few studies incorporate new water supply sources in planning approaches. *Matrosov et al.* [2013] examined the impact of climate change on London's water supply system expansion in the Thames basin, UK. However, the 20 water infrastructure portfolios investigated only included large-scale, centralised infrastructure options, such as desalination plants. *Groves et al.* [2008a; 2008b] and *Lempert and Groves* [2010] examined the reuse of treated wastewater and an increase in sustainable groundwater use, incorporating stormwater and recycled water recharge programs for the Inland Empire, Southern California, under climate change projections. However, these studies

are limited to supply portfolios incorporating large-scale water supply sources and while stormwater is included, it is not used directly as a water supply source for the city. Therefore, the increased modelling complexity of non-potable supplies from multiple, decentralised locations is not investigated.

In addition to adapting water supply systems to climate change pressures (e.g., by introducing non-traditional water sources), mitigating climate change impacts by minimising greenhouse gas (GHG) emissions in the water sector is also warranted, particularly because: (1) the water sector is highly sensitive to climate change; (2) energy use is both considerable and increasing in the water sector; and (3) water resource adaptation often requires greater energy use [*Rothausen and Conway*, 2011]. For example, GHG emissions associated with water supply services in South East Queensland, Australia, are likely to increase 3-fold in the next 50 years, as new sources (such as desalination) are introduced, which have considerably higher energy intensities than traditional surface water supply systems [*Hall et al.,* 2011]. It is particularly concerning that water resource adaptation will most likely increase GHG emissions, given that: (a) GHG emissions contribute to climate change; (b) climate change will in many places exacerbate water scarcity; and (c) water scarcity is a driver for water resource adaptation. However, while cities around the world are increasingly engaged in climate action and mitigating greenhouse gas (GHG) emissions [*Miller et al.*, 2013], in the context of responding to climate change pressures, very few studies have investigated the impacts of changing water use on GHG emissions [*Rothausen and Conway*, 2011]. Thus, minimising GHG emissions, and thus focusing on both mitigation and adaptation responses to climate change in planning and managing urban water supply systems, is both timely and necessary.

However, the minimisation of GHG emissions is likely to conflict with other objectives, such as maximising water supply security, so multiple objectives will need to be balanced. The application of multi-objective evolutionary algorithms (MOEAs) can help achieve this balance because they can evolve an approximation of entire tradeoff (Pareto) fronts of multiple objectives in a single run [*Reed*

et al., 2003]. An approximation of the Pareto front is usually sufficient, because it would be computationally impossible to quantify the true Pareto front, given the exceptionally large decision spaces typical of water resources problems [*Nicklow et al.*, 2010].

Minimising GHG emissions has been considered as an objective in a number of MOEA studies concerned with the design and operation of water distribution networks [Wu et al., 2009; 2010; Wu et al., 2013; Wu et al., 2010]. However, focusing solely on water supply networks ignores a number of important issues in reducing GHG emissions of urban water supply systems, such as in assessing alternative water supply sources (e.g., desalination plants) that may be introduced as adaptation responses to climate change for a city's water supply system. Furthermore, of the MOEA studies focussing on regional scale water supply system management and planning, none have considered GHG emission reduction as an objective [*Kasprzyk et al.*, 2009; *Kasprzyk et al.*, 2012; *Kasprzyk et al.*, 2013; *Mortazavi et al.*, 2012]. Thus, it is necessary to develop an approach to enable the exploration of optimal trade-offs between GHG emissions and other objectives, such as minimising cost and maximising water supply security, for urban water supply systems at the regional scale.

In summary, while numerous approaches exist for planning and managing urban water supply systems at the city scale under climate change, there still exist a number of key knowledge gaps, specifically in:

1. Understanding the relative magnitudes of uncertainty sources in assessing the impacts of climate change on water supply systems that can help water authorities plan for, and manage, the impacts of climate change;
2. Assessing water supply security for a city in explicitly acknowledging and accounting for the additional complexities associated with simulating non-traditional water sources and the additional uncertainties associated with climate change impacts; and

3. Multi-objective evolutionary algorithm studies in regional-scale water supply system management and planning that incorporate GHG emission reduction as an objective and thus consider both adaptation and mitigation responses to climate change.

1.1 Research Objectives

The main aim of this research is to develop methods for assessing and improving urban water supply security planning under climate change to better understand: (1) relative magnitudes of uncertainty sources in assessing climate change impacts; (2) enhanced simulation complexity of non-traditional water sources and increased uncertainty of climate change impacts; and (3) both adaptation and mitigation responses to climate change. To achieve this overall aim, three major objectives are developed for this research, with nine sub-objectives:

Objective 1 To develop a scenario-based sensitivity analysis to understand the relative magnitudes of uncertainty sources in assessing the impacts of climate change on water supply systems.

Sub-objective 1.1 To assess the relative magnitudes of the major sources of uncertainty.

Sub-objective 1.2 To identify critical points in the future when water supply security is threatened.

Sub-objective 1.3 To present projected ranges of water supply security.

Sub-objective 1.4 To test and validate the approach for a case study based on Adelaide's southern water supply system.

Objective 2 To develop a framework for the assessment of water supply security for a city that explicitly acknowledges and accounts for both the additional complexities and uncertainties associated with non-traditional water sources and climate change impacts, respectively.

Sub-objective 2.1 To develop a generalised framework that could be applied to any city's water supply system that outlines the additional complexities due to the incorporation of non-traditional water sources and the additional uncertainties due to climate change impacts.

Sub-objective 2.2 To test and validate the generalised framework for a case study based on Adelaide's southern water supply system to illustrate the approach and draw conclusions about planning Adelaide's water supply system.

Objective 3 To incorporate greenhouse gas (GHG) emissions as an objective function within a multi-objective evolutionary algorithm (MOEA) framework to take into consideration both adaptation and mitigation responses to climate change.

Sub-objective 3.1 To use GHG emissions as an objective function and include both mitigation and adaptation options to climate change in a MOEA framework for a city's water supply system.

Sub-objective 3.2 To evaluate the implications of optimising for GHG emissions on economic cost and system security.

Sub-objective 3.3 To test and validate the framework and to demonstrate practical management implications of it by applying it to a case study based on Adelaide's southern water supply system.

These objectives and sub-objectives are related to one another, as illustrated by Figure 1.1.

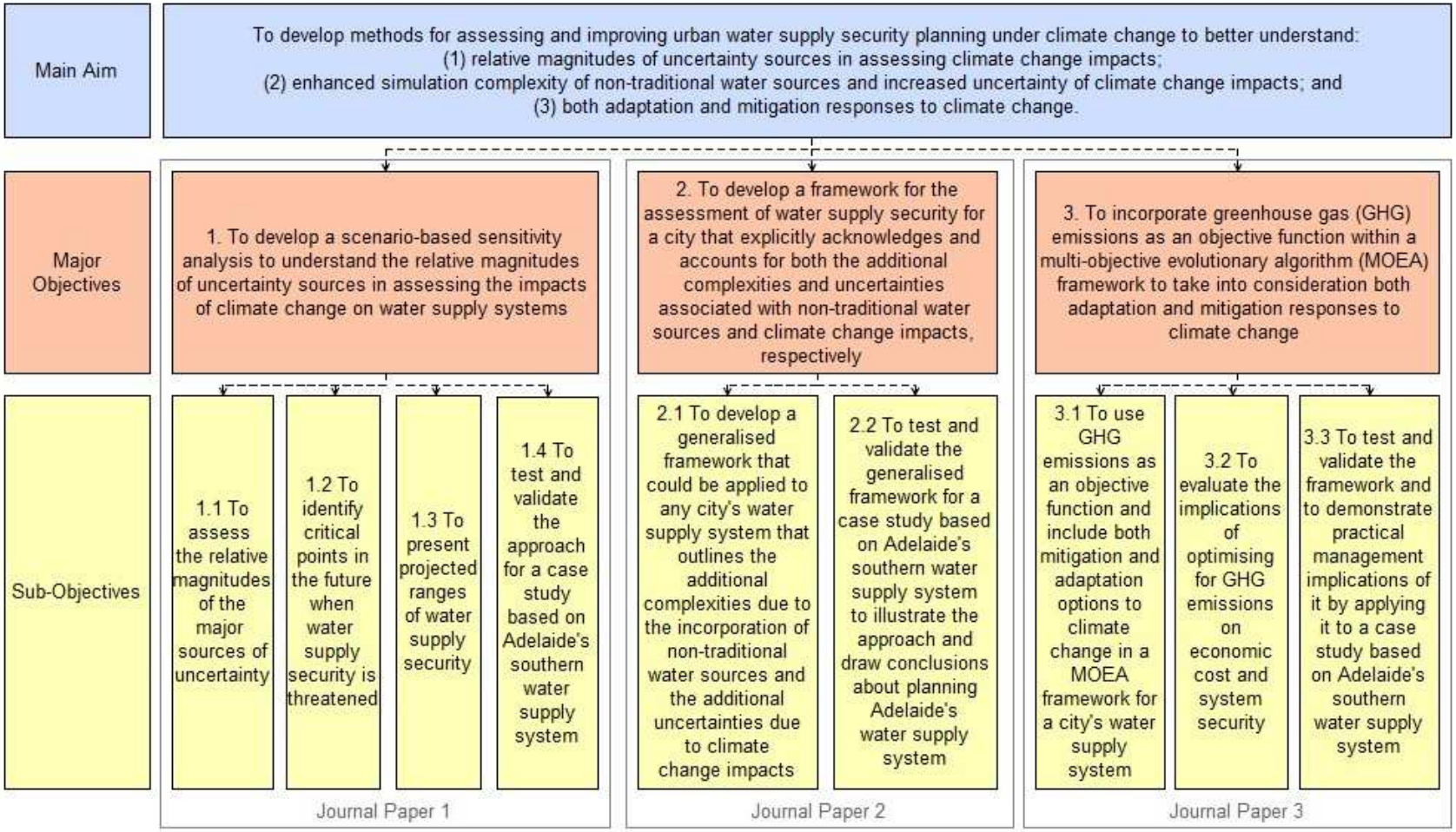

Figure 1.1: Hierarchy and linkage of the main aim, three major objectives, and nine sub-objectives of this research. The three journal papers developed to address the main aim, and each of the major objectives and sub-objectives, are also depicted.

1.2 Thesis Organisation

Five chapters constitute this thesis by publication with the main body of work comprising the middle three chapters. Chapter 2 comprises journal paper 1 and explores major objective 1, which also includes addressing sub-objectives 1.1 to 1.4 (Figure 1.1). Chapter 3 (journal paper 2) addresses major objective 2 and sub-objectives 2.1 and 2.2, while Chapter 4 (journal paper 3) concentrates on major objective 3 and sub-objectives 3.1 to 3.3 (Figure 1.1). These three chapters are copies of the journal papers as published or resubmitted for publication, albeit reformatted for the purpose of this thesis. The conclusions of this research are detailed in Chapter 5, which also summarises: (1) the research contributions of the thesis; (2) the limitations of the thesis; and (3) future work to further the research contained within this thesis.

Appendices are supplied to support each of the journal papers. Specifically, Appendix A is a replicate of the first journal paper as published in *Water Resources Research* in February, 2013. Appendices B-D contain supplementary material resubmitted with journal paper 2 to *Environmental Modelling and Software* in June, 2014, while supplementary material resubmitted with journal paper 3 to *Water Resources Research* in May, 2014 appear in Appendices E-G. Finally, a complete reference list for the main chapters and appendices is provided.

Chapter 2

2 Relative magnitudes of sources of uncertainty in assessing climate change impacts on water supply security for the southern Adelaide water supply system (Paper 1)

Statement of Authorship

Title of Paper	Relative magnitudes of sources of uncertainty in assessing climate change impacts on water supply security for the southern Adelaide water supply system
Publication Status	◉ Published, ○ Accepted for Publication, ○ Submitted for Publication, ○ Publication style
Publication Details	Paton, F. L., H. R. Maier, and G. C. Dandy (2013), Relative magnitudes of sources of uncertainty in assessing climate change impacts on water supply security for the southern Adelaide water supply system, Water Resour. Res., 49, 1643–1667, doi:10.1002/wrcr.20153.

Author Contributions

By signing the Statement of Authorship, each author certifies that their stated contribution to the publication is accurate and that permission is granted for the publication to be included in the candidate's thesis.

Name of Principal Author (Candidate)	Fiona Paton		
Contribution to the Paper	Designed general methodology, constructed case study, conducted modeling and analysis, and wrote manuscript.		
Signature		Date	11/06/2014

Name of Co-Author	Holger Maier		
Contribution to the Paper	Supervised manuscript preparation and reviewed draft.		
Signature		Date	11/06/2014

Name of Co-Author	Graeme Dandy		
Contribution to the Paper	Supervised manuscript preparation and reviewed draft.		
Signature		Date	11/06/2014

Name of Co-Author			
Contribution to the Paper			
Signature		Date	

Abstract

The sources of uncertainty in projecting the impacts of climate change on runoff are increasingly well recognised; however, translating these uncertainties to urban water security has received less attention in the literature. Furthermore, runoff cannot be used as a surrogate for water supply security when studying the impacts of climate change due to the non-linear transformations in modelling water supply and the effects of additional uncertainties, such as demand. Consequently, this study presents a scenario-based sensitivity analysis to qualitatively rank the relative contributions of major sources of uncertainty in projecting the impacts of climate change on water supply security through time. This can then be used by water authorities to guide water planning and management decisions. The southern system of Adelaide, South Australia, is used to illustrate the methodology, for which water supply system reliability is examined across six greenhouse gas (GHG) emissions scenarios, seven general circulation models, six demand projections, and 1000 stochastic rainfall time series. Results indicate the order of the relative contributions of uncertainty changes through time; however, demand is always the greatest source of uncertainty and GHG emissions scenarios the least. In general, reliability decreases over the planning horizon illustrating the need for additional water sources or demand mitigation, while increasing uncertainty with time suggests flexible management is required to ensure future supply security with minimum regret.

2.1 Introduction

Water supply systems in the developed world have previously been planned and managed assuming that natural systems, although exhibiting fluctuations, operate in an unchanging envelope of variability [*Milly et al.,* 2008]. However, as pointed out by *Milly et al.* [2008] this assumption of stationarity is dead because of the impacts of substantial anthropogenic global warming on the hydrologic cycle. Thus, using historic climate to plan and manage future water supply systems is no longer valid; instead projections of future climate should be used to guide decision-making. However, there still exist large uncertainties in projecting future climate and in understanding how these projections translate to water resources, such as runoff or water supply. Consequently, water

resource planners must understand the greatest sources of uncertainty, so as to be able to undertake the difficult task of implementing robust management policies in an uncertain environment [*Salas et al.,* 2012].

Chen et al. [2011b] developed the following cascade of the sources of uncertainty when determining climate change impacts on hydrology: (1) greenhouse gas (GHG) emissions scenarios; (2) general circulation model (GCM) structures and parameters; (3) GCM initial conditions; (4) downscaling methods; (5) hydrological model structures; and (6) hydrological model parameters. A brief description of the sources of uncertainty in this cascade is given below.

In 2000, the Intergovernmental Panel on Climate Change (IPCC) published the Special Report on Emissions Scenarios (SRES) [*Intergovernmental Panel on Climate Change*, 2000], in which GHG emissions scenarios (labelled SRES scenarios) were defined. These reflect different world development pathways based on demographic, economic, and technological drivers [*Intergovernmental Panel on Climate Change*, 2007]. For the various SRES scenarios, General Circulation Models (GCMs) are the best tools available for simulating climate at global and regional scales [*Mpelasoka and Chiew*, 2009]; however, the modelling uncertainty associated with GCMs contributes to the total uncertainty of the future climate. Although there is considerable confidence in GCMs to provide credible, quantitative future climate projections, particularly at the continental scale or greater, the models do differ considerably in terms of estimating the strength of different feedbacks in the climate system [*Randall et al.*, 2007]. Consequently, the projections of future climate variables differ between GCMs and this is more pronounced for certain variables, such as precipitation [*Randall et al.*, 2007]. Furthermore, initial conditions of a GCM run can alter the output, reflecting natural variability of the climate system [*Cubasch et al.*, 2001]. It is important to note that while this discussion relates to the set of coordinated climate model experiments comprising the World Climate Research Programme's Coupled Model Intercomparison Project CMIP3, a new set of simulations (CMIP5) are currently being developed.

Additional uncertainty is introduced when the coarse-scale resolution variables produced by GCMs are downscaled to a finer spatial scale; one that is suitable for modelling the impacts of climate change on catchment runoff. The first major method to do this is statistical downscaling, which uses statistical methods to establish empirical relationships between GCM outputs and local climate variables [*Fowler et al.*, 2007]. Dynamical downscaling, the other major method, achieves fine scale variables by embedding a higher-resolution climate model within a GCM [*Fowler et al.*, 2007]. An overview of these downscaling methods is presented by *Fowler et al.* [2007], which includes a comparison of the methods, including their merits and caveats. Hydrological modelling also causes uncertainty in projecting climate change impacts. For example, there are a myriad of rainfall-runoff (RRO) models that are used to translate local-scale climate variables, such as precipitation and evaporation, to runoff projections. The various RRO models use different climate inputs, different model parameters, run at different time-steps and must be calibrated.

In terms of the impact of climate change on future runoff, there has been increasing attention given to uncertainties in GHG emissions scenarios, GCM models, GCM initial conditions, downscaling techniques, and hydrological models and parameters [*Boé et al.*, 2009; *Chen et al.*, 2011a; *Chen et al.*, 2011b; *Chiew and McMahon*, 2002; *Chiew et al.*, 2009b; *Chiew et al.*, 2009c; *Chiew et al.*, 2010; *Diaz-Nieto and Wilby*, 2005; *Dibike and Coulibaly*, 2005; *Forbes et al.*, 2011; *Majone et al.*, 2012; *Manning et al.*, 2009; *Mpelasoka and Chiew*, 2009; *Wilby and Harris*, 2006; *Wilby et al.*, 2006]. A number of these studies have also explicitly compared the magnitude of runoff changes caused by the different sources of uncertainty associated with climate change and hydrological modelling [*Boé et al.,* 2009; *Chen et al.,* 2011a; *Chen et al.,* 2011b; *Chiew et al.,* 2009c; *Mpelasoka and Chiew,* 2009; *Wilby and Harris,* 2006]. The most comprehensive comparison by *Chen et al.* [2011b] assessed the overall uncertainty of hydrological impacts of climate change for a Canadian watershed, by examining six GCMs, five GCM initial conditions, two GHG emissions scenarios, four statistical downscaling techniques, three hydrological model structures, and 10 sets of hydrological model parameters. For mean annual discharge, the study concluded the following order of uncertainty

source significance (from greatest to least): GCM > GCM initial conditions > GHG emissions scenario > statistical downscaling technique > hydrological model > hydrological model parameters.

While in many cases runoff is a good indicator of water availability, the impacts of climate change on runoff do not necessarily correlate with those on water supply. For example, *Zhu et al.* [2005] discovered that in California most climate change scenarios with increased precipitation resulted in less available water because of the seasonal rainfall pattern and the storage capacities; that is, less summer runoff was not compensated by more winter runoff, because the storages could not accommodate the increased winter flows. Water supply systems also have additional complexities in comparison to runoff. These include the uncertainties associated with future population, per capita water demand, regulatory requirements, water law, consumer preferences, and environmental standards [*Wiley and Palmer*, 2008]. Furthermore, model complexity is enhanced when modelling climate change impacts on water supply because not only do water simulation models incorporate demand, but they can also model: (1) water storages; (2) transmission systems; (3) treatment systems; and (4) user-specified operating rules [*Traynham et al.*, 2011]. Consequently, because of the additional complexity and uncertainty when moving from analysing runoff to water supply, it cannot be assumed that the magnitude of uncertainties of climate change impacts on runoff equal that for water supply.

A number of studies have examined the impact of climate change on water supply systems [*Fowler et al.*, 2003; *Gober et al.*, 2010; *Groves et al.*, 2008c; *Kaczmarek et al.*, 1996; *Lopez et al.*, 2009; *O'Hara and Georgakakos*, 2008; *Traynham et al.*, 2011; *Vicuna et al.*, 2010; *Wiley and Palmer*, 2008; *Zhu et al.*, 2005], with most of these studies developing projected ranges of water availability based on a number of different uncertainties. For example, *Wiley and Palmer* [2008] examined uncertainty of GCMs, *O'Hara and Georgakakos* [2008] analysed uncertainty of GCMs and population growth, *Vicuna et al.* [2010] examined uncertainty of GCMs and GHG emissions scenarios, while *Gober et al.* [2010] investigated uncertainty of GCMs, GHG emissions scenarios, runoff factors, supply and

demand management policies, and population growth. However, none of the studies compared the uncertainty sources in terms of their relative magnitudes. This is important because water authorities must understand the greatest sources of uncertainties for water supply system security and whether these are epistemic (systematic) or aleatoric (statistical). Systematic uncertainties, such as model inadequacy or data measurement inaccuracies, are potentially reducible (by the water authority's means or others) whereas statistical uncertainties, such as natural rainfall variability, are inherent and will always exist. If major sources of uncertainty are reducible by the water authority then effort can be directed towards reducing this uncertainty, while if irreducible uncertainties dominate impacts on water supply security, then adaptation responses must be developed to cope with this uncertainty. Furthermore, an understanding of how these uncertainties interact through the development of "best" and "worst" cases will help water authorities establish likely bounds of future water supply security, which is imperative for them to understand the degree to which water supply may need to be supplemented, or demand reduced, in the future. In order to understand the impacts of the uncertainties associated with modelling the likely impacts of climate change on water supply security, a number of approaches can be applied. A 'top-down' or 'scenario-based' approach, in which uncertainty is added at each point of the modelling process from GHG emissions scenarios through to water supply system models, is the most commonly used approach within scientific evidence reviewed by the IPCC [*Wilby and Dessai,* 2010], and is the approach applied in the current paper. However, as discussed by *Wilby and Dessai* [2010], 'bottom-up' and 'sensitivity-based' approaches can also be applied to analyse uncertainties surrounding the likely impacts of climate change on water supply systems.

When examining the impacts of climate change on water supply systems it is also important to consider the temporal aspects of water supply security. Due to the large-scale infrastructure associated with water supply systems and the potentially long lead times for expanding these systems, it is necessary to identify when water supply security will be jeopardised in the future, so that plans to avoid water scarcity can be implemented well in advance. With the many uncertainties

associated with analysing the impacts of climate change on water supply security, it would be prudent to assume that the estimated point in time when water security is threatened will vary considerably depending on the choices made in modelling climate change, hydrology, and the water supply system. Consequently, monitoring how water supply security will change progressively through time at regular intervals over a long-term planning horizon of 30-50 years is very important. This is quite different to analysing the impacts of climate change on runoff because in the case of water supply security, the addition of demand means a "failure" of supply to meet demand can be identified at a critical point in time, while there are no such critical points when examining runoff.

In summary, there still exists a gap in understanding the relative magnitudes of uncertainty sources in assessing the impacts of climate change on water supply systems that can help water authorities plan for, and manage, the impacts of climate change. A scenario-based sensitivity analysis has therefore been developed and applied to Adelaide's southern water supply system that focuses on the three objectives of this paper, namely: (i) to assess the relative magnitudes of the major sources of uncertainty, (ii) to identify critical points in the future when water supply security is likely to be threatened, and (iii) to present projected ranges of water supply security. The results obtained from addressing these objectives are used to draw conclusions about the planning and management of Adelaide's southern water supply system. While the methodology is illustrated for this particular case study, its generic nature means it could easily be adapted and applied to other water supply systems around the world.

The remainder of the paper is organised as follows. Firstly, the Adelaide southern system case study is introduced (Section 2.2), followed by the methodology applied to meet the three objectives of this paper (Section 2.3). The results of the case study are then presented and discussed (Section 2.4), before the main components of the paper are summarised and conclusions drawn (Section 2.5).

2.2 Case Study

Adelaide, the capital of South Australia (Figure 2.1), is the driest Australian capital city with an average annual rainfall of 552 millimetres (mm). Adelaide's rainfall is strongly seasonal, falling predominantly during mild winters, which are separated by dry, hot summers. Adelaide also experiences high interannual variability, with a minimum recorded annual rainfall of 274 mm and a maximum of 883 mm (for Kent Town, Adelaide: 1889-2010 [*Jeffrey et al.*, 2001]). Furthermore, there is high interdecadal variability in Adelaide. For example, the 1920s were 13% wetter than the long-term average, while the 1960s were 9% drier (for Kent Town, Adelaide [*Jeffrey et al.,* 2011]).

Historically, water has been sourced from reservoirs in nearby catchments in the Mount Lofty Ranges. These storages can hold a total of approximately 200 Gigaliters (GL) of water, equivalent to a little more than one year's water supply for Adelaide. In most years, water from the River Murray is pumped about 50-60 kilometres (km) to supplement Adelaide's water supply.

This study focuses on Adelaide's southern system of reservoirs, namely Myponga, Mount Bold, and Happy Valley. The southern system, which supplies approximately half of Adelaide's demand, can be considered separately from Adelaide's northern system of reservoirs because the two systems act largely independently of each other [*Crawley and Dandy*, 1993].

Myponga Reservoir in the South (Figure 2.1) has a capacity of 26.8 GL and is a 'supply and storage' reservoir, with water collected from its 124 km^2 catchment (Figure 2.1), before being treated at Myponga Water Treatment Plant (WTP), which has a capacity of 50 Megalitres/day (ML/day) (see www.sawater.com.au). Mount Bold Reservoir has a much larger catchment and storage capacity (Figure 2.1) – 388 km^2 and 46.2 GL, respectively (see www.sawater.com.au) – but is considered a 'storage' reservoir because it cannot directly supply water to the water distribution network. Instead, water is released from Mount Bold Reservoir and diverted six kilometres downstream at Clarendon Weir via the Horndale Flume to Happy Valley Reservoir (Figure 2.1) [*Teoh*, 2002]. Clarendon Weir is a small reservoir with capacity of 0.3 GL, while Happy Valley Reservoir has a

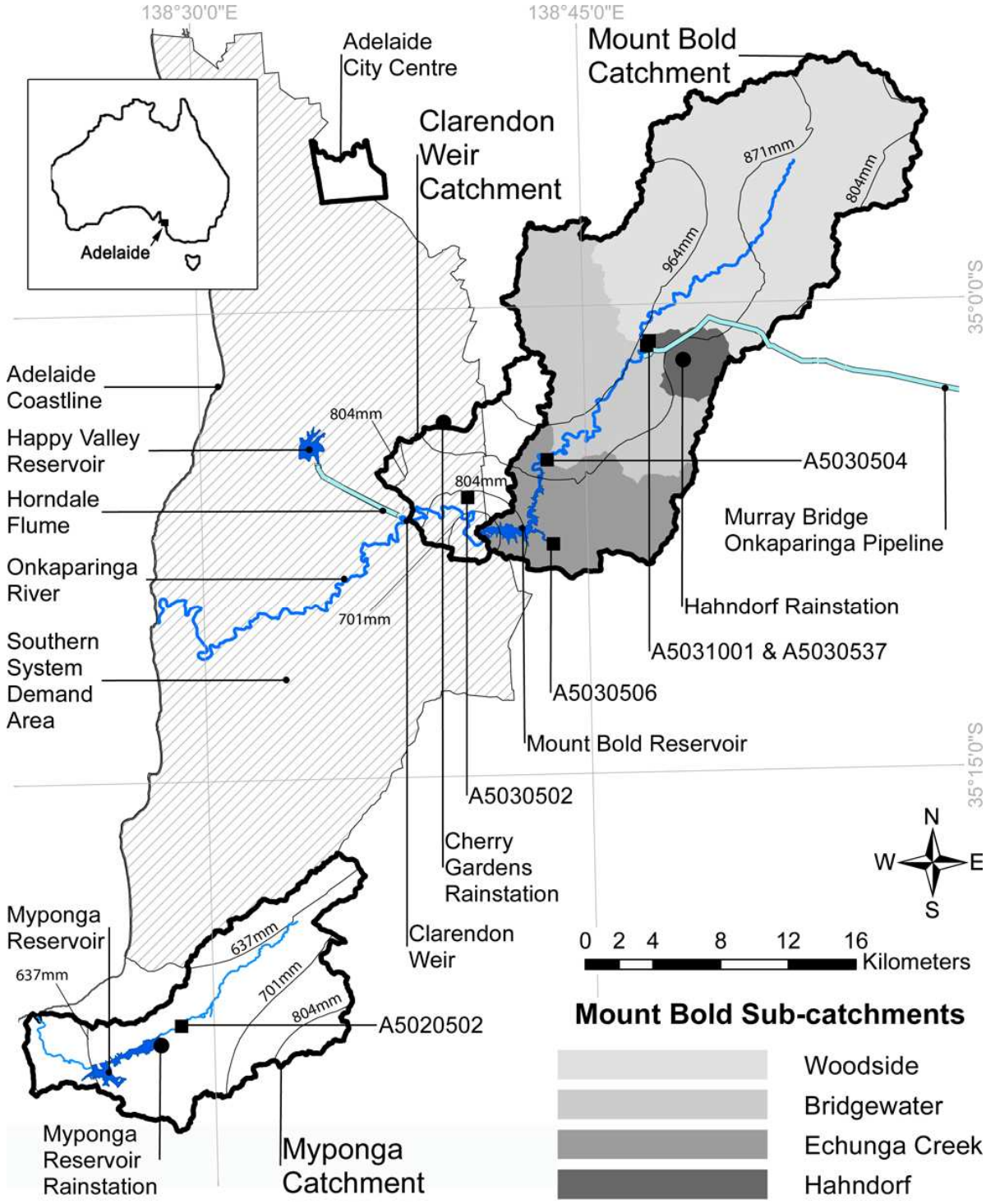

Figure 2.1: Map of Adelaide's southern water supply system, detailing reservoirs, reservoir catchments, major rivers, pipelines, and the southern system demand area. Gauging stations, rainfall stations, Mount Bold sub-catchments, and isoheytal lines that have been defined for calibrating RRO models for each catchment are also illustrated. Insert of map of Australia highlighting location of Adelaide.

capacity of 11.6 GL (see www.sawater.com.au). Happy Valley Reservoir is considered an "off-stream" reservoir, with water only being supplied via the Horndale Flume, while Clarendon Weir receives

water released from Mount Bold Reservoir, as well as run-off from its 54 km^2 catchment (Figure 2.1). The main purpose of Happy Valley Reservoir is to store water prior to treatment at the Happy Valley WTP, which has a capacity of 850 ML/day (see www.sawater.com.au).

Mount Bold Reservoir also receives water from the River Murray via the Murray Bridge-Onkaparinga (MBO) Pipeline (Figure 2.1). Although flows in the River Murray are affected by rainfall in the basin, the upper limit of water that Adelaide has previously been able to source from the River Murray has been determined by licenses, rather than rainfall. For example, licenses have allowed for up to 90% of Adelaide's water to be sourced from the River Murray in the past in dry years, whereas about 40% of Adelaide's demand has been supplied by the River Murray on average [*Government of South Australia*, 2009]. Furthermore, and contrary to the common principle that a license does not necessarily guarantee water availability, Adelaide's River Murray usage is almost certainly guaranteed because: (1) it constitutes less than one percent of total River Murray flow; (2) critical human needs, including for Adelaide, are the highest priority in allocating River Murray water; and (3) the significant storage of the River Murray system helps to dampen out temporal variability in flow that might restrict water availability for a particular time period. The amount of River Murray water that Adelaide can use is based on a 5-year rolling license of 650 GL, with the license period beginning on May 1st each year. However, the license alone cannot supply all of Adelaide's water demand, as the maximum River Murray supply over five years is about 65% of total demand. Furthermore, with projections of population growth resulting in future increases in demand, the percentage of demand potentially met by the River Murray will reduce (as the 5-year license is fixed at 650 GL). Hence, supply from local catchments is vital in order to meet demand.

2.3 Methods

Figure 2.2 illustrates the methodology and data used to assess water supply security at a number of discrete times in the future and the relative contributions of sources of uncertainty of climate change impacts on water supply security for Adelaide's southern system. The first step was the

development of RRO models (Figure 2.2), which were necessary to determine runoff from the Myponga, Mount Bold and Clarendon Weir catchments, while the second step was to develop climate change affected rainfall and evaporation (Figure 2.2). For clarity, data that were used in the case study for both the RRO models and the development of climate change affected rainfall and evaporation are highlighted in Figure 2.2. The validated RRO models from Step 1 and the climate change affected rainfall and evaporation from Step 2 were then applied in the development of the water supply system model for the southern Adelaide system (Figure 2.2). Specifically, the RRO model and the climate change affected rainfall and evaporation were used to determine supply from the climate-dependent water sources, namely the three reservoirs – Myponga, Mount Bold and Happy Valley (Step 3, Figure 2.2). The supply component also incorporated the climate-independent water source of the River Murray (as explained above – see also Section 2.3.3.1.1), while demand was a combination of per capita consumption and population (Step 3, Figure 2.2). Finally, in Step 4, water supply security was assessed for various uncertain water supply scenarios in a systematic fashion, investigating uncertainties in future development pathways, general circulation models, and demand (Figure 2.2). Steps 3 and 4 are very important because as illustrated in Section 2.1, studies have examined the relative magnitudes of uncertainty associated with climate change impacts on

runoff, but there is a need to extend this to water supply systems, for which there are additional uncertainties (e.g. demand) and additional complexities (e.g. storages).

The four major steps of the flowchart are discussed in more detail in the following sections, while justification for the scenario options considered in this paper (delineated by the black boxes in Figure 2.2), is provided in Section 2.3.4. While the following discussion focuses on Adelaide's southern water supply system, the methodology presented in Figure 2.2 could also be readily applied to other water supply systems. However, some alterations may be required. For example, in the case study, stochastic rainfall time series were generated for a historical record and then perturbed for climate change, while in other cases, calibrating a weather generator on a climate-

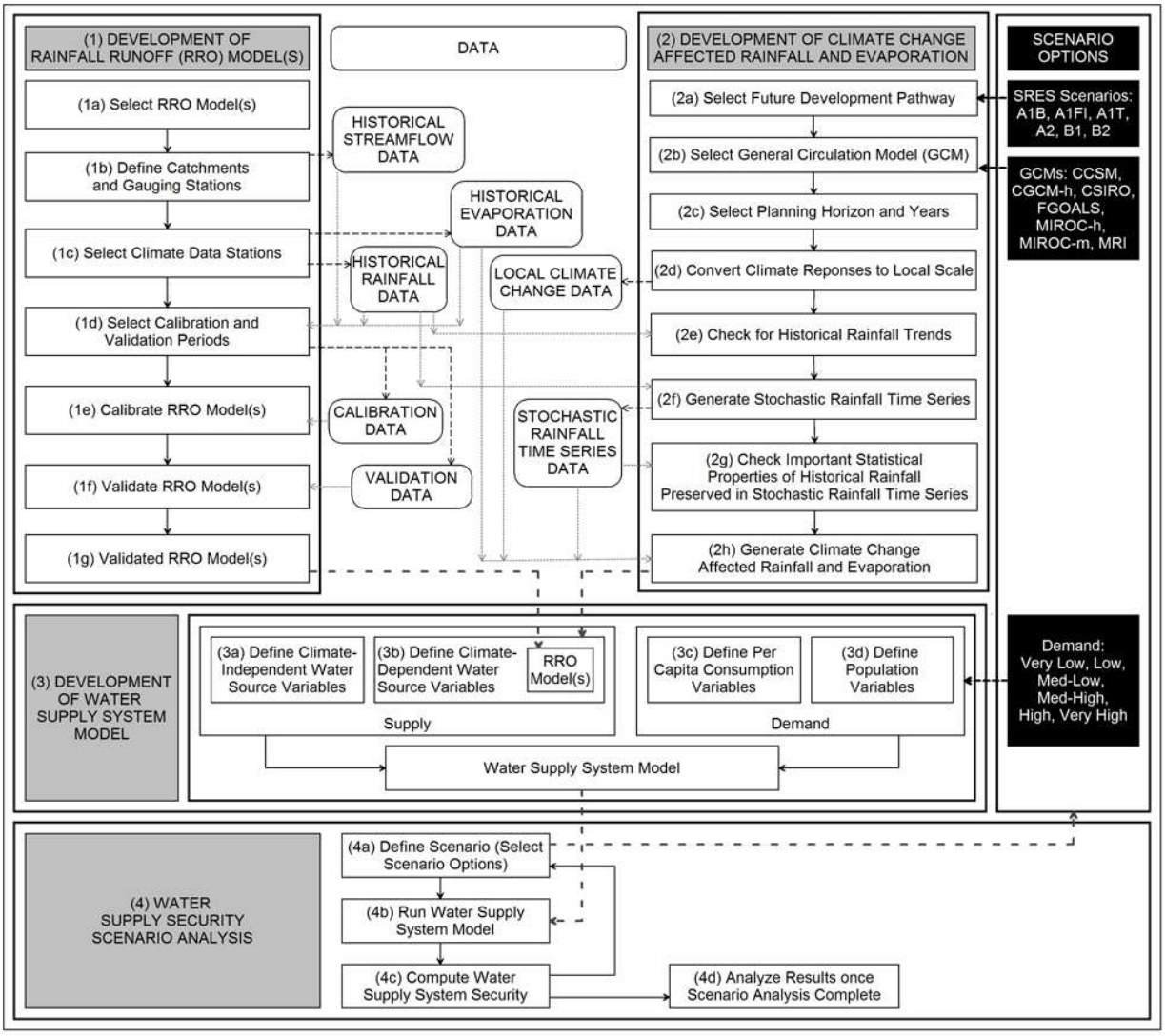

Figure 2.2: Flowchart of the methodology followed for the Adelaide southern water supply system case study.

change perturbed record (for example see *Kilsby et al.* [2007]), or conditioning the parameters of a weather generator using GCM output to directly incorporate the climate change signal, may be more appropriate. In addition, the focus in this case study is on the impacts of climate change on supply; however, climate change impacts on demand could also be incorporated. For example, *Groves et al.* [2008c] found outdoor water demand was projected to increase by 10% in southern California by 2040 due to the impacts of climate change.

2.3.1 Development of Rainfall Runoff (RRO) Model(s)

2.3.1.1 Select RRO Model(s)

The WC1 model was selected to determine runoff in this case study (Step 1a, Figure 2.2) because it has been used previously throughout the Mount Lofty Ranges [*Alcorn*, 2006; *Savadamuthu*, 2003; *Teoh*, 2002] and because it was developed based on experience with South Australian RRO calibration in the Mount Lofty Ranges and other parts of the state (see www.waterselect.com.au). WC1 is a 10-parameter, conceptual RRO model that employs a three-bucket concept, in which the three storage components (or buckets) of the model, are: (1) interception store; (2) soil moisture store; and (3) groundwater store. Surface, interflow, and groundwater flow potentially contribute to surface runoff. Further details of the WC1 model can be found in the WaterCress user manual, available from www.waterselect.com.au. Both daily rainfall and monthly evaporation are required for WC1 to compute runoff.

2.3.1.2 Define Catchments and Gauging Stations

Daily flow data from gauging stations A5020502, A5030504, A5030506, and A5030502 (Figure 2.1) were selected for this case study (Step 1b, Figure 2.2) because large areas of the Myponga, Mount Bold, and Clarendon Weir catchments contribute flow at these stations and because the datasets span three to four decades and are relatively complete (Table 2.1). Furthermore, a catchment model of increased complexity was also defined for the Mount Bold catchment to assess the impact of model complexity on model performance. For the complex model, which contains four RRO models (one for each sub-catchment), a further two suitable gauging stations for the Mount Bold catchment (A5031001 and A5030537 – see Figure 2.1) were selected (Table 2.1).

For each of the six gauging stations, streamflow data were sourced from the Government of South Australia's surface water archive (www.waterconnect.sa.gov.au/SWA). Long and complete records were available for A5030502 and A5030504, long but incomplete records were available for A5030506 and A5020502, while relatively shorter and incomplete records were available for

Table 2.1: Gauging station data for each catchment.

Catchment	Catchment Area (km^2)	Gauging Station Identification	Gauging Station Area (Percentage of Catchment Area)	Gauging Station Data Period Available	Data Record Completeness (Percentage of Data Period Available)
Myponga	124	A5020502	61%	Oct'79-Feb'11	98.8%
Mount Bold	388	A5030504	83%	May'73-Jan'11	100%
		A5030506	9%	Apr'73-Dec'10	97.1%
		A5031001	59%	Jul'02-Jul'11	99.2%
		A5030537	4%	Apr'93-Mar'96; Jul'02-Jul'11	98.1%
Clarendon Weir	54	A5030502	49%	Apr'69-Dec'10	100%

A5030537 and A5031001 (Table 2.1). For records that contained missing streamflow data at the very beginning or very end of the data periods, the data were excluded, while if the missing data were in the middle of the dataset, they were estimated using regression analysis with nearby flow gauges. Flow records downstream of the MBO pipeline were also adjusted to take into account volumes supplied from the River Murray. Furthermore, an assessment of the rainfall and streamflow records for the Myponga catchment illustrated that from about the late 1990s, there was a marked decrease in large streamflow events but no decreasing trend in rainfall. A5020502 data were predominantly tagged as good quality, so errors in gauging seem unlikely to have caused this trend. The altered flow regime is more likely due to an increase in small farm dams and an intensification of dairying, viticulture, and olive horticulture that has occurred in the catchment over time. Consequently, calibration and validation were only carried out for Myponga catchment from January 1999 to December 2010.

2.3.1.3 Select Climate Data Stations

The Bureau of Meteorology (BoM) stations Myponga Reservoir (23738), Hahndorf (23720), and Cherry Gardens (23709) were selected as suitable climate data stations (Step 1c, Figure 2.2) to represent Myponga, Mount Bold, and Clarendon Weir catchments, respectively. These stations were selected because they are part of the Patched Point Dataset (PPD) [*Jeffrey et al.*, 2001], a dataset comprising approximately 4600 locations around Australia and spanning from 1890 to the current day. The PPD is based on observed BoM daily meteorological records that have been enhanced by high-quality, rigorously-tested data infilling (when data are missing) and deaccumulation of any records that represented rainfall over multiple days, rather than a single day [*Charles et al.*, 2008].

2.3.1.3.1 Rainfall

A number of advantages exist in using the PPD dataset for rainfall data in this study. Firstly, the data from each site span identical time periods with inter-station correlations being upheld. Secondly, the data cover a long timeframe, so that the existing long-term variability in rainfall experienced in Adelaide is incorporated, while thirdly, the rainfall data are a continuous time series, which is a necessary input requirement for the modelling and analysis tools used in this study. Finally, rainfall data in the original BoM datasets for these stations span a significant time period and are relatively complete (Table 2.2), ensuring that the potential errors occurring through the infilling process are minimised because the use of observed data is maximised. For example, the stations selected have greater than 90 years of rainfall records and are between 89% and 98% complete (Table 2.2).

The climate data stations were also selected because of their location within each catchment (Figure 2.1), which is an important consideration in attempting to obtain an accurate representation of rainfall for a particular area because rainfall displays the largest spatial variability among meteorological variables [*Srikanthan and McMahon*, 2001]. In this case study, the average annual rainfall for each catchment was estimated using ArcGIS. Firstly, all BoM stations that occurred in the PPD and that were within 15 kilometres of the three catchments were selected. The average annual

rainfalls for all stations were then spatially interpolated using the inverse distance weighted tool and with the resulting interpolation classified into seven categories (isoheytal areas) using the Natural Breaks (Jenks) method. The average of the bounding rainfall values for each of the isoheytal areas was taken as the average rainfall for each respective area (Figure 2.1). These average values were then weighted by area to calculate an average annual rainfall for each of the catchments (Table 2.2). The resulting differences between these values and the average annual rainfall amounts for each respective climate data station were then used to create a rainfall scaling factor (Table 2.2), by which all daily rainfall amounts in the historical datasets were multiplied.

2.3.1.3.2 Evaporation

Evaporation (which is treated as equivalent to actual evapotranspiration in WC1) was calculated by multiplying recorded daily evaporation by the pan factor for soil (which is one of the RRO parameters to be calibrated). Recorded daily evaporation was converted from monthly Pan A evaporation inputs, which in this case study were sourced from averaging values in the PPD between 1975 and 2004 (Table 2.3). While the PPD contain daily evaporation values from 1889 onwards, Class A evaporation pans were only installed in Australia during the 1960s [*Rayner*, 2005], so values in the PPD pre-1970 were interpolated from long-term averages and were thus not included. Furthermore, to develop the climate change scenarios for evaporation later in this study, evaporation data based on the 30 years from 1975-2004 are required (see Section 2.3.2.3), so this 30-year period was selected.

2.3.1.4 Select Calibration and Validation Periods

Approximately 60-70% of the available data were used for calibration and 30-40% for validation (Step 1e, Figure 2.2), ensuring that at least five years of data were used in calibration and at least three years were used in validation (Table 2.4). The calibration and validation periods for Myponga, Woodside, Hahndorf and Bridgewater were very short, which could potentially limit the RRO models in accurately capturing the catchments' RRO behaviour, particularly if these time periods do not

Table 2.2: Rainfall station data for each catchment.

Catchment or Sub-catchment		Climate Data Station (BoM identification number)	BoM record length	BoM dataset completeness (%)	Average annual rainfall for climate data station (mm/yr)	Average annual rainfall for catchment (mm/yr)		Rainfall Scaling Factor	
						Calibration & Validation	Whole catchment	Calibration & Validation	Whole catchment
Myponga		Myponga Reservoir (23738)	1914-2010	89%	752	736	728	0.9785	0.9677
Mount Bold (simple)		Hahndorf (23720)	1884-2010	95%	849	919	914	1.0828	1.0770
Mount Bold (complex)	Woodside						906		1.0671
	Hahndorf						856		1.0085
	Bridgewater						990		1.1659
	Echunga (& Mount Bold Reservoir)					842	841	0.9918	0.9911
Clarendon Weir		Cherry Gardens (23709)	1899-2010	98%	929	943	859	1.0150	0.925

Table 2.3: Average monthly evaporation for climate data stations.

Rainfall Station	Average evaporation (mm/month)											
	Jan	Feb	Mar	Apr	May	Jun	Jul	Aug	Sep	Oct	Nov	Dec
Myponga Reservoir	219	188	151	96	62	45	50	67	90	130	165	199
Hahndorf	233	201	162	102	66	47	52	72	95	139	179	213
Cherry Gardens	217	188	149	92	57	39	44	61	84	124	161	195

Table 2.4: Calibration and validation periods for catchments and sub-catchments.

Catchment or Sub-catchment		Calibration Period	Validation Period
Myponga		Jan'99 - Dec'06	Jan'07 - Dec'10
Mount Bold (simple)		Jan'74 - Dec'99	Jan'00 - Dec'10
Mount Bold (complex)	Woodside	Jan'03 - Dec'07	Jan'08 - Dec'10
	Hahndorf	Jan'03 - Dec'07	Jan'08 - Dec'10
	Bridgewater	Jan'03 - Dec'07	Jan'08 - Dec'10
	Echunga	Jan'75 - Dec'99	Jan'00 - Dec'10
Clarendon Weir		Jan'70 - Dec'97	Jan'98 - Dec'09

contain particular extreme events, such as droughts. Calibration and validation periods began in January and were multiples of 12 months, so as not to bias the RRO models' calibrated parameters towards a particular month's flow properties.

Adelaide also suffered a severe drought from 2003 to 2009, so data from this time period alone possibly suffered from a dry rainfall bias. While it is important to understand water supply security

during dry periods, it is also critical to accurately simulate runoff during wet periods as this runoff can replenish storages and potentially be used to buffer droughts. Furthermore, RRO models calibrated only on dry periods may not be able to accurately simulate the response to wet periods, so this was avoided where possible. However, it could not be helped when calibrating Woodside,

Hahndorf and Bridgewater catchments (Table 2.4) because of the need to use overlapping data from identical periods, a result of the Bridgewater gauging station (A5030504) being downstream of both the Woodside and Hahndorf gauging stations (A5031001 and A5030537, respectively) (Figure 2.1).

2.3.1.5 Calibrate RRO Model(s)

A genetic algorithm (GA) was chosen over classical methods of optimisation to calibrate the WC1 models (Step 1f, Figure 2.2), because genetic algorithms have shown to be successful in optimising RRO models [*Wang,* 1991]. Upper and lower limits for each parameter for WC1 were defined to restrict the search space of the GA and ensure the physical plausibility of the parameter values. The bounds for WC1 parameters were based on limits defined in the WaterCress user manual (see www.waterselect.com.au), which were similar to those used in the Mount Lofty Ranges' studies by *Teoh* [2002] and *Savadamuthu* [2003].

Initial GA parameter trials examined populations of 100 to 400, generations of 100 to 300, and values of 0.6 to 0.9 for the probability of crossover, with final GA parameter selection being 200 for population, 150 for maximum number of generations, and 0.7 for probability of crossover. The probability of mutation was taken as 0.1 – the inverse of the number of model parameters. In order to check whether parameter equifinality [*Beven*, 2006] is a potential problem, each calibration run was repeated ten times from different starting positions in parameter space. Firstly, there was little change in the calibration errors for the ten trials. Similarly, the calibrated RRO parameters were reasonably stable over the ten calibration runs and the flows were not sensitive to these slight changes in parameters.

The Root Mean Squared Error (RMSE) of the monthly flows was selected as the performance criterion; such that RMSE was minimised in the optimisation process (an RMSE equal to zero indicates a perfect fit). RMSE is biased towards minimising error in high flows but was selected as the objective because, as mentioned in Section 2.3.1.4, when studying water supply security, accurately simulating runoff from the large rainfall events is likely to be more important than simulating runoff from the more frequent low rainfall events, because of the ability of reservoirs to store water. If the amount of runoff from wet periods was under- or over-estimated, the amount of water available in the storages could be quite different from reality, and would thus affect the estimated supply security during dry periods when demand exceeded runoff. Hence, high flows have the potential to have a much bigger impact on water supply security than low flows and as such, minimising errors in these high flows is critical. A monthly time step was chosen over a daily time step for assessing model performance because the storage of the reservoirs was likely to buffer any daily errors obtained in runoff. The average annual flows for the observed and modelled datasets and the monthly Nash-Sutcliffe (NS) were also calculated following optimisation. A minimal difference between the annual observed and modelled flows and a NS value approaching one were sought. However, *Jain and Sudheer* [2008] point out that a high value of NS can be achieved for a model with a poor fit. Consequently, although more subjective than the use of statistical measures of goodness-of-fit, plots of simulated and observed hydrographs were also inspected following optimisation. *Refsgaard and Storm* [1996] note that the visual inspection of plots is an efficient means of assimilating information, as well as providing a good overall insight into a model's capabilities. To compare the simple and complex Mount Bold catchment models, an additional criterion was required that could penalise model complexity as well as error. This is based on the principle that for a given level of accuracy a more parsimonious model is preferable [*Bozdogan*, 1987]. The application of the principle of parsimony in hydrological modelling is discussed by *Wagener et al.* [2004], but, in brief, complexity control is advantageous as it reduces parameter equifinality by identifying the

simplest model that explains the observed data [*Schoups et al.,* 2008]. The Akaike Information Criterion (AIC) [*Akaike*, 1973] based on monthly flows was used for this purpose.

2.3.1.6 Validate RRO Model(s)

Model validation (Step 1f, Figure 2.2) was necessary to check that the RRO parameters optimised during calibration also performed well on independent data. A model was to be rejected as being not behavioural (i.e. not consistent with observations) [*Beven*, 2006] for this case study if: (1) the modelled hydrographs were judged to not adequately match the observed hydrographs based on visual inspection; (2) NS was < 0.50 [*Moriasi et al.,* 2007]; and/or (3) the RMSE was more than half the standard deviation of the observed flows [*Singh et al.,* 2004]. Validation periods for the case study were as defined in Section 2.3.1.5, while the validation performance evaluation measures were the same as those defined above for calibration.

2.3.1.7 Validated RRO Model(s)

To have confidence in using the optimised WC1 model parameters to estimate runoff for the case study, it was necessary to analyse whether the RRO models produced results within the range of accuracy identified in Section 2.3.1.6 for the validation data. All RRO models developed for this case study had an NS > 0.50, while the RMSE values for most catchments were considered low, as they were less than 50% of their respective standard deviations, except for the calibration periods of the Hahndorf and Bridgewater sub-catchments, for which they were slightly greater than 50% (Table 2.5). However, this was considered obsolete, because based on the NS efficiency values (Table 2.5) and AIC values (1515 for the complex model compared to 1480 for the simple model), it was decided the simple Mount Bold model should be used rather than the complex one. An assessment of the modelled monthly hydrographs indicated that the WC1 models recreated the observed flow hydrographs reasonably well. The WC1 model parameter values (Table 2.6) were similar to those obtained in previous calibration studies on nearby catchments [*Alcorn*, 2006; *Teoh*, 2002] indicating

Table 2.5: Root Mean Squared Error (RMSE), Nash-Sutcliffe (NS), ratio of RMSE to standard deviation (SD), and average observed and modelled flows for the calibration and validation periods of the WC1 models for the Myponga, Mount Bold (simple), Mount Bold (complex), and Clarendon Weir catchments.

Catchment or Sub-catchment		Accuracy Criteria for Calibration					Accuracy Criteria for Validation				
		RMSE (ML/month)	NS	RMSE/SD	Average Observed Flow (GL/yr)	Average Modelled Flow (GL/yr)	RMSE (ML/month)	NS	RMSE/SD	Average Observed Flow (GL/yr)	Average Modelled Flow (GL/yr)
Myponga		228	0.92	0.28	7.5	7.9	315	0.80	0.44	5.2	3.2
Mount Bold (simple)		1775	0.95	0.22	51.9	51.6	1996	0.88	0.35	41.4	41.2
Mount Bold (complex)	Woodside	798	0.90	0.31	16.9	15.8	888	0.94	0.24	20.6	17.4
	Hahndorf	122	0.74	0.51	1.9	1.6	105	0.88	0.34	2.1	1.8
	Bridgewater	1277	0.75	0.50	19.8	16.8	919	0.81	0.43	16.9	18.2
	Echunga	203	0.89	0.34	3.4	3.3	148	0.87	0.35	2.6	2.6
Clarendon Weir		134	0.94	0.25	3.9	3.9	138	0.87	0.36	3.0	3.5

Table 2.6: Parameter values for the WC1 RRO models for each of the catchments.

Catchment or Sub-catchment	WC1 Model Parameter									
	Median Soil Moisture (mm)	Catchment Distribution (mm)	Interception Store (mm)	Ground Water Discharge	Soil moisture discharge	Pan factor for soil	Fraction Groundwater Loss	Store Reduction Coefficient	Groundwater Recharge	Creek Loss (mm)
Myponga	160	59.4	8.1	0.0015	0.00015	0.94	0.49	0.90	0.45	0.01
Mount Bold	186	60.0	9.3	0.0015	0.00012	0.84	0.49	1.39	0.15	0.00
Clarendon Weir	195	59.5	8.0	0.0015	0.00015	0.99	0.20	0.85	0.30	0.01

that the model parameters obtained were reasonable. Thus the calibrated RRO models were considered valid (Step 1g, Figure 2.2) and could be applied to the case study with confidence.

2.3.2 Development of Climate Change Affected Rainfall and Evaporation Data

2.3.2.1 Select Future Development Pathway and General Circulation Model (GCM)

The first step in developing the climate change affected rainfall and evaporation data was to select the SRES scenario to represent a future development pathway (Step 2a, Figure 2.2). A GCM was then selected (Step 2b, Figure 2.2) to translate the future emissions pathway to regional climate responses. The scenario options selected for SRES scenarios and GCMs for the case study are discussed in Section 2.3.4.1.

2.3.2.1 Select Planning Horizon and Years

A planning horizon and the years for which to progressively analyse system security for the case study must be selected (Step 2c, Figure 2.2) to ensure that future critical points in time for water supply security will be recognised. For the case study, a 40-year period from 2010 to 2050 was selected, with 2010, 2020, 2030, 2040 and 2050 identified as regular but discrete years to analyse.

2.3.2.2 Convert Climate Responses to Local Scale

The constant scaling or delta change approach was used in the case study to obtain local rainfall and evaporation responses (Step 2d, Figure 2.2). The constant scaling approach meant that for each month and for each climate site, the historical baseline climate was scaled by a factor representing the change projected in that month for the closest GCM grid point.

Specifically, monthly factors for rainfall and areal potential evapotranspiration (equivalent to Pan A Evaporation and calculated according to the method described in *Morton* [1983]), were obtained from the Australian Commonwealth Scientific and Industrial Research Organisation's (CSIRO) OzClim (www.csiro.au/ozclim/). Ozclim is a tool developed for the scientific research community and policy makers that provides data on a 25 km grid over Australia. Change factors for each grid point are developed by: (1) using linear regression to obtain the local change in the value of a climate variable

(e.g. rainfall) per degree of global warming for a particular GCM; and (2) multiplying this result by the degree of global warming associated with a SRES scenario. These change factors can then be applied to the baseline climatology of the climate variable (defined from 1975-2004), to produce future climate projections. For this case study, the change factors for rainfall and evaporation were extracted for 2020, 2030, 2040 and 2050.

The delta change approach is a simple downscaling approach and has a number of limitations that include: (1) the mean, maxima and minima are the only data properties that are different between the scaled and baseline climate; (2) the spatial pattern of the present climate is assumed for the future; (3) the approach, without modification, cannot simulate changes in the occurrence of rainfall, nor changes to the size of extreme events; and (4) values for a single grid cell may contain gross biases [*Wilby and Fowler,* 2011]. However, the constant scaling approach was selected to downscale GCM data because: (1) simple downscaling approaches can accurately simulate flow [*Fowler et al.*, 2007]; and (2) the constant scaling approach can be applied easily using multiple GCMs and SRES scenarios [*Mpelasoka and Chiew*, 2009], which was important in this case study in order to analyse uncertainties associated with these factors.

2.3.2.3 Check for Historical Rainfall Trends

It was important that the historical rainfall time series were checked for trends before generating the stochastic rainfall time series because the stochastic rainfall generator used in this case study – Stochastic Climate Library (SCL) (Section 2.3.2.5), assumes that the input data (i.e. the historical rainfall) have already been checked for stationarity. Consequently, the rainfall data were run through TREND (www.toolkit.net.au/trend) (Step 1d, Figure 2.2), a tool developed by the Cooperative Research Centre (CRC) for Catchment Hydrology, which enables statistical testing for trend, change, and randomness in time series data [*Chiew and Siriwardena*, 2005]. As the distribution of the rainfall is unknown, only the non-parametric tests were used. The Mann-Kendall and Spearman's Rho tests were used to test for a trend; the Distribution-Free Cumulative Sum

(CUSUM) was used to test for a step jump in the mean; while the Rank-Sum test was used to check for a difference in median between two sections of the dataset. In this case study, rainfall from May 1974 to April 2004 was elected as the baseline data from which to derive future climate change scenarios because 1975 to 2004 is the OzClim baseline (see Section 2.3.2.3), and the River Murray license year runs from May 1st to April 30th (see Section 2.2). Consequently, rainfall data from the three sites spanning this time period were analysed in TREND. For each of the three rainfall stations, none of the aforementioned tests returned a significant result (indicating that there were no trends or step jumps in the nominated time series), apart from the Mann-Kendall test for Hahndorf. However, the significance level of this test suggested that there was little evidence of a trend, and given the Spearman's Rho test (which also tests for a trend) did not return a significant result, it was presumed that if such a trend in the Hahndorf dataset existed, it was insignificant for the purposes of this study.

2.3.2.4 Generate Stochastic Rainfall Time Series

Generating stochastic rainfall time series for the case study (Step 2e, Figure 2.2) was important because urban water supply planning should include the stochasticity in precipitation [*O'Hara and Georgakakos*, 2008] and because Adelaide has such high, natural temporal rainfall variability (see Section 2.2). Use of stochastic rainfall data ensured that: (1) the results produced were not simply a reflection of the historical rainfall time series; and (2) water supply system security could be reported as a distribution to reflect the inherent variability in historical rainfall, rather than a single deterministic value. A probability-based approach is particularly useful from a water management perspective because it establishes ranges and confidence levels to help understand future levels of risk to the system. It is important to note that while this distribution will reflect historical rainfall variability, it does not necessarily reflect future rainfall variability. To correctly achieve projections of future rainfall variability would require applying a perturbed physics ensemble or weather generator to generate rainfall sequences based on climate characteristics. For example, a weather generator could be calibrated on a climate change perturbed record or its parameters could be conditioned on

large-scale atmospheric predictors, weather states or rainfall properties to directly incorporate climate change [*Wilby and Fowler,* 2011]. These methods are beyond the scope of this paper.

The stochastic rainfall time series were constructed using the multi-site daily rainfall model of the Stochastic Climate Library (SCL) (www.toolkit.net.au/scl), developed by the CRC for Catchment Hydrology [*Srikanthan*, 2005]. It is a multi-site two part daily model, nested in a monthly and annual model. The first part consists of rainfall occurrence, which is determined using a first-order two-state Markov chain, while the second part relates to rainfall amounts, derived using a gamma distribution [*Srikanthan*, 2005]. This daily model is then nested in a monthly and annual model in order to preserve the monthly and annual characteristics. The monthly and annual models are driven by the noise term derived from the generated daily rainfall data. The mathematical development of the monthly and annual models is provided by *Srikanthan* [2005] and *Srikanthan and Pegram* [2009]. Because of the great spatial variability of rainfall (see Section 2.3.1.3.1), a multi-site model was necessary to account for the spatial dependence between rainfall stations, while the SCL was selected because it preserves the important characteristics of rainfall at daily, monthly, and annual time scales [*Srikanthan*, 2005].

2.3.2.5 Check Important Statistical Properties of Historical Rainfall Preserved in Stochastic Rainfall Time Series

Statistical analyses of the developed stochastic time series were necessary to ensure that the important statistical properties of the historical data were preserved in the stochastic time series (Step 2f, Figure 2.2). *Srikanthan et al.* [2004] provide suggested tolerances for each statistical parameter but also suggest that users make their own assessment of the quality of the data produced by SCL because certain statistics may be more important than others depending on the application. First of all, because these stochastic time series represent natural rainfall variability, measures of variability (e.g. standard deviation) must be assessed and because of the high interannual and interdecadal variability experienced by Adelaide (see Section 2.2), preservation of interannual and interdecadal variability was also necessary. For this case study, the 2-, 3-, 5-, 7-, and

10-year low rainfall sums were particularly important, because the accumulation of a number of years with below-average rainfall creates water supply security concerns, rather than a single year. This is because Adelaide currently has the ability to buffer an extremely low rainfall year through reservoir storage and pumping water from the River Murray with a 5-year rolling license, whereas an accumulated dry spell of a number of years may result in reservoirs running dry and the River Murray license being fully allocated. The annual mean rainfall was also considered an important measure, so as not to over- or under-predict runoff. Furthermore, the coincidence of below-average rainfall years across the three rainfall sites could also impact total water supply from the reservoirs, so matching the observed annual cross-correlation between rainfall sites was also important.

For the case study, 1000 stochastic rainfall time series of 30 years were developed. Differences between the annual standard deviation of the historical and generated series for all sites (Table 2.7) were no greater than 1 millimetre per year (mm/yr), which is well within the tolerance of 5 mm/yr suggested by *Srikanthan et al.* [2004]. Similarly, differences in the maximum and minimum annual rainfall values for all three sites (Table 2.7) fell within the 10% tolerance suggested by *Srikanthan et al.* [2004]. The average difference in multi-year rainfall sums was 1.5%, with all multi-year rainfall sums (Table 2.7) well within the 10% tolerance suggested by *Srikanthan et al.* [2004]. The mean annual rainfall amounts in the generated data for the three sites (Table 2.7) were within 0.02% of the historical means, while the average difference in mean monthly rainfall amounts for the three sites was 2.0%, with only the February rainfall for Hahndorf and March rainfall for Cherry Gardens, not being within the 7.5% tolerance suggested by *Srikanthan et al.* [2004]. Finally, the differences in annual cross-correlation values between the three rainfall sites ranged from 0.01 to 0.04, well within the tolerance of 0.2 suggested by *Srikanthan et al.* [2004]. Consequently, based on the similarity in statistical properties that were considered important to this case study, the generated stochastic data were considered to preserve the important characteristics of the historical rainfall and were thus appropriate for further use in this study. However, it is recognised that the time period elected to base the stochastic rainfall time series on (30 years from 1974-2004), is relatively short and may

Table 2.7: Important annual statistical properties of the historical and generated rainfall time series.

Parameter		Unit	Climate Data Station					
			Hahndorf		Cherry Gardens		Myponga	
			Historical	Generated	Historical	Generated	Historical	Generated
Mean		mm/yr	794	794	905	906	756	756
Standard Deviation		mm/yr	158	159	145	146	163	163
Maximum		mm/yr	1248	1139	1335	1220	1111	1113
Minimum		mm/yr	479	487	665	619	467	444
Low rainfall sums	2-yr	mm/2yrs	1188	1204	1441	1452	1107	1087
	3-yr	mm/3yrs	1931	1938	2261	2301	1852	1771
	5-yr	mm/5yrs	3474	3452	4140	4044	3316	3197
	7-yr	mm/7yrs	4975	5003	5864	5821	4626	4663
	10-yr	mm/10yrs	7368	7375	8665	8530	6813	6920

therefore not represent the true natural rainfall variability of the system. While longer time periods were considered to increase the representation of natural rainfall variability, the average monthly mean rainfalls of the longer datasets were considerably different to those for OzClim's 30-year baseline (see Section 2.3.2.3), and so could not be used in this case study.

2.3.2.6 Generate Climate Change Affected Rainfall and Evaporation

Climate change affected rainfall and evaporation were subsequently developed by applying the percentage changes obtained from OzClim to the stochastic rainfall time series and the historical evaporation data, respectively (Step 2g, Figure 2.2). A caveat of this methodology is that the stochastic rainfall time series and historical evaporation data are not mutually consistent, which may affect daily runoff because it is a response to both of these variables acting together. However, uncorrelated daily rainfall and evaporation is not expected to influence water supply system security because the storage of the reservoirs is likely to buffer any daily errors obtained in runoff. Furthermore, evaporation is less variable compared with rainfall; for example, for the baseline period of 1974-2005 for Kent Town, the average standard deviation of evaporation per month was approximately half of that for rainfall.

2.3.3 Development of Water Supply System Model

The water supply system model consisted of both supply and demand components, with supply requiring the definition of climate-independent (Step 3a, Figure 2.2) and climate-dependent (Step 3b, Figure 2.2) water sources and demand requiring per capita consumption (Step 3c, Figure 2.2) and population (Step 3d, Figure 2.2) variables to be defined. Climate change affected rainfall and evaporation data from Step 2 were used to determine supply from the reservoirs (climate-dependent sources), while the validated RRO models of Step 1 were used to calculate runoff from the catchments that flowed into the reservoirs (Figure 2.2).

2.3.3.1 Water Supply System Model

The continuous time series, water resources model WaterCress (available from www.waterselect.com.au) was chosen for this case study because it can not only balance supply and demand and uphold system constraints, but it can also: (1) readily incorporate multiple rainfall time series (see Section 2.3.2.5); (2) model multiple catchment-reservoir relationships; (3) incorporate an external supply to represent the River Murray; and (4) output data to easily compute water security. Furthermore, the model is freely available and has the advantage of being developed and supported within South Australia.

2.3.3.1.1 Supply

As mentioned in the introduction to Section 2.3, both climate-dependent and climate-independent supply sources were defined for Adelaide's southern system. For Adelaide, the availability of River Murray supply is dictated by licenses, rather than by climate, and as Adelaide only takes about 1% of River Murray flow, the amount prescribed is virtually guaranteed, irrespective of climatic conditions (see Section 2.2). Consequently, the River Murray supply was considered a climate-independent source for this case study, with its 5-year rolling Adelaide license of 650 GL converted to an annual license and then reduced by half to represent the southern system demand. Consequently, supply from the River Murray was capped at 65 GL per year, with a year defined as being from May 1st to April 30th. Simplifying the 5-year rolling license to an annual license was necessary due to limitations of the water supply system model. This simplification is therefore considered a conservative approach because it has the potential to underestimate water supply security. The daily pumping capacity for the MBO pipeline of 447 ML/day (see www.sawater.com.au) was also defined as a constraint in the model. Furthermore, water was only pumped from the River Murray when the volume of water in Mount Bold Reservoir dropped below the levels defined in Table 2.8 (provided that the annual cap of 65 GL had not already been reached). These levels were calibrated in WaterCress using a trial and error approach in order to provide a balance between minimising the

Table 2.8: Monthly Mount Bold reservoir levels (as a percentage of full capacity) that trigger use of River Murray supply.

Jan	Feb	Mar	Apr	May	Jun	Jul	Aug	Sep	Oct	Nov	Dec
90%	90%	90%	90%	2%	2%	2%	2%	2%	2%	80%	90%

loss of water through spillage (due to the reservoir exceeding full capacity) and maximising water supply security.

To simplify the reservoir modelling and because of the relationship between Clarendon Weir and Happy Valley Reservoir (see Section 2.2) these two storages were treated as a single reservoir and are hereafter referred to as Happy Valley Reservoir. Water was supplied from Myponga reservoir and Happy Valley reservoir (which included water from Clarendon Weir catchment, Mount Bold catchment and the River Murray) in equal priority and equal proportions, provided that water was available in each of the reservoirs. For Myponga, Mount Bold, and Happy Valley Reservoirs, evaporation and rainfall data were obtained from the same climate data stations as used for their respective catchments (see Section 2.3.1.3). Minimum volumes were taken as the physical minimum operating levels as per *Crawley* [1995] and maximum volumes were as specified by SA Water (see Section 2.2) (Table 2.9). The first of two mathematical expressions provided in WaterCress were used to describe the reservoir volume-area relationships (which enabled evaporation losses from the reservoir surface to be computed):

$$SA = aV^b \tag{2.1}$$

where SA is the surface area of the reservoir (hectare), V is the volume of the reservoir (ML) and a and b are parameters. For each reservoir, the resulting value for the volume-area relationship parameter a (Table 2.9) was determined by assuming the reservoir was at full capacity and holding the other volume-area relationship parameter b at 0.68 (the default value in WaterCress). This equation and parameter selection appeared reasonable, as when the modelled surface areas for

Table 2.9: Properties of Mount Bold, Happy Valley and Myponga reservoirs.

Reservoir	Minimum volume (GL)	Maximum volume (GL)	Volume-Area relationship parameters	
			a	b
Myponga	4.6	26.8	0.2729	0.68
Mount Bold	0.4	46.2	0.2073	0.68
Happy Valley	4.5	11.9	0.3066	0.68

Mount Bold reservoir were compared to measured values provided by *Crawley* [1995], there was generally less than 2% difference over a broad range of volumes.

2.3.3.1.2 Demand

In 2008, Adelaide's total mains water consumption, with severe water restrictions in place, was approximately 166 GL (effectively 83 GL for the southern system), with water restrictions estimated to have saved 50 GL for the whole of Adelaide [*Government of South Australia*, 2009]. However, because water restrictions have now been lifted in Adelaide, demand for the southern system was modelled at the higher rate of 108 GL for 2010. This demand was assumed to be a function of individual per capita consumption and population and both of these variables were adjusted on an annual basis over the 40-year planning horizon to constitute the demand scenario options (see Section 2.2.3.4.1).

Initial individual per capita consumption for the case study was based on the breakdown of demand between sectors in Adelaide for 2008, such that 63% was accounted for by the residential sector (with 40% of this demand attributed to outdoor use and 60% attributed to in-house use), while the remaining 37% was split between primary production, industrial, commercial and public purposes, and other [*Government of South Australia*, 2009]. Thus, total annual demands for the southern system in 2010 were assumed to be 40.8 GL for residential indoor use, 27.2 GL for residential outdoor demand, and 40.0 GL for non-residential demand. Due to Adelaide's high natural intra-

annual rainfall variability, outdoor demand in Adelaide also varies with time of year. Consequently, outdoor residential demand was varied using the percentages of ex-house usage estimated by *Barton* [2005] for Adelaide (Table 2.10).

Adelaide's population in 2010 was about 1.2 million people, so assuming the southern system demand is approximately half of Adelaide's demand (see Section 2.2) the initial population for the southern system was assumed to be approximately 600,000 people. Australia's average household size in 2001 was 2.6 people, while in 2026 this is projected to decrease to between 2.2 and 2.3 people, a reflection of the increase in single-person households [*Australian Bureau of Statistics*2008]. For simplicity in the modelling, average household size was held at a constant 2.3 people throughout the planning period.

2.3.4 Water Supply Security Scenario Analysis

2.3.4.1 Define Scenario (Select Scenario Options)

For the water supply security scenario analysis, scenario options were selected (Step 4a, Figure 2.2) in accordance with the objectives of the paper. Sixteen scenario options were defined to: (1) assess the relative magnitude of the impacts of major sources of uncertainty; and (2) identify critical points in the future for water supply security for Adelaide's southern water supply system. Average, Best and Worst cases were defined to project a likely scenario and establish likely bounds of water supply security for Adelaide's southern water supply system.

2.3.4.1.1 Scenarios to Assess the Relative Magnitudes of Major Sources of Uncertainty and Identify Critical Points in the Future for Water Supply Security for Adelaide's Southern Water Supply System

Different SRES scenarios, GCMs, and demands were considered as scenario options in the case study (Figure 2.2).

The six SRES scenarios of A1B, A1FI, A1T, A2, B1 and B2 were selected (Figure 2.2) to cover the full range of potential future development pathways defined by the IPCC. The A1B scenario explores the

Table 2.10: Monthly outdoor water use as a percentage of total annual outdoor water use [*Barton*, 2005].

Jan	Feb	Mar	Apr	May	Jun	Jul	Aug	Sep	Oct	Nov	Dec
22.9%	18.8%	14.2%	6.4%	3.0%	0.0%	0.1%	0.7%	1.4%	4.9%	10.7%	17.0%

situation of rapid economic growth and introduction of new and efficient technologies, a peak in global population at about 2050 and a balance across all energy sources, while A1FI and A1T are based on the same assumptions except in terms of technological advancement; A1FI assumes intense fossil fuel use while A1T assumes a non fossil fuel-directed future [*Intergovernmental Panel on Climate Change*, 2007]. A2 assumes a future with high population growth, slow economic growth, and gradual technological development; B1 reflects the same population outcomes as the A1 family but with quicker changes in economic structures to enable a service and information economy; while B2 represents intermediate population and economic growth with a focus on local sustainable solutions [*Intergovernmental Panel on Climate Change*, 2007].

In selecting GCMs for this case study, CSIRO's Climate Futures Framework (CFF) [*Clarke et al.*, 2011] was applied, in which plausible climates simulated by GCMs for different SRES scenarios are classified into a small set of Representative Climate Futures (RCFs) defined by, and represented by, a matrix of two climate variables [*Whetton et al.*, 2012]. Consequently, a smaller sub-set of models can be selected that covers the identified RCFs to reduce computational effort but still address the uncertainty in GCM projections. Skill-based GCM assessments are another method used to define smaller sub-sets of GCMs, but these suffer from: (1) the assumption that a good estimation of past climate correlates with a good estimation of future climate; and (2) the lack of a robust method [*Whetton et al.*, 2012], and community-agreed metric [*Perkins and Pitman*, 2009], to use when attempting to identify "best performing" models.

Before constructing the RCFs and in consultation with a CSIRO climate scientist, five GCMs were removed from the 24 available CGMs in the CFF (23 CMIP GCMs and CSIRO's Mk3.5 model) because

they did not simulate the El Niño-Southern Oscillation (ENSO) phenomenon (L. Webb, pers. comm.), which was critical because: (1) Adelaide's climate is influenced by ENSO interannual variability; and (2) natural climate variability is important for this case study. The five GCMs excluded based on their poor simulation of ENSO were INM-CM3.0, PCM, GISS-EH [*Irving et al.*, 2011], GISS-AOM and GISS-ER [*Irving et al.*, 2011; *van Oldenborgh et al.*, 2005].

The two indices used to categorise the models into RCFs for this case study were annual change in rainfall and annual change in temperature. Temperature was used as a surrogate for evaporation because: (1) there exists a 90% correlation between temperature and potential evaporation for Australia [*Whetton et al.*, 2012]; and (2) evaporation data were only available for eight of the GCMs, while temperature data were available for all 19 models.

Using these models and indices, six RCFs were defined for the Adelaide and Mount Lofty Ranges region for the A1B scenario in 2050, ranging from “warmer with little precipitation change” to “hotter and much drier”. However, only five RCFs from this matrix were represented by the seven GCMs in OzClim that: (1) were not eliminated based on poor ENSO simulation; and (2) had both rainfall and evaporation data available. Maintaining physically consistent combinations of rainfall and evaporation data was necessary in order to maximise the robustness of the impact assessment [*Clarke et al.*, 2011]. The GCMs in OzClim were CCSM3 (hereinafter CCSM), CGCM3.1(T63) (hereinafter CGCM-h), CSIRO-MK3.5 (hereinafter CSIRO), FGOALS-g1.0 (hereinafter FGOALS), MIROC3.2(hires) (hereinafter MIROC-h), MIROC3.2(medres) (hereinafter MIROC-m) and MRI-CGCM2.3.2 (hereinafter MRI). These seven GCMs did not represent the “warmer and much drier” RCF but they still represented the most and least severe RCF. Furthermore, while three of these models fell within the same RCF, they were all included in the case study, because the RCF matrix only examined annual changes to the variables, while monthly changes are analysed in the case study, which are potentially dissimilar between models.

Six demand options were investigated to cover a broad range of potential future demand scenarios (Figure 2.2), constituted from two per capita consumption projections and three population projections (Table 2.11). The first individual per capita consumption case (labelled Reduction, Table 2.11) included a reduction in per capita consumption due to the effects of permanent water conservation measures, savings due to government incentives and increasing water price, and increases in the use of water efficient technologies. By 2050, total water savings due to demand management strategies for Adelaide are expected to be 48 Litres/capita/day (Lcd) for households and 21 Lcd for other demands [*Government of South Australia*, 2009]. *Water for Good* does not differentiate the 48 Lcd savings between in-house and ex-house use; however, the preceding water security plan for Adelaide – W*aterproofing Adelaide: A Thirst for Change 2005-2025* [*Government of South Australia*, 2005], provides an estimate of the breakdown to 2025. For example, in-house measures such as low-flow showerheads, water-efficient washing machines, and dual-flush toilets are projected to account for about 37% of household savings by 2025, while permanent water conservation measures, urban consolidation, more efficient practices, and low water use vegetation are expected to contribute the remaining 63% of household savings [*Government of South Australia*, 2005]. Consequently, annual linear (i.e. non-compounded) percentage decreases were applied to per capita consumption over the 40-year planning horizon to account for demand management savings; residential indoor use was reduced by 0.237% per annum, residential outdoor demand was reduced by 0.606% per annum, while non-residential demand was reduced by 0.281% per annum. The second case (labelled "Constant", Table 2.11) reflected the possibility that no savings in individual per capita consumption would be made over the planning horizon, such that individual per capita consumptions remained constant over the planning horizon at 187 Lcd for residential indoor demand, 124 Lcd for residential outdoor demand, and 183 Lcd for non-residential demand. The impacts of climate change on demand have not been investigated in this study because future projections are not available for Adelaide. Furthermore, while demand is affected by weather and climate factors [*House-Peters and Chang,* 2011], it is also a response to the complex interaction of

Table 2.11: Demand Scenario Options.

Demand Scenario	Per capita consumption	Population
Very Low	Reduction	Small
Low	Constant	Small
Medium-Low	Reduction	Medium
Medium-High	Constant	Medium
High	Reduction	Large
Very High	Constant	Large

multiple variables, including economic and social factors (e.g. water pricing); consequently, projecting the impacts of climate change on demand is not as straightforward as simply correlating demand to climate variables. However, the "constant" variation defined above can be considered a very conservative approach to demand projection and thus does not only reflect the possibility of "no savings" but could represent the possibility of making some savings (which is highly likely) in combination with increasing demand due to climate change.

Taking into account fertility, mortality, net interstate migration, and net overseas migration rates, the Australian Bureau of Statistics' (ABS) median population projection (from 72 population projections) for Adelaide in 2050 is approximately 1.56 million people [*Australian Bureau of Statistics*, 2008]. Therefore, the first population case (labelled "Medium", Table 2.11) applied a linear (i.e. non-compounded) percentage increase of 0.736% per year to the southern system population. Two additional population options (labelled "Small" and "Large", Table 2.11) were also defined to investigate futures with small and large populations. Consequently, the 5^{th} and 95^{th} percentile values of the 72 population projections made by the ABS for Adelaide were used, corresponding to annual linear percentage changes of -0.680% (Small) and 1.579% (Large), respectively. The resulting demand

scenarios formulated from combinations of the two per capita consumption cases and the three options for population are labelled Very Low, Low, Medium-Low, Medium-High, High and Very High (Table 2.11).

A "Base case", from which to compare the scenario options, was defined as a combination of the A1B SRES scenario, the FGOALS GCM, and the Medium-Low demand scenario (Base case, Table2.12). As no likelihoods have been assigned to the SRES scenarios [*Intergovernmental Panel on Climate Change*, 2007], the A1B SRES scenario was selected for the Base case as it represents a A caveat of this study is that rainfall and evaporation datasets derived from different downscaling methods are not available and thus the impact of the downscaling model on supply reliability could not be tested as a source of uncertainty. However, in previous studies of the impact of climate change on runoff, downscaling models were shown to contribute less uncertainty than GCMs [*Boé et al.*, 2009; *Chen et al.*, 2011a; *Chen et al.*, 2011b; *Mpelasoka and Chiew*, 2009; *Wilby and Harris*, 2006], less uncertainty than SRES scenarios [*Chen et al.*, 2011a; *Chen et al.*, 2011b], and less uncertainty than GCM initial conditions [*Chen et al.*, 2011b] (see Section 2.1). Direct comparisons of downscaling approaches are also difficult to achieve because they use different spatial domains, predictor variables, predictands, and assessment criteria [*Fowler et al.* 2007]. GCM initial conditions were not examined in the case study because: (1) the authors did not run the GCMs; and (2) the data sourced from OzClim did not include multiple ensemble runs.

Different RRO models and their parameters were also not tested in the case study because *Chiew et al.* [2009a] illustrated that RRO models exhibited less uncertainty in determining the impacts of climate change on runoff than GCMs; *Chen et al.* [2011b] illustrated that in estimating runoff under climate change impacts, hydrological models and hydrological model parameters contributed less uncertainty than GCMs, GCM initial conditions and GHG emissions scenarios; while *Wilby and Harris* [2006] showed hydrological models and their parameters contributed less uncertainty in estimating

Table 2.12: Scenario options defined for the case study of Adelaide's southern water supply system.

Scenario Options		Scenario ID																		
		Base case	1	2	3	4	5	6	7	8	9	10	11	12	13	14	15	16	Best Case	Worst Case
SRES Scenario	A1B	x						x	x	x	x	x	x	x	x	x	x	x		
	A1FI		x																	x
	A1T			x																
	A2				x															
	B1					x													x	
	B2						x													
GCM	FGOALS	x	x	x	x	x	x							x	x	x	x	x		
	CCSM							x												
	CGCM-h								x										x	
	CSIRO									x										x
	MIROC-h										x									
	MIROC-m											x								
	MRI												x							
Demand	Medium-High	x	x	x	x	x	x	x	x	x	x	x	x							
	Very Low													x					x	
	Low														x					
	Medium-Low															x				
	High																x			
	Very High																	x		x

runoff under climate change impacts than GCMs (see Section 2.1). However, *Wilby and Harris* [2006] did show that hydrological models and their parameters contributed more uncertainty to estimating runoff under climate change impacts than SRES scenarios, so this study is limited in that it only assesses one RRO model and one set of RRO model parameters.

It should be noted that the relatively insensitive responses of runoff to the downscaling model and the choice of RRO model and parameters, compared to other sources of uncertainty, cannot necessarily be generalised to other cases. However, a water supply manager with limited resources for impact assessments must make some assumptions as to the importance of uncertainty sources based on previous case studies to ensure effort is directed towards the greatest expected sources of uncertainty.

2.3.4.1.2 Scenarios to project ranges of water supply security for Adelaide's southern water supply system

To project the likely range of the impact of climate change on water supply security for Adelaide's southern water supply system (and thus address the third objective of this paper), Best and Worst cases were defined, with scenario options only selected from those detailed in Section 2.3.4.1.1. For the Best case the Very Low demand scenario was selected, while for the Worst case the Very High demand scenario was selected (Table 2.12). However, it was not so clear which SRES scenario and GCM would be associated with the lowest and highest water supply securities. Consequently, the SRES scenarios and GCMs for the Best and Worst cases were selected after the Base case and scenarios 1-11 (Table 2.12) were run and analysed. Following this analysis (Section 2.4.1), B1 was found to return the highest water supply security and thus was selected for the Best case (Table 2.12), while choosing A1FI resulted in the lowest water supply security at the end of the planning horizon, so it was selected for the Worst case (Table 2.12). Similarly for the GCMs, CGCM-h was selected for the Best case because it returned the highest reliability in 2050, while CSIRO was selected for the Worst case as it corresponded to the smallest reliability for all years (Table 2.12).

The results for these Best and Worst cases were discussed in reference to those obtained for an 'Average' case, which for this case study was defined as Scenario 6 (Table 2.12). The Average case was different to the Base case, because the Base case was comprised of a combination of the most likely projections, or when there was no understanding of their likelihood of occurrence, median projections were used (e.g. for population growth). Consequently, while the A1B scenario and Medium-Low demand scenarios were appropriate to use for both the Base case and Average case (see Figures 3, 6 and 7), CCSM provided reliabilities that were closer to representing the average for the GCM scenarios than FGOALS, which was used for the Base case (see Figures 4 and 5).

2.3.4.2 Run Water Supply System Model and Compute Water Supply System Security

The scenarios listed in Table 2.12 were run through the WaterCress model (Step 4b, Figure 2.2) for each of the 1000 stochastic rainfall time series for 2020, 2030, 2040 and 2050. Water supply system security, represented by reliability calculated on a daily time step for the case study, was then determined for each scenario (Step 4c, Figure 2.2). Reliability was selected to represent water supply system security for the case study because it provides information as to the proportion of time spent in failure, an important factor in understanding water supply security.

Reliability for each of the future years is defined as:

$$R_{yi} = \frac{T_{syi}}{T_{tyi}} \tag{2.2}$$

where R_{yi} is the reliability for stochastic time series i (i=1-1000) for year y (y=2010, 2020, 2030, 2040 or 2050), T_{syi} is the total number of days that available supply exceeds demand for stochastic time series i and year y and T_{tyi} is the total number of days for stochastic time series i and year y. For each year and for each of the 1000 stochastic rainfall time series (developed in Step 2e of Figure 2.2), the model was run and reliability was computed (Equation 2.2), such that for each scenario, 1000 different reliabilities were calculated. Consequently, reliability could be presented as a probability

(based on the 1000 stochastic rainfall time series), rather than a deterministic value. This meant that uncertainties in natural rainfall variability, expressed by the probabilities of reliability for each scenario, could be analysed and compared to the uncertainties in selecting SRES scenarios, GCMs and demand.

From a planning perspective, it is also important to understand how reliability changes through time so that additional supply or demand management schemes can be sequenced to come on line when they are required to raise reliability to an acceptable level (see Section 2.1). Consequently, changes in reliability between years over the planning horizon were also analysed by linear interpolation.

2.4 Results and Discussion

The analysis of reliability in Section 2.4.1 addresses the first objective of this paper, which is to understand the relative magnitudes of major sources of uncertainty when analysing the impacts of climate change on water supply security. It is important to note that the cumulative distribution functions (cdfs) presented herein purely reflect the stochastic nature of the natural rainfall variability, rather than any other systematic uncertainty. Changes in reliability over the planning horizon are then analysed in Section 2.4.2 in order to illustrate future critical points in time for water supply security and thereby address the second objective of the paper. Finally, Section 2.4.3 examines the Best and Worst cases to understand water supply security ranges projected for Adelaide's southern system, thus satisfying the third objective of the paper. The Base case and scenarios 1-16 (Table 2.12) are analysed in Sections 2.4.1 and 2.4.2, while the Average, Best and Worst cases are analysed in Section 2.4.3.

2.4.1 Relative Magnitudes of Sources of Uncertainty

In this section, the cdfs of the 1000 stochastic rainfall time series are illustrated for each of the 16 scenarios (Table 2.12) for 2020 and 2050 (Figures 2.3-2.7); for 2030 and 2040, median reliability values are illustrated in Figures 2.8-2.10 and 0.05 and 0.95 probabilities of exceedance values summarised in Table 2.13; while the cdf for natural rainfall variability for 2010 is illustrated in Figure

2.11. Cdfs of natural rainfall variability for the 16 scenarios for 2030 and 2040 are not illustrated, as the patterns were similar to those for 2020 and 2050 and the differences could be well illustrated in Table 2.13. Furthermore, the following discussion focuses on the median or 50th percentile values representing natural rainfall variability because the patterns between the scenarios are similar for all percentiles.

The cdfs of reliability based on the 1000 stochastic rainfall time series of Adelaide's southern water supply system for different SRES scenarios for 2020 and 2050 are shown in Figure 2.3. For the Base case, the difference in median reliability across the SRES scenarios was 0.4% in 2020, which by 2050 had increased progressively to 2.0% (Figure 2.3 and Table 2.14). The order of SRES scenarios in terms of impact on reliability changed depending on the future year (Figure 2.3, Table 2.13). By 2050, A1B returned greater reliabilities than A1FI and A1T, but smaller reliabilities than A2, B2 and B1 (Figure 2.3). While it was expected that B1 and B2 would produce more favourable reliabilities due to their more moderate development pathways (see Section 2.3.4.1.1), it was not intuitive that A1T would produce the lowest reliabilities for 2020 and 2030, and the second lowest reliabilities in 2040 and 2050, because it represents the least fossil-fuel intensive pathway of the A1 family (see Section2.3.4.1.1). However, this can be explained by examining the impacts of the development pathways in terms of changes to precipitation (sourced from OzClim for the FGOALS GCM) up until the end of the 21st century. A1FI has a greater impact on precipitation than A1T from 2040 onwards, while A1B has a greater impact on precipitation than A1T from 2080 onwards. Consequently, although by the end of the 21st century the impact on water supply security of A1FI and A1B should be greater than that of A1T, it did not occur for this case study due to the timeframe only extending to 2050.

The cdfs of reliability (representing stochastic uncertainty in rainfall) of Adelaide's southern water supply system for different GCMs for 2020 and 2050 are illustrated in Figures 2.4 and 2.5, respectively. The difference in reliability across the GCMs was approximately twenty times that for

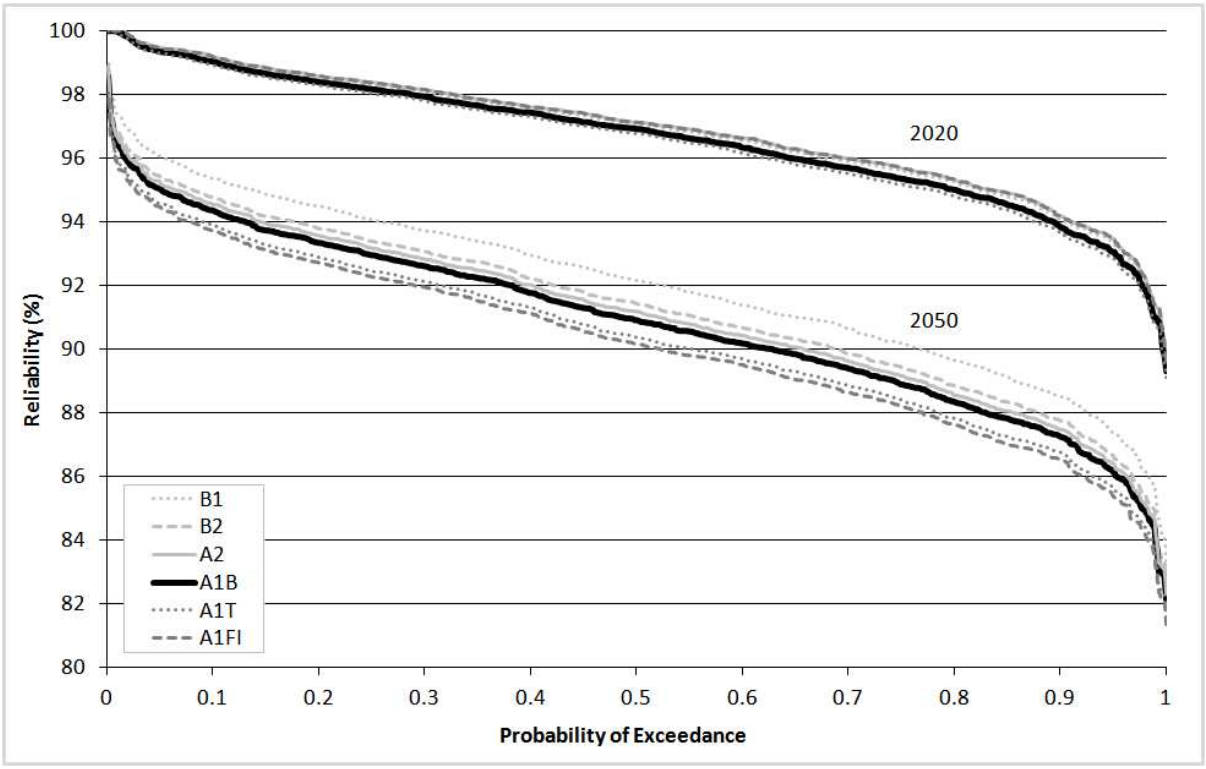

Figure 2.3: Cumulative distribution function (cdf) of reliability (based on 1000 stochastic rainfall time series) of Adelaide's southern water supply system for different SRES scenarios for 2020 and 2050.

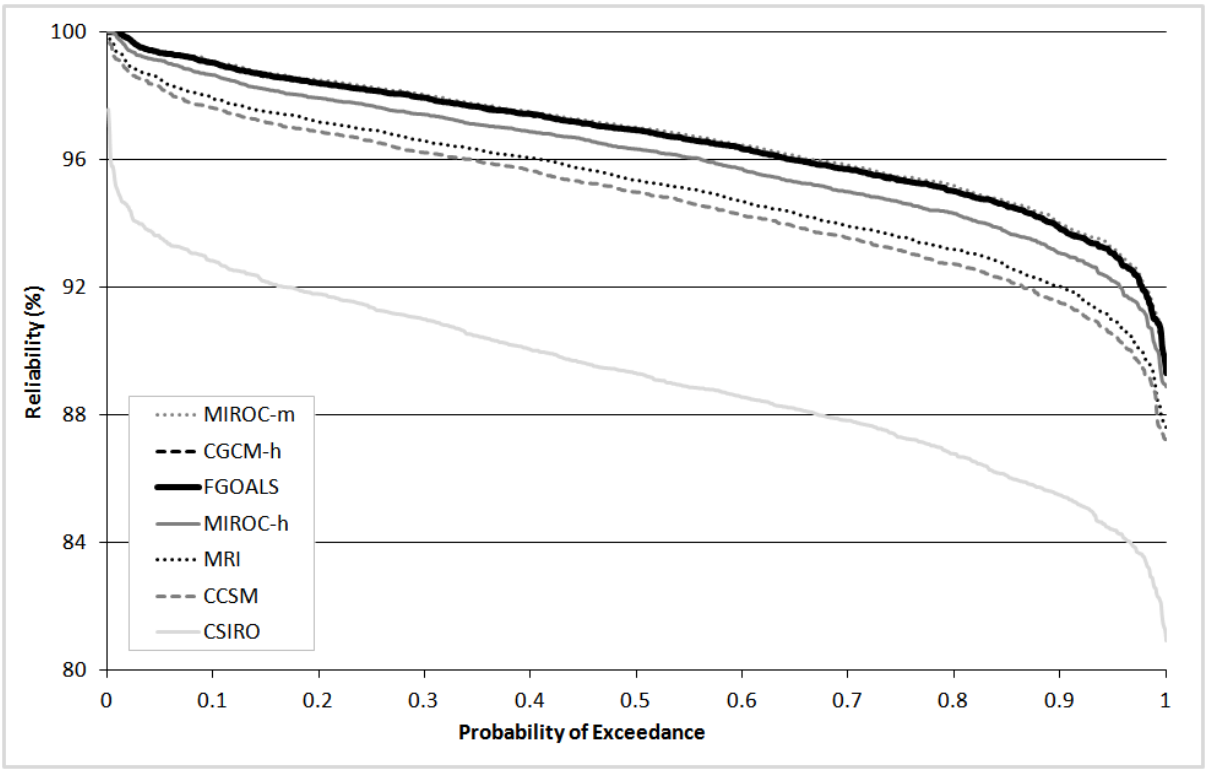

Figure 2.4: Cdf of reliability (based on 1000 stochastic rainfall time series) of Adelaide's southern water supply system for different GCMs for 2020.

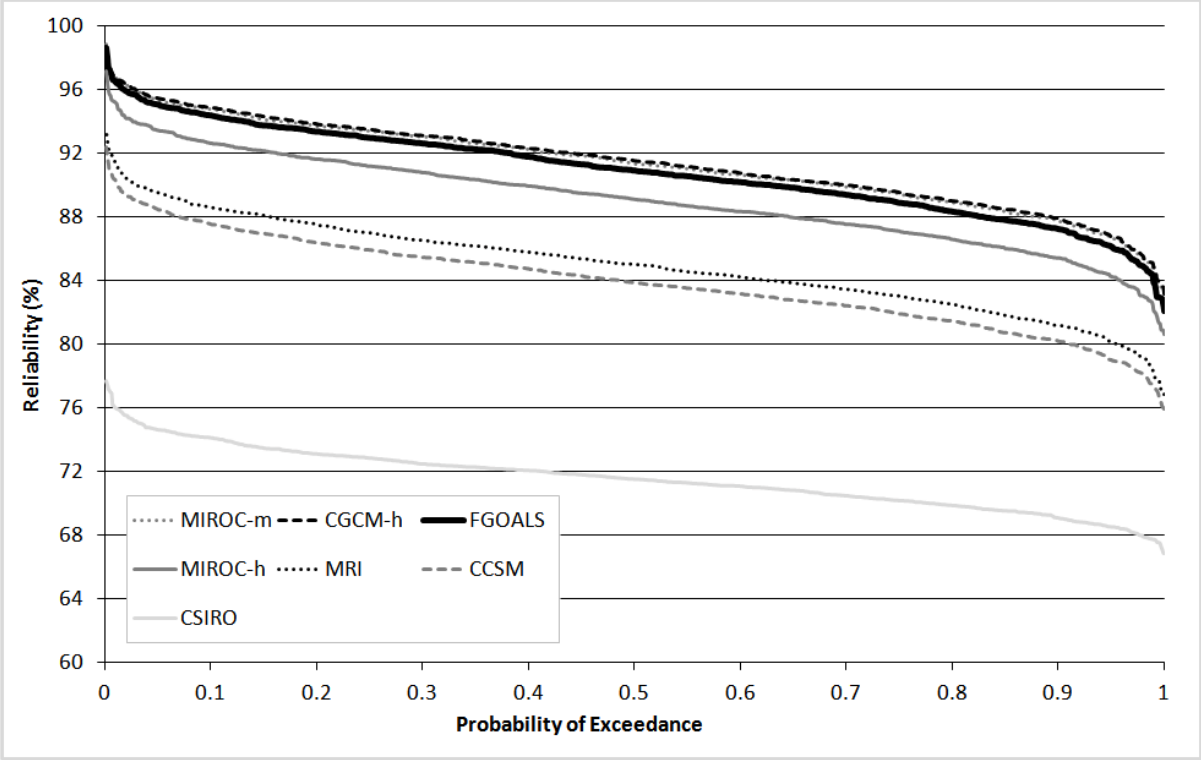

Figure 2.5: Cdf of reliability (based on 1000 stochastic rainfall time series) of Adelaide's southern water supply system for different GCMs for 2050.

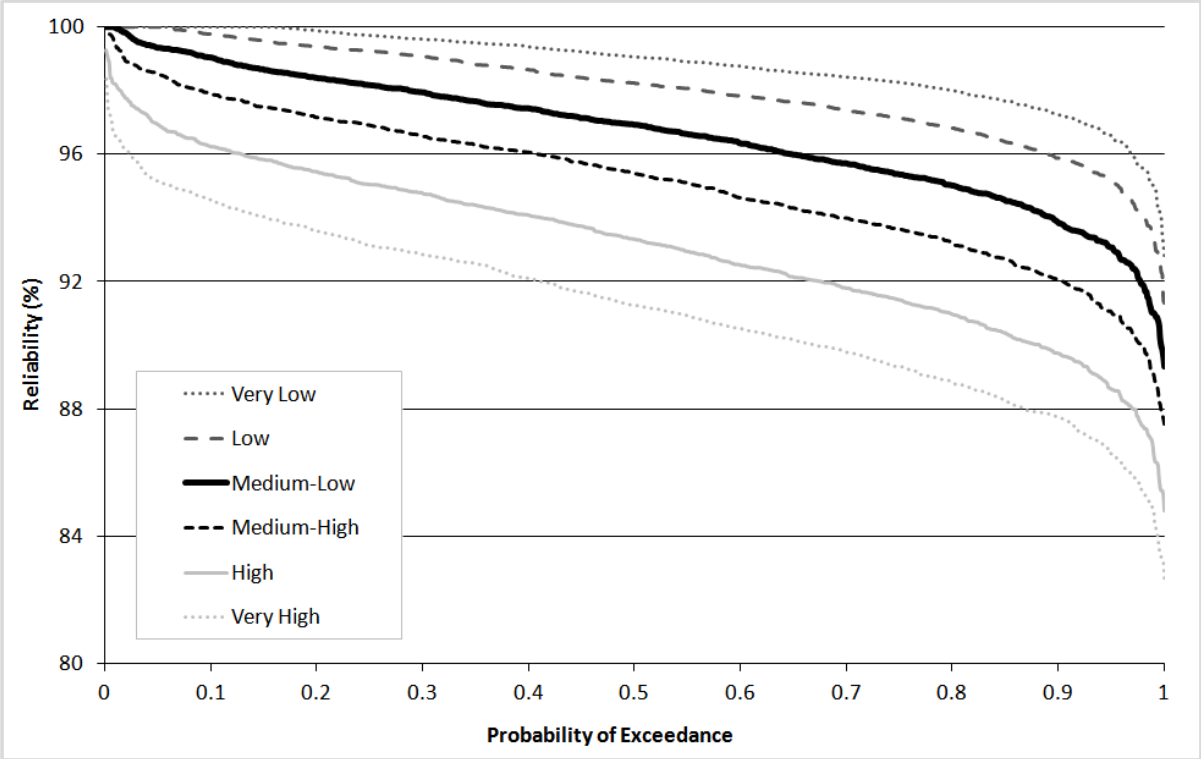

Figure 2.6: Cdf of reliability (based on 1000 stochastic rainfall time series) of Adelaide's southern water supply system for different demands for 2020.

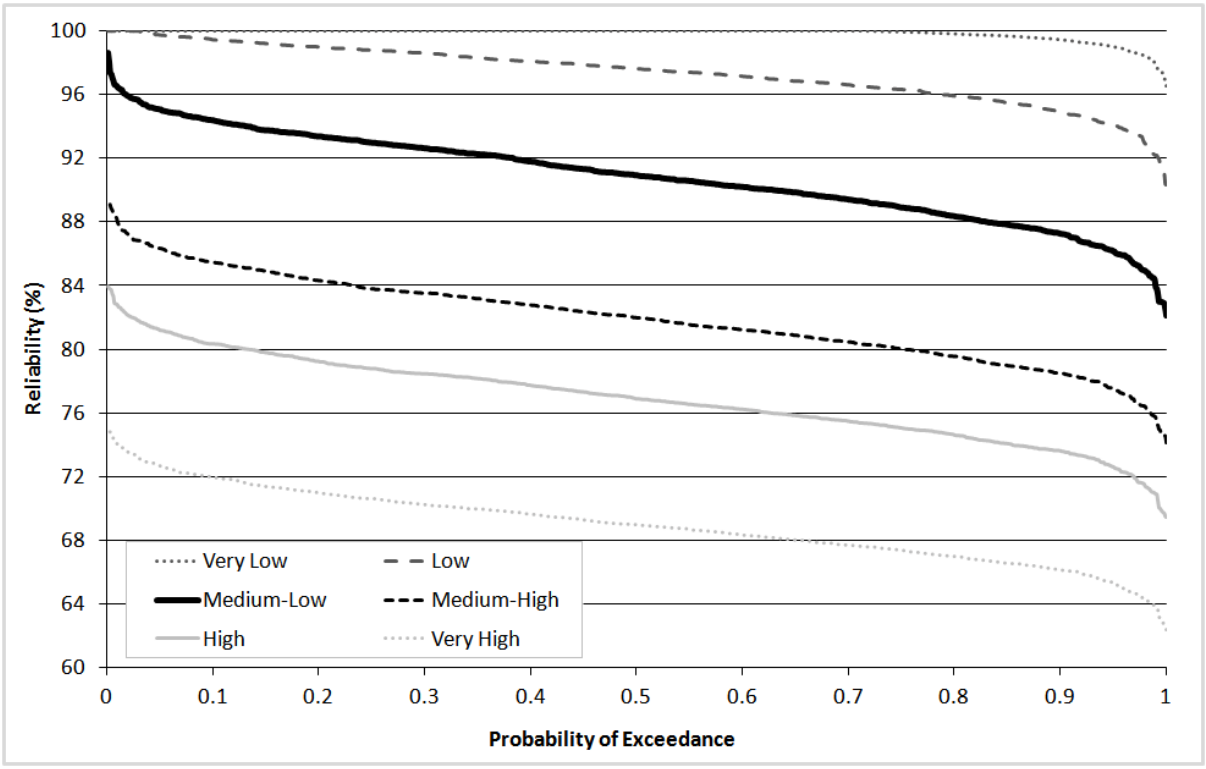

Figure 2.7: Cdf of reliability (based on 1000 stochastic rainfall time series) of Adelaide's southern water supply system for different demands for 2050.

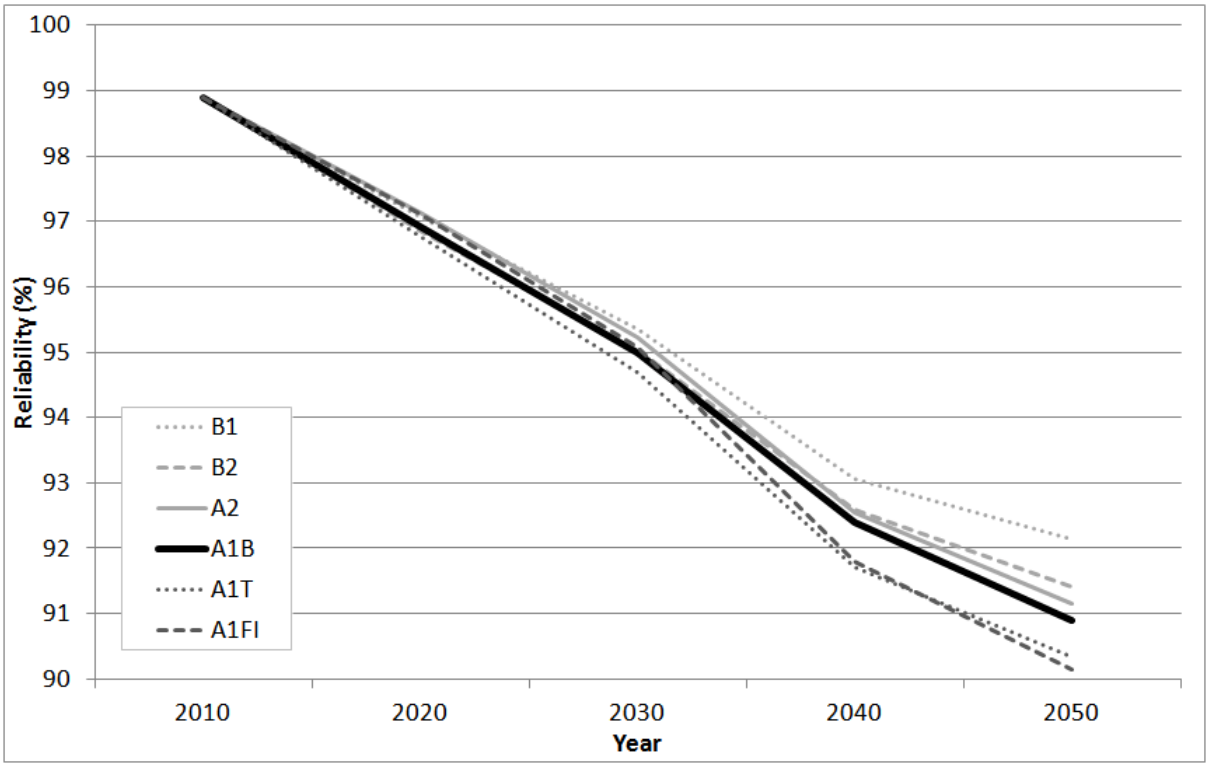

Figure 2.8: Change in median reliability over the planning horizon of Adelaide's southern water supply system for different SRES scenarios.

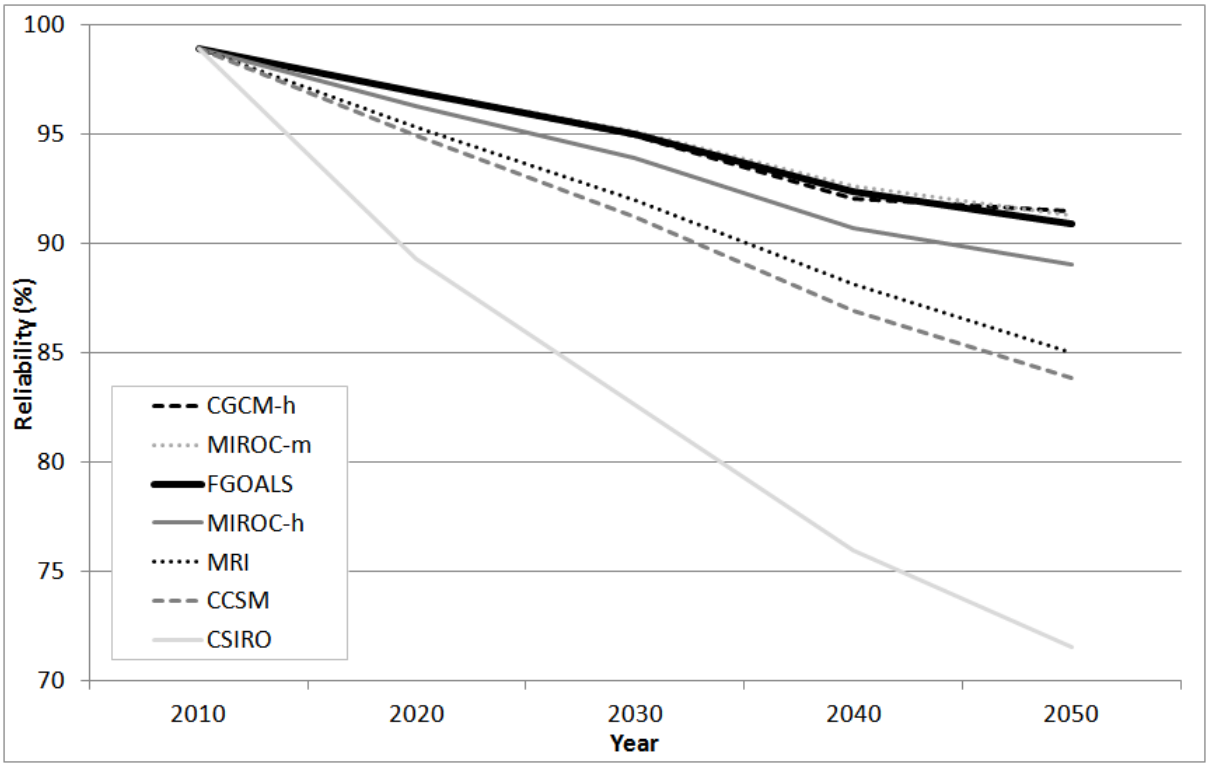

Figure 2.9: Change in median reliability over the planning horizon of Adelaide's southern water supply system for different GCMs.

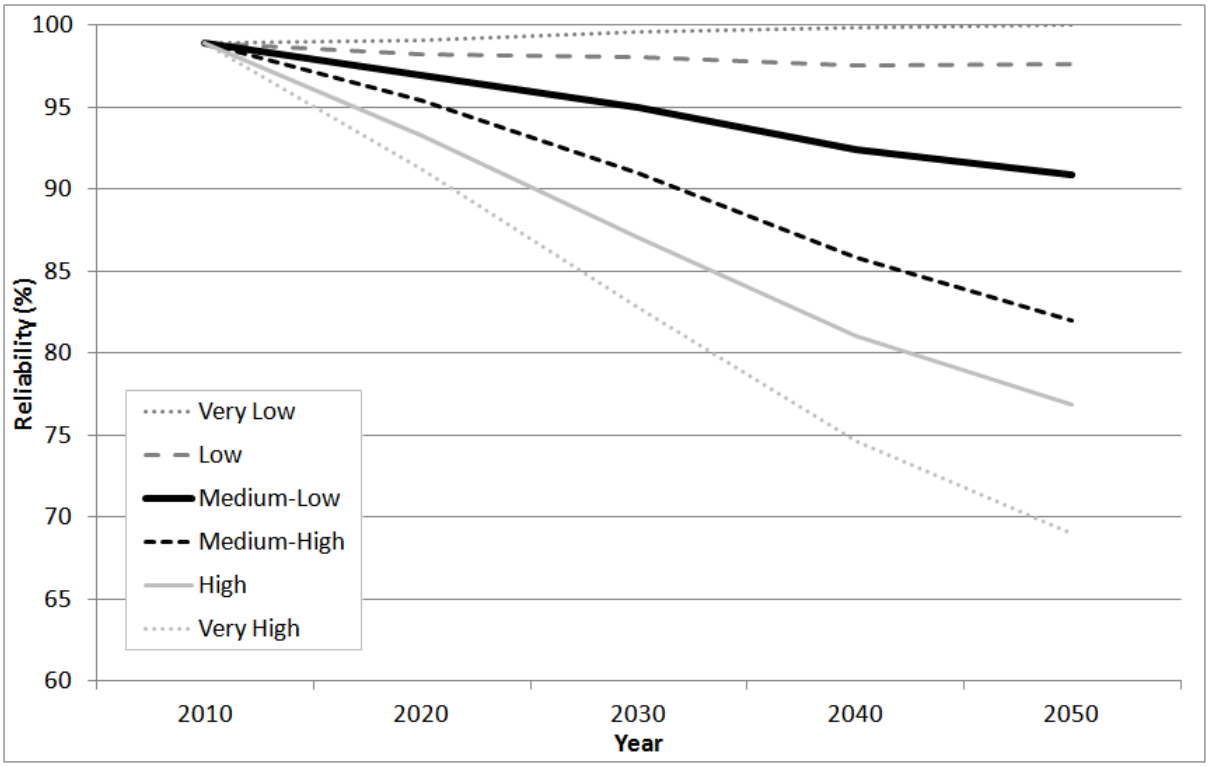

Figure 2.10: Change in median reliability over the planning horizon of Adelaide's southern water supply system for different demands.

Table 2.13: Probability of Exceedance summary for reliability for years 2030 and 2040 for each of the 16 scenarios detailed in Table 2.12

Uncertainty source	Year	2030		2040	
	Probability of Exceedance	0.05	0.95	0.05	0.95
SRES scenario	B1	98.5	91.0	96.8	88.3
	B2	98.3	90.5	96.4	87.8
	A2	98.4	90.8	96.4	87.8
	A1B	98.3	90.5	96.2	87.6
	A1T	98.0	90.2	95.7	86.8
	A1FI	98.3	90.6	95.7	86.9
GCM	MIROC-m	98.3	90.7	96.4	87.9
	FGOALS	98.3	90.5	96.2	87.6
	CGCM-h	98.2	90.4	95.9	87.3
	MIROC-h	97.5	89.3	94.7	85.9
	MRI	96.0	87.4	92.6	83.2
	CCSM	95.3	86.3	91.4	81.9
	CSIRO	87.1	78.1	79.7	72.3
Demand	Very Low	100.0	97.5	100.0	98.2
	Low	100.0	94.8	99.7	94.0
	Medium-Low	98.3	90.5	96.2	87.6
	Medium-High	94.9	86.2	90.3	81.3
	High	91.5	82.4	85.4	76.5
	Very High	87.2	78.3	78.8	70.7

Table 2.14: Range in median reliability caused by uncertainty in SRES scenario, GCM and demand for 2020, 2030, 2040 and 2050 for each of the 16 scenarios in Table 2.12.

Year	Uncertainty Source		
	SRES scenario	GCM	Demand
2020	0.4	7.7	7.8
2030	0.6	12.5	16.8
2040	1.4	16.6	25.2
2050	2.0	20.0	31.0

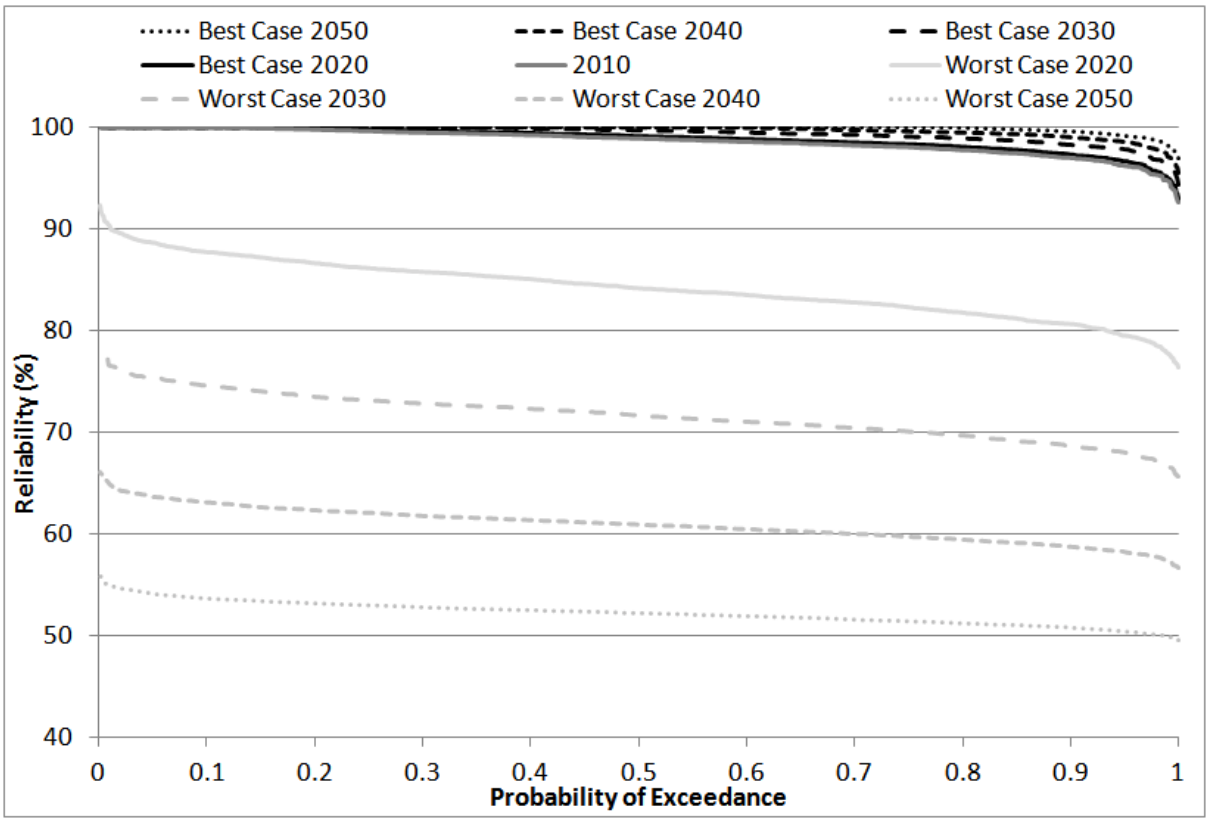

Figure 2.11: Cdf of reliability (based on 1000 stochastic rainfall time series) of Adelaide's southern water supply system for 2010 and for the Best and Worst Cases for 2020, 2030, 2040 and 2050.

the SRES scenarios in 2020, decreasing progressively to ten times by 2050 (Figures 2.4 and 2.5). The lowest median reliability in 2050 was 71.5% under CSIRO (Figure 2.5). This was expected because the CSIRO GCM resulted in the greatest overall decrease in annual rainfall (23% reduction by 2050) compared to the other GCMs. Lower rainfall translated to Mount Bold storage levels being lower for longer periods, thus requiring water to be pumped from the River Murray for more days of the year, such that the annual River Murray license was used up earlier in the year and there were, therefore, more days of failure. MIROC-m and CGCM-h resulted in the greatest median reliabilities of 91.3% and 91.5% in 2050, respectively, which was expected considering these two GCMs resulted in very slight annual rainfall increases of 0.7% and 0.5% by 2050, respectively. Interestingly though, FGOALS with a 5.3% annual reduction in rainfall by 2050 only resulted in a slightly smaller median reliability of 90.9%, even though a similar reduction in annual rainfall was exhibited by CCSM (6.6% reduction by 2050), which returned reliabilities approximately 7% smaller than FGOALS (Figure 2.5). CCSM actually projected a smaller decrease in annual rainfall than MIROC-h (7.3%) and MRI (7.4%) but still

returned a lower reliability. Furthermore, the similarity in annual rainfall reduction between MIROC-h and MRI was not translated into reliability with an approximate 4% difference between the two by 2050. These differences in the reliability patterns appear to be the result of differences in rainfall distribution over the year. Furthermore, these results illustrate both the complexity of studying the impacts of climate change on Adelaide's water supply security, and the importance of considering seasonal variations for climate change scenarios.

The cdfs of reliability based on natural rainfall variability of Adelaide's southern water supply system for different demand scenarios for 2020 and 2050 are shown in Figures 2.6 and 2.7, respectively. In a similar way to the SRES scenarios and GCMs, the range of water supply security increased with time across demand scenarios, so by 2050 reliability ranged from 69.0% for the Very High demand scenario to 100% for the Very Low scenario (Figure 2.7). Thus, the range in median AAR of 31.0% across the demand scenarios was more than one and a half times that obtained across the seven GCMs and more than fifteen times that observed for the six SRES scenarios. The changes in reliability for each of the demand scenarios were to be expected, such that an increasing demand (due to a greater population and/or less water savings) resulted in a lower reliability (Figures 2.6 and 2.7).

The six cdfs of natural climate variability (Figures 3-7) illustrate that reliability noticeably changed depending upon the particular stochastic rainfall time series. For example, for the Base case, the difference between the minimum and maximum reliabilities was 10.7% in 2020, 12.9% in 2030, 15.5% in 2040 and 16.5% in 2050. This meant that demand uncertainty was always greater and SRES uncertainty always smaller than uncertainty due to natural rainfall variability, but compared to GCM uncertainty it was dependent on the future year; for 2020 and 2030 inherent natural rainfall variability created more uncertainty than GCMs, for 2040 the uncertainties were almost identical, and by 2050 GCMs were the second greatest source of uncertainty (Table 2.14). However, the extremely low probabilities of exceedance for reliability correspond to extremely large return periods (e.g. the maximum probability of exceedance is equivalent to a 1 in 1000 year event), so

these events are very unlikely. While this may appear to lessen the significance of the impact of natural rainfall variability, a 1 in 1000 year event is still possible. Secondly, as the probability of occurrence is unknown for each of the scenarios listed in Table 2.12, these scenarios could also be as unlikely to occur as a 1 in 1000 year event. Furthermore, when considering all scenarios in Table 2.12, natural rainfall variability can only cause up to 16-17% variability at any of the years. This is because the greatest variation occurs when reliability ranges from 78-95% and this does not always occur for the Base case. This pattern is believed to be a function of the large River Murray supply (65 GL/yr) that is, in this case study, unaffected by natural rainfall variability. In other words, when reliability is low (<78-95%), the River Murray dominates supply, so natural variability in reservoir supply (reflecting natural rainfall variability) is dampened out by the climate-independent River Murray supply. However, when less River Murray supply is required, greater natural rainfall variability is expressed in the reliability, through reservoir supply. At very high reliabilities, the natural rainfall variability has less effect because there are fewer failures.

2.4.1.1 Summary of Relative Magnitude of Uncertainty Sources

For this case study, uncertainty source significance was dependent on the future year; however, demand was always the greatest source of uncertainty on water supply security and SRES scenario the least. Natural rainfall variability was second only to demand for the first half of the planning horizon, essentially equal to GCM uncertainty by 2040 and then of less importance than GCM choice by 2050. However, it is important to also remember, that while the synthetic rainfall data are believed to be representative of the historical 30-year time series they were derived from (Section 2.3.2.6), this short time period may not reflect the real natural rainfall variability over a 100-year period. Therefore, natural rainfall variability could be underestimated in this analysis and could be an even greater source of uncertainty than determined here. These findings indicate that, in analysing the uncertainties of the impact of climate change on water supply systems, demand uncertainties, and natural rainfall variability, should not be excluded, as these can be greater sources of uncertainty than those associated with climate change modelling. They also illustrate the

importance of analysing changes in reliability progressively through time, such that if a longer planning horizon is selected, more effort can be directed to characterizing uncertainty of supply security due to demand and GCMs, while a shorter time period would suggest focus be directed on natural rainfall variability, as well as demand uncertainty.

In terms of management implications, demand uncertainty could be reduced in the future by the water authority if they could control per capita consumption through demand management schemes and, while outside the scope of most water authorities, climate scientists working towards improving GCMs may also be able to reduce uncertainties associated with these model outputs. Of comfort to water authorities is the knowledge that the impact of SRES scenarios, in which uncertainty is irreducible, was minor compared to the other sources of uncertainty. Similarly, the planning of supply systems under demand uncertainty and natural rainfall variability is traditional for water authorities, so it is encouraging that these two sources were discovered to be the dominant sources of uncertainty, at least in the short-term.

2.4.2 Identifying Critical Points in Time for Water Supply Security

Changes in median reliability of Adelaide's southern water supply system for different SRES scenarios are shown in Figure 2.8, while changes in median reliability for different GCMs are shown in Figure 2.9 and changes in median reliability for different demands are shown in Figure 2.10. Median reliability for the Base case decreased from 98.9% in 2010 to 90.9% in 2050 (Figure 2.8), which was expected due to population growth and the increasingly adverse impacts of climate change. However, there was a good degree of variability in the trajectories of supply reliability over the planning horizon (Figures 2.8-2.10).

As mentioned in Section 2.1, understanding these changes in reliability with time, and their associated uncertainties, is important from a planning perspective, as additional supply sources or demand management schemes could be sequenced to come online when they are required to maintain reliability at an acceptable level. However, defining what an acceptable level is for

reliability is subjective. While 100% reliability is desirable, when considering other objectives such as cost, water planners may accept a lower reliability for economic gain or accept the need for temporary water restrictions or other demand management actions. For example, if water supply planners accepted reliability levels in excess of 95%, then most of the 16 scenarios analysed would at some stage over the planning horizon require supply to be increased or demand reduced. While this would occur around 2030 for the SRES scenarios (Figure 2.8); for the GCM scenarios water supply security would be threatened between 2015 to 2030 (Figure 2.9); while for the demand scenarios, supply augmentation or demand mitigation would be required between 2015 to 2030 or not at all (Figure 2.10).

While the order of median reliability remained constant with time when comparing the different demand scenarios, the order of median reliability for the SRES scenarios and GCM scenarios changed slightly depending on the year (Figures 2.8 and 2.10). For example, A1FI resulted in a sharper decline in median reliability over the planning horizon than the other SRES scenarios, but this decline only accelerated after 2030 (Figure 2.8). Hence, the order of the impact of SRES scenarios and GCMs on water supply security is dependent on the year, which again highlights the importance of considering the temporal dimension when analyzing the impacts of climate change on water supply security.

Over the planning horizon, the uncertainty in median reliability increased (Figures 2.8-2.10). While reliabilities were similar at the beginning of the planning horizon, the lowest median reliability for 2050 was 69.0% for the Very High demand scenario, while the greatest median reliability was 100% for the Very Low demand scenario (Figure 2.10). Furthermore, differences in median reliability caused by the different sources of epistemic uncertainty were in agreement with the order of the magnitude of uncertainty sources defined in Section 2.4.1 (without natural rainfall variability). A number of planning options, including the addition of alternative sources or demand management schemes could reduce this window of uncertainty in terms of water supply security; however, should the very low demand scenario ensue, then there would be a level of regret (for example unnecessary

economic expenditure) associated with the selected option. Consequently, the findings illustrate that continual reassessment of planning may be necessary to ensure maximum reliability with minimal regret.

2.4.3 Water Supply Security Ranges

For the Best case, Adelaide's southern supply system had slightly greater reliability in 2050 than in 2010, which progressively increased with time over the planning horizon (Figure 2.11). While counter-intuitive, this increase in reliability over time is caused by the very low demand scenario, which corresponds to a slight decrease in population and decreasing per capita consumption over the planning horizon (see Section 2.3.4.1.1). If the Best case ensued and water supply planners accepted reliability levels greater than 95%, then there is only a very slight probability that the supply system will not quite reach the target reliability in 2020 and 2030 due to natural rainfall variability, while for 2040 and 2050 it will always be met (Figure 2.11). In stark contrast, the Worst case has reliabilities that decreased with time over the planning horizon and by 2050, for all stochastic rainfall time series, reliability was less than 56% (Figure 2.11). If 95% is considered the reliability threshold by the water authority and the Worst case was to occur, then as early as 2020, the system would exhibit failures, regardless of natural rainfall variability. This stark contrast between the Best and Worst cases was expected, due to selecting SRES scenarios, GCMs and demands that corresponded to the best and worst outcomes for reliability, respectively. As mentioned in Section 2.4.2, the increasing uncertainty envelope with time was also expected, as projections made for the more distant future are less certain than those for the near future.

The Best and Worst cases are both extreme cases, and have low probabilities of occurrence. To place them in perspective, the Average case was analysed, which had a median reliability of 84% by 2050 (Figure 2.5), considerably smaller than the Best case (100%), and much greater than the Worst case (52%). However, while the Best and Worst cases are unlikely to occur, they do provide water authorities with the likely upper bound on the range of water supply security up to 2050. If some

uncertainties can be reduced, which is likely in the future with projected improvements to GCM model accuracy and potential demand management actions implemented by the water authority, then the overall uncertainty envelope will also be reduced. If the uncertainties are irreducible though, then the water authority must consider adaptation options that are extremely flexible, so as not to regret adaptation responses nor jeopardise water supply security. For example, if plans were made based on findings from the Worst case to ensure maximum water supply security and should the Best case occur, there would be a relatively high level of regret (such as unnecessary economic expenditure) associated with the selected option.

These results from the Best and Worst cases also illustrate that the multiplicative impacts of epistemic uncertainty sources on supply reliability lessen the importance of natural rainfall variability. However, these cases are firstly not likely to occur and secondly, while the stochastic time series were found to preserve the important characteristics of the historical rainfall time series (Section 2.3.2.6), the short 30-year historical rainfall time series may not have included the entire range of possible natural rainfall events, and so natural rainfall variability may be underestimated.

2.5 Summary and Conclusions

Previous studies that have compared the magnitude of uncertainty sources associated with climate change impacts on water resources have largely focused on runoff. However, because of the non-linear translation of runoff to water supply (due to a number of complexities in modelling water supply systems including the incorporation of demand and storages), there is a need to understand the importance of major uncertainty sources for climate change impacts on water supply security. Understanding the major sources of uncertainty and whether they are reducible or not, will help water authorities to focus efforts towards reducing uncertainty where possible, or to develop strategies to cope with the uncertainties if they are irreducible. Furthermore, from a planning perspective it is also important to understand changes in water supply security with time, and their associated uncertainties, so that additional supply sources or demand management schemes can be

sequenced to come on line when they are required to raise water supply security to an acceptable level. This paper presents a scenario-based sensitivity approach for analysing the impacts of climate change on water supply security tailored to the case study of Adelaide's southern water supply system. The methodology developed ensured that the three objectives of this paper were met, these being that: (1) relative magnitudes of major sources of uncertainty on water supply security were assessed; (2) changes in water supply security through time were traced; and (3) water supply security ranges were established. Three major sources of systematic uncertainty – SRES scenarios, GCMs, and demand – were compared in the case study, as well as stochastic natural climate variability.

In the earlier half of the adopted planning horizon of 2010 to 2050, the level of demand created the most uncertainty in water supply security, followed by natural rainfall variability, GCM, and lastly SRES scenario. By the later stages of the planning horizon though, GCMs created more uncertainty in reliability than natural rainfall variability. This suggests that, for studies analysing the impacts of climate change on water supply security, uncertainties other than those associated with climate change and hydrological modelling should in fact be considered as they could have as great, or greater, impacts on water supply security projections. Furthermore, in the short-term, efforts by water authorities should be directed towards demand and natural rainfall variability, but that for longer-term plans, uncertainties in GCMs should be analysed.

The case study also illustrated that reliability generally decreased over the planning horizon, a result of increasing demands and decreasing rainfall under climate change. From a local policy perspective, the projected reduction in system reliability realised in this analysis of Adelaide's southern system justifies: (1) the production of flexible plans to ensure the security of Adelaide's future water supply; and (2) the need for current and future initiatives to supplement Adelaide's water supply as well as curb demand.

Furthermore, the findings illustrate the benefits from a water management perspective of assessing reliability progressively over a planning horizon to determine when to reduce demand and/or augment supply to maintain water supply security. However, the uncertainty envelope or range of uncertainty increased with time for Adelaide's southern system, which was particularly noticeable when comparing the Best and Worst cases. While some of this uncertainty may be reducible (by the water authority or others), stochastic uncertainty and some epistemic uncertainty will always exist, so flexible management may therefore be necessary to strike a balance between water supply security and regret. Thus a move away from single, long-lived and large-scale centralised water sources towards decentralised, diverse water sources at much smaller scales is necessary [*Pahl-Wostl*, 2007]. For Adelaide's southern system, this would mean that if supply were to be augmented by additional sources, local stormwater harvesting schemes or household rainwater tanks, would be preferred over centralised, larger-scale sources, such as a desalination plant. However, such climate-dependent sources have disadvantages compared with climate-independent sources (such as desalination), as climate-independent sources can guarantee supply (subject to loss of power and mechanical faults) regardless of whether it rains or not. Consequently, for Adelaide's southern system, trade-offs exist in selecting planning initiatives when attempting to maintain system reliability and minimise system regret. Future research should focus on identifying potential solutions for the southern system and the associated trade-offs.

Furthermore, extending this research to examine multiple case studies and assess an increased number of uncertainty sources and scenarios would be valuable to determine whether generalised patterns and rules regarding the relative degree of uncertainty associated with particular major sources of uncertainty can be established. This would assist water planners in understanding where the greatest level(s) of effort should be focused when: (1) attempting to reduce epistemic uncertainty; and (2) developing tools to assist in planning for the future under great uncertainty. However, the findings of this case study clearly show that, in addition to examining demand

uncertainty, natural rainfall variability must be considered in short-term plans, while in the longer-term, the focus will need to shift to consider the uncertainties of GCMs.

Acknowledgements

This work is financed by The University of Adelaide and eWater CRC. We thank David Cresswell for his technical support of WaterCress and for adapting the program to suit the requirements of the case study. Thank you also to Sri Srikanthan for his assistance with SCL, Leanne Webb for running the CFF for this case study, Matthew Gibbs for his help with programming, Mark Thyer and Michael Leonard for their advice on catchment calibration, and the three anonymous reviewers, who have assisted with improving the quality of this paper significantly.

Appendices Supporting Journal Paper 1

Appendix A contains a copy of this Journal Paper printed in *Water Resources Research*.

Chapter 3

3 Integrated framework for assessing urban water supply security of systems with non-traditional sources under climate change (Paper 2)

Statement of Authorship

Title of Paper	Integrated framework for assessing urban water supply security of systems with non-traditional sources under climate change
Publication Status	○ Published, ○ Accepted for Publication, ◉ Submitted for Publication, ○ Publication style
Publication Details	Paton, F.L., G.C. Dandy, and H.R. Maier, Integrated framework for assessing urban water supply security of systems with non-traditional sources under climate change. Submitted to Environmental Modelling and Software on 11th June, 2014.

Author Contributions

By signing the Statement of Authorship, each author certifies that their stated contribution to the publication is accurate and that permission is granted for the publication to be included in the candidate's thesis.

Name of Principal Author (Candidate)	Fiona Paton		
Contribution to the Paper	Designed general methodology, developed climate change and demand scenarios, conducted modeling and analysis, and wrote manuscript.		
Signature		Date	11/06/2014

Name of Co-Author	Graeme Dandy		
Contribution to the Paper	Supervised manuscript preparation and reviewed draft.		
Signature		Date	11/6/2014

Name of Co-Author	Holger Maier		
Contribution to the Paper	Supervised manuscript preparation and reviewed draft.		
Signature		Date	11/06/2014

Name of Co-Author			
Contribution to the Paper			
Signature		Date	

Abstract

Assessing water supply security for urban water supply system (UWSS) planning is now more challenging with the inclusion of non-traditional sources, which increases simulation complexity, and the need to account for climate change impacts, which increases uncertainty. This paper addresses this by developing an integrated framework for assessing the security of UWSSs with non-traditional sources under climate change. The framework is applied to a case study based on the southern Adelaide UWSS. The case study objectives include minimizing cost and maximizing supply security, with the latter assessed using reliability, maximum failure duration, maximum vulnerability, and robustness. Robustness represents the performance of the UWSS across plausible future scenarios, comprising of realizations of climate change and consumer demand. Trade-offs exist between cost and supply security for solutions that use desalination and harvested stormwater to augment water supply; however, use of rainwater tanks is undesirable, as they are an expensive source.

3.1 Introduction

The assessment of water supply security has traditionally been used in the planning of a city's water supply system. However, in recent times, cities' water supply systems have become more challenging to model due to both increased complexity and increased uncertainty. Consequently, the decision-making process of water supply planning has become more challenging. Firstly, in order to accommodate growth, there has been a reduced reliance on traditional water supplies, accompanied by a move towards combinations of large, engineering water projects, water reuse and conservation measures [*Chung et al.*, 2009]. For example, the harvesting of urban stormwater to supply non-potable water demands is emerging as a viable option for augmenting stressed water supply systems [*Mitchell et al.*, 2008a], water reuse is on the rise in the United States, Western Europe, Australia and Israel [*Wade Miller*, 2006], and desalination is approaching exponential growth worldwide [*Dolnicar and Schaefer*, 2009]. Secondly, substantial climate change means that the usual assumption of stationarity (traditionally relied upon in water supply system planning) is no longer

valid [*Milly et al.*, 2008]. Consequently, integrating non-traditional sources and climate change impacts into urban water supply security assessment is both timely and necessary. However, to date, this has not been achieved.

A number of studies have considered incorporating non-traditional water sources as alternatives to traditional water sources in the context of urban water supply planning. *Chung et al.* [2008] developed an integrated water supply system model in an object-orientated system dynamics simulation environment, to evaluate decentralized treatment options, allowing for multiple sources, users, and transportation and treatment systems. *Makropoulos et al.* [2008] developed a decision-support tool (Urban Water Optioneering Tool (UWOT)) for the development (or cluster) scale, which had the functionality to supply water from rainwater harvesting and greywater recycling and *Beh et al.* [2014] included non-traditional sources as part of a study on the optimal sequencing of urban water supply augmentation options, However, the focus of these papers is on the model for simulating the urban water supply system or, in the case of *Beh et al.* [2014], on the proposed sequencing approach, rather than an integrated assessment framework for urban water supply system planning that not only incorporates a simulation model that can model non-traditional water sources, but also the impacts, and associated uncertainties, of climate change.

From a climate change impact assessment perspective, there are multiple studies that have examined its impact on water supply systems [*Gober et al.*, 2010; *Groves et al.*, 2008a; *Groves et al.*, 2008b; *Groves et al.*, 2008c; *Lempert and Groves*, 2010; *Maheepala and Perera*, 2003; *Matrosov et al.*, 2013; *O'Hara and Georgakakos*, 2008; *Paton et al.*, 2013; *Wiley and Palmer*, 2008]. Of these studies, only a few investigated the impacts of climate change in a planning approach for a city that includes new water supply sources. For example, *Matrosov et al.* [2013] examined the impacts of climate change on London's water supply system expansion in the Thames basin, UK. They investigated 20 water infrastructure portfolios; however, these only included large-scale, centralized enterprises, such as desalination plants. On the other hand, *Groves et al.* [2008a], *Groves et al.*

[2008b] and *Lempert and Groves* [2010] examined the reuse of treated wastewater and an increase in sustainable groundwater use, incorporating stormwater and recycled water recharge programs for the Inland Empire, Southern California, under climate change projections. However, these studies are limited to supply portfolios incorporating large-scale water supply sources and while stormwater is included, it is not used directly as a water supply source for the city. Therefore, the increased modelling complexity of non-potable supplies from multiple, decentralized locations is not investigated. In fact, to the authors' knowledge, there are no studies that investigate the impacts of climate change on different supply portfolios to augment a city's water supply system that incorporate non-traditional, localized water sources. Consequently, there remains a need to develop an integrated framework for assessing urban water supply security of systems with non-traditional sources. Furthermore, the inclusion of non-traditional sources is particularly warranted under climate change impact assessment, given that some alternative water sources, such as rainwater and stormwater reuse, are dependent on climate.

In summary, there still exists a gap in assessing water supply security for a city in explicitly acknowledging and accounting for both the additional complexities and uncertainties associated with non-traditional water sources and climate change impacts. The specific objectives of this paper are therefore to (1) develop a generalized framework that could be applied to any city's water supply system that explicitly outlines the additional complexities due to the incorporation of non-traditional water sources and the additional uncertainties due to climate change impacts that must be considered; and (2) apply the generalized framework to a case study based on of Adelaide's southern water supply system to illustrate the approach and draw conclusions about planning Adelaide's water supply system. Adelaide, the capital city of South Australia, is an appropriate case study because of proposals to include non-traditional water sources in the city's future water supply system as part of the recent Water Plan [*Government of South Australia*, 2009].

The remainder of the paper is organized as follows. The integrated framework for assessing urban water supply security of systems with non-traditional sources under climate change is introduced in Section 3.2. The application of the framework to the case study is presented in Section 3.3, followed by the results and discussion in Section 3.4. Finally, in Section 3.5, the paper is summarized and major conclusions are drawn.

3.2 Integrated framework for assessing urban water supply security of systems with non-traditional sources under climate change

The integrated framework for assessing urban water supply security of systems with non-traditional sources under climate change (Figure 3.1) is based on the steps of systems analysis, defined as "an analytical study that helps a decision-maker to identify and select a preferred course of action among several feasible alternatives" [*Biswas*, 1976]. For water resource system analysis, there are five basic steps: (1) selection of objectives, (2) translation of objectives into measurable criteria, (3) identification of alternatives, (4) assessment of alternatives in terms of the nominated criteria, and (5) comparative evaluation of results from the assessment of alternatives [*Biswas*, 1976] (Figure 3.1). However, this basic framework for solving water resource problems has been tailored to the water supply system planning problem defined herein. Of particular note is the integration of non-traditional sources in Step 3, and the subsequent additional model complexity in Step 4 in representing the water supply system in a simulation model (Figure 3.1). Furthermore, in considering uncertainty sources when assessing the impacts of climate change, a sensitivity-based scenario analysis to examine uncertainty in demand and climate change impacts also forms part of Step 4 (Figure 3.1). These components of particular interest in the framework are discussed in more detail below, while all components of this framework are presented for the case study in Section 3.3.

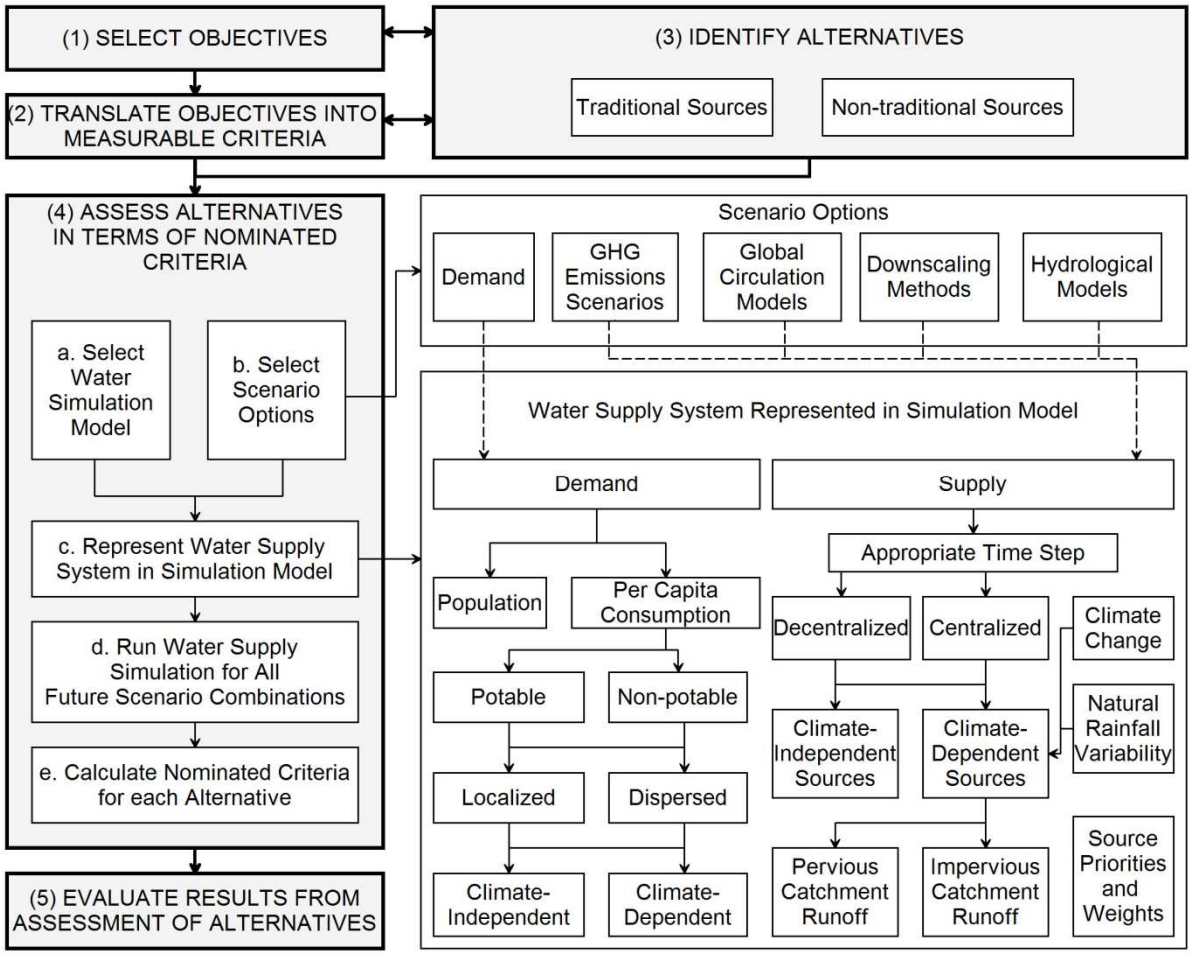

Figure 3.1: Integrated framework for assessing urban water supply security of systems with non-traditional sources under climate change, explicitly illustrating the additional complexity and uncertainty that need to be considered

3.2.1 Non-traditional Sources

As illustrated in Figure 3.1, the inclusion of non-traditional sources as alternatives in Step 3 warrants a more complex approach to representing the water supply system in the simulation model in Step 4(b), because their inclusion requires additional considerations in terms (a) levels of usability (e.g., potable and non-potable), (b) degree of climate dependence, (c) spatial and temporal scales, and (d) source integration and priority.

Not all non-traditional sources will provide water that is of an acceptable drinking standard (e.g., due to public health concerns or social acceptability), so both potable and non-potable per capita consumption must be defined (Figure 3.1). Non-potable demand for a household could include

garden, toilet, and laundry demands. In addition, non-potable supply could also be used to irrigate community parks, gardens, and large open spaces (such as golf courses), or supply large industrial non-potable demand; however, this would require delivery via a third-pipe network. Thus, non-potable supply could be used both at the residential (localized) and non-residential (dispersed) scales (Figure 3.1). Finally, there is a delineation between those non-potable end uses that are climate-dependent (e.g., garden watering) and those that are climate-independent (e.g., toilet flushing) (Figure 3.1) to account for seasonal variation in climate-dependent demand. Climate-dependent demand may fluctuate considerably with the seasons, particularly at locations where rainfall is unevenly distributed throughout the year.

Secondly, from a supply perspective, the selection of an appropriate time-step for this problem requires due consideration (Figure 3.1). Water sources with much smaller storages (e.g. household rainwater tanks), may require a smaller time-step to more accurately estimate yield than has traditionally been used for larger, centralized storage sources, such as local reservoir catchments. For example, if rainfall events were temporally lumped to such an extent that a rainwater tank's storage would be frequently exceeded (while in reality it would not be exceeded as demand would continually draw down the tank storage), the yield of a rainwater tank could be severely underestimated. However, decreasing the time-step used in modelling will increase computational effort, which may be a problem when considering multiple future scenario combinations. These are integral to the approach because they address the uncertainties in assessing climate change impacts. Furthermore, the selection of an appropriate time-step must also take into consideration the properties of the available data. For example, using an hourly time-step may be unwarranted if the rainfall data are only available on a daily time-step.

It is also important to consider the decentralized (localized) or centralized nature of sources (Figure 3.1). The localized nature of many non-traditional water sources has implications on the distribution of supply from these sources. For example, household rainwater tanks collect water from a single

household, so distributing rainwater to other households or commercial/industrial uses may be infeasible or uneconomical considering the distribution network infrastructure that would be required.

In terms of estimating yield, defining the sources as climate-independent (e.g. desalination or wastewater reuse) or climate-dependent (e.g. rainwater harvesting and local reservoir catchments) is also essential (Figure 3.1). Climate change impacts can then be incorporated into estimating yield from climate-dependent sources, as can natural rainfall variability (Figure 3.1). This is important as urban water supply planning should include stochasticity of precipitation [*O'Hara and Georgakakos*, 2008]. *Mortazavi et al.* [2012] illustrate that evaluating water supply security criteria based on short input time series could be meaningless with results being sensitive to the choice of the particular input time series. In fact, *Paton et al.* [2013] discovered that the supply reliability of a city's water supply system was not only highly sensitive to the uncertainties surrounding the impacts of climate change modelling, but also demand, and particularly in the near future, natural rainfall variability. Consequently, using stochastic rainfall data in the framework ensures that natural variability is considered. This means that (1) the results produced are not simply a reflection of the historical rainfall time series, and (2) water supply security can be reported as a percentile value to reflect the inherent variability in historical rainfall, rather than a single deterministic value.

Another side-effect of introducing non-traditional sources is the need to define both pervious and impervious catchments. For example, while reservoirs are fed from predominantly pervious catchments, household rainwater tanks receive runoff from impervious catchments, while urban stormwater harvesting schemes will have a combination of pervious and impervious catchments. Pervious and impervious catchments react differently to rainfall events, with impervious catchments having higher harvest efficiencies due to only experiencing small losses at the beginning of a rainfall event [*Coombes and Kuczera*, 2003]. Conversely, *Coombes and Kuczera* [2003] report that a reservoir catchment (that is predominantly pervious in nature) displays a threshold effect, where annual

runoff will be insignificant when annual rainfall is below about 500mm. This infers that sources with impervious catchments may be less affected during a drought or under adverse climate change impacts compared to sources with pervious catchments. Furthermore, the differing spatial scales over which non-traditional sources operate means that sometimes catchments will overlap. For example, a household roof could provide the impervious catchment for a household rainwater tank, or it could contribute to urban stormwater harvesting. Consequently, catchments for the sources must be modelled with this interdependency in mind. Finally, the sources must be integrated with priorities and weights defined (Figure 3.1) for each of the different end uses. Considerations in defining these supply operations should include the suitability of water sources to supply particular demands in terms of their water quality and spatial scale.

3.2.2 Climate Change Impact

Defining future scenario combinations is considered an essential component of the proposed methodology (Step 4b, Figure 3.1) in order to enable the impact of sources of uncertainty to be investigated, particularly those associated with projecting future climate and in understanding how these projections translate to water resources, such as runoff or water supply. For climate change impacts, uncertainty sources start with GHG emissions scenarios that represent future development pathways, for example the Special Report on Emissions Scenarios (SRES) scenarios developed by the Intergovernmental Panel on Climate Change (IPCC). The global climate responses to each of these different pathways are projected using global circulation models (GCMs), which can then be further downscaled to local climate impacts using a variety of downscaling methods, both statistical and dynamical. Finally, these are translated to runoff effects through hydrological models, and finally to water supply security by incorporating demand, through both population and future per capita consumption estimates.

As part of the scenario-based sensitivity analysis proposed in this framework, the water supply simulation model is run for all future scenario combinations (Step 4d, Figure 3.1), which enables the

magnitude of the uncertainty sources to be investigated. Understanding the greatest sources of uncertainty, and whether they are epistemic (systematic) or aleatoric (statistical), is very important for water managers. Systematic uncertainties, such as model inadequacy or data measurement inaccuracies, are potentially reducible (by the water authority's means or others); whereas statistical uncertainties, such as natural rainfall variability, are inherent and will always exist. If major sources of uncertainty are reducible by the water authority, then effort can be directed towards reducing this uncertainty, while if irreducible uncertainties dominate the impacts on water supply security, then adaptation responses must be developed to cope with this uncertainty.

3.3 Case Study

Adelaide is the capital city of South Australia (Figure 3.2), with a population of approximately 1.2 million people and a historical water demand over the past 20 years averaging about 200 Gigalitres per year (GL/yr) [*Government of South Australia*, 2009]. Historically, Adelaide has received much of its water from local catchment reservoirs in the Mount Lofty Ranges and water pumped about 60 kilometres (km) via three pipelines from the River Murray. The case study focuses on Adelaide's southern water supply system, which can be considered separate from the northern system because they are largely independent of each other [*Crawley and Dandy*, 1993]. The southern system supplies approximately half of Adelaide's population, with an indicative demand area illustrated in Figure 3.2.

Adelaide's southern system has three reservoirs, namely Myponga, Mount Bold and Happy Valley Reservoirs (Figure 3.2), with a total capacity of 85 GL. Myponga Reservoir is independent of the other reservoirs, with runoff collected from Myponga catchment (Figure 3.2) and treated at Myponga Water Treatment Plant (WTP) before being released into the distribution system. Conversely, runoff from the Mount Bold catchment collects in Mount Bold Reservoir before it is released downstream via the Onkaparinga River to Clarendon Weir, which is a very small storage that also receives runoff from its catchment (Figure 3.2). Water from Clarendon Weir is then either

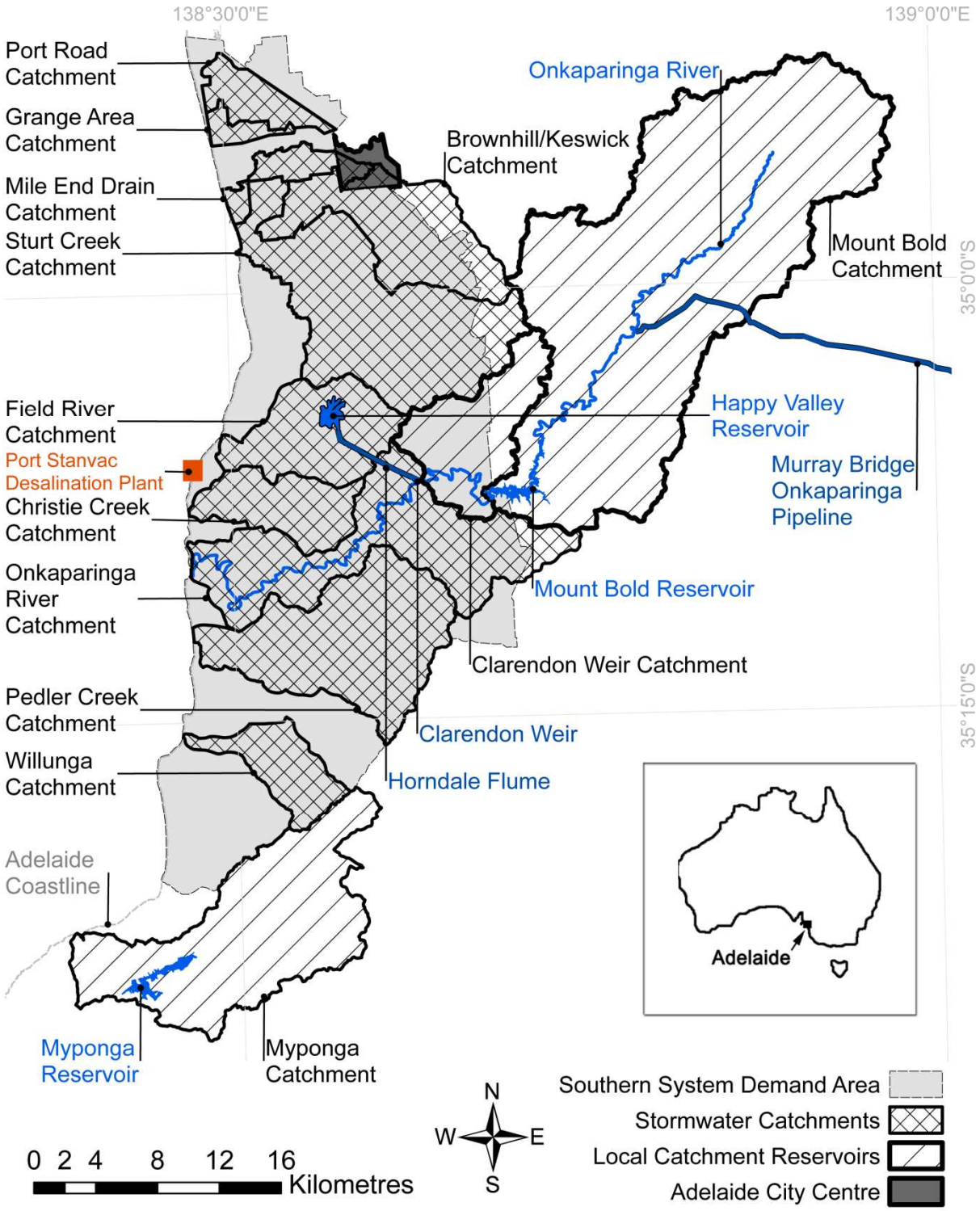

Figure 3.2: Map of the existing Adelaide southern water supply system, showing reservoirs, reservoir catchments, major rivers, pipelines, and an indicative southern system demand area. The Port Stanvac desalination plant and the ten stormwater harvesting scheme catchments used in modelling are also shown. Inset is a map of Australia highlighting the location of Adelaide.

transferred to Happy Valley Reservoir via the Horndale Flume or released downstream (Figure 3.2).

Water from Happy Valley Reservoir is treated at Happy Valley WTP before being distributed to

consumers. See *Paton et al.* [2013] for a more detailed description of Adelaide's southern reservoir system.

For the southern system, River Murray water is pumped into the Onkaparinga River via the Murray Bridge-Onkaparinga (MBO) Pipeline, where it is captured and stored in Mount Bold Reservoir (Figure 3.2). Adelaide's River Murray supply is based on a 5-year rolling license of 650 GL, with the license period beginning on May 1st each year. Although a license does not always guarantee supply, River Murray water has usually been available to meet Adelaide's needs in the past, with up to 90% of Adelaide's annual demand being met by the River Murray in dry years [*Government of South Australia*, 2009].

However, as illustrated by *Paton et al.* [2013], supply augmentation is needed for Adelaide's southern water supply system in order to respond to the projected increases in demand and the projected impacts of climate change. Furthermore, *Water for Good* (a water security plan for Adelaide released by the South Australian government) nominates diversification of water sources as an appropriate mechanism to help secure Adelaide's water supply into the future up to 2050 [*Government of South Australia*, 2009]. Thus, in this case study, different supply augmentation alternatives based on *Water for Good* are analysed to determine a suitable mix of supply sources from 2010 to 2050 for the case study based on Adelaide's southern water supply system as it was in 2009. To represent the system's mid-term and long-term viability, 2030 and 2050 were chosen as appropriate years to assess each alternative. Figure 3.2 illustrates how the general methodology of Figure 3 is applied to the case study, with more detail provided in the subsequent sections.

3.3.1 Objectives

The objectives for the case study were to maximize risk-based water supply security and minimize economic cost (Step 1, Figure 3.3). These two objectives enabled trade-offs between alternatives to be compared in terms of water supply security and economic cost, which is important, because for water supply systems, often the best option in terms of water supply security is too expensive to

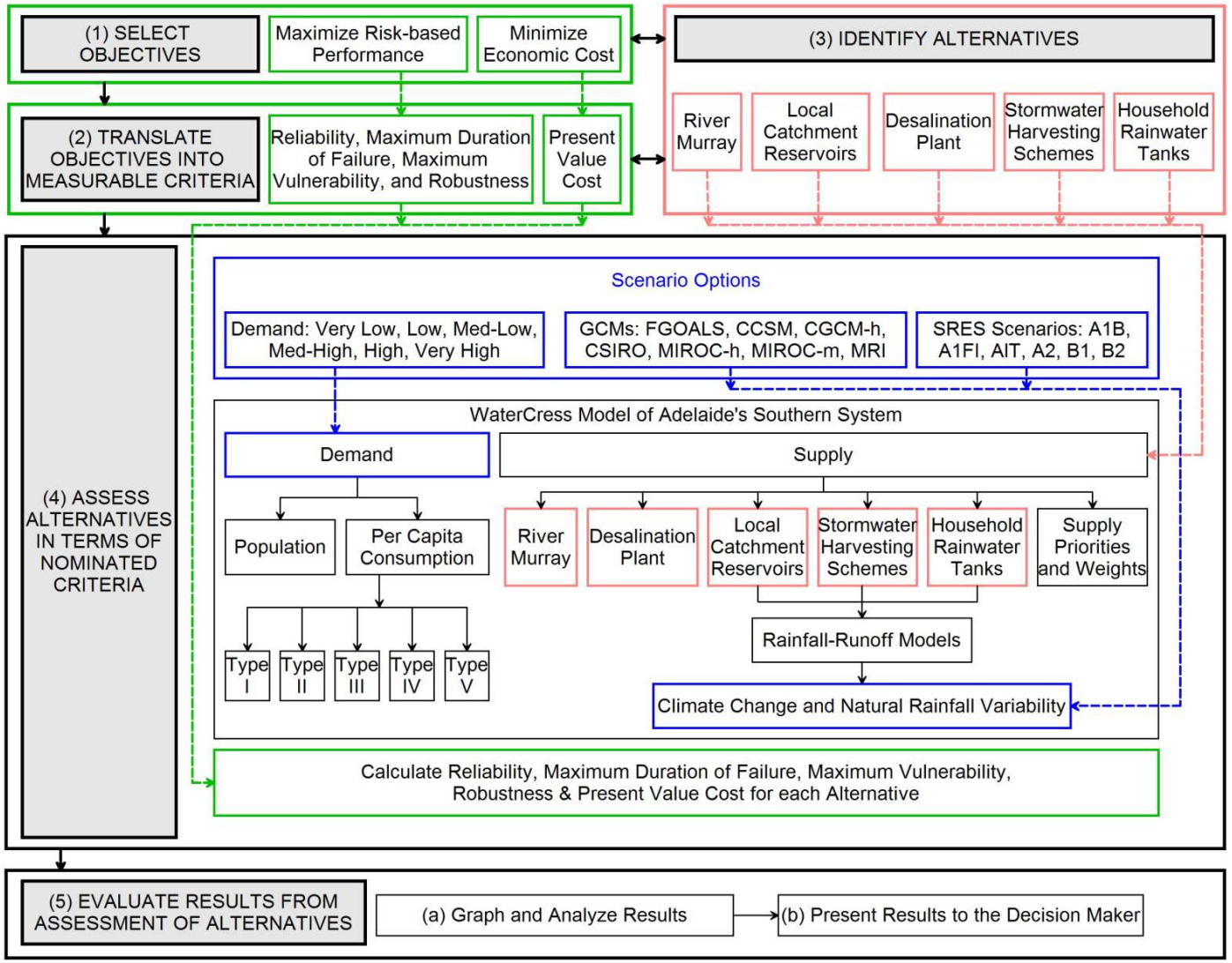

Figure 3.3: Flowchart of the general integrated framework applied to the case study based on the southern Adelaide water supply system.

warrant selection. Indeed, as *Alcubilla and Lund* [2006] propose, the cost associated with any increase in the frequency of water security should be balanced against the benefits of resulting reductions in the frequency of water scarcity. While present value of cost was used as the sole economic cost criterion, reliability, maximum duration of failure, maximum vulnerability and robustness were used for risk-based water supply security assessment (Step 2, Figure 3.3). These criteria cater for both natural variability and impacts due to changes in climate and demand over time. Details of how these criteria were calculated are given in Section 3.3.3.4.

3.3.2 Water Supply Alternatives

The alternatives considered for the water supply system configuration (Step 3, Figure 3.3) include nine feasible alternatives (Table 3.1) to examine various combinations of traditional and non-traditional water supply sources to be compared.

Alternative 1 includes only the current, traditional water sources of the local catchment reservoirs and the River Murray supply, with River Murray supply limited to 65 GL/yr to represent half of Adelaide's current 5-year rolling license (as the southern system represents about half of Adelaide's demand) (Table 3.1). Refer to *Paton et al.* [2013] for more details. This provides a baseline against which future options for supply augmentation can be compared.

Alternatives 2-4 include the addition of one of the non-traditional water supply sources (Table 3.1), namely a 5.0KL rainwater tank for all households (Alternative 2), stormwater harvesting schemes (Alternative 3) or a 25 GL/yr desalination plant (Alternative 4). Alternatives 5-7 examine the current system supplemented with two of the three aforementioned non-traditional water source options (Table 3.1), while Alternative 8 includes the addition of all three non-traditional sources. Alternative 9 examines the option of considering a desalination plant of larger capacity (i.e. 50 GL/yr), without rainwater tanks or stormwater harvesting.

Table 3.1: Alternatives considered for Adelaide's southern water supply system configuration

Water Supply Source Volume/Capacity	Alternative Number								
	1	2	3	4	5	6	7	8	9
Local Catchment Reservoir Volume (GL)	85	85	85	85	85	85	85	85	85
River Murray Maximum Transfer (GL/yr)	65	65	65	65	65	65	65	65	65
Desalination Plant Capacity (GL/yr)	0	0	0	25	0	25	25	25	50
Household Rainwater Tank Volume (kL/tank)	0	5	0	0	5	5	0	5	0
Stormwater Harvesting Schemes Capacity (GL/yr)	0	0	22	0	22	0	22	22	0

These were considered feasible alternatives for Adelaide's southern water supply system, because household rainwater tanks, stormwater harvesting schemes and a desalination plant at Port Stanvac (Figure 3.2) have all been investigated as potential future water supply options for Adelaide [*Government of South Australia*, 2009]. Specifically, two capacities were considered for Adelaide's desalination plant, namely 50 GL/yr and 100 GL/yr [*Government of South Australia*, 2009]. However, these two capacities were halved for this case study, because the southern system accounts for approximately half of Adelaide's demand, and thus it was assumed that only half of the desalinated water produced would be available for the southern system. Furthermore, of 20 potential stormwater harvesting schemes nominated for Adelaide [*Wallbridge and Gilbert*, 2009], only the catchments of 10 schemes fall predominantly within Adelaide's southern system supply area, with Port Road being the most northern catchment and Willunga the most southern (Figure 3.2). Consequently, only these 10 schemes were included in this case study when harvested stormwater was included as a source. A tank size of 5kL was selected when rainwater harvesting was considered because *Coombes and Kuczera* [2003] conclude that in order to achieve mains water savings the optimum sized rainwater tank was about 5kL for a number of Australian cities, including Adelaide.

3.3.3 Simulation Model

The water resources model WaterCress (Water – Community Resource Evaluation and Simulation System) was selected (Step 4, Figure 3.2) because it can: (1) model the traditional and non-traditional water sources; (2) model across multiple spatial scales, so as to incorporate the household rainwater tanks, the local stormwater catchment schemes, and the much larger, centralized supply sources; (3) model at a daily time step (see Section 3.3.3.2); (4) consider water quality so that rainwater and stormwater could be assigned to non-potable end uses; and (5) readily incorporate multiple scenarios. As described in the WaterCress manual (www.waterselect.com.au), WaterCress is a PC-based continuous time series, water balance model for designing and testing layouts of water systems incorporating non-traditional water sources. Central features include: (1) water sources represented by nodes (representing various functions or operations of water infrastructure/processes) and joined by flow paths (either 'free flow' gravity drainage paths or fixed capacity water supply pipes) to simulate the water system; (2) a set of core mathematical relations (e.g. rainfall-runoff models) and data bases (e.g. sequential rainfall), which contain the variables and constraints necessary to enable quantities and qualities of water to be estimated and tracked; and (3) tables and graphs of outputs of performance for components of the water system over the modelling period (e.g. reservoir storage levels). Data requirements vary for each particular case study. However, each node has an associated database containing the variables necessary to enable quantities and qualities of water to be manipulated as rainfall or flow is passed through it. Time series inputs for rainfall and evaporation are the usual prime drivers in the rainfall-runoff models (being provided as individual ASCI files). WaterCress was also considered suitable for the case study as it is freely available (www.waterselect.com.au), has the benefits of being developed and supported locally in Adelaide, and the model for Adelaide's southern water supply system has already been partially established by *Paton et al.* [2013]. The WaterCress model representation of Adelaide's southern water supply system consisted of two main components – demand and supply, as detailed in the subsequent sections.

3.3.3.1 Demand

Demand was computed from population and per capita consumption (Step 4, Figure 3.3). The initial population for the southern system in 2010 was assumed to be approximately 600,000 people (half of Adelaide's population). Depending on the future scenario selected (see Section 3.3.3.3), an annual linear percentage change, derived from projections of Adelaide's future population, was then applied to this value to determine the population of the southern system in 2030 and 2050. For per capita consumption, consideration was firstly given to whether the demand was potable or non-potable. These demands were then divided into either residential or non-residential demand, and again to either climate-dependent or climate-independent demand, resulting in the definition of a total of five demand types for the case study (Step 4, Figure 3.3) (Table 3.2). Residential demand included potable, climate-independent demand (Type I), non-potable, climate-dependent garden demand (Type II), and non-potable, climate-independent toilet demand (Type III) (Table 3.2). The splitting of the non-potable residential demands was particularly important for this case study to account for the high seasonal variability in garden demand (Table 3.3), a result of Adelaide's Mediterranean-style climate of hot, dry summers and wet, cool winters. Non-residential demand included demand for primary production, public purposes, commercial and industrial uses, unmetered water and water lost in the mains distribution network due to leaks. For non-residential demand, there was both potable supply (Type IV) and non-potable supply (Type V). Non-residential, non-potable supply was not split into climate-dependent and climate-independent demand, as WaterCress could not accommodate seasonal variation in demand outside of the residential demand node. Individual per capita consumption for the five demand categories in 2010 (Table 3.2) reflect the breakdown of Adelaide's demand in 2008 without water restrictions in place (see *Paton et al.* [2013]). Depending on the demand scenario selected (see Section 3.3.3.3), these demands were either kept constant or reduced over the planning horizon by annual linear percentage changes.

Table 3.2: Demand type, water source, and 2010 individual per capita consumption for the five demand categories defined for the Adelaide southern system case study

Category	Demand Type	Water Source(s)	2010 demand (Litres per capita per day)
Type I	Residential – Potable	Mains water only	144
Type II	Residential (Garden) Non-potable, Climate-dependent	Rainwater & Mains water	115
Type III	Residential (Toilet) - Non-potable, Climate-independent	Rainwater & Mains water	28
Type IV	Non-residential – Potable	Mains water only	144
Type V	Non-residential – Non-potable	Stormwater & Mains water	62
TOTAL			493

Table 3.3: Monthly residential garden water demand as a percentage of total annual residential garden water demand [*Barton*, 2005]

Jan	Feb	Mar	Apr	May	Jun	Jul	Aug	Sep	Oct	Nov	Dec
22.9%	18.8%	14.2%	6.4%	3.0%	0.0%	0.1%	0.7%	1.4%	4.9%	10.7%	17.0%

3.3.3.2 Supply

A daily time-step was selected for the model. Any greater time step could have underestimated harvested rainwater yield (see Section 3.2.1) or inaccurately estimated yield from the desalination plant because it produces water as needed and has very limited storage capacity, while any smaller time-step would have required excessive computational effort that was not necessary for accurately determining yield. For example, studies by *Mitchell et al.* [2008a] and *Mitchell et al.* [2008b] showed that a sub-daily time step had an insignificant impact on the estimation of volumetric reliability of (a) an urban stormwater storage and (b) rainwater tanks greater than 1kL, respectively.

For centralized sources, namely the desalination plant, local catchment reservoirs and the River Murray, which all have water treated to a potable level, supply was through the main distribution network, which was thus available to each of the five demand types defined in Table 3.2. However, as harvested stormwater only produced water of a non-potable standard, a third-pipe network was required. As this would have been costly and disruptive to provide for residential users, stormwater was only supplied to non-residential, non-potable demands (e.g. irrigation of public reserves) (Table 3.2) [*Government of South Australia*, 2009]. Similarly, as the distribution of household rainwater for non-residential purposes would have necessitated a non-potable, third-pipe network and thus have been very expensive, rainwater was only used on site to supply the non-potable demands of residential garden and toilet demand (Table 3.2).

Both the River Murray supply and desalination plant were defined as climate-independent sources in the model, so yield from these sources was not limited by climate, but was instead limited by Adelaide's River Murray License and the capacity of the desalination plant (Table 3.1). See Appendix B for supporting documentation and further information on these two sources.

However, the yields from local catchment reservoirs, stormwater harvesting schemes, and household rainwater tanks were dependent on climate. Consequently, rainfall-runoff (RRO) models were developed within WaterCress for the source catchments (Step 4, Figure 3.3) to enable future climate to be translated to runoff, and subsequently yield. WC1 was the RRO model option selected in WaterCress because it has previously been used for studies in the Mount Lofty Ranges' catchments [*Alcorn*, 2006; *Savadamuthu*, 2003; *Teoh*, 2002] and in the *Urban Stormwater Harvesting Options Study* for Adelaide [*Wallbridge and Gilbert*, 2009]. WC1 is a 10-parameter, conceptual three-bucket model with buckets or storage components for interception, soil moisture, and groundwater. Surface, interflow, and groundwater flow potentially contribute to surface runoff. The catchment response is defined by six parameters: median soil moisture, catchment standard deviation, interception store, soil wetness multiplier, soil moisture discharge, and pan factor for soil. For

groundwater simulation, three parameters are defined, namely groundwater recharge, groundwater discharge, and fraction groundwater loss. The final parameter – creek loss, is used to simulate runoff reduction, for example, the uptake of water by riparian vegetation. For further details of WC1 see www.waterselect.com.au. Reservoir catchments were considered totally pervious, rainwater catchments were considered totally impervious, while stormwater catchments were a combination of both pervious and impervious catchments. Appendix B contains details on the calibration of the WC1 models for both the impervious and pervious catchments. It particularly illustrates the challenge of incorporating urban stormwater harvesting in this step of the modelling process, as calibrating and validating the stormwater catchments was difficult due to limited, good-quality, streamflow data.

To incorporate the impact of climate change on the climate-dependent sources (Step 4, Figure 3.3), the constant scaling or delta-change approach was applied to obtain local rainfall and evaporation responses for each of the climate change scenarios modelled (see Section 3.3.3.3). The delta change approach is a simple downscaling approach and has a number of limitations, such as maintaining the same probability distribution for rainfall even though changes in wet and dry spell lengths are projected to occur. However, it has been used because (1) *Fowler et al.* [2007] have shown that simple downscaling approaches can accurately simulate flow and multiple climate change scenarios can easily be modelled, and (2) this approach has already been applied to this case study [*Paton et al.*, 2013]. Specifically, 2030 and 2050 change factors (based on the 30-year baseline from 1975-2004) for monthly rainfall and areal potential evapotranspiration (equivalent to Pan A evaporation) were obtained from the Australian Commonwealth Scientific and Industrial Research Organization's (CSIRO) OzClim (www.csiro.au/ozclim/). For evaporation, change factors were applied to the average monthly historical evaporation data derived for each climate station (which were based on the 30-year baseline from 1975-2004), while for rainfall, these change factors were applied to stochastic rainfall time series.

One thousand 30-year stochastic rainfall time series were developed to ensure that the impact of natural rainfall variability was included in the approach (Step 4, Figure 3.3). This was particularly important for this case study because (1) Adelaide experiences high variability in both seasonal, annual and decadal rainfall and (2) natural rainfall variability has been shown to be at least as important as GCM uncertainty and SRES emissions uncertainty when modelling the impacts of climate change on water supply security [*Paton et al.*, 2013]. For example, in 2050, the range in reliability for Alternative 1 caused by uncertainty in natural rainfall variability was 16.5% [*Paton et al.*, 2013]. Further details on the development of the stochastic time series for this case study are provided in Appendix C.

The final step in representing the water supply system in WaterCress was to integrate the water sources and define the supply priorities and weights (i.e. operational strategies) of the system (Step 4, Figure3.3). In the WaterCress model, runoff from the three local reservoir catchments was stored in their respective reservoirs. However, because water is simply transferred from Clarendon Weir to Happy Valley Reservoir, these two storages were treated as a single reservoir in the model and are hereafter referred to as Happy Valley Reservoir. Consequently, in the model, runoff from Clarendon Weir catchment flowed directly into Happy Valley Reservoir. Minimum and maximum volumes of the reservoirs (Table 3.4) were based on values reported by *Crawley* [1995] and by SA Water (www.sawater.com.au). For harvested stormwater, pervious and impervious runoff was transferred from buffer storages or waterways to wetlands [*Wallbridge and Gilbert*, 2009]. The wetlands had a minimum residence time of seven days, after which water was pumped into aquifers for storage until the harvested stormwater was required to supply Type V demand. However, due to a lack of suitable aquifer storage near the Christie Creek and Onkaparinga River schemes, *Wallbridge and Gilbert* [2009] propose that water from the Christie Creek wetland and Onkaparinga River wetland be transferred to the Pedler Creek aquifer. Consequently, in the WaterCress model, there were only four aquifers for storing harvested stormwater, namely Brownhill-Keswick aquifer, Sturt Creek aquifer, Field River aquifer and Pedler Creek aquifer. Wetland and aquifer properties for the

Table 3.4: Properties and constraints of reservoirs, wetlands, and aquifers for the southern water supply system model

Reservoir or Stormwater Scheme	Reservoir or Wetland Properties			Aquifer Properties	
	Minimum Volume (GL)	Maximum Volume (GL)	Maximum Infill Rate (ML/day)	Maximum Recharge Rate (ML/day)	Maximum Extraction Rate (ML/day)
Myponga Reservoir	4.6	26.8	n/a	n/a	n/a
Mount Bold Reservoir	0.4	46.2	n/a	n/a	n/a
Happy Valley Reservoir	4.5	11.9	n/a	n/a	n/a
Brownhill-Keswick	0.48	0.73	20.3	90.9	67.3
Sturt Creek	0.49	0.74	28.7	101.4	69.1
Field River	0.24	0.37	3.1	66.1	4.3
Christie Creek	0.13	0.19	6.7	n/a	n/a
Onkaparinga River	0.17	0.26	10.7	n/a	n/a
Pedler Creek	0.08	0.12	5.0	57.7	25.9

stormwater schemes (Table 3.4) were based on *Wallbridge and Gilbert* [2009]: (1) the maximum infill rate of the wetland represented the capacity of the pumps used to divert water from the buffer storage or waterway to the wetland; (2) the maximum recharge rate to the aquifers represented the overall rate that wells for a scheme could inject to groundwater; and (3) the maximum extraction rate was assumed to be 10 litres per second per well. Furthermore, for Alternatives 5 and 8, which included both harvested stormwater and household rainwater tanks (Table 3.1), there was a reduction in the proportion of household roof area contributing to the impervious catchment of the

stormwater schemes, due to the overlap of the impervious catchments of these two sources. See Appendix B for more detail.

In terms of source priorities and weightings, for Type II and Type III demands (Table 3.2), rainwater was preferentially supplied over mains water when it was available, while stormwater was used over mains water for Type V demand (Table 3.2), when it was available. However, in the absence of sufficient harvested rainwater and stormwater to meet the non-potable demands (and for the potable demands), mains water was used (Table 3.2), with water sourced in equal proportions (when it was available) from the desalination plant, Myponga reservoir and Happy Valley Reservoir (which included River Murray supply). Equal priority and weighting was assumed for these sources because *Water for Good* did not stipulate operational regimes for the different supply augmentation options [*Government of South Australia*, 2009].

3.3.3.3 Run Water Supply System for All Future Scenario Combinations

The WaterCress model was used to simulate the supply system for 2030 and 2050 conditions for all nine alternatives (Section 3.3.2), for all future scenario combinations, and for the 1,000 30-year stochastic time series). Future scenario combinations were defined for the case study to explore the impacts of future demand and climate change uncertainty (Step 4, Figure 3.3). Six potential demand projections, six potential SRES scenarios, and seven potential GCM scenarios (from the set of coordinated climate model experiments comprising the World Climate Research Programme's Coupled Model Intercomparison Project CMIP3) were combined to create a total of 252 future scenario combinations. These are illustrated in Figure 3.3 and are identical to those developed by *Paton et al.* [2013] to explore the relative magnitudes of sources of uncertainty in modelling climate change impacts on water supply security for Adelaide's current southern water supply system.

The six demand options consisted of three population projections and two per capita consumption projections. The population projections – labelled small, medium and large (Table 3.5), corresponded to the 95th, 50th and 5th percentiles of the 72 population projections for Adelaide in

Table 3.5: Demand Scenario Options

Demand Scenario	Per capita consumption	Population
Very Low	Reduction	Small
Low	Constant	Small
Medium-Low (Base case)	Reduction	Medium
Medium-High	Constant	Medium
High	Reduction	Large
Very High	Constant	Large

2050 [*Australian Bureau of Statistics*, 2008], respectively. Specifically, population projections as annual linear percentage changes were -0.680% (small), 0.736% (medium), and 1.579% (large). The first per capita consumption scenario (labelled Reduction, Table 3.5) was for future savings of 0.35% per year, representative of projections made by *Government of South Australia* [2009] due to the effects of permanent water conservation measures, savings due to government incentives and increasing water price, and increases in the use of water-efficient technologies. The second scenario (labelled Constant, Table 3.5) was more conservative, assuming the same per capita water use as 2010. This second scenario also represents the possibility of water savings being negated by potential increases in individual per capita consumption as a result of the impact of climate change (see *Paton et al.* [2013]). The resulting demand scenarios formulated were labelled Very Low, Low, Medium-Low, Medium-High, High, and Very High (Table 3.5).resulting demand scenarios formulated were labelled Very Low, Low, Medium-Low, Medium-High, High, and Very High (Table 3.5).

In selecting GCMs, CSIRO's Climate Futures Framework (CFF) [*Clarke et al.*, 2011] was applied, whereby plausible climates simulated by GCMs for different SRES scenarios were classified into a small set of representative climate futures (RCFs) [*Whetton et al.*, 2012]. For this case study, seven GCMs were available in OzClim that represented five out of six future RCFs identified for the

Adelaide and Mount Lofty Ranges region, including the least severe (warmer with little precipitation change) and most severe (hotter and much drier) (see *Paton et al.* [2013] for more detail on the approach). As illustrated in Figure 3.3, the seven GCMs were CCSM3 (hereinafter CCSM), CGCM3.1(T63) (hereinafter CGCM-h), CSIRO-MK3.5 (hereinafter CSIRO), FGOALS-g1.0 (hereinafter FGOALS), MIROC3.2(hires) (hereinafter MIROC-h), MIROC3.2(medres) (hereinafter MIROC-m), and MRICGCM2.3.2 (hereinafter MRI).

3.3.3.4 Calculate Nominated Criteria for Each Alternative

Given that for each of the nine alternatives, the system was simulated for 252 scenarios, which were each represented by 1,000 30-year time series in both 2030 and 2050, each alternative was simulated in WaterCress 504,000 times. In order to obtain meaningful summary outputs from such a large volume of generated data, , reliability, maximum duration of failure, maximum vulnerability and economic cost for each alternative and each scenario in 2030 and 2050 were averaged across the 1000, 30-year stochastic time series. This enabled the results to reflect the inherent stochasticity in natural precipitation without producing too large a data set. Consequently, for each alternative, there were 252 values for reliability, maximum duration of failure, maximum vulnerability, and present value of economic cost for both 2030 and 2050. As illustrated below, robustness was a function of meeting acceptable 'level of service' (LOS) objectives, defined in terms of values of reliability, maximum duration of failure, and maximum vulnerability across the 252 scenarios, so only a single value of robustness was obtained for each alternative in both 2030 and 2050.

3.3.3.4.1 Risk Based Performance Criteria

Reliability, maximum failure duration, maximum vulnerability, and robustness were used as the four risk-based performance criteria because, from the perspective of natural variability, risk-based water supply security assessment should consider the likelihood, duration, and magnitude of supply shortfalls. Failure duration and vulnerability, in addition to reliability, are considered important criteria for water supply systems, because the risks of either extreme shortages or lengthy, smaller

shortages during critical periods are not desirable [*Zongxue et al.*, 1998]. Other studies have used alternative terminology to describe reliability, failure duration and vulnerability, for example, *Griffin and Mjelde* [2000] described failures in terms of their probability, strength and duration, while *Hashimoto et al.* [1982b] defined failures in terms of their reliability, resilience and vulnerability: reliability describing the probability of the system being in a satisfactory state (i.e. the probability of supply exceeding demand); resilience measuring how quickly the system returns to a satisfactory state after a failure occurs; and vulnerability describing the likely magnitude of failure (provided a failure occurs).

Robustness was also used because from the perspective of changes in climate and demand, risk-based water supply security assessment should consider the degree to which the system performs at an acceptable level under a range of possible scenarios. Robustness has been used as an indicator for water resources system performance for many years (e.g., see *Hashimoto et al.* [1982a]) but is gaining prominence in analysis (e.g. see *Korteling et al.* [2013] and *Matrosov et al.* [2013]) as significant future uncertainties are acknowledged, many of which are associated with climate change [*Moody and Brown*, 2013]. Robustness can be measured as the degree to which water supply systems perform at a satisfactory level across a broad range of plausible future conditions [*Groves et al.*, 2008c]. This definition of the robustness performance metric is in line with that proposed in Robust Decision Making (RDM), where robustness reflects counts or fractions of scenarios with acceptable performance (e.g. *Groves and Lempert* [2007]). However, alternative robustness metrics have also been defined in the literature, including a ratio of desirable configurations possible from an initial decision or set of decisions [*Wong and Rosenhead*, 2000], and a climate-informed index that explicitly accommodates probabilities of future climates with associated uncertainties and incorporates credible climate information [*Moody and Brown*, 2013].

Average reliability was calculated as follows:

$$\mathrm{Re}l_{sy} = \frac{\sum_{t=1}^{T_{sy}} (\frac{S_{tsy}}{D_{tsy}} * 100)}{T_{sy}} \quad (3.1)$$

where Rel_{sy} was the average reliability for scenario s (s=1-252) and year y (y=2030 or 2050) given as a percentage; S_{tsy} was the number of days supply exceeded demand (success state) for time series t (t=1-1000), scenario s, year y; D_{tsy} was the total number of days evaluated for time series t, scenario s, year y (D_{tsy}=10,958); and T_{sy} was the total number of time series evaluated for scenario s, year y (T_{sy}=1,000). Average maximum duration of failure was calculated as:

$$M.D.F_{sy} = \frac{\sum_{t=1}^{T_{sy}} \max(\{F_{tsy}\})}{T_{sy}} \quad (3.2)$$

where $M.D.F_{sy}$ was the average maximum duration of failure for scenario s (s=1-252), year y (y=2030 or 2050) given in days; F_{tsy} was the number of consecutive days that demand exceeded supply for time series t (t=1-1,000), scenario s, year y; and T_{sy} was the total number of time series evaluated for scenario s, year y (T_{sy}=1,000). Average maximum annual vulnerability as a percentage of demand was calculated as:

$$M.Vul_{sy} = \frac{\sum_{t=1}^{T_{sy}} \max(\left\{\frac{V_{atsy}}{D_{sy}}\right\})}{T_{sy}} * 100 \quad (3.3)$$

where $M.Vul_{sy}$ was the average maximum annual vulnerability for scenario s (s=1-252), year y (y=2030 or 2050) given as a percentage; V_{atsy} was the volume by which demand exceeded supply for year a of the stochastic time series (a=1-30), time series t (t=1-1000), scenario s, year y; D_{sy} was the

annual demand for scenario s, year y; and T_{sy} was the number of time series evaluated for scenario s, year y (T_{sy} =1,000).

Maximum (rather than average) values for failure duration and vulnerability were applied because an understanding of the worst possible future failure in terms of both duration (maximum failure duration) and severity (maximum vulnerability) was necessary to relate the criteria to water restrictions. This was required as failures that could be addressed by imposing water restrictions were considered acceptable in terms of meeting LOS objectives, Water restrictions are also not uncommon in water supply system planning, because, given that the construction of generous buffer supplies are often associated with high economic and environmental cost [*Erlanger and Neal*, 2005], enforcing temporary water restrictions to reduce deficits that may only occur infrequently, such as once every 20 years (e.g., in a drought), may be advantageous over "gold plating" the system to ensure no failures. Furthermore, while temporary water restrictions come at a cost to the water consumer, there is a culture in Australia to accept periodic water restrictions because of the highly-variable rainfall in many locations [*Erlanger and Neal*, 2005].

Robustness was calculated as:

$$Rob_y = S_y / T_y \tag{3.4}$$

where Rob_y was the robustness for year y (y=2030 or 2050), S_y was the number of scenarios for which the system was considered to exhibit "acceptable performance" for year y, (y = 2030 or 2050) and T_y was the total number of scenarios evaluated for year y (T_y=252). The LOS objectives for acceptable performance were defined as average reliability >95% [*Chong et al.*, 2009a], average maximum duration <365days [*Chong et al.*, 2009a] and average maximum annual vulnerability ≤ 27% of demand [*Chong et al.*, 2009b]. In the absence of Adelaide-specific data, the first two LOS objectives are based on the LOS objectives of Melbourne, the closest capital city to Adelaide and one that shares a similar climate, while the last LOS objective coincides with the projected savings under

Adelaide's level five water restrictions. The cost of these LOS objectives have not been included, as it was beyond the scope of the study; however, with the increasing body of research into consumers' willingness-to-pay (WTP) to avoid restrictions (for example see *Dandy* [1992], *Alcubilla and Lund* [2006], *Griffin and Mjelde* [2000], and *Hensher et al*., [2006]), future work could look at incorporating the cost to the consumer of water restrictions and the societal benefits of meeting specified reliability targets.

3.3.3.4.2 Present Value of Costs

The 2010 present value (PV) of the capital and ongoing costs accrued over the planning horizon from 2010 to 2050 was calculated for each alternative. Capital costs of the existing Adelaide southern system water sources (i.e. catchment reservoirs and River Murray supply infrastructure) were not included (as these are sunk costs), but capital costs were attributed to the desalination plant, household rainwater tanks and stormwater harvesting schemes. Ongoing costs for all supply sources were considered and discounted in order to equitably account for future costs in terms of their 2010 present value. Weitzman's gamma discounting (where the discount rate reduces with time) was applied to place greater emphasis on near future costs relative to the usual exponential discounting. For the first five years, a discount rate of 4% was used, from 1st May 2015 to 31st April 2035 (inclusive) the discount rate was reduced to 3%, while this was reduced further to 2% from 1st May 2035 to the end of the planning horizon [*Weitzman*, 2001]. Furthermore, for each alternative, this PV cost was averaged across the 1,000 30-year stochastic time series for each of the 252 scenarios in 2030 and 2050. Consequently, like reliability, maximum duration of failure and maximum vulnerability, 252 PV costs were obtained for both 2030 and 2050 for each of the nine alternatives.

Only ongoing costs for the local catchment reservoirs and the River Murray were accounted for, as these water sources already exist in Adelaide's southern water supply system (Table 3.6). However, labour, chemical, and power costs, as well as upgrades and replacement of assets, were accounted for as ongoing costs for the reservoirs (Table 3.6). For the River Murray, the cost to purchase

Table 3.6: Summary of economic cost estimations for the Adelaide's southern system water supply sources

Water Source	Capital Cost	Ongoing Costs	
Local Catchment Reservoirs (HV = Happy Valley; Myp = Myponga)	n/a	Labour	$1Million/yr (HV) $0.32Million/yr (Myp)
		Chemicals and Power	$37/ML (HV) $87/ML (Myp)
		Chlorination Facility Upgrade	$17.8Million in 2012 (HV)
		Plant Replacement	$162.5Million (HV in 2041) $28.4Million (Myp in 2043)
		Mechanical Asset Replacement	$22.4Million/7yrs (HV) $3.9Million/7yrs (Myp)
River Murray	n/a	Power	Derived from first principles (flow-dependent)
		Treatment	As per Happy Valley Reservoir
Port Stanvac Desalination Plant	$1.35Billion (50GL/yr); $1.83Billion (100GL/yr)	Power	$0.68/kL
		Labour, Chemicals, and Maintenance	$34.2Million/yr (50GL/yr) $68.4Million/yr (100GL/yr)
		RO membrane replacement	$15.5Million/5yrs (50GL/yr) $31.0Million/5yrs (100GL/yr)
		PSHV Pipeline pump replacement	$30 Million in 2030
Stormwater Harvesting Schemes	$260Million	Operation and Maintenance	$1.23/kL
Household Rainwater Tanks	$2,708/tank $355/pump	Tank replacement	$2,708/tank/30yrs
		Pump replacement	$355/pump/15yrs
		Operation and Maintenance	$0.05/kL
		Annual Maintenance Fee	$20/yr
		Pump power	$0.18/kL

electricity for pumping from Murray Bridge to Onkaparinga River was accounted for, along with treatment costs at Happy Valley Reservoir (Table 3.6).

For the Port Stanvac desalination plant, stormwater schemes, and rainwater tanks, capital costs were included (Table 3.6). In addition, fixed ongoing costs for the desalination plant were associated with power, chemicals and maintenance, RO membrane replacement and the Port Stanvac Happy Valley (PSHV) Pipeline pump replacement (Table 3.6). However, the cost of power was dependent on yield (Table 3.6). Similarly, ongoing costs of rainwater were a combination of fixed costs and yield-dependent costs (Table 3.6). Fixed costs were attributed to tank and pump replacement, and annual maintenance, whereas ongoing costs were associated with power, as well as an operation and maintenance cost (Table 3.6). Ongoing costs for the harvested stormwater schemes, attributed to operation and maintenance, were based on yield only (Table 3.6). Detailed information supporting these costs, including assumptions used in their derivation, is provided in Appendix D.

3.4 Results and Discussion

The performance of the alternatives against the different criteria considered is presented in Section 3.4.1. An investigation into the sources of uncertainty affecting variability in average reliability, average maximum duration of failure, and average maximum annual vulnerability in 2050 across the 252 scenarios is provided in Section 3.4.2, while the results are summarized from a practical management perspective in Section 3.4.3 (which is particularly important in terms of addressing the second objective of the paper).

3.4.1 Comparative Analysis of Alternatives

The performance of the nine alternatives in 2030 and 2050 in terms of the selected criteria is summarized in Table 3.7. As can be seen Alternatives 1 (current system), 2 (rainwater) and 3 (stormwater) do not perform acceptably in 2030 nor 2050 for the median case, with Alternatives 4 (25 GL/yr desalination plant), 5 (rainwater and stormwater), and 6 (rainwater and 25 GL/yr desalination plant) not meeting acceptable performance in 2050 (Table 3.7) for the median case. Consequently, in 2050, only Alternatives 7 (stormwater and 25 GL/yr desalination plant), 8, (rainwater, stormwater and 25 GL/yr desalination plant) and 9 (50 GL/yr desalination plant) have

Table 3.7: Median values (based on 252 scenarios) for Average Reliability, Average Maximum Resilience, Average Maximum Annual Vulnerability expressed as a percentage of demand and Net Present Value of Total System Cost, and Robustness for the nine alternatives in 2030 and 2050.

Year	Alternative	Average Reliability (%)	Average Maximum Resilience (Maximum Consecutive Days of Failure)	Average Maximum Annual Vulnerability (Maximum Shortfall in % of Demand)	NPV Total System Cost (2010$Billion)	Robustness (%)
2030	1	88.45	245	82.2	0.56	9.1
	2	93.67	193	62.2	1.59	25.0
	3	95.97	159	47.9	1.03	36.1
	4	99.16	58	14.9	1.75	57.9
	5	99.20	56	14.6	2.04	57.9
	6	99.97	3	0.6	2.75	79.0
	7	100.00	0	0.0	2.17	91.3
	8	100.00	0	0.0	3.17	97.6
	9	100.00	0	0.0	2.38	97.6
2050	1	78.67	329	89.0	1.01	12.3
	2	84.59	279	80.1	2.71	22.2
	3	87.09	257	75.2	1.66	26.2
	4	91.61	217	61.6	2.58	40.9
	5	92.78	204	59.3	3.33	39.7
	6	97.03	134	34.7	4.23	47.6
	7	98.81	75	17.3	3.17	56.0
	8	99.94	6	1.3	4.79	71.8
	9	99.88	11	2.1	3.53	64.7

acceptable performance for the median case. However, this improved performance generally comes at a greater economic cost (Table 7).

There are no trade-offs between reliability, duration of failure and vulnerability, but trade-offs exist between risk-based performance and economic cost, which are illustrated using a plot of cost versus reliability versus robustness (Figure 3.4). As can be seen, the dominated solutions (in terms of maximizing reliability, maximizing robustness, and minimizing cost) all contain rainwater tanks (i.e. Alternatives 2, 6 and 8 in 2030 and Alternatives 2, 5 and 6 in 2050). This is not surprising because the addition of 5.0 kL rainwater tanks to Alternative 1 (current system) translates to an average additional 11.2 GL/yr of supply to the system at an additional cost of $1.7 billion in 2050, whereas Alternative 4 contributes an additional 25 GL/yr of water for a smaller cost increase of only $1.57 billion. Similarly, stormwater harvesting contributes more water to the supply system than rainwater tanks (14.6 GL/yr on average in 2050) for only an extra $650 million to the cost of the current system. Consequently, from both a risk-based performance and an economic cost perspective, these results suggest that rainwater tanks are not a good supply augmentation option.

The slope of the lines between non-dominated alternatives in Figure 3.4 also draws attention to how much additional cost is required for an increase in reliability and robustness. For example, the very steep slope between Alternatives 4 (25 GL/yr desalination plant) and 5 (rainwater and stormwater) in 2030 illustrates that when moving from Alternative 4 to Alternative 5, the very small gain in reliability of less than 0.1%, which is also accompanied by no increase in robustness, comes at a relatively large increase in cost (of about $30 million). Conversely, a shallow slope of the line between non-dominated alternatives, for example between Alternative 1 (current system) and Alternative 3 (stormwater) in 2030 and 2050 (Figure 3.4), represents a large gain in reliability and robustness for a relatively small cost increase.

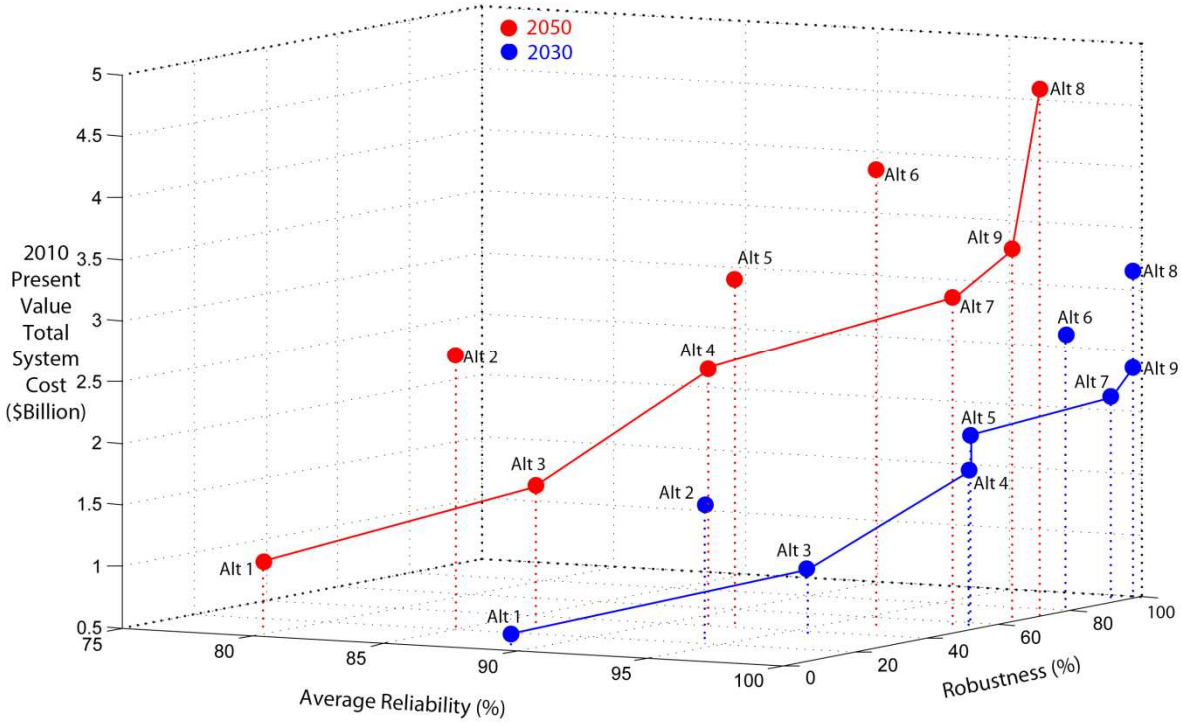

Figure 3.4: Median Average Reliability versus Robustness versus Median Average Present Value Cost for the Nine Alternatives for 2030 and 2050 (derived from 252 scenarios). The two solid lines join the non-dominated solutions across all three objectives for 2030 and 2050.

Finally, as illustrated in Table 3.7 and Figure 3.4, risk-based performance of the system generally decreases from 2030 to 2050, an indication that the longer-term projections for climate change and demand are likely to have a predominantly negative impact on water supply system security. Interestingly, Alternative 1 (current system) exhibits an increase in robustness from 9% in 2030 to 12% in 2050 (Table 3.7), but this reflects the possibility accounted for in this case study of a slightly-declining population for Adelaide through time and thus an improvement in system performance over time for some scenarios. Furthermore, considering the values for reliability, maximum duration of failure, and maximum vulnerability for each scenario and those values required for "acceptable performance", the limiting criterion for this case study is maximum vulnerability. This means that for any scenario where maximum vulnerability is < 27%, reliability is always > 95% and maximum duration of failure is always < 1 year. Therefore, if maximum vulnerability can be reduced, system robustness could be increased.

3.4.2 Variation in Criteria Across the 252 scenarios

The scatter plots derived from the 252 scenarios for all nine alternatives for average reliability, average maximum duration of failure, and average maximum annual vulnerability in 2050 are illustrated in Figures 3.5-3.7, respectively. Each scatter plot has three sections – the top section compares across the GCMs, the middle section across the SRES scenarios and the bottom section across the demands. Within each section, the six or seven different scenario options are illustrated, and within each of these, there are 9 columns of points that represent each of the alternatives (from Alternative 1 in the furthest left column through to Alternative 9 in the furthest right column). For example, in the top section of the figure, for each GCM and each alternative, the columns are comprised of 36 points (one for each of the 6 SRES scenarios combined with the 6 demands).

The scatter plots firstly confirm the general trends across the alternatives illustrated in Table 3.7. For example, Alternative 1 (current system) performs worst, while Alternatives 8 (rainwater, stormwater and 25 GL/yr desalination plant) and 9 (50GL/yr desalination plant) are the best performing alternatives (Figures 3.5-3.7), and all other alternatives are somewhere in-between. Secondly, the large ranges for each criterion across the scenarios confirm that reliability, maximum duration of failure, and maximum vulnerability are highly sensitive to future uncertainties. For example, for Alternative 1 (current system), average reliability ranges from about 35% to just less than 100% (Figure 3.5); average maximum duration of failure ranges from 5 to about 800 consecutive days (Figure 3.6); and average maximum annual vulnerability ranges from 1.7% to almost 100% of demand (Figure 3.7). However, there is often less variability in the better-performing alternatives, as these alternatives usually exhibit no failures for more scenarios, e.g., for the Very Low demand scenarios, average maximum annual vulnerability shows no variation from 0% for over half the alternatives, although variation in Alternative 1 (current system) is about 98% (Figure 3.7). Furthermore, a comparison between Alternatives 4 (25GL/yr desalination plant) and 5 (stormwater and rainwater) (which have reasonably similar water supply security), indicates there is less variability in the risk-based performance criteria for Alternative 4 for the Very

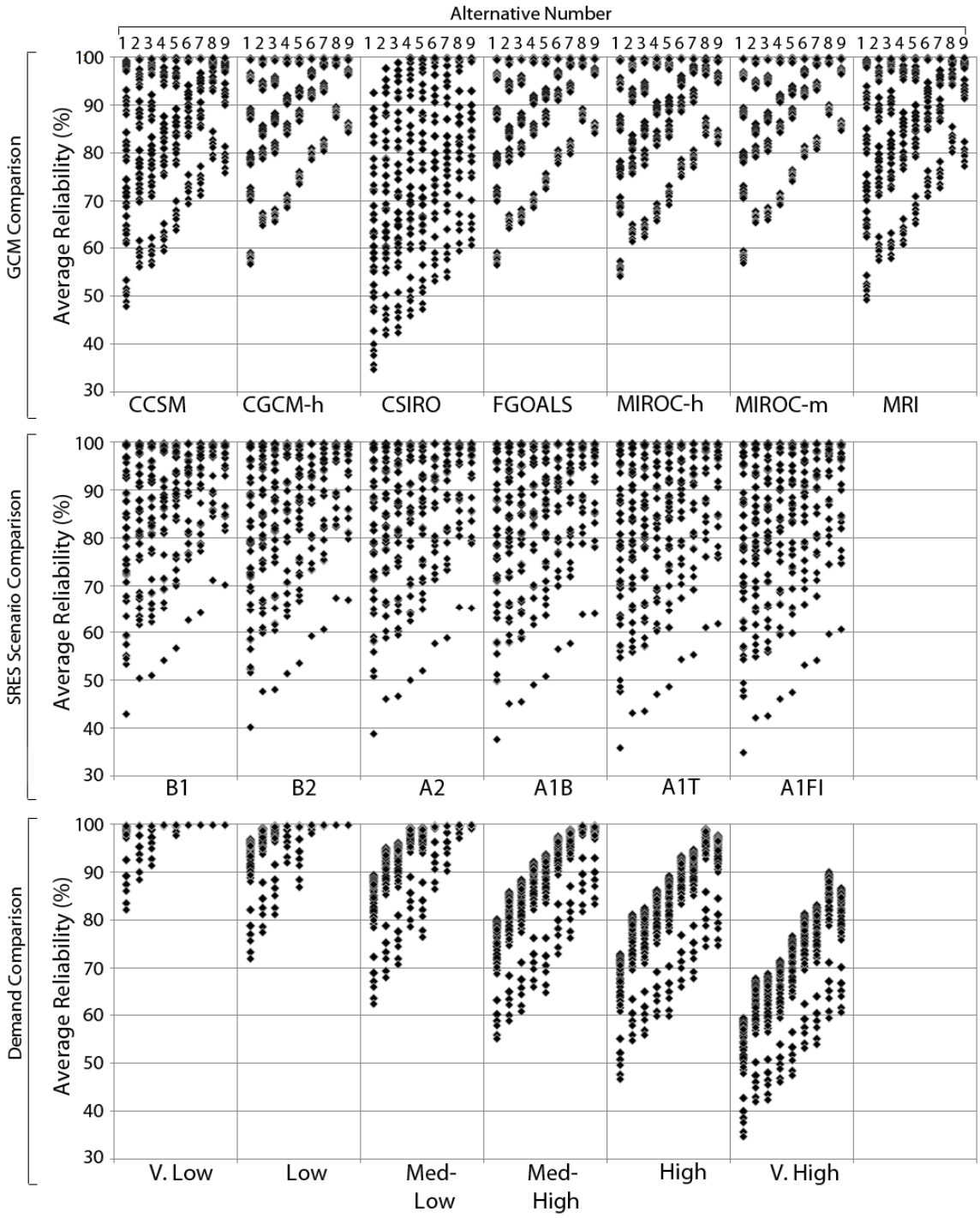

Figure 3.5: Scatter plot of average reliability in 2050 comparing the different GCMs (top section), different SRES scenarios (middle section) and different demands (bottom section). Within each section and for each different GCM, SRES scenario or demand, the alternatives are illustrated consecutively from one to nine in columns from left to right, as indicated at the top of the figure.

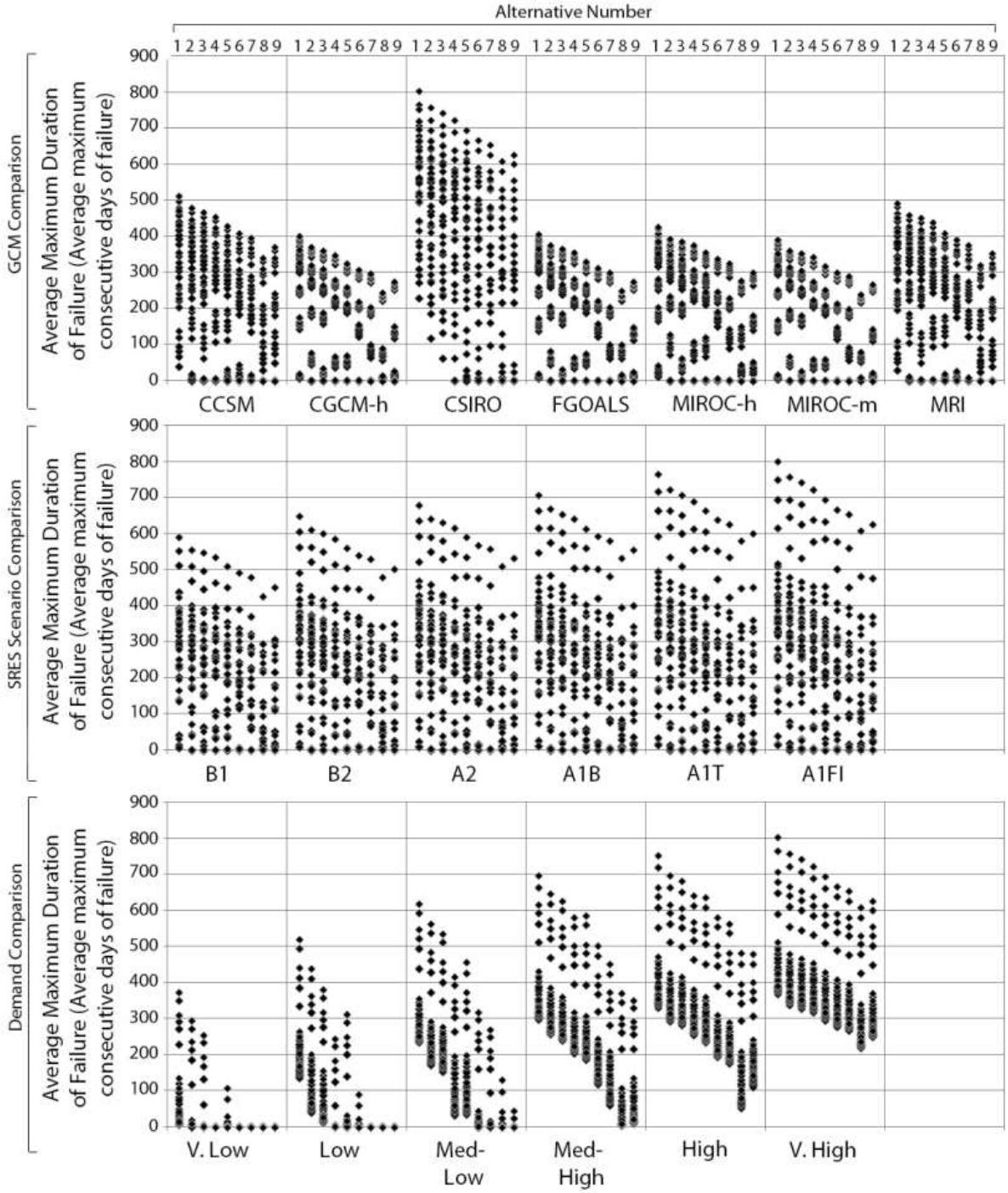

Figure 3.6: Scatter plot of average maximum duration of failure in 2050 comparing the different GCMs (top section), different SRES scenarios (middle section) and different demands (bottom section). Within each section and for each different GCM, SRES scenario or demand, the alternatives are illustrated consecutively from one to nine in columns from left to right, as indicated at the top of the figure.

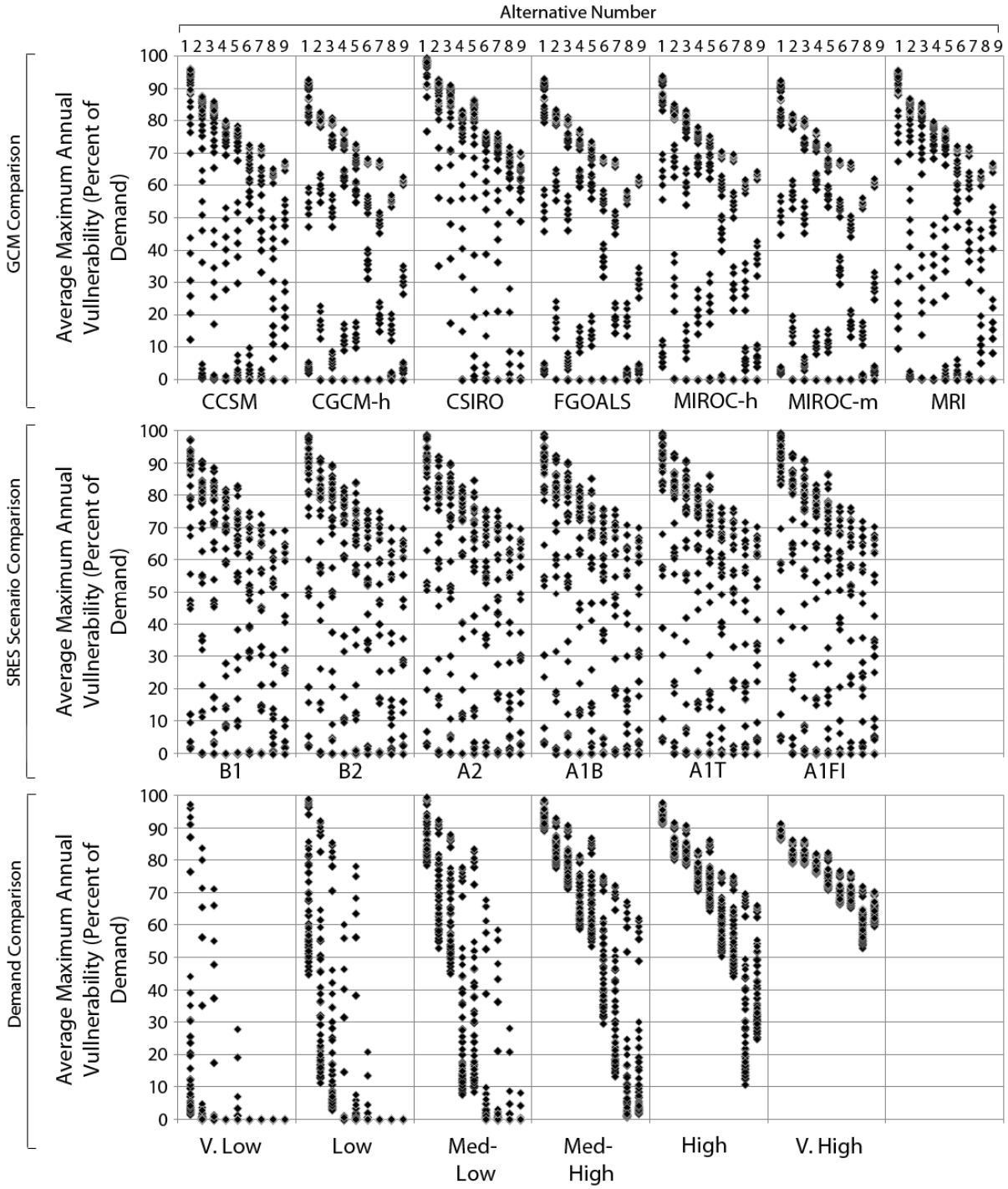

Figure 3.7: Scatter plot of average maximum annual vulnerability in 2050 comparing the different GCMs (top section), different SRES scenarios (middle section) and different demands (bottom section). Within each section and for each different GCM, SRES scenario or demand, the alternatives are illustrated consecutively from one to nine in columns from left to right, as indicated at the top of the figure.

Low and Low demand scenarios (Figures 3.5-3.7). For example, the average maximum annual vulnerability ranges from about 0-30% for Alternative 5 for the Very Low demand scenarios, compared with a constant 0% value for Alternative 4, inferring that Alternative 5 will be more sensitive to uncertainties in climate change than Alternative 4 (Figure 3.7). A similar trend is apparent when comparing Alternative 8 (rainwater, stormwater and 25 GL/yr desalination plant) to Alternative 9 (50GL/yr desalination plant), whereby Alternative 9 shows less variability; although this is noticeable only for the higher-demand scenarios, when these alternatives begin to exhibit failures (Figures 3.5-3.7). Given the climate-independent nature of desalination, these trends are as expected.

Thirdly, changes to demand result in the biggest changes to values for reliability, maximum duration of failure, and maximum vulnerability, followed by GCMs, and then SRES scenarios (Figures 3.5-3.7). For example, as demand shifts from the Very Low to Very High demands, average reliability drops from above 80% for all scenarios and all alternatives, to between about 35% and 90% for all scenarios and alternatives, whereas there is less change in average reliability when shifting between the GCMs and even less change when shifting between the SRES scenarios (Figure 3.5). In addition, when comparing across the GCMs, the CSIRO GCM projects the smallest values for average reliability and the largest values for average maximum duration of failure. For example, for Alternative 1, average reliability is 35% and the longest duration of failure is 803 days under CSIRO, but under any other GCM, the lowest reliability is 48% and the maximum length of failure is 511 days (Figures 3.5-3.6). It is to be expected that the CSIRO GCM results in the lowest performance, because it projects the most severe climate change scenario. However, the same pattern is not apparent for average maximum annual vulnerability, whereby the largest maximum annual vulnerabilities for the CSIRO GCM are relatively similar to those obtained using other GCMs (Figure 3.7). This is a result of demand having a much greater impact on average maximum annual vulnerability than it does on either reliability or average maximum duration of failure, which is illustrated in the bottom section of Figure 3.7 by the great changes to average maximum annual vulnerability as a result of the

demand scenario. This illustrates the importance of the impact of demand on average maximum annual vulnerability, which, as pointed out in Section 3.4.1, is an important conclusion from a management perspective, because maximum vulnerability is the limiting factor when calculating the robustness of an alternative.

Figures 3.5-3.7 also illustrate that the worst system performance exists for the CSIRO GCM, A1FI SRES, and Very High demand scenario. Furthermore, the extent to which selection of an alternative can limit unacceptable system performance under this scenario is poor. In fact, regardless of the SRES scenario and GCM, under the Very High demand, no alternative reaches the > 95% average reliability target (Figure 3.5), nor the ≤ 27% average maximum vulnerability target (Figure 3.7). Consequently, should the Very High Future demand scenario ensue, alternatives other than those proposed in this study would need to be considered to ensure acceptable system performance was achieved.

Thus, not only do these findings confirm that there is great variability of the criteria as a result of future uncertainties, they also demonstrate that GCM uncertainty and even more importantly, demand uncertainty, are critical for managing this system. For example, the CSIRO GCM gives high levels of the frequency of forecast failures and the maximum duration of forecast failures, while changes in demand affect both of these criteria, and have considerable implications for maximum vulnerability. Consequently, while outside the scope of most water authorities, climate scientists working toward improving GCMs may be able to reduce uncertainties associated with these model outputs. Alternatively, per capita consumption could be controlled through demand management schemes imposed by the water authority, which could reduce maximum vulnerability and raise the robustness of some of the alternatives. Also of comfort to water authorities is the knowledge that the impact of SRES scenarios, in which uncertainty is irreducible, is minor compared to the other sources of uncertainty over the timeframes considered.

3.4.3 Practical Management Implications

The very poor risk-based performance of Alternative 1 (current system) highlights the need to investigate augmentation of supply options for the current Adelaide southern system. Similarly, Alternatives 2 (rainwater) and 3 (stormwater) have such poor risk-based performance in both 2030 and 2050, that these alternatives by themselves are unlikely to be appropriate to ensure acceptable performance of the system in the future. However, in the mid-term (2030 planning horizon), all other alternatives exhibit reasonable risk-based performance for at least half of the future scenarios, while in 2050 "acceptable performance" is achieved for at least half of the future scenarios for Alternatives 7 (stormwater and 25 GL/yr desalination plant), 8 (rainwater, stormwater and 25 GL/yr desalination plant) and 9 (50 GL/yr desalination plant). However, when taking the trade-offs between reliability, robustness and cost into account, Alternative 8 should not be considered, as discussed previously. Consequently, in the mid-term, Alternatives 4 (25 GL/yr desalination plant) and 7 (stormwater and 25 GL/yr desalination plant) would be most appropriate, while Alternative 7 (stormwater and 25 GL/yr desalination plant) or Alternative 9 (50 GL/yr desalination plant) would be appropriate in the longer-term. However, Alternative 9 is a large-scale, long-lived, centralized source that is not conducive to flexible management. Consequently, if less severe climate change impacts and lower demands eventuate, the two-pronged approach of stormwater and a smaller desalination plant may be more appropriate (with one of these sources implemented now and the other source only if it is needed). However, in 2050, even these best-performing alternatives will not perform at an acceptable level for some future scenarios representing conditions of higher GHG emission futures, greater projected impacts of climate change and greater demands.

3.5 Summary and Conclusions

A city's water supply system has traditionally been planned through the assessment of water supply security. However, the inclusion of non-traditional water sources and the need to account for climate change impacts means assessing water supply security is now more challenging. In modelling urban water supply systems, the inclusion of non-traditional water sources increases complexity,

while there is greater uncertainty through incorporating climate change impacts, making the assessment of urban water supply security more challenging. Therefore, in order to address this issue, an integrated framework for assessing urban water supply security of systems with non-traditional sources under climate change was introduced in this paper and applied to a case study based on the southern Adelaide water supply system.

The integrated framework was based on the steps of systems analysis, with additional complexity (associated with including non-traditional sources as alternatives) developed in Step 4 - assessing the alternatives in terms of nominated criteria. Additional complexity occurred at a number of steps of the assessment stage, namely (a) defining end uses in terms of potable versus non-potable, localized versus centralized, and climate-independent versus climate-dependent; (b) selecting an appropriate time step for accurately simulating yield from water supply sources while keeping in mind computational effort; (c) defining supply sources in terms of centralized versus decentralized, climate-dependent versus climate-independent, and pervious versus non-pervious catchments; and (d) integrating sources and defining source priority. The uncertainty associated with assessing the impacts of climate change was incorporated through a sensitivity-based scenario analysis. Specifically, the uncertainty sources of (a) GHG emissions scenarios, (b) GCMs, (c) downscaling methods, (d) hydrological models, and (e) demand were incorporated. An important component of the sensitivity analysis was the ability to compare the uncertainty sources in terms of their magnitude of impact on water supply security, which has benefits for planning and managing urban water supply systems.

For the case study, five criteria, namely reliability, maximum duration of failure, maximum vulnerability, robustness, and present value cost, were used to represent the two objectives of maximizing risk-based performance and minimizing economic cost. Nine alternatives, comprised of existing traditional water sources and new non-traditional water sources were modelled for Adelaide's southern water supply system in WaterCress. Each alternative was trailed under 252

different future scenarios that varied based on different demand and climate change projections. This extensive, scenario-based sensitivity analysis helped to determine how robust each alternative was to future uncertainties. For each of the 252 scenarios, 1,000 30-year stochastic rainfall time series were modelled to account for the large uncertainty in Adelaide's natural rainfall variability.

The results from the case study indicated that there was usually a trade-off between cost and risk-based performance, e.g. a better performing alternative in terms of reliability, duration of failure, vulnerability, and robustness was usually more expensive. However, some alternatives were completely dominated by other alternatives for all criteria. These dominated alternatives were usually the ones that included household rainwater harvesting. Keeping this in mind, and the fact that some alternatives did not provide "acceptable performance" (e.g. Alternative 3 - stormwater), then for the mid-term, Alternatives 4 (25 GL/yr desalination plant) and 7 (25 GL/yr desalination plant and stormwater) would be most appropriate, while Alternative 7 (25 GL/yr desalination plant and stormwater) or Alternative 9 (50 GL/yr desalination plant) would be appropriate in the longer-term, although Alternative 9 lacks the benefits of flexibility. The case study findings also illustrated the significant impact of demand uncertainty on system performance. As this uncertainty is at least partially within the control of the water authority, demand management could be an option worth considering for increasing future system performance, especially since maximum vulnerability was the factor controlling system robustness.

There are limitations of this case study that, while beyond the scope of this paper, could be addressed with future research. Firstly, the objectives could be expanded to address the growing awareness of sustainability issues [*Sahely and Kennedy*, 2007], which calls for consideration of additional performance criteria when investigating appropriate supply augmentation strategies, such as minimizing environmental impacts. The inclusion of such objectives could potentially alter which alternative a decision-maker selects. For example, should minimizing greenhouse gas emissions be an objective, the high-energy of desalination plants would render these alternatives as less

favourable than indicated by this study. Secondly, per capita consumption was classified as an uncertainty in this paper, rather than a potential management option. In doing so, the economic costs of reducing per capita consumption through demand management were not accounted for, which could be addressed in future work. Thirdly, if demand management was considered an alternative, along with operational strategies and a larger number of potential capacities of supply augmentation options, more alternatives than the nine presented in this paper could be considered. This could lead to the identification of alternatives that outperform those listed herein. However, analysing more alternatives would require increased computational effort. Consequently, with such a large number of possible alternatives, and with multiple criteria requiring evaluation, multi-objective optimization (MOO) may prove a useful tool. MOO will not produce a single, optimal alternative, because conflicting criteria mean it is unlikely that one solution will achieve the best value for all criteria. However, MOO can produce a Pareto optimal front containing only non-dominated solutions (that cannot be improved in one objective without degrading at least one other objective), to illustrate trade-offs between alternatives for multiple criteria.

In summary, in this paper, an integrated framework for assessing water supply security of a city with non-traditional sources under climate change was introduced. Further, the approach was demonstrated for a case study based on the southern Adelaide water supply system, explicitly detailing the challenges faced in doing so and exploring the resulting management implications.

Acknowledgements

We acknowledge the financial support of this research by the University of Adelaide and eWater CRC. Thanks to David Cresswell and Richard Clark for their ongoing support of WaterCress and Sri Srikanthan for assistance with Stochastic Climate Library. We also thank the three anonymous reviewers for their contributions in improving this paper considerably.

Appendices Supporting Journal Paper 2

Appendix B provides information on the climate-independent and climate-dependent water sources for the case study of this paper.

Appendix C details the development of stochastic rainfall time series for the case study of this paper.

Appendix D includes further information on the economic costs derived for the case study in this paper.

Chapter 4

4 Including adaptation and mitigation responses to climate change in a multi-objective evolutionary algorithm framework for urban water supply systems incorporating GHG emissions (Paper 3)

Statement of Authorship

Title of Paper	Including both adaptation and mitigation responses to climate change in a MOEA framework for urban water supply systems incorporating GHG emissions
Publication Status	○ Published, ○ Accepted for Publication, ◉ Submitted for Publication, ○ Publication style
Publication Details	Paton, F.L., H.R. Maier, and G.C. Dandy, Including adaptation and mitigation responses to climate change in a multi-objective evolutionary algorithm framework for urban water supply systems incorporating GHG emissions. Submitted to Water Resources Research on 12th May, 2014.

Author Contributions

By signing the Statement of Authorship, each author certifies that their stated contribution to the publication is accurate and that permission is granted for the publication to be included in the candidate's thesis.

Name of Principal Author (Candidate)	Fiona Paton		
Contribution to the Paper	Designed general methodology, derived costs and GHG emissions for case study, conducted modeling and analysis, and wrote manuscript.		
Signature		Date	11/06/2014

Name of Co-Author	Holger Maier		
Contribution to the Paper	Supervised manuscript preparation and reviewed draft.		
Signature		Date	11/06/2014

Name of Co-Author	Graeme Dandy		
Contribution to the Paper	Supervised manuscript preparation and reviewed draft.		
Signature		Date	11/06/2014

Name of Co-Author			
Contribution to the Paper			
Signature		Date	

Abstract

Cities around the world are increasingly involved in climate action and mitigating greenhouse gas (GHG) emissions. However, in the context of responding to climate pressures in the water sector, very few studies have investigated the impacts of changing water use on GHG emissions, even though water resource adaptation often requires greater energy use. Consequently, reducing GHG emissions, and thus focusing on both mitigation and adaptation responses to climate change in planning and managing urban water supply systems, is necessary. Furthermore, the minimisation of GHG emissions is likely to conflict with other objectives. Thus, applying a multi-objective evolutionary algorithm (MOEA), which can evolve an approximation of entire tradeoff (Pareto) fronts of multiple objectives in a single run, would be beneficial. Consequently, the main aim of this paper is to incorporate GHG emissions into a MOEA framework to take into consideration both adaptation and mitigation responses to climate change for a city's water supply system. The approach is applied to a case study based on Adelaide's southern water supply system to demonstrate the framework's practical management implications. Results indicate that trade-offs exist between GHG emissions and risk-based performance, as well as GHG emissions and economic cost. Solutions containing rainwater tanks are expensive, while GHG emissions greatly increase with increased desalinated water supply. Consequently, while desalination plants may be good adaptation options to climate change due to their climate-independence, rainwater may be a better mitigation response, albeit more expensive.

4.1 Introduction

Cities around the world are increasingly engaged in climate action and mitigating greenhouse gas (GHG) emissions [*Miller et al.*, 2013; *National Research Council*, 2009]. However, *Rothausen and Conway* [2011] conclude that energy use and GHG emissions associated with water management are poorly understood and have only been partially considered in water resources management. Consequently, the consideration of GHG emissions in the water sector is both timely and necessary,

particularly because of: (1) the high sensitivity of the water sector to climate change [*Rothausen and Conway*, 2011]; and (2) the close link between water and energy [*Stokes and Horvath*, 2009; *Stokes et al.*, 2014], often referred to as the water-energy nexus and referencing the use of water in many processes of electricity generation, as well as the use of energy in water supply and wastewater treatment [*Miller et al.*, 2013]. In addition, energy and carbon use in the water sector is both intensive [*Roshani et al.*, 2012] and increasing [*Rothausen and Conway*, 2011].

The trend of increasing energy use in the water sector is expected to continue, because as *Rothausen and Conway* [2011] note, water resource adaptation will often mean that more energy is required to meet rising demand, regulatory standards, and the effects of climate change. For example, some adaptation options to climate change, such as desalination and pumping, are very energy intensive. This means that GHG emissions are also likely to rise, given the extensive use of non-renewable sources, such as fossil fuels, to produce energy around the world. It is therefore concerning that water resource adaptation will most likely increase GHG emissions, given that: (a) GHG emissions contribute to climate change; (b) climate change will in many places exacerbate water scarcity; and (c) water scarcity is a driver for water resource adaptation. Consequently, reducing GHG emissions, and focusing on both mitigation and adaptation responses to climate change in planning and managing urban water supply systems, is necessary.

While the consideration of GHG emissions from urban water supply systems is both timely and necessary, the minimisation of GHG emissions is likely to conflict with other objectives, such as maximising water supply security. Thus, multiple objectives will need to be balanced and negotiated [*Reed et al.*, 2003]. Balancing such objectives can be greatly aided by the application of multi-objective evolutionary algorithms (MOEAs) because they can rapidly evolve an approximation of entire tradeoff (Pareto) fronts of multiple objectives in a single run [*Reed et al.*, 2003].

In recent years, a number of MOEA studies concerned with the design and operation of water distribution systems have considered GHG emissions reduction as one of the objectives [*Stokes et*

al., 2014; *Wu et al.*, 2009; 2010; *Wu et al.*, 2013; *Wu et al.*, 2012], or as a component of a broader environmental objective [*Herstein et al.*, 2009; 2011; *Herstein and Filion*, 2011]. Similarly, *Roshani et al.* [2012] examined the cost of GHG emissions (that is the cost associated with a carbon price levied on electricity used for pumping water) as a component of total system costs for a water distribution network expansion in a single-objective, evolutionary algorithm optimisation problem. However, this focus on water supply infrastructure ignores a number of important issues related to the minimisation of GHG emissions from urban water supply systems, such as in assessing alternative water supply sources (e.g., desalination plants) that may be introduced as adaptation responses to climate change for a city's water supply system. Consequently, there is a need to explore the optimal trade-offs between GHG emissions and other objectives, such as minimising cost and maximising water supply security, for urban water supply systems at the regional scale.

A number of studies have examined GHG emissions of regional-scale urban water supply systems [*Barjoveanu et al.*, 2014; *Lundie et al.*, 2004; *Sahely et al.,* 2005; *Sahely and Kennedy*, 2007; *Stokes and Hovarth*, 2006; *Slagstad and Brattebø*, 2014]. However, while these studies thoroughly explore GHG emissions from an environmental impact perspective, they do not include multiobjective optimisation, let alone a MOEA. In fact, of the MOEA studies that have focused on regional scale water supply system management and planning, none has considered GHG emissions reduction as an objective [*Kasprzyk et al.*, 2009; *Kasprzyk et al.*, 2012; *Kasprzyk et al.*, 2013; *Mortazavi et al.*, 2012]. Consequently, in order to address this shortcoming, the main aim of this paper is to develop a MOEA framework for urban water supply systems that takes into consideration both adaptation and mitigation responses to climate change. The specific objectives are: (1) to use GHG emissions as an objective function and to include both mitigation and adaptation options to climate change in a MOEA framework for urban water supply systems at the regional scale; (2) to evaluate the implications of optimising for GHG emissions on economic cost and water supply system security; and (3) to demonstrate practical management implications of the framework by applying it to a case study based on Adelaide's southern water supply system. While the approach is applied to a case

study, its generic nature means it could be readily applied to other city's water supply systems around the world.

The remainder of this paper is organized as follows. In Section 4.2, the issues and challenges of incorporating GHG emissions into multiobjective optimisation of regional water supply systems are highlighted. The case study is then introduced in Section 4.3, followed by a description of the MOEA framework applied to the case study to demonstrate the value of the approach (Section 4.4). The results are discussed in Section 4.5. Section 4.6 summarises the paper, focusing on the key conclusions drawn.

4.2 Incorporation of GHG emissions in the multiobjective optimisation of regional water supply systems

As mentioned in the Introduction, the adaptation of city water supply systems to climate change can often lead to an increase in energy and GHG emissions, which thus conflicts with any aims by the water sector to mitigate climate change. Therefore, to balance adaptation to and mitigation of climate change, it is not only necessary to estimate how well solutions perform under future climate change conditions (i.e. adaptation), but also the quantity of GHG emissions that are associated with each solution (j.e. mitigation). Furthermore, given that there are (1) other objectives to consider, such as economic cost, and (2) a great number of potential solutions, there is a compelling argument for applying multiobjective optimisation of regional water supply systems incorporating GHG emissions. However, this is not a straightforward task.

The first difficulty for modelers is the issue of how to evaluate GHG emissions, particularly given the uncertainty in estimating the quantity of emissions that are created by any given process. In accounting for GHG emissions of an urban water supply system, operational GHG emissions need to be estimated for existing supply sources, and both capital and operational GHG emissions need to be estimated for new supply sources. However, GHG emissions data specific to supply sources may not be readily available (particularly for non-traditional sources, such as stormwater harvesting).

Furthermore, if these data were available, they may be heavily dependent on local conditions (e.g. the rate of emissions), so transferring data from a case study in one city to another may be inappropriate. To overcome this problem, capital emissions for supply sources can be derived from embodied energy of material use, while operating emissions for supply sources can be derived from annual energy consumption [*Wu et al.,* 2010]. However, the modeler then faces the issue of estimating energy use and selecting an appropriate emission factor (tonnes of CO_2 equivalent emissions per megawatt hour of electricity generated), which will be heavily dependent on the fuel mix used: electricity generated predominantly from fossil fuels will have a much higher emission factor than electricity generated from renewable sources, such as wind energy. Furthermore, the sources of electricity for a particular city may vary in time and space, so more detailed, coupled modelling studies that include electricity generation may thus be required to increase our understanding of this topic in the future [*Stokes et al.*, 2014].

There is also the issue of whether GHG emissions estimated to occur in the future should be discounted. *Wu et al.* [2010] explain that a discount rate of zero (i.e. no discounting) is very often used for GHG impact evaluation, reflecting the notion that future GHG emissions do not have a lower impact than emissions at the current time. However, a positive discount rate may be appropriate for GHG emissions if, for example, technology advancement can significantly reduce the cost of GHG abatement or carbon sequestration in the future [*Wu et al.* 2010] or one takes into account that all GHG emissions undergo natural decay in the atmosphere. If so, then as is the case with discounting economic costs, a decision must be made as to what is an appropriate discount rate to apply. For economic costs, high discount rates match the prevailing rates in the private sector but discourage investment in long-term conservation of natural resources; while low discount rates, which are less likely to be justified economically, are set to favor long-term environmental conservation projects [*Cai et al.*, 2002]. On the contrary, when discounting GHG emissions of water supply systems, the application of a positive discount rate, particularly a high discount rate, will favor sources with high operational emissions and lower embodied energy (such as desalination

plants), because the future GHG emissions will be discounted, thus reducing the total GHG emissions of these sources.

Finally, GHG emissions or energy data might not be readily available, or easy to estimate, for all components of a water supply system. Consequently, modelers may have to work with imperfect GHG emissions data for some supply sources, until further research into energy and/or GHG emissions for such water supply sources occurs.

4.3 Case Study: The Southern Adelaide System

With a population of about 1.2 million people, the capital city of South Australia - Adelaide (Figure 4.1), has an average water demand over the past 20 years of about 200 gigalitres per year (GL/yr) [*Government of South Australia*, 2009]. However, this case study focuses on Adelaide's southern water supply system, which supplies approximately half of Adelaide's demand, with an indicative demand area illustrated in Figure 4.1. Furthermore, in the case study, the current system refers to Adelaide's southern water supply system as it was in 2009, which included three local catchment reservoirs and water pumped about 50 kilometers (km) from the River Murray via the Murray Bridge-Onkaparinga Pipeline.

There are three local catchment reservoirs in Adelaide's southern water supply system – Myponga, Mount Bold and Happy Valley (Figure 4.1), which can hold up to a total of 85 GL of water. Myponga is independent of the other two reservoirs, with water being treated at the Myponga Water Treatment Plant (WTP) before being released into the mains distribution network. However, water from Mount Bold Reservoir must be released downstream and diverted at Clarendon Weir via the Horndale Flume to Happy Valley Reservoir before being treated at Happy Valley WTP and released into mains distribution (Figure 4.1). Happy Valley Reservoir also receives water from Clarendon Weir Catchment (Figure 4.1), which is similarly transferred via the Horndale Flume. For a more thorough description of the reservoir properties and operations see *Paton et al.* [2013].

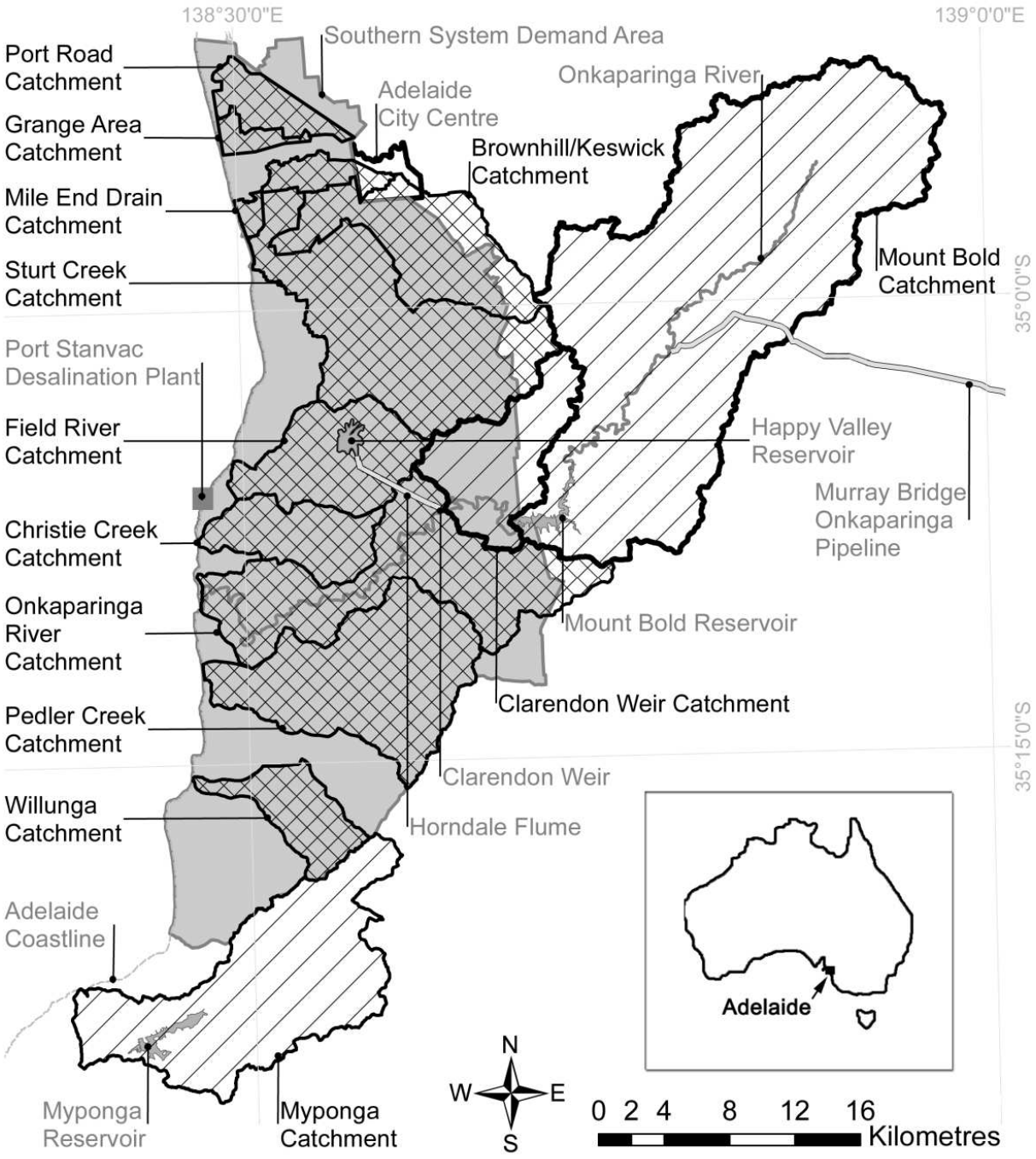

Figure 4.1: Map of the existing Adelaide southern water supply system, showing reservoirs, reservoir catchments, major rivers, pipelines, and an indicative southern system demand area (illustrated by grey shading). The Port Stanvac desalination plant and the ten southern water supply system stormwater harvesting scheme catchments are also shown. Inset is a map of Australia highlighting the location of Adelaide.

Water from the River Murray is transferred to the southern system via the 48 km-long Murray Bridge-Onkaparinga (MBO) Pipeline (Figure 4.1). It is released upstream of Mount Bold Reservoir (Figure 4.1), where it can be stored before treatment and distribution. As, explained in *Paton et al.*

[2013], supply from the River Murray for Adelaide is capped at 650 GL over 5 years under the terms of SA Water's license. While a license does not always guarantee supply, Adelaide's River Murray license has previously always been met, with up to 90% of Adelaide's demand being catered for by the River Murray in dry years [*Government of South Australia*, 2009].

However, to respond to the uncertainties of climate change in the future and an increasing demand due to population growth, supply augmentation for the current Adelaide southern water supply system is necessary to avoid demand shortfall [*Paton et al.*, 2013]. *Maier et al.* [2013] illustrated that a diversification of water supply sources could help the system meet future demand shortfall through an assessment of five feasible sources for water supply, which were comprised of the two current supply sources and three potential supply sources. The current sources included pumping from the River Murray via the MBO Pipeline (Figure 4.1) and local catchment reservoirs (Figure 4.1). Potential supply sources included a reverse osmosis (RO) desalination plant at Port Stanvac (Figure 4.1), stormwater harvesting schemes that collect water from ten catchments extending from Port Road catchment in the north to Willunga catchment in the south (Figure 4.1), and household rainwater tanks.

This paper extends the current understanding of future options for Adelaide's current southern water supply system by using optimisation, specifically a multi-objective evolutionary optimisation approach, to search a greater number of potential feasible alternatives (including supply operations, as well as increased supply augmentation options), rather than simply analyzing a limited number of discrete options. Demand-side management options are not examined, as they are outside the scope of this paper. However, as the consideration of water demand reduction strategies can have significant urban water system-wide benefits (in terms of the environment and economic cost) [*Sahely and Kennedy*, 2007], they should be included in future studies. A 40-year planning horizon from 2010 to 2050 was used to assess the alternatives.

4.4 Methods

4.4.1 Objectives and Constraints

The selected objectives for the case study include: (1) to minimise system vulnerability; (2) to minimise economic cost; and (3) to minimise GHG emissions. Constraints on system reliability and duration of failure were also applied. Details of how the objectives and constraints were calculated are given in Sections 4.4.4 and 4.4.5. It should be noted that while the objectives and constraints were kept constant in this study, the benefit of using an adaptive decision-making framework that continually updates the objectives and constraints and enables the GHG emissions objective to be readily assimilated into existing trade-off studies [*Kasprzyk et al.*, 2012] could be explored in future studies.

4.4.2 Water Supply Alternatives

The water supply alternatives were comprised of both supply source selection and supply system operation. For the supply sources, options included the existing River Murray supply and the three local catchment reservoirs (see Section 4.3), as well as the three potential sources of a desalination plant, stormwater harvesting schemes, and household rainwater tanks.

The capacity of the Port Stanvac desalination plant can range between 100 to 500 megalitres per day (ML/day) in 50 ML/day increments (Table 4.1). These capacities were nominated as they provided a good range of feasible sizes for desalination plants based on current and planned expansion capacities of desalination plants in Australia. However, these capacities were halved for the case study, because the southern system accounts for approximately half of Adelaide's demand. The option of not including a desalination plant was also considered (Table 4.1).

For stormwater, there were four schemes for the southern system that could be selected, namely Brownhill-Keswick, Sturt River, Field River, and Pedler Creek (Table 4.1). As explained by *Beh et al.* [2014] these schemes represent a total of ten stormwater catchments that predominantly fall in the indicative southern system demand area (Figure 4.1).

Table 4.1: Values for options of supply source augmentation and supply system operation defined for the case study

Option	Values for Option
Desalination Plant Capacity (ML/day)	0, 100, 150, 200, 250, 300, 350, 400, 450, 500
Stormwater Schemes	Brownhill-Keswick, Sturt River, Field River and Pedler Creek
Rainwater Tank Size (m^3)	0, 1, 2, 3, 4, 5, 6, 7, 10, 15, 22.5, 27
Rainwater Tank Roof Connectivity (%)	50, 60, 70, 80, 90
Rainwater Tank End Use	Garden, Toilet, Laundry Cold Water, Hot Water
Supply Priority	1, 2, 3, …, 7
Supply Weight	1, 2, 3, …, 10
Mount Bold Level to trigger River Murray Pumping (monthly values, %)	0, 5, 10, …, 100

Rainwater tanks could be selected as a supply source, based on a Government policy introduced in 2006 requiring most new homes and home extensions in South Australia to have rainwater tanks installed [*Government of South Australia*, 2009]. The rainwater tanks could take one of 11 sizes, ranging from 1 m^3 up to 27 m^3 (Table 4.1), as these are feasible sizes when taking the physical size constraints of residential backyards into account. In addition, the fraction of roof connected to the tank could range from 50% up to 90% (Table 4.1).

When rainwater tanks and harvested stormwater schemes were both selected as supply options, the roof connectivity for stormwater harvesting was reduced because less roof runoff was assumed to be entering the stormwater collection network. Finally, while the rainwater tank was always assumed to be connected to the garden, it could also be connected to one or more of three indoor end uses, namely the toilet, laundry cold water, and hot water (Table 4.1).

In addition to decisions regarding the size and properties of supply sources, alternatives were also a function of different operating rules of the system. These included determining: (1) which sources would have priority of supply, if water was available from more than one source; (2) whether more water should be drawn from one source than another if sources had equal priority; and (3) what level Mount Bold Reservoir should reach to trigger pumping of water from the River Murray. For priority of supply, options ranged from one to seven (Table 4.1), with one being the highest priority and seven being the lowest. For supply weights, options ranged from one to ten (Table 4.1), with weights being considered relative to each other, so that a source of weighting five would supply five times the amount of water of a source of weighting one (provided the sources had equal priority). For the Mount Bold Reservoir target level (to trigger pumping from the River Murray), each month of the year was assigned a value, ranging from 0% to 100% in 5% increments (Table 4.1). Given the number of decision variables, the decision space for the optimisation problem was 3.26×10^{33}, clearly justifying the need to use MOEAs to efficiently search the space and produce an approximation of the Pareto Front.

4.4.3 Simulation Model

The water resources model WaterCress (www.waterselect.com.au/watercress/watercress.html) was selected to evaluate alternatives because the model can (1) cater for the alternative water sources and supply operations of the case study (see Section 4.4.2), (2) easily incorporate multiple scenarios (see Section 4.4.7), and (3) be easily linked with an optimisation module through the use of text input and output files. It is also freely available, locally supported in Adelaide, and has been previously applied to this case study [*Beh et al.*, 2014; *Maier et al.*, 2013; *Paton et al.*, 2013]. These publications provide further details of the model, its benefits, and its suitability for the case study.

The WaterCress representation of Adelaide's southern water supply system consisted of two major components – demand and supply. Demand was a function of both population and per capita consumption. The population in 2050 was assumed to be approximately 775,000 people, about half

of Adelaide's 2050 population based on the median population projection (derived from 72 projections) [*Australian Bureau of Statistics,* 2008]. For the optimisation process, per capita consumption was assumed to remain constant over the planning horizon at 494 litres per capita per day (Lcd) [*Paton et al.,* 2013]. This is a conservative approach to demand projection; however, options considering demand reduction through water savings were investigated post-optimisation (see Section 4.4.7). In the WaterCress model, per capita consumption was split into five categories (Type I-V) to account for residential and non-residential, potable and non-potable, and climate-dependent and climate-independent demands (Table 4.2). These were important delineations to make in terms of allocating water sources to appropriate end use categories (Table 4.2). Firstly, rainwater was only used for residential use, rainwater and harvested stormwater were both considered non-potable, and garden demand varied considerably depending on the season (see *Paton et al.* [2013]), so this variability needed to be modelled.

In terms of supply, sources could be considered as climate-independent or climate-dependent. The River Murray and desalination plant were both classified as climate-independent sources, which is intuitive for the desalination plant but not so for the River Murray. However, in the past, River Murray supply for Adelaide has depended on licenses, rather than climate, and this supply is guaranteed [*Paton et al.*, 2013]. In addition to the Mount Bold level to trigger River Murray pumping, River Murray supply was also constrained to 447 ML/day (the pumping capacity of the MBO pipeline), and 325 GL over five years. This second constraint represented half of the 5-year rolling license (see Section 4.3) and was a necessary simplification because WaterCress could not incorporate a rolling license. The local catchment reservoirs, stormwater harvesting schemes and household rainwater tanks were considered to be climate-dependent sources. Consequently, runoff from their catchments (either pervious, impervious or both in the case of stormwater), were modelled as a function of rainfall and evaporation, which were sourced from eight representative climate data sites across the indicative demand area and local reservoir catchments (Figure 4.1).

Table 4.2: Demand type and water source for the five demand categories defined for the Adelaide southern system case study

Category	Demand Type	Water Sources
Type I	Residential – Potable	River Murray, Local Catchment Reservoirs, Desalination Plant
Type II	Residential (Garden) Non-potable, Climate-dependent	Rainwater, River Murray, Local Catchment Reservoirs, Desalination Plant
Type III	Residential (Toilet) - Non-potable, Climate-independent	Rainwater, River Murray, Local Catchment Reservoirs, Desalination Plant
Type IV	Non-residential – Potable	River Murray, Local Catchment Reservoirs, Desalination Plant
Type V	Non-residential – Non-potable	Stormwater, River Murray, Local Catchment Reservoirs, Desalination Plant

Details on the rainfall-runoff models and the rainfall and evaporation data for this case study can be found in *Paton et al.* [2013] and *Beh et al.* [2014].

The impact of climate change on local catchment reservoirs, stormwater harvesting schemes and household rainwater tanks was projected by firstly considering outputs from different world development pathways, represented by SRES scenarios, and different global circulation models (GCMs). For the optimisation process, the A1B emissions scenario was used in combination with the CCSM3 GCM. These selections proved to return middle of the range estimates for water supply security when compared with a selection of SRES scenarios and GCMs for a number of different water supply configurations. Alternative SRES scenarios and GCMs were considered post-optimisation (see Section 4.4.7). The constant scaling or delta-change approach was then applied to obtain local rainfall and evaporation responses to these climate change projections, as this has been used for this case study previously [*Paton et al.*, 2013].

One thousand 30-year stochastic rainfall time series were generated, ensuring the impact of natural rainfall variability was considered, as this number of replicates guaranteed that the important statistical characteristics of the historical datasets were preserved in the generated datasets (see *Paton et al.,* [2013] for more detail). However, due to computational constraints, only 10 stochastic time series were selected for the optimisation process, with the full 1000 stochastic time series subsequently applied in the post-optimisation robustness assessment (see Section 4.4.7). The 10 time series were selected to be representative of the 1000 series for a range of different water supply system configurations with different combinations of sources. This was achieved by minimising the difference between the average maximum annual vulnerabilities obtained using the 10 selected time series and the 1000 time series with the aid of a genetic algorithm.

Finally, the supply priorities and weights were applied (decision variables in the optimisation process), to integrate the supply sources in the WaterCress model. However, given the limited capacity of rainwater tanks to store water, if rainwater was available, it was always used as a first priority for its allocated household uses.

4.4.4 Objective Function Evaluation

Synopses of how vulnerability and economic cost were evaluated for the case study are provided below. More extensive detail is provided for the GHG emissions evaluation due to the significance of incorporating the reduction of GHG emissions as an objective in this paper.

4.4.4.1 Vulnerability

The vulnerability objective was represented by the maximum annual vulnerability as a percentage of demand averaged over the 10 stochastic time series as follows:

$$M.Vul = \frac{\sum_{t=1}^{T} \max\left(\left\{\frac{V_{at}}{D}\right\}\right)}{T} * 100 \quad (4.1)$$

where M.Vul was the average maximum annual vulnerability given as a percentage; V_{at} was the volume by which demand exceeded supply (given a failure occurred) for year a of the stochastic time series (a=1-30) and time series t (t=1-10); D was the average annual demand; and T was the number of time series evaluated (T=10).

4.4.4.2 Economic Cost

Economic costs for existing supply sources (River Murray and local catchment reservoirs) were purely a function of operational costs over the 40-year planning horizon, as their capital costs were considered sunk costs. However, economic costs for new supply sources were a function of both the capital costs incurred in 2010 and operational costs over the planning horizon. Consequently, the 2010 present value total system cost was calculated as:

$$\text{2010 PV Total System Cost} = \text{2010 PV } OC_{[RM+Res+Des+SW+RW]} + CC_{[Des+SW+RW]} \quad (4.2)$$

where 2010 PV $OC_{[RM+Res+Des+SW+RW]}$ was the sum of the 2010 PV operational costs for the five supply sources and $CC_{[Res+SW+RW]}$ was the sum of the capital costs for desalination, stormwater and rainwater. Due to the extensive economic cost data for supply sources, a summary of economic costs for each supply source is included in Table 4.3, while a full derivation is provided as auxiliary material. An indicative cost of 12 cents per kilowatt hour (c/kWh) was assumed as the purchase price for electricity, which is slightly higher than SA Water's average electricity purchase price of approximately 10 c/kWh (see SA Water's 2010 annual report at www.sawater.com.au), so as to account for potential electricity price increases in South Australia over the planning horizon. To convert future operational costs to their 2010 present value, a discount rate of 4% was used for the first five years, from 2015 to 2035 (inclusive) the discount rate was reduced to 3%, while this was reduced further to 2% from 1st May 2035 to the end of the planning horizon [*Weitzman*, 2001]. Application of a declining discount rate (DDR) is supported by *Rambaud and Torrecillas* [2005] because of (1) uncertainty about the future, (2) future fairness and (3) observed individual choice.

Table 4.3: Economic cost summary for different water supply sources

Supply Source	Capital Costs	Operational Costs
Local Catchment Reservoirs	n/a	- power and chemical of treating water at the water treatment plants (WTPs), - labor to run the WTPs - mechanical asset replacement - upgrading infrastructure
River Murray	n/a	- treatment at Happy Valley WTP (see above) - electricity for pumping for MBO pipeline
Desalination	- desalination plant - materials and construction for the transfer pipeline pipe and fittings - pumps and pump station building for transfer pipeline	- electricity - labour - chemicals - membrane and plant replacement - electricity for pumping, and pump replacement, for transfer pipeline
Stormwater	- stormwater wetland material and construction - aquifer storage recovery material and construction - water distribution network material and construction	- labor - replacement capital - maintenance - electricity for pumping - UV treatment - monitoring fees
Rainwater	- tank - delivery and installation - dolomite base - pump (and for indoor use a mains switch) - plumbing	- electricity for pumping - tank maintenance - pump and tank replacement

4.4.4.3 Greenhouse Gas Emissions

In a similar way to economic costs, only operational GHG emissions were attributed to existing supply sources, while for new potential supply sources, both operational GHG emissions and capital

(embodied) GHG emissions were included. Specifically, total system GHG emissions were calculated as:

$$\text{Total System GHG Emissions} = OGHG_{[RM+Res+Des+SW+RW]} + CGHG_{[Des+SW+RW]} \quad (4.3)$$

where $OGHG_{[RM+Res+Des+SW+RW]}$ was the sum of the operational GHG emissions for the five supply sources and $CGHG_{[Res+SW+RW]}$ was the sum of the capital GHG emissions for desalination, stormwater and rainwater. Due to the extensive GHG emissions data for supply sources, a summary of GHG emissions for each supply source is included below, while further detail is provided as auxiliary material. No discount rate was used for GHG emissions; however, a sensitivity analysis on different discount rates should be investigated in future work. The GHG emissions factor for electricity was assumed to be 0.73 kilograms of carbon dioxide equivalents per kilowatt hour ($kgCO_2^{-e}$/kWh), which is the latest full fuel cycle emissions factor (FFCEF) estimate for purchased electricity by South Australian end users [*Department of Industry, Innovation, Climate Change, Science, Research, and Tertiary Education*, 2013]. South Australia's generated electricity is sourced predominantly from natural gas (52%), wind (27%), coal (17%), and solar (4%) [*Australian Energy Market Operator*, 2014]. Its FFCEF for purchased electricity is thus lower than the Australia-wide average of 1.00 $kgCO_2^{e-}$/kWh, reflecting South Australia's greater uptake of renewable fuels and lower reliance on coal compared to states such as Victoria and New South Wales (FFCEFs of 1.35 and 1.05 $kgCO_2^{e-}$/kWh, respectively) [*Department of Industry, Innovation, Climate Change, Science, Research, and Tertiary Education*, 2013]. However, it is comparatively high compared to Tasmania's FFCEF of 0.22 $kgCO_2^{e-}$/kWh [*Department of Industry, Innovation, Climate Change, Science, Research, and Tertiary Education*, 2013], which relies heavily on hydropower. From an international perspective, Australia's FFCEF for purchased electricity is relatively high due to its energy sector being one of the most CO_2-intensive in the world, along with other coal-dependent countries such as South Africa, India and Indonesia [*Foster and Bedrosyan*, 2014]. Natural-gas dependent countries, such as Mexico and Egypt, have lower emissions factors, while even lower emissions factors exist for hydropower-

dependent countries, such as Canada and Brazil [*Foster and Bedrosyan*, 2014]. For example, in 2009, Canada's electricity generation emissions factor, including transmission losses and associated emissions, was 0.20 $kgCO_2^{e-}$/kWh [*Canadian Government*, 2011].

4.4.4.3.1 Local Catchment Reservoirs and River Murray

For local catchment reservoirs, operational GHG emissions associated with the energy required for treatment at the WTPs and those associated with chemical use were accounted for. Operational GHG emissions of River Murray supply included GHG emissions of treating the water at Happy Valley WTP and GHG emissions due to pumping. GHG emissions due to pumping were derived from first principles, using the Darcy-Weisbach head loss equation and the pump power equation (see Section 2 of auxiliary material on economic costs). The pump power was then converted to energy requirements, based on 24-hour operation, before being transferred to GHG emissions.

4.4.4.3.2 Desalination

Capital GHG emissions for the desalination plant were attributed to the materials, electricity, and diesel used to construct the main plant and onsite power facilities, which account for just less than 1% of operational GHG emissions over a 20-year plant lifetime. Using this relationship and the derived operational GHG emissions, the capital GHG emissions were estimated for each desalination plant capacity. For the desalination plant transfer pipeline, capital GHG emissions associated with materials for the mild steel cement lined (MSCL) pipeline and construction of the pipeline were accounted for. GHG emissions associated with the materials for the pumps were considered insignificant based on the GHG emissions inventory of the similarly-sized Murrumbidgee to Googong pipeline [*ACTEW Corporation*, 2009].

Operational GHG emissions included electricity required for treatment; chemicals; and membrane and plant replacement. The GHG emissions associated with membrane replacement were applied every five years and were independent of the amount of water produced by the plant. Furthermore, the GHG emissions associated with plant replacement were accounted for once in 2030 and were

estimated to be the same as the initial capital GHG emissions. However, GHG emissions associated with power and chemicals depended on the amount of water supplied by the desalination plant. The operating GHG emissions for the transfer pipeline were attributed to the electricity required to power the transfer of water. The power required to pump the water was estimated using first principles (see Section 2 of auxiliary material on economic costs). GHG emissions associated with pump replacement were excluded, as they were negligible compared with GHG emissions associated with pumping.

4.4.4.3.3 Rainwater Tanks

Capital GHG emissions were attributed to the rainwater tank, pump, pipes, fixtures, and installation. However, the transport of the rainwater tank system to site was not accounted for, as this was expected to vary considerably for each house. All rainwater tanks were assumed to be made from high density polyethylene (HDPE).

Operational GHG emissions for rainwater tanks were attributed to electricity use of the pump and replacement of the tank (25 years) and pumps (10 years). However, no replacement GHG emissions associated with pipes nor fixtures were accounted for, as these were assumed to have a lifetime greater than the planning horizon. Replacement GHG emissions for the tanks and pumps were assumed to be the same as the initial capital GHG emissions.

4.4.4.3.4 Stormwater Schemes

The capital material and construction GHG emissions for the stormwater schemes were attributed to the materials and construction of the wetland, aquifer storage and recovery (ASR) wells, and the distribution network. The GHG emissions associated with pumps were not considered, given that GHG emissions for pumps of large pipelines were found to be negligible compared to other capital GHG emissions and the operating GHG emissions of pumps. For the wetlands and ASR wells, GHG emissions were attributed to the concrete and steel used in their construction and the excavation of soil required to create the wetlands and wells.

For the distribution network, pipes were assumed to be made from high density polyethylene (HDPE), have a pressure rating of 600 kilopascal (kPa), an outside diameter of 280 mm, and a wall thickness of 10.8 mm. The length of pipeline required for the distribution of harvested stormwater to non-potable industrial and commercial users was estimated from a number of similar stormwater schemes in Adelaide. Specifically, the following equation was derived to estimate pipe length based on the potential yield of the schemes:

$$L = 18.108 * Y^{0.5681} \tag{4.4}$$

where L is the length of pipeline (in km) and Y is the potential yield of the stormwater scheme (in GL/yr).

Operational GHG emissions for the stormwater harvesting schemes were based on operating GHG emissions, namely those associated with pumping the stormwater. The wetlands, wells and distribution network were assumed to have lifetimes greater than the planning horizon of 40 years considered, so no GHG emissions associated with replacement were attributed to stormwater harvesting. GHG emissions for pump replacement were also ignored, as these were assumed to be negligible compared with those associated with the electricity required for pumping.

4.4.5 Evaluation of Constraints

Constraints were based on the definition of “acceptable performance” representing the extent of water savings that can be expected from temporary water restrictions, which is a function of the “acceptable” frequency, duration and severity of restrictions [*Chong et al.*, 2009a]. As Adelaide has no defined ‘level of service’ objectives in terms of these measures [*Chong et al.*, 2009a], “acceptable performance” was based on the ‘level of service’ objectives for Melbourne, Australia, which include reliability >95% and duration of failure <365days [*Chong et al.*, 2009a].

Reliability was calculated as:

$$\mathrm{Re}I = \frac{\sum_{t=1}^{T}(\frac{S_t}{D_t} * 100)}{T} \tag{4.5}$$

where Rel was the average reliability of the system given as a percentage; S_t was the number of days available supply exceeded demand (success state) for time series t (t=1-10); D_t was the total number of days evaluated for time series t (D_t=10,958); and T was the number of time series evaluated (T=10).

Average maximum duration of failure was calculated as:

$$M.D.F. = \frac{\sum_{t=1}^{T}\max(\{F_t\})}{T} \tag{4.6}$$

where M.D.F. was the average maximum duration of failure given in days; F_t was the number of consecutive days that demand exceeded supply given a failure occurred for time series t (t=1-10); and T was the total number of time series evaluated (T=10).

4.4.6 Optimisation

The Water System Multiobjective Genetic Algorithm (WSMGA) developed by *Wu et al.* [2010], which is based on the non-dominated sorting genetic algorithm II (NSGA-II) [*Deb et al.*, 2002], was used as the multi-objective genetic algorithm (MOGA), as it has been shown to perform well in previous studies and caters to discrete decision variables.

In order to calibrate the WSMGA, various values of the population (P) (50-300), number of generations (G) (100-400), probability of crossover (P_c) (0.6-0.9), and probability of mutation (P_m) (0.05-0.2) were trialled. In order to identify the most appropriate combination of these parameters, the hypervolume of the different Pareto Fronts produced whilst varying the parameters was analysed. The hypervolume was selected for this purpose because it is the most difficult metric to satisfy, given it rigorously captures both convergence and diversity of the Pareto Front [*Reed et al.*,

2013]. Specifically, for different combinations of P, P_c and P_m, the hypervolume was plotted against the number of generations, with the aim of determining which combination of P, G, P_c, and P_m returned the largest hypervolume (and so resulted in a Pareto front with good convergence and diversity) with the least computational effort. The parameters obtained through this process were P=150, G=150, P_c=0.9, and P_m=0.1.

The random initialization of the first generation in WSMGA was repeated ten times, with the final Pareto Front comprised of Pareto optimal points sourced from all ten runs. A number of runs was necessary to ensure that near-globally optimum solutions were found, because WSMGA is a stochastic algorithm and will thus find different solutions depending on the starting position in the search space [*Keedwell and Khu*, 2006].

4.4.7 Post-Optimisation Robustness Assessment

To provide an indication of how robust the solutions were to future uncertainties in demand and impacts of climate change projections (see *Paton et al.* [2013]), six solutions from the Pareto front were subjected to multiple future scenarios in a post-optimisation robustness assessment.

These solutions were selected because they (a) represented break-points in trade-offs between two of the three objectives (Figures 4.2b-4.2d); (b) spanned a wide range of values of the objectives, i.e., solutions were across the Pareto surface, rather than only from a small section of the surface (Figure 4.2a); and (c) had average maximum annual vulnerabilities of less than 27% of demand. This cut-off was employed as it is equivalent to the projected savings under Adelaide's toughest Level 5 water restrictions [*Chong et al.*, 2009b], and thus the upper limit of this objective to ensure system failure was prevented.

Overall, 252 scenarios comprised of six SRES scenarios, seven GCMs (from the set of coordinated climate model experiments comprising the World Climate Research Programme's Coupled Model Intercomparison Project CMIP3), and six demands were included in the robustness assessment. This is consistent with the scenarios applied to this case study by *Paton et al.* [2013]. The six SRES

scenarios included B1, B2, A2, A1B, A1T and A1FI, which were selected to cover the full range of potential future development pathways defined by the Intergovernmental Panel on Climate Change. The GCMs were selected using CSIRO's Climate Futures Framework (CFF) [*Clarke et al.*, 2011], in which plausible climates simulated by GCMs are classified into a small set of representative climate futures (RCFs) [*Whetton et al.*, 2012]. Consequently, a smaller subset of GCMs can be selected that cover the identified RCFs (in this case study six RCFs were identified), thus reducing computational effort but still maintaining the uncertainty in GCM projections. The seven GCMs selected for this case study using the CFF included CCSM3 (hereinafter CCSM), CGCM3.1(T63) (hereinafter CGCM-h), CSIRO-MK3.5 (hereinafter CSIRO), FGOALS-g1.0 (hereinafter FGOALS), MIROC3.2(hires) (hereinafter MIROC-h), MIROC3.2(medres) (hereinafter MIROC-m), and MRICGCM2.3.2 (hereinafter MRI). The six demand scenario options, labelled Very Low, Low, Medium-Low, Medium-High, High, and Very High, represented three population estimates combined with two per capita consumption estimates (Table 4.4), as detailed in *Paton et al.* [2013].

For each of the six selected solutions, the WaterCress model was run for each of the 252 scenario options in combination with the 1000 stochastic time series. Robustness was then estimated as:

$$Rob = S / T \tag{4.7}$$

where Rob was the robustness, S was the number of scenarios for which the system was considered to exhibit "acceptable performance" and T was the total number of scenarios evaluated (T=252,000). As discussed earlier, "Acceptable performance" was defined in terms of a reliability > 95%, a maximum duration of failure < 365days, and a maximum vulnerability of ≤ 27% of demand.

In addition, the median values for the 1000 stochastic time series for each of the 252 scenarios for the each of the selected solutions for average maximum annual vulnerability, average reliability, average maximum duration of failure, total system cost, and total GHG emissions were calculated so as to assess how the uncertainty sources (GCMs, SRES scenarios and demands) affected the

Table 4.4: Demand Scenario Options

Demand Scenario	Per capita consumption	Population
Very Low	Reduction	Small
Low	Constant	Small
Medium-Low	Reduction	Medium
Medium-High	Constant	Medium
High	Reduction	Large
Very High	Constant	Large

performance criteria. This was important from a practical management perspective, as if the greatest sources of uncertainty are within the control of the water authority, any effort may be best spent by reducing this uncertainty, thus resulting in a smaller future window of uncertainty and increasing the robustness of solutions. It should be noted that while in this instance median values were selected for comparison, a more conservative approach would be to look at the values for which only 5% or 10% of future scenarios would be more vulnerable, more costly, more GHG emissions intensive, less reliable, and have more consecutive days of failure.

4.5 Results

The Pareto front illustrating the range of values of the objectives and the trade-offs between objectives for the non-dominated solutions is presented in Section 4.5.1. Analysis of the Pareto front, in terms of the similarities in decision variables for solutions comprising the Pareto front, is presented in Section 4.5.1.1, while Section 4.5.1.2 examines how decision variable selection affects the objectives. In Section 4.5.2, the post-optimisation robustness results are presented, thereby investigating (a) how robust the six solutions are to future uncertainties when assessing the impacts of climate change on water supply (including demand uncertainty) and (b) which uncertainty sources

have the greatest impact on the objective values. A summary of the results from a practical management perspective is given in Section 4.5.3.

4.5.1 Optimisation

Four different views of the Pareto front (comprising of 792 non-dominated solutions) are presented to fully illustrate the trade-offs between the three objectives (Figures 4.2a-4.2d). Because of the large number of non-dominated solutions, decision-makers may also benefit from investigating a number of interactive visual analytics, as highlighted by *Kasprzyk et al*. [2009], *Kasprzyk et al.* [2012] *and Kasprzyk et al.* [2013]. However, the Pareto fronts do illustrate a number of patterns, the most evident being that trade-offs exist between all three objectives. Firstly, decreases in average maximum annual vulnerability result in increases in costs and/or GHG emissions (Figures 4.2b and 4.2d). However, the rate of increase varies. Relatively large vulnerabilities can be reduced to small values with only small increases in costs and/or GHG emissions, while completely removing system failure is much more expensive and/or GHG emissions intensive. For example, in moving from solution 1 to 3, a reduction in average maximum annual vulnerability of 9% is associated with a relatively small 3% increase in economic cost, whereas a further reduction of 15% in average maximum annual vulnerability to achieve no system failure (e.g., solution 4) comes at a minimum additional 27% increase in economic cost (Figure 4.2d). Similarly, for GHG emissions, in moving from solution 2 to 6, average maximum annual vulnerability can be cut from 23.5% to 7.3% with only a 3.5% increase in GHG emissions, whereas a further reduction of 7.3% of average maximum annual vulnerability (e.g. solution 5) means a minimum additional 44.0% increase in GHG emissions (Figure 4.2b). Furthermore, there is also a trade-off between costs and GHG emissions, whereby an improvement in GHG emissions or cost does not necessarily correlate with an improvement in the other objective (Figure 4.2c). For example, for solutions 1 and 2, which have very similar average maximum annual vulnerability (Figures 4.2b and 4.2d), solution 2 costs $1.15 billion more than solution 1, while solution 1 has greater GHG emissions, specifically 1.19 million tonnes of CO_2^{e-} more than solution 2 (Figure 4.2c). The objective values also range considerably, with average maximum

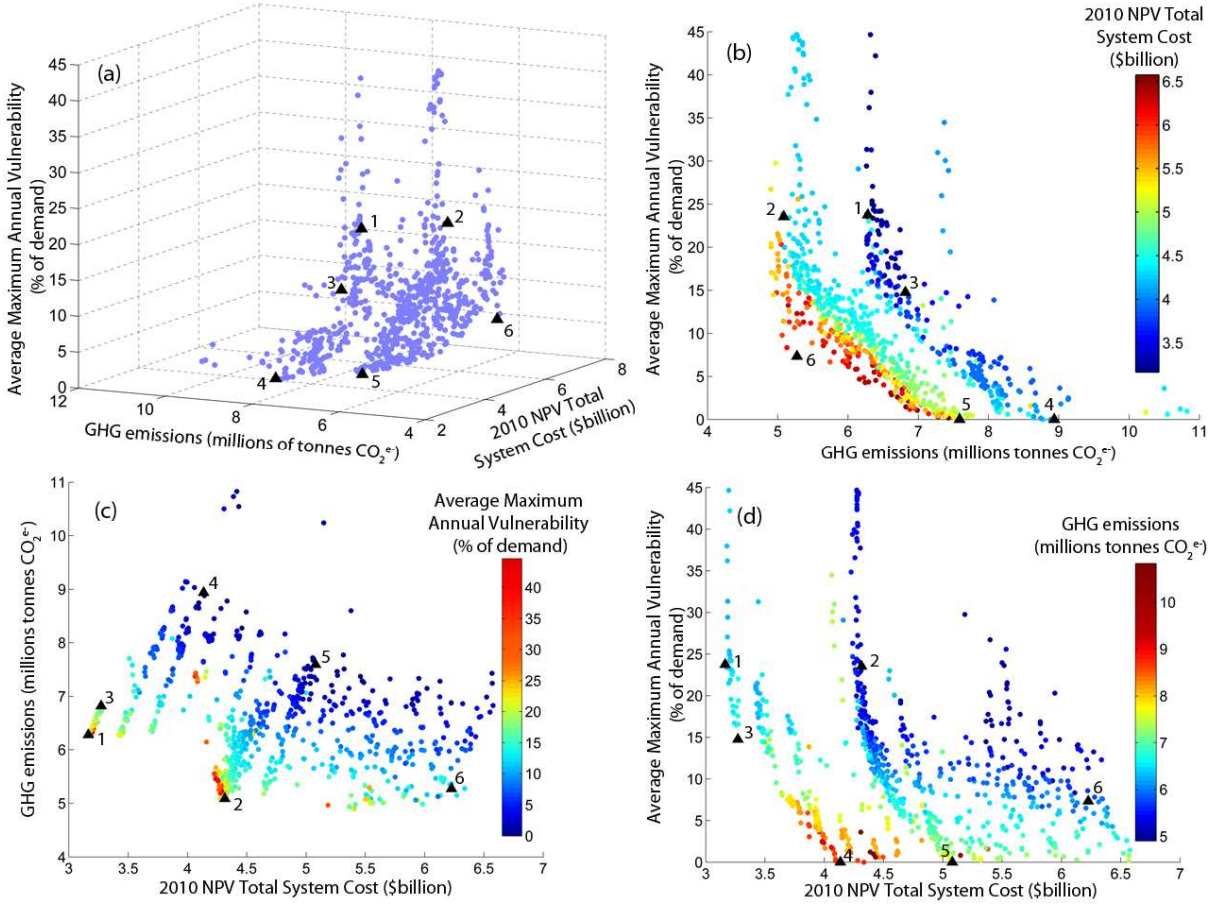

Figure 4.2: The Pareto front for the case study illustrating tradeoffs between (a) all three objectives; (b) average maximum annual vulnerability and GHG emissions; (c) GHG emissions and 2010 PV total system cost; and (d) average maximum annual vulnerability and 2010 NPV total system cost. The black triangles indicate the six solutions (numbered to correspond with Tables 4.6 and 4.7) selected for the post-optimisation robustness assessment.

annual vulnerability varying from zero to 44.7% of demand, total system cost from $3.17 to $6.58 billion, and GHG emissions from 4.90 to 10.83 million tonnes of CO_2^{e-} (Figure 4.2).

4.5.1.1 Decision Variables

A number of trends in the values for the decision variables are apparent when studying the solutions that comprise the Pareto front (Figure 4.2). Firstly, a desalination plant is always selected, with capacity between 100 and 500 ML/day (representing the full range of options specified for this variable, except for the option of no desalination plant). This seems counterintuitive from purely studying the unit costs and GHG emissions of desalination, as desalination is almost the most expensive source and is the most GHG emissions intensive (Table 4.5). However, this source is being selected because of the third objective – risk-based performance. That is, even the smallest

Table 4.5: Median unit costs and GHG emissions (includes both capital and operational costs and GHG emissions) derived from the 792 Pareto optimal solutions for the different supply sources

Supply Source	Median Unit Cost ($/kL)	Median Unit GHG emissions ($kgCO_2^{e-}$/kL)
Myponga Reservoir local catchment	0.35	0.18
Happy Valley Reservoir local catchment	0.09	0.09
River Murray	0.16	0.82
Desalination Plant	2.32	3.78
Household Rainwater Tanks	2.36	1.89
Brownhill-Keswick Stormwater Harvesting Scheme	1.12	0.48
Sturt Stormwater Harvesting Scheme	1.39	0.57
Field Stormwater Harvesting Scheme	1.42	0.59
Pedler Stormwater Harvesting Scheme	1.26	0.54

desalination plant capacity (approx. 36.5 GL/yr) could supply more water than all of the stormwater schemes (maximum supply from Pareto solutions of 17 GL/yr) and rainwater (maximum supply from Pareto solutions of 25 GL/yr). Thus, the reliability and duration of failure constraints of the optimisation problem may not be met without the desalination plant, resulting in all solutions on the Pareto front containing desalination. The four stormwater harvesting schemes are also present in almost every option. This is expected, considering they have both lower unit costs and GHG emissions compared with the two other augmentation options of desalination and rainwater (Table 4.5). However, as demonstrated by the results, augmentation options in addition to stormwater (desalination or desalination plus rainwater) are necessary, as the total potential yield from all of the stormwater schemes is insufficient to meet projected future demand.

Rainwater tanks are only present in 70% of the Pareto front solutions, so depending on how important the water authority considers each objective, rainwater tanks may or may not have a place in the future water supply system. Furthermore, when tanks are selected, they are always sized between 2 and 7 m^3, there is a roof connectivity of 0.9 in most cases, and rainwater is usually selected to supply all but the toilet end use (i.e. garden, cold laundry and hot water). It is not surprising that large tank sizes do not feature in the Pareto solutions, because larger tanks do not necessarily supply much more water than smaller tanks in Adelaide's climate, even though they are more expensive and are associated with the emission of more GHGs.

As far as optimal operational decisions are concerned, the desalination plant and Happy Valley Reservoir have the lowest priorities of supply in 84% and 85% of the Pareto solutions, respectively. The relatively high unit costs and GHG emissions for desalination (Table 4.5) offer a good reason for why desalination has such a low priority. Furthermore, while supply from the Happy Valley Reservoir local catchment has the smallest unit GHG emissions and smallest unit costs, water supplied from Happy Valley Reservoir also contains River Murray supply, which has the second highest unit GHG emissions and thus explains why Happy Valley Reservoir also has a low priority in many solutions. These results suggest that to reduce costs and/or GHG emissions of the system, desalinated and River Murray supply should be used sparingly. There were no distinguishing features in regard to the weights of supply, or the Mount Bold reservoir trigger levels, suggesting that the value these variables take do not have as large an impact on the objective functions as either the capital decisions associated with source augmentation, or the priorities of supply.

4.5.1.2 Correlations between the decision variables and objectives

There is a 71% positive correlation coefficient between rainwater tank size and economic cost, together with a similar positive correlation coefficient, albeit it slightly less at 60%, between desalination plant capacity and economic cost. This was to be expected, given that larger rainwater tanks and larger desalination plants are more expensive. Supply from local catchment reservoirs, the

River Murray, and harvested stormwater have much less of an impact on cost, although all correlations are slightly negative. This was to be expected, as increases in rainwater and desalination supply (which are positively correlated with cost) generally mean less water is supplied from the other sources. However, the exception to this is the relationship between supply from desalination and harvested stormwater, in which a positive correlation coefficient of 44% exists. This occurs because when rainwater tanks are an option, there is a reduction in the impervious catchment of harvested stormwater. Consequently, harvested stormwater yield decreases when rainwater tanks are implemented, which is matched by a decrease in supply from the desalination plant, as less water is required to be supplied by this source (supply from rainwater tanks and the desalination plant have a negative correlation coefficient of 84%).

Rainwater tank selection also influences GHG emissions considerably. For example, all solutions without rainwater tanks have GHG emissions of more than 6.26 million tonnes CO_2^{e-}, in combination with a negative 52% correlation coefficient between rainwater tank size and GHG emissions. In fact, only two out of 69 Pareto solutions with GHG emissions of more than 8 million tonnes CO_2^{e-} include a rainwater tank. This infers that rainwater tanks could be useful adaptation measures that also maintain relatively low GHG emissions for the system. While desalination plant capacity only exhibits a 12% correlation coefficient with GHG emissions, desalination plant supply has a 91% positive correlation coefficient with GHG emissions. This implies that: (a) the desalination plant should be used sparingly to minimise GHG emissions (supporting the conclusion in Section 4.5.1.1); and (b) the operational GHG emissions of desalination are more significant than the capital GHG emissions, which is consistent with estimations of capital versus operational energy for desalination plants. Furthermore, there is a negative 56% correlation coefficient between River Murray supply and GHG emissions, inferring that use of the River Murray may also help reduce GHG emissions of the system. This is as expected, because there is also a negative 45% correlation coefficient between River Murray supply and desalination supply, so when more water is sourced from the River Murray, generally less is sourced from the desalination plant, resulting in fewer GHG emissions. While supply

from the local catchment reservoirs also exhibited a similar negative correlation with GHG emissions, there was a slight (25%) positive correlation coefficient between GHG emissions and supply from the harvested stormwater schemes. This was expected though, because there is a positive correlation between supply from harvested stormwater schemes and the desalination plant, as explained in the preceding paragraph.

4.5.2 Post-Optimisation Robustness Assessment

The capital decision variables for the six solutions selected for the post-optimisation robustness assessment are summarized in Table 4.6, while Table 4.7 summarises the criteria values derived from the optimisation process, as well as the robustness of each solution. While the six solutions all contained the four stormwater schemes, the desalination plant capacity ranged from 100 to 500 ML/day and rainwater tanks from 3 to 5 m^3, if they were selected (Table 4.6). For the three scenarios with rainwater tanks, each had a constant roof connectivity of 0.9, with rainwater used for the garden, cold laundry, and hot water (Table 4.6). While solutions 1 and 3 have the same capital decision variables (Table 4.6), the average maximum annual vulnerability is somewhat less for solution 3 (Table 4.7). Moreover, solution 6, which has a larger supply infrastructure portfolio than solutions 4 and 5 (Table 4.6), exhibits a few short, small system failures, while solutions 4 and 5 can still provide the required demand (Table 4.7). These occurrences illustrate that system operation can influence the objectives, even if they may not affect them to the same extent as capital decisions.

The most robust solution to the climate change impact assessment uncertainties is solution 5 at 80.6%, although this is only slightly better than solutions 4 and 6, which share a robustness of 78.7% (Table 4.7). This is to be expected, given that solutions 4 and 5 exhibit no failures from the optimisation runs and thus have the best risk-based performance, while solution 6 in the optimisation run only exhibits infrequent failures that are short and of a small magnitude (Table 4.7). The least robust solution is solution 2, while solutions 1 and 3 (which share the same initial capital decision variables) perform acceptably for about two thirds of future scenarios (Table 4.7). So,

Table 4.6: Values for the capital decision variables for the six solutions selected for the post-optimisation robustness assessment

Solution Number	Desalination Plant Capacity (ML/day)	Rainwater Tank Size (m^3)	Rainwater Roof Connectivity	Rainwater End Use	Stormwater Schemes
1	150	0	n/a	n/a	All schemes
2	100	3	0.9	Garden, Cold Laundry, Hot Water	All schemes
3	150	0	n/a	n/a	All schemes
4	250	0	n/a	n/a	All schemes
5	150	4	0.9	Garden, Cold Laundry, Hot Water	All schemes
6	500	5	0.9	Garden, Cold Laundry, Hot Water	All schemes

Table 4.7: Criteria values for the six solutions nominated for the post-optimisation robustness assessment

Solution Number	2010 NPV total system cost ($billion)	Total system GHG emissions (millions tonnes CO_2^{e-})	Average maximum annual vulnerability (% of demand)	Reliability (%)	Average maximum duration of failure (days)	Robustness (% of scenarios exhibiting acceptable performance)
1	3.16	6.28	23.7	95.1	92.9	64.8
2	4.31	5.09	23.5	95.5	116.6	43.9
3	3.27	6.82	14.7	95.1	73.6	63.9
4	4.14	8.94	0.0	100.0	0	78.7
5	5.08	7.59	0.0	100.0	0	80.6
6	6.23	5.27	7.3	97.3	28.5	78.7

although solutions 1 and 2 both exhibit very similar average maximum annual vulnerability in the optimisation process (Table 4.7), solution 1 is considerably more robust than solution 2, inferring it has a better overall risk-based performance than solution 1. This makes sense, as the 3 m^3 rainwater tank cannot supply as much water as an additional 50 ML/day capacity for the desalination plant (Table 4.6).

A summary of the variation in performance criteria due to the different sources of uncertainty for the six solutions (Table 4.6) is provided below, including boxplots of the variation in average maximum annual vulnerabilities (Figure 4.3), while boxplots for the other performance criteria are included in the auxiliary material. Each boxplot has three sections – the top section compares across GCMs, the middle section across SRES scenarios and the bottom section across demands (e.g., Figure 4.3). Within each section, the six or seven different scenario options are illustrated, and within each of these, there are six columns that represent each of the six solutions considered in the post-optimisation robustness assessment (consecutively from solution 1 in the furthest left column through to solution 6 in the furthest right column). For example, in the top section of each boxplot, for each GCM and each alternative, the columns represent 36 points (one for each of the 6 SRES scenarios combined with the 6 demands).

System cost is most insensitive to future uncertainty; however, the costs of solutions with rainwater tanks are more sensitive to changes in population than solutions without rainwater tanks (see auxiliary material). This is expected, considering the large impact rainwater tanks have on economic cost and given that for larger populations, there are more houses and thus more rainwater tanks. GHG emissions similarly increase for scenarios with bigger populations, as well as bigger per capita consumptions (see auxiliary material). This is because larger demands require more water to be supplied, which is likely to increase the supply from desalination plants, which has a major impact on GHG emissions. As illustrated by the increase in average maximum annual vulnerability (Figure 4.3), larger demands also decrease the risk-based performance of the system (see auxiliary material). In

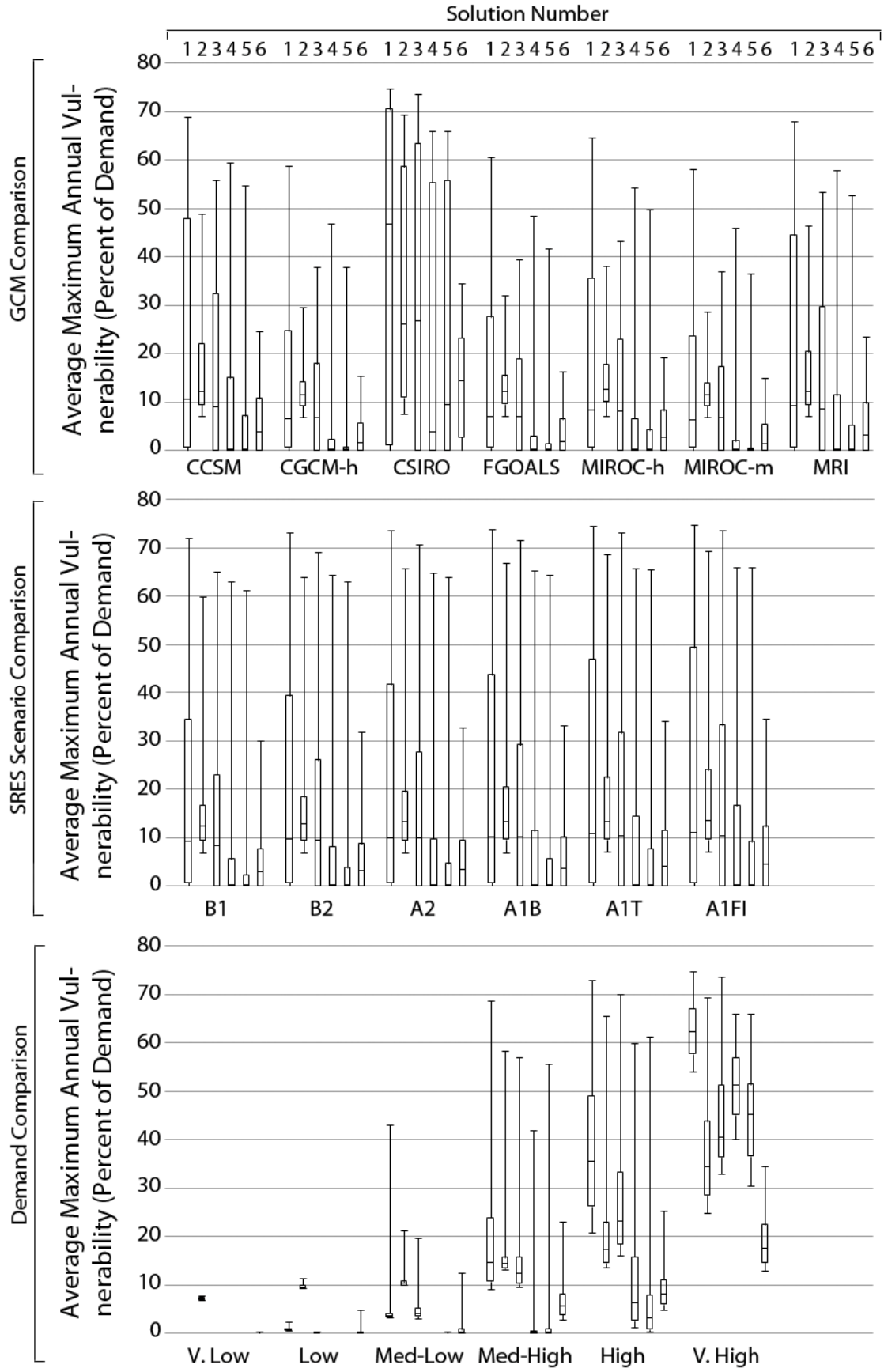

Figure 4.3: Boxplot of average maximum annual vulnerability comparing the different GCMs (top section), different SRES scenarios (middle section), and different demands (bottom section).

fact, of the uncertainty sources, demand has the greatest impact on the performance criteria, followed by GCMs and SRES scenarios, as illustrated by a greater variation in the performance criteria when comparing across the different demands, than exists when comparing across the GCMs and SRES scenarios (Figure 4.3 and auxiliary material).

4.5.3 Practical Management Implications

The results from this case study have a number of practical management implications. Firstly, considerable tradeoffs exist between (1) cost and risk-based performance and (2) GHG emissions and risk-based performance, which is to be expected, as a system that has enhanced water security, will generally cost more and/or emit more GHG emissions. However, results also illustrated that while large system failures may be reduced to smaller ones relatively cheaply and/or without many additional GHG emissions, to reduce average maximum annual vulnerability to zero will be relatively expensive and/or produce many more GHG emissions. Consequently, it may be better to operate the system with the need for some water restrictions in order to avoid system shortfalls.

A trade-off also exists between economic cost and GHG emissions. The main drivers of this tradeoff are the presence of rainwater tanks and the supply of water from the desalination plant. That is, rainwater tanks are an expensive adaptation source and desalination is a GHG emissions-intensive source. Consequently, for a water authority aiming to minimise GHG emissions (as would be the aim in attempting to mitigate the impacts of climate change), water supply from the desalination plant should be kept to a minimum. Therefore, while a desalination plant may be a good adaptation measure to climate change due to its climate independence, other water sources, such as rainwater tanks and stormwater harvesting schemes, may be better mitigation measures. This illustrates the importance of accounting for GHG emissions in urban water supply system planning, as if simply cost and risk-based performance were considered as objectives, solutions would favour adaptation responses, rather than mitigation responses.

However, in the future water supply system plan, a desalination plant of some capacity should be included, as it is required to maintain "acceptable" risk-based performance of the system. Similarly, stormwater schemes should be included. However, as discussed above, from a mitigation perspective (with the aim of minimising GHG emissions), the desalination plant should be used sparingly and rainwater tanks between 2 and 7 m^3 should be included, connected to as much of the roof area as possible and supplying garden, cold water laundry and hot water use. Furthermore, to cope with future uncertainty, some consideration should be given to the outcome of the scenario-based sensitivity analysis. Solutions with a combination of a desalination plant of ≥ 150 ML/day and rainwater tanks of 4 or 5 m^3, or a desalination plant ≥ 250 ML/day, are more robust than solutions with a 100 ML/day desalination plant and 3 m^3 rainwater tanks, or a desalination plant ≤150 ML/day. Consequently, planning a system with a desalination plant ≥150 ML/day in combination with rainwater tanks will help the system cope with future uncertainty. Furthermore, while uncertainties in GCMs and SRES scenarios both influence the risk-based performance of the system, the greatest impact is due to demand uncertainty. This is comforting to water managers, as per capita consumption is, to an extent, within their control, unlike GCMs and SRES scenarios, for which they cannot reduce the uncertainty. Consequently, reducing per capita consumption, and thus the uncertainty in demand projections, would be a good focus for the water authority, as it would reduce the uncertainty in projecting risk-based performance, and thus improve the robustness of solutions.

4.6 Summary and Conclusions

While the adaptation of urban water supply systems to climate change has been given due consideration in the literature (see for example *Wilby and Dessai* [2010]), there still exists a lack of understanding of mitigation responses in planning urban water supply systems. In fact, energy use and GHG emissions are on the rise in the water sector, with some water resource adaptation measures (e.g., desalination plants) having greater energy intensities than traditional sources. However, mitigation responses to climate change require the reduction of GHG emissions.

Therefore, due to this contradiction, there is a need to account for both adaptation and mitigation responses to climate change in urban water supply planning. Furthermore, the mitigation of climate change by minimising GHG emissions will inevitably conflict with other water supply system objectives, such as maximizing risk-based performance. Thus, balancing and negotiating multiple objectives is a necessary focus. MOEAs are particularly useful tools for addressing such a problem, because they can evolve an approximation to the entire tradeoff (Pareto) fronts of multiple objectives in a single run [*Reed et al.*, 2003].

In order to address this issue, a MOEA approach was used to optimise future water supply options for the southern portion of Adelaide's water supply system in terms of costs, GHG emissions, and water supply security. The results showed that GHG emissions produced by urban water supply systems can vary considerably (between 4.90 and 10.83 million tonnes of CO_2^{e-} for Pareto solutions of Adelaide's southern water supply system). In addition, there is a trade-off between GHG emissions and risk-based performance and, the rate of increase in GHG emissions with increase in risk-based performance varies. To reduce relatively large system failures to relatively small ones does not necessarily increase GHG emissions (and/or economic cost) by much; although to completely remove system failure may greatly increase GHG emissions (and/or economic cost). There is also a trade-off between GHG emissions and cost, with solutions resulting in lower GHG emissions potentially costing more. The results also indicated that Pareto solutions comprising a large supply from the desalination plant result in greater GHG emissions, while low GHG emissions solutions favour household rainwater tanks. Thus, while a desalination plant may be a good adaptation measure to climate change due to its climate independence, other water sources, such as rainwater tanks and stormwater harvesting schemes, which emit fewer GHG emissions, may be better mitigation measures. Including GHG emissions as an objective in an optimisation framework for urban water supply system planning under climate change is thus imperative to ensure that both adaptation and mitigation measures to climate change are considered.

All Pareto solutions are generally comprised of stormwater schemes and a desalination plant to ensure "acceptable performance", and a little over two thirds of solutions incorporate rainwater tanks between 2 and 7 m^3, inclusive. Rainwater tanks are usually always connected to 90% of the roof, and supply the garden, laundry cold water, and hot water end uses, but not toilets. The operational variables have less of an impact on the objectives compared with the capital investment decisions, although results indicate that operation of the system still influences the objective values, so system operation is still important to consider. Finally, the post-optimisation robustness assessment highlighted that three of the six solutions analysed satisfy the security of supply criteria for about 80% of future scenarios. These three relatively robust solutions include either: (1) a combination of a desalination plant of ≥ 150 ML/day and rainwater tanks of 4 or 5 m^3; or (2) a desalination plant ≥ 250 ML/day. Furthermore, demand uncertainty has the greatest impact on the objectives, so effort directed towards reducing per capita consumption (and thus demand) may be warranted to increase the robustness of solutions to future uncertainties of climate change.

There are a number of limitations of this study that could be addressed in future work. Firstly, a number of assumptions were made regarding values used in modelling the water supply system (e.g., in the catchment rainfall-runoff models) and in estimating costs and GHG emissions (e.g., the price and emissions factor for electricity and the discount rate). These may affect the results of the case study, thus a sensitivity analysis on these factors should be conducted as part of future work. Secondly, a limitation of the approach is the use of a robustness measure post-optimisation. By only considering robustness post-optimisation, system operation could not be optimised for each of the scenarios, even though in reality once the initial capital decisions are made, the operation of the system enables some flexibility to react to the actual scenario that eventuates. Further work could therefore focus on re-optimising just the operational rules for fixed infrastructure options for different future scenarios, to investigate how much adaptive capacity selected infrastructure options have. Thirdly, demand management options (e.g., water rebates for water efficient appliances) were not included as decision variables, as there were insufficient economic cost and GHG emissions data

to do so. Therefore, future work should focus on collecting these data, or developing approaches to estimate the costs and GHG emissions for such options, so they can be included as decision variables in the optimisation process. Finally, due to the large integrated nature of the approach and the effort required to demonstrate it for a city's water supply system, the approach could only be illustrated for one case study. While the practical management implications drawn from this case study are useful and may be applicable to other urban water supply systems, the application of the approach to a number of cities around the world would enable more generic conclusions to be drawn about the role of GHG emissions in urban water supply systems and the tradeoffs that may exist between adaptation and mitigation responses to climate change.

Acknowledgements

Thanks are due to the University of Adelaide and eWater CRC for their financial support of this research. The assistance of David Cresswell and Richard Clark for their ongoing support of WaterCress and Sri Srikanthan for his help with SCL is gratefully acknowledged. We also thank the three anonymous reviewers who provided valuable assistance in improving the quality of this paper considerably.

Appendices Supporting Journal Paper 3

Appendix E details the derivation of economic costs for water supply sources.

Appendix F explains the derivation of GHG emissions for water supply sources.

Appendix G contains boxplots illustrating results from the post-optimisation robustness assessment.

Chapter 5

5 Thesis Conclusions

Water supply system planning can no longer be based on the traditional concept of stationarity because of substantial climate change. However, there still exist large uncertainties in projecting future climate and understanding how these projections relate to urban water supply. Furthermore, adaptation options to augment stressed water supply systems, such as non-traditional water sources, are increasing the simulation complexity of water supply systems, while consideration of mitigation options in the water sector is lacking. Consequently, this thesis has developed approaches for assessing and improving urban water supply security planning under climate change to better understand: (1) relative magnitudes of uncertainty sources in assessing climate change impacts; (2) enhanced simulation complexity of non-traditional water sources and increased uncertainty of climate change impacts; and (3) both adaptation and mitigation responses to climate change by minimising GHG emissions. These approaches have been applied to a case study based on Adelaide's southern water supply system to demonstrate their practical management implications.

5.1 Research Contributions

The overall contribution of this thesis was the development of methods for assessing and improving urban water supply security planning under climate change to better understand: (1) relative magnitudes of uncertainty sources in assessing climate change impacts; (2) enhanced simulation complexity of non-traditional water sources and increased uncertainty of climate change impacts; and (3) both adaptation and mitigation responses to climate change. Improvements to these three areas of urban water supply system planning were achieved by addressing the three major objectives of this thesis (as documented in the Introduction). By addressing these objectives, the following research contributions were made:

1) A scenario-based sensitivity analysis was developed, and applied to Adelaide's southern water supply system, to understand the relative magnitudes of uncertainty sources in assessing the impacts of climate change on water supply systems. This is a valuable extension to a body of current research that explores the relative magnitudes of uncertainty sources in assessing the impacts of climate change on runoff because in moving from runoff to water supply security, there is: (a) additional model complexity involving, for example, water storages and operating rules; and (b) additional uncertainties, such as population and per capita demand projections. For the case study of Adelaide's southern system, three major sources of systematic uncertainty – SRES scenarios, GCMs and demand – were compared, as well as stochastic natural rainfall variability. Results indicated that uncertainty source significance is dependent on the future year; however, demand is always the greatest source of uncertainty on water supply security and SRES scenario the least. Natural rainfall variability is second only to demand up to 2030, essentially equal to GCM uncertainty by 2040, and then of less importance than GCM choice by 2050. Therefore, for studies analysing the impacts of climate change on water supply security, uncertainties other than those associated with climate change and hydrological modelling should be considered, as they could have as great, if not greater, impacts on water supply security projections

(particularly in the short-term). From a management perspective, it is useful to know that demand is the greatest source of uncertainty, as focussing effort toward demand management schemes to reduce per capita consumption may considerably help to reduce future uncertainty. Moreover, of comfort to water authorities is the knowledge that the impact of SRES scenarios, in which uncertainty is irreducible, is minor compared to the other sources of uncertainty. Similarly, the planning of supply systems under demand uncertainty and natural rainfall variability is traditional for water authorities, so it is encouraging that these two sources are the dominant sources of uncertainty, at least in the short-term. Results also indicated that supply reliability decreases over the planning horizon for Adelaide's southern water supply system, justifying the need for initiatives to augment supply or reduce demand. Finally, the range of uncertainty in reliability increases with time. While some uncertainty may be reducible, stochastic uncertainty and some epistemic uncertainty will always exist, so flexible management may therefore be required to strike a balance between water supply security and regret.

2) Following on from the research above and the conclusion that Adelaide's current water supply system requires source augmentation, a generalised framework for the assessment of water supply security for a city was developed, that explicitly acknowledged and accounted for both the additional complexities and uncertainties associated with non-traditional water sources and climate change impacts, respectively. The additional complexities of modelling non-traditional water sources that were explicitly detailed in the approach relate to: (a) levels of usability (e.g., potable and non-potable); (b) degree of climate dependence; (c) spatial and temporal scales; and (d) source integration and priority. The uncertainties of climate change impacts were based on the cascade of uncertainty sources in projecting the impacts of climate change on water supply security, namely: (a) GHG emissions scenarios; (b) GCMs; (c) downscaling methods; (d) hydrological models; and (e) demand. This was an important contribution, as previously there had not been an urban

water supply system framework that explicitly detailed these additional complexities and uncertainties associated with non-traditional water sources and climate change impacts. The practical management implications of the framework were also demonstrated for a case study based on Adelaide's southern water supply system. Five criteria (reliability, resilience, vulnerability, robustness, and total system life cycle cost), were used to represent the two objectives of maximising risk-based performance and minimising economic cost for nine supply system alternatives comprised of existing traditional sources and new non-traditional sources, namely a desalination plant, stormwater harvesting schemes and household rainwater tanks. Furthermore, the scenario-based sensitivity analysis included 252 future scenarios that varied based on different demand and climate change projections, as well as 1000 stochastic rainfall time series. Results showed that trade-offs exist between cost and water supply security for solutions including desalination and stormwater. However, solutions containing rainwater are undesirable, as similar water supply security can be obtained more cheaply when desalination and stormwater are used. The case study findings also illustrated the importance from a management perspective of identifying demand as: (1) the greatest source of uncertainty; and (2) having the greatest impact on maximum vulnerability, which is the limiting factor in determining a strategy's robustness. Consequently, if the water authority can reduce per capita consumption through demand management schemes, they could increase a strategy's robustness to future uncertainties.

3) The above framework was then extended to incorporate GHG emissions as an objective function within a multi-objective evolutionary algorithm (MOEA) framework, to take into consideration both adaptation and mitigation responses to climate change. This is a valuable contribution in the field of urban water supply system planning, because while cities are increasingly engaged in mitigating GHG emissions, few studies have investigated the impacts of changing water use on carbon dioxide emissions. Furthermore, energy use in the water sector is rising and water resource adaptation options often require greater energy use, so

an investigation into conflicting adaptation and mitigation responses to climate change is timely and necessary. In addition, this framework was also an improvement on the framework developed to assess the second objective of this thesis, as the MOEA approach enabled many potential alternatives (including operational strategies) to be assessed efficiently. Practical management implications of the approach were also illustrated by applying the framework to a case study based on Adelaide's southern water supply system. In doing so, a valuable contribution was the collation and synthesis of economic cost and GHG emissions data for a number of traditional and non-traditional water sources, as these data, particularly for GHG emissions, are not readily available in the literature. Results demonstrated that trade-offs exist between all three objectives of maximising risk-based performance, minimising economic cost, and minimising GHG emissions. However, while large system failures may be reduced to smaller system failures relatively cheaply and/or without many additional GHG emissions, to completely reduce average maximum annual vulnerability to zero would be relatively expensive and/or produce many more GHG emissions. Consequently, it may be cheaper and/or better for the environment to operate the system with the need for some water restrictions in order to avoid system shortfalls. In terms of the trade-off between economic cost and GHG emissions, the main drivers are the presence of rainwater tanks and the supply of water from the desalination plant – rainwater tanks are an expensive option, while supply from the desalination plant greatly increases GHG emissions. Therefore, while a desalination plant may be a good adaptation measure to climate change due to its climate independence, other water sources, such as rainwater tanks and stormwater harvesting schemes, may be better mitigation measures. This illustrates the importance of accounting for GHG emissions in urban water supply system planning, as if maximising risk-based performance and minimising costs are the only objectives considered, solutions may favour adaptation responses (such as desalination plants) over mitigation responses (such as rainwater tanks). However, a desalination plant of

some size, along with the stormwater harvesting schemes, should be included for the system to maintain "acceptable" risk-based performance. To minimise GHG emissions, the desalination plant should be used sparingly though, and rainwater tanks between 2 and 7kL, connected to as much of the roof area as possible and supplying garden, cold water laundry and hot water use should be used. Robust solutions to future uncertainties in demand and climate include: (1) a desalination plant ≥ 150ML/day and a rainwater tank of 4 or 5 kL; and (2) a desalination plant ≥ 250ML/day. Thus, planning a system with a desalination plant ≥ 150ML/day in combination with a rainwater tank will help the system cope with future uncertainty. Finally, future uncertainty in demand has the largest impact on the performance criteria, so water authorities directing effort toward demand management schemes could reduce future uncertainty.

5.2 Additional Publications of this Research

In addition to the journal papers contained in Chapters 2 to 4 of this thesis, a number of other publications and presentations have arisen from this doctoral research. These are as follows:

Book Chapters

Maier, HR, FL Paton, GC Dandy, and JD Connor (2013), Impact of drought on Adelaide's water supply system: Past, present and future, in *Drought in Arid and Semi-Arid Regions: A Multi-Disciplinary and Cross-Country Perspective*, edited by K. Schwabe, J. Albiac, J. D. Connor, R. M. Hassan and L. M. Gonzalez, pp. 41-62, Springer, New York.

Peer-Reviewed Conference Papers

Paton FL, Dandy GC and Maier HR, Sensitivity of urban water security based on various Global Circulation Models and emission scenarios*, Practical Responses to Climate Change National Conference 2010*, Melbourne, Australia, September 29 - October 1, 2010.

Paton FL, Gibbs MS, Maier HR and Dandy GC, Impacts of Climate Change Downscaling Method on Rainwater Tank Yield, *10th International Conference on Hydroinformatics,* Hamburg, Germany, July 14-18, 2012.

Conference Presentations

Paton FL, Maier HR and Dandy GC, *Impacts of climate variability and uncertainty on urban water supply systems over a range of spatial and temporal scales*, Climate: Science + Humanities GO8-Harvard Conference, Harvard University, Boston, March 2-4, 2010.

Paton FL, Dandy GC and Maier HR, *Impacts of implementing alternative water sources for a city's water supply*, e-Water CRC Annual Conference, Gold Coast, Australia, February 16-18, 2010.

5.3 Research Limitations

Limitations of this research have resulted from model, data and computational limitations, as well as the scope of the research and time constraints. These limitations, and the resulting implications, include:

1) **Model limitations of WaterCress.** This meant that certain aspects of Adelaide's southern water supply system could not be modelled, such as the 5-year rolling licence of the River Murray and the seasonal variation in non-residential outdoor demand.
2) **Limited access to climate change data.** Thus, the constant scaling or delta change method was the only climate change method that was applied to translate global to local climate responses for the case study. The delta change method has a number of limitations, namely: (1) the mean, maxima, and minima are the only data properties that are different between the scaled and baseline climate; (2) the spatial pattern of the present climate is assumed for the future; (3) the approach, without modification, cannot simulate changes in the occurrence of rainfall, nor changes to the size of extreme events; and (4) values for a single grid cell may contain gross biases [*Wilby and Fowler*, 2011]. Furthermore, OzClim only

provides evaporation data for nine GCMs, limiting the ability to compare projected impacts of climate change from the 19 GCMs in the Climate Futures Framework that were available and appropriate for this case study.

3) **Limited access to cost and GHG emissions data for demand management schemes.** Consequently, the economic costs and GHG emissions of reducing per capita consumption through demand management could not be accounted for. Consequently, per capita consumption was treated as an uncertainty, even though reducing per capita consumption is a potential management option for urban water supply system management, which, when compared to supply augmentation for reducing future water security, may be a better measure in terms of both economic cost and GHG emissions.
4) **Time constraints for the sensitivity-based scenario analysis.** Therefore, scenario-based sensitivity analyses focused solely on uncertainty in GCMs, SRES scenarios, demand, and natural rainfall variability, even though a broad range of uncertain variables exist within the analyses, such as the choice of economic discount rate used in estimating economic cost and the selection of the rainfall-runoff models and parameters.
5) **Computational constraints in the MOEA approach.** This meant that uncertainty in climate change and demand, and to a lesser extent natural rainfall variability, had to be analysed post-optimisation, as run times for multiple scenarios during optimisation would have been too long. Thus, robustness and flexibility could not be incorporated into the portfolio selection process, and could only be analysed post-optimisation. Furthermore, system operation could not be optimised for each of the future scenarios, even though in reality once the initial capital decisions are made, the operation of the system enables some flexibility to react to the actual scenario that eventuates. Finally, computational limitations also meant only 10 stochastic rainfall time series could be used (out of a potential 1,000) for the optimisation approach, preventing the full representation of natural rainfall variability.

6) **Time constraints, research scope and data availability in the MOEA approach.** These factors limited the number of objectives for the case study to maximising risk-based performance, minimising economic cost and minimising GHG emissions. However, there are additional objectives that may warrant consideration, such as maximising water quality of the local marine environment (which will be affected, for example, by brine disposal from the desalination plant and pollutants in stormwater discharge) and maximising environmental flows of rivers for aesthetic, recreational and environmental benefits (e.g., for the River Murray downstream of Murray Bridge and the Onkaparinga and Myponga Rivers downstream of the local catchment reservoirs).
7) **Time constraints for demonstrating the frameworks.** Due to the integrated nature of the approach and thus the effort required to collate large amounts of data and develop the models for a case study, the frameworks developed in this thesis could only be illustrated for a case study based on Adelaide's southern water supply system. Consequently, while the practical management implications that have been drawn are useful and may be applicable to other urban water supply systems, the application of the approaches to multiple cities around the world would enable more generic conclusions to be drawn. Furthermore, only a 40-year planning horizon was considered for the case study, which is not long enough to take into account the long-term effects of climate change.
8) **The absence of incorporating a sequencing approach.** The methods adopted in this thesis utilise a 'precautionary approach', whereby supply options are assumed to be implemented at the start of the planning horizon, while in reality the options could be sequenced to come on-line at any time during the planning horizon.
9) **The absence of consideration of social or governance issues associated with the implementation of a number of options.** For example, requiring every household to have rainwater tanks, or integrating harvested stormwater supply into the water supply system.

5.4 Recommendations for Future Work

Based on the research limitations mentioned in Section 5.3, future work in this field should focus on the following ten key areas:

1) **Water Supply System Model** – Modifying the WaterCress simulation model to enhance its capabilities to represent real-life water supply systems, for example, including rolling licences for supply sources and the ability to account for seasonal variation of demand for non-residential uses.
2) **Data** – Collating data on GHG emissions and economic costs for demand management schemes, or in the absence of empirical data, developing approaches to estimate the costs and GHG emissions for such options. This will enable demand management to be included as a management option in the approaches developed and enable the reduction of per capita consumption to be compared with supply augmentation options.
3) **Scenario-based Sensitivity Analysis** – Extending the sources of uncertainty from GCMs, SRES scenarios, demand, and natural rainfall variability, to also incorporate other uncertainties, such as the selection of the economic discount rate and different climate change downscaling approaches.
4) **Objectives** – Increasing the number of objectives of the MOEA optimisation approach to include additional objectives that may be important considerations for planning and managing the system, such as maximising the water quality of local marine waters and rivers. This will ensure water authorities have a greater understanding of trade-offs between objectives for feasible alternatives.
5) **Robustness Assessment** – Incorporating robustness and flexibility into the portfolio selection process.
6) **Post-Optimisation Robustness Assessment** – Re-optimising just the operational rules for fixed infrastructure options for different future scenarios, to investigate how much adaptive capacity selected infrastructure options have. Reporting robustness in this context will

provide a more realistic understanding of a fixed infrastructure solution's ability to respond to future uncertainties than is offered in the current MOEA framework.

7) **Optimisation –** Addressing the problem of reducing 1,000 stochastic series to 10 when applying the multi-objective evolutionary algorithm framework.
8) **Demonstration of Frameworks** – Extending the demonstration of the approaches developed herein to multiple water supply system case studies from cities around the world to determine whether any generalised rules or patterns from the results can be established, and to enable more generic conclusions to be drawn in terms of the practical management implications of the approaches. Furthermore, extending the planning horizon to take into account the long-term effects of climate change, for example, to the end of the 21st Century.
9) **Sequencing –** Extending the approach to incorporate sequencing of different options in time along the planning horizon.
10) **Social and Governance Issues** – Considering these issues in relation to the implementation of a number of options, such as requiring every household to install a particular sized rainwater tank.

Appendix A – Journal Paper 1 as published in *Water Resources Research*

Reference: Paton, F. L., H. R. Maier, and G. C. Dandy (2013), Relative magnitudes of sources of uncertainty in assessing climate change impacts on water supply security for the southern Adelaide water supply system, *Water Resour. Res.,* 49*,* 1643–1667*,* doi:10.1002/wrcr.20153

WATER RESOURCES RESEARCH, VOL. 49, 1643–1667, doi:10.1002/wrcr.20153, 2013

Relative magnitudes of sources of uncertainty in assessing climate change impacts on water supply security for the southern Adelaide water supply system

F. L. Paton,[1] H. R. Maier,[1] and G. C. Dandy[1]

Received 14 May 2012; revised 12 February 2013; accepted 15 February 2013; published 28 March 2013.

[1] The sources of uncertainty in projecting the impacts of climate change on runoff are increasingly well recognized; however, translating these uncertainties to urban water security has received less attention in the literature. Furthermore, runoff cannot be used as a surrogate for water supply security when studying the impacts of climate change due to the nonlinear transformations in modeling water supply and the effects of additional uncertainties, such as demand. Consequently, this study presents a scenario-based sensitivity analysis to qualitatively rank the relative contributions of major sources of uncertainty in projecting the impacts of climate change on water supply security through time. This can then be used by water authorities to guide water planning and management decisions. The southern system of Adelaide, South Australia, is used to illustrate the methodology for which water supply system reliability is examined across six greenhouse gas (GHG) emissions scenarios, seven general circulation models, six demand projections, and 1000 stochastic rainfall time series. Results indicate the order of the relative contributions of uncertainty changes through time; however, demand is always the greatest source of uncertainty and GHG emissions scenarios the least. In general, reliability decreases over the planning horizon, illustrating the need for additional water sources or demand mitigation, while increasing uncertainty with time suggests flexible management is required to ensure future supply security with minimum regret.

Citation: Paton, F. L., H. R. Maier, and G. C. Dandy (2013), Relative magnitudes of sources of uncertainty in assessing climate change impacts on water supply security for the southern Adelaide water supply system, *Water Resour. Res.*, *49*, 1643–1667, doi:10.1002/wrcr.20153.

1. Introduction

[2] Water supply systems in the developed world have previously been planned and managed assuming that natural systems, although exhibiting fluctuations, operate in an unchanging envelope of variability [*Milly et al.*, 2008]. However, as pointed out by *Milly et al.* [2008], this assumption of stationarity is dead because of the impacts of substantial anthropogenic global warming on the hydrologic cycle. Thus, using historic climate to plan and manage future water supply systems is no longer valid; instead, projections of future climate should be used to guide decision making. However, there still exist large uncertainties in projecting future climate and in understanding how these projections translate to water resources, such as runoff or water supply. Consequently, water resource planners must understand the greatest sources of uncertainty, so as to be able to undertake the difficult task of implementing robust management policies in an uncertain environment [*Salas et al.*, 2012].

[3] *Chen et al.* [2011b] developed the following cascade of the sources of uncertainty when determining climate change impacts on hydrology: (1) greenhouse gas (GHG) emissions scenarios, (2) general circulation model (GCM) structures and parameters, (3) GCM initial conditions, (4) downscaling methods, (5) hydrological model structures, and (6) hydrological model parameters. A brief description of the sources of uncertainty in this cascade is given below.

[4] In 2000, the Intergovernmental Panel on Climate Change (IPCC) published the "Special Report on Emissions Scenarios" (SRES) [*Intergovernmental Panel on Climate Change*, 2000], in which GHG emissions scenarios (labeled SRES scenarios) were defined. These reflect different world development pathways based on demographic, economic, and technological drivers [*Intergovernmental Panel on Climate Change*, 2007]. For the various SRES scenarios, GCMs are the best tools available for simulating climate at global and regional scales [*Mpelasoka and Chiew*, 2009]; however, the modeling uncertainty associated with GCMs contributes to the total uncertainty of the future climate. Although there is considerable confidence in GCMs to provide credible, quantitative future climate projections, particularly at the continental scale or greater, the models do differ considerably in terms of estimating

[1]School of Civil, Environmental and Mining Engineering, University of Adelaide, Adelaide, Australia.

Corresponding author: F. L. Paton, School of Civil, Environmental and Mining Engineering, University of Adelaide, Adelaide 5005, Australia. (fpaton@civeng.adelaide.edu.au)

0043-1397/13/10.1002/wrcr.20153

the strength of different feedbacks in the climate system [*Randall et al*., 2007]. Consequently, the projections of future climate variables differ between GCMs, and this is more pronounced for certain variables, such as precipitation [*Randall et al*., 2007]. Furthermore, initial conditions of a GCM run can alter the output, reflecting natural variability of the climate system [*Cubasch et al*., 2001]. It is important to note that while this discussion relates to the set of coordinated climate model experiments comprising the World Climate Research Programme's Coupled Model Intercomparison Project CMIP3, a new set of simulations (CMIP5) are currently being developed.

[5] Additional uncertainty is introduced when the coarse-scale resolution variables produced by GCMs are downscaled to a finer spatial scale; one that is suitable for modeling the impacts of climate change on catchment runoff. The first major method to do this is statistical downscaling, which uses statistical methods to establish empirical relationships between GCM outputs and local climate variables [*Fowler et al*., 2007]. Dynamical downscaling, the other major method, achieves fine scale variables by embedding a higher-resolution climate model within a GCM [*Fowler et al*., 2007]. An overview of these downscaling methods is presented by *Fowler et al*. [2007], which includes a comparison of the methods, including their merits and caveats. Hydrological modeling also causes uncertainty in projecting climate change impacts. For example, there are a myriad of rainfall-runoff (RRO) models that are used to translate local-scale climate variables, such as precipitation and evaporation, to runoff projections. The various RRO models use different climate inputs, different model parameters, run at different time steps and must be calibrated.

[6] In terms of the impact of climate change on future runoff, there has been increasing attention given to uncertainties in GHG emissions scenarios, GCM models, GCM initial conditions, downscaling techniques, and hydrological models and parameters [*Boé et al*., 2009; *Chen et al*., 2011a, 2011b; *Chiew and McMahon*, 2002; *Chiew et al*., 2009b, 2009c, 2010; *Diaz-Nieto and Wilby*, 2005; *Dibike and Coulibaly*, 2005; *Forbes et al*., 2011; *Majone et al*., 2012; *Manning et al*., 2009; *Mpelasoka and Chiew*, 2009; *Wilby and Harris*, 2006; *Wilby et al*., 2006]. A number of these studies have also explicitly compared the magnitude of runoff changes caused by the different sources of uncertainty associated with climate change and hydrological modeling [*Boé et al*., 2009; *Chen et al*., 2011a, 2011b; *Chiew et al*., 2009c; *Mpelasoka and Chiew*, 2009; *Wilby and Harris*, 2006]. The most comprehensive comparison by *Chen et al*. [2011b] assessed the overall uncertainty of hydrological impacts of climate change for a Canadian watershed, by examining six GCMs, five GCM initial conditions, two GHG emissions scenarios, four statistical downscaling techniques, three hydrological model structures, and 10 sets of hydrological model parameters. For mean annual discharge, the study concluded the following order of uncertainty source significance (from greatest to least): GCM > GCM initial conditions > GHG emissions scenario > statistical downscaling technique > hydrological model > hydrological model parameters.

[7] While in many cases runoff is a good indicator of water availability, the impacts of climate change on runoff do not necessarily correlate with those on water supply. For example, *Zhu et al*. [2005] discovered that in California most climate change scenarios with increased precipitation resulted in less available water because of the seasonal rainfall pattern and storage capacities; that is, less summer runoff was not compensated by more winter runoff, because the storages could not accommodate increased winter flows. Water supply systems also have additional complexities in comparison to runoff. These include the uncertainties associated with future population, per capita water demand, regulatory requirements, water law, consumer preferences, and environmental standards [*Wiley and Palmer*, 2008]. Furthermore, model complexity is enhanced when modeling climate change impacts on water supply because not only do water simulation models incorporate demand, but they can also model (1) water storages, (2) transmission systems, (3) treatment systems, and (4) user-specified operating rules [*Traynham et al*., 2011]. Consequently, because of the additional complexity and uncertainty when moving from analyzing runoff to water supply, it cannot be assumed that the magnitude of uncertainties of climate change impacts on runoff equal that for water supply.

[8] A number of studies have examined the impact of climate change on water supply systems [*Fowler et al*., 2003; *Gober et al*., 2010; *Groves et al*., 2008; *Kaczmarek et al*., 1996; *Lopez et al*., 2009; *O'Hara and Georgakakos*, 2008; *Traynham et al*., 2011; *Vicuna et al*., 2010; *Wiley and Palmer*, 2008; *Zhu et al*., 2005], with most of these studies developing projected ranges of water availability based on a number of different uncertainties. For example, *Wiley and Palmer* [2008] examined uncertainty of GCMs, *O'Hara and Georgakakos* [2008] analyzed uncertainty of GCMs and population growth, *Vicuna et al*. [2010] examined uncertainty of GCMs and GHG emissions scenarios, while *Gober et al*. [2010] investigated the uncertainty of GCMs, GHG emissions scenarios, runoff factors, supply and demand management policies, and population growth. However, none of the studies compared the uncertainty sources in terms of their relative magnitudes. This is important because water authorities must understand the greatest sources of uncertainties for water supply system security and whether these are epistemic (systematic) or aleatoric (statistical). Systematic uncertainties, such as model inadequacy or data measurement inaccuracies, are potentially reducible (by the water authority's means or others), whereas statistical uncertainties, such as natural rainfall variability, are inherent and will always exist. If major sources of uncertainty are reducible by the water authority, then effort can be directed toward reducing this uncertainty, while if irreducible uncertainties dominate impacts on water supply security, then adaptation responses must be developed to cope with this uncertainty. Furthermore, an understanding of how these uncertainties interact through the development of "best" and "worst" cases will help water authorities establish likely bounds of future water supply security, which is imperative for them to understand the degree to which water supply may need to be supplemented, or demand reduced, in the future. In order to understand the impacts of uncertainties associated with modeling the likely impacts of climate change on water supply security, a number of approaches can be applied. A "top-down" or "scenario-based" approach, in which

uncertainty is added at each point of the modeling process from GHG emissions scenarios through to water supply system models, is the most commonly used approach within scientific evidence reviewed by the IPCC [*Wilby and Dessai*, 2010], and is the approach applied in the current paper. However, as discussed by *Wilby and Dessai* [2010], "bottom-up" and "sensitivity-based" approaches can also be applied to analyze uncertainties surrounding the likely impacts of climate change on water supply systems.

[9] When examining the impacts of climate change on water supply systems, it is also important to consider the temporal aspects of water supply security. Due to the large-scale infrastructure associated with water supply systems and the potentially long lead times for expanding these systems, it is necessary to identify when water supply security will be jeopardized in the future, so that plans to avoid water scarcity can be implemented well in advance. With the many uncertainties associated with analyzing the impacts of climate change on water supply security, it would be prudent to assume that the estimated point in time when water security is threatened will vary considerably depending on the choices made in modeling climate change, hydrology, and the water supply system. Consequently, monitoring how water supply security will change progressively through time at regular intervals over a long-term planning horizon of 30–50 years is very important. This is quite different to analyzing the impacts of climate change on runoff because in the case of water supply security, the addition of demand means a "failure" of supply to meet demand can be identified at a critical point in time, while there are no such critical points when examining runoff.

[10] In summary, there still exists a gap in understanding the relative magnitudes of uncertainty sources in assessing the impacts of climate change on water supply systems that can help water authorities plan for, and manage, the impacts of climate change. A scenario-based sensitivity analysis has therefore been developed and applied to Adelaide's southern water supply system that focuses on the three objectives of this paper: (i) to assess the relative magnitudes of the major sources of uncertainty, (ii) to identify critical points in the future when water supply security is likely to be threatened, and (iii) to present projected ranges of water supply security. The results obtained from addressing these objectives are used to draw conclusions about the planning and management of Adelaide's southern water supply system. While the methodology is illustrated for this particular case study, its generic nature means it could easily be adapted and applied to other water supply systems around the world.

[11] The remainder of the paper is organized as follows. First, the Adelaide southern system case study is introduced (section 2), followed by the methodology applied to meet the three objectives of this paper (section 3). The results of the case study are then presented and discussed (section 4), before the main components of the paper are summarized and conclusions are drawn (section 5).

2. Case Study

[12] Adelaide, the capital of South Australia (Figure 1), is the driest Australian capital city with an average annual rainfall of 552 mm. Adelaide's rainfall is strongly seasonal, falling predominantly during mild winters, which are separated by dry, hot summers. Adelaide also experiences high interannual variability, with a minimum recorded annual rainfall of 274 mm and a maximum of 883 mm (for Kent Town, Adelaide: 1889–2010 [*Jeffrey et al*., 2001]). Furthermore, there is high interdecadal variability in Adelaide. For example, the 1920s were 13% wetter than the long-term average, while the 1960s were 9% drier (for Kent Town, Adelaide [*Jeffrey et al*., 2011]).

[13] Historically, water has been sourced from reservoirs in nearby catchments in the Mount Lofty Ranges. These storages can hold a total of approximately 200 GL of water, equivalent to a little more than one year's water supply for Adelaide. In most years, water from the River Murray is pumped about 50–60 km to supplement Adelaide's water supply.

[14] This study focuses on Adelaide's southern system of reservoirs, namely Myponga, Mount Bold, and Happy Valley. The southern system, which supplies approximately half of Adelaide's demand, can be considered separately from Adelaide's northern system of reservoirs because the two systems largely act independently of each other [*Crawley and Dandy*, 1993].

[15] Myponga Reservoir in the South (Figure 1) has a capacity of 26.8 GL and is a "supply and storage" reservoir, with water collected from its 124 km^2 catchment (Figure 1), before being treated at Myponga Water Treatment Plant (WTP), which has a capacity of 50 ML/day (see www.sawater.com.au). Mount Bold Reservoir has a much larger catchment and storage capacity (Figure 1)—388 km^2 and 46.2 GL, respectively (see www.sawater.com.au)—but is considered a "storage" reservoir because it cannot directly supply water to the water distribution network. Instead, water is released from Mount Bold Reservoir and diverted 6 km downstream at Clarendon Weir via the Horndale Flume to Happy Valley Reservoir (Figure 1) [*Teoh*, 2002]. Clarendon Weir is a small reservoir with a capacity of 0.3 GL, while Happy Valley Reservoir has a capacity of 11.6 GL (see www.sawater.com.au). Happy Valley Reservoir is considered an "off-stream" reservoir, with water only being supplied via the Horndale Flume, while Clarendon Weir receives water released from Mount Bold Reservoir, as well as runoff from its 54 km^2 catchment (Figure 1). The main purpose of Happy Valley Reservoir is to store water prior to treatment at the Happy Valley WTP, which has a capacity of 850 ML/day (see www.sawater.com.au).

[16] Mount Bold Reservoir also receives water from the River Murray via the Murray Bridge-Onkaparinga (MBO) Pipeline (Figure 1). Although flows in the River Murray are affected by rainfall in the basin, the upper limit of water that Adelaide has previously been able to source from the River Murray has been determined by licenses, rather than rainfall. For example, licenses have allowed for up to 90% of Adelaide's water to be sourced from the River Murray in the past in dry years, whereas about 40% of Adelaide's demand has been supplied by the River Murray on average [*Government of South Australia*, 2009]. Furthermore, and contrary to the common principle that a license does not necessarily guarantee water availability, Adelaide's River Murray usage is almost certainly guaranteed because (1) it constitutes less than 1% of total River Murray flow; (2)

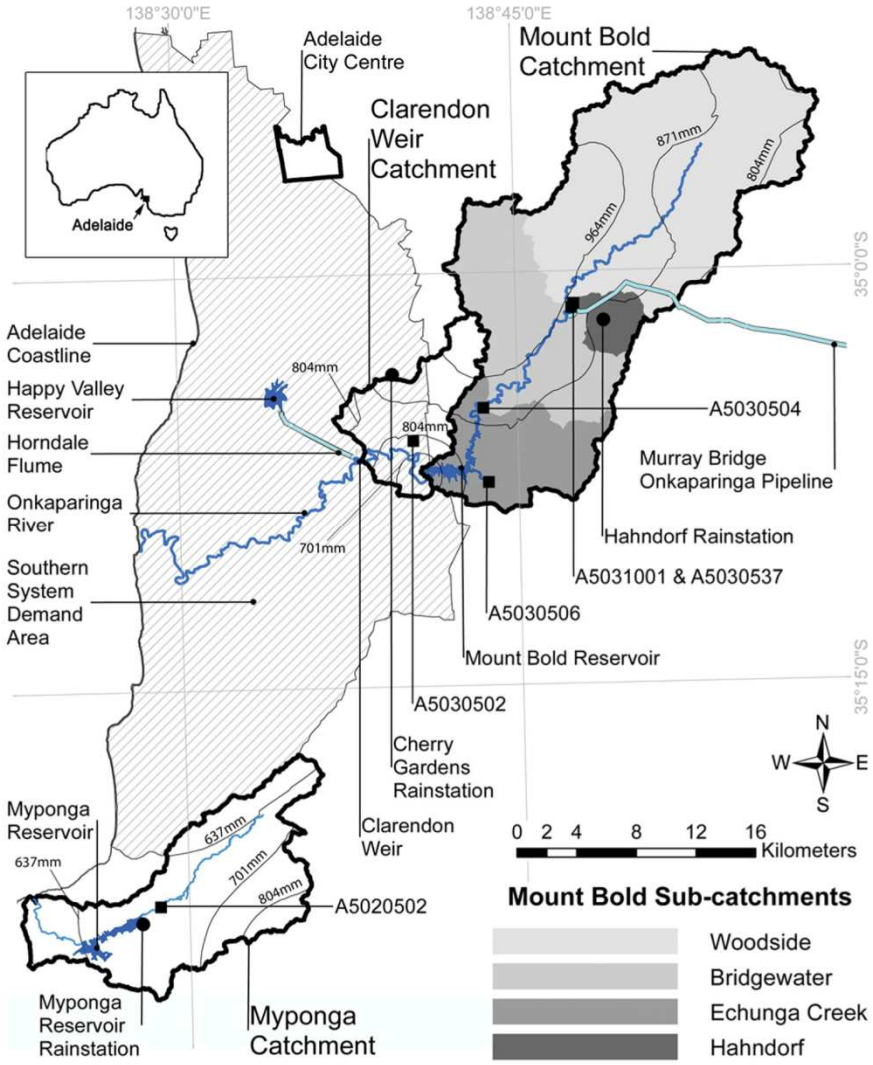

Figure 1. Map of Adelaide's southern water supply system, detailing reservoirs, reservoir catchments, major rivers, pipelines, and the southern system demand area. Gauging stations, rainfall stations, Mount Bold subcatchments, and isoheytal lines that have been defined for calibrating RRO models for each catchment are also illustrated. Inset of map of Australia highlighting location of Adelaide.

critical human needs, including for Adelaide, are the highest priority in allocating River Murray water; and (3) the significant storage of the River Murray system helps to dampen out temporal variability in flow that might restrict water availability for a particular time period. The amount of River Murray water that Adelaide can use is based on a 5 year rolling license of 650 GL, with the license period beginning on 1 May each year. However, the license alone cannot supply all of Adelaide's water demand, as the maximum River Murray supply over 5 years is about 65% of total demand. Furthermore, with projections of population growth resulting in future increases in demand, the percentage of demand potentially met by the River Murray will reduce (as the 5 year license is fixed at 650 GL). Hence, supply from local catchments is vital in order to meet demand.

3. Methods

[17] Figure 2 illustrates the methodology and data used to assess water supply security at a number of discrete times in the future and the relative contributions of sources of uncertainty of climate change impacts on water supply security for Adelaide's southern system. The first step was the development of RRO models (Figure 2), which were necessary to determine runoff from the Myponga, Mount Bold, and Clarendon Weir catchments, while the second step was to develop climate change affected rainfall and

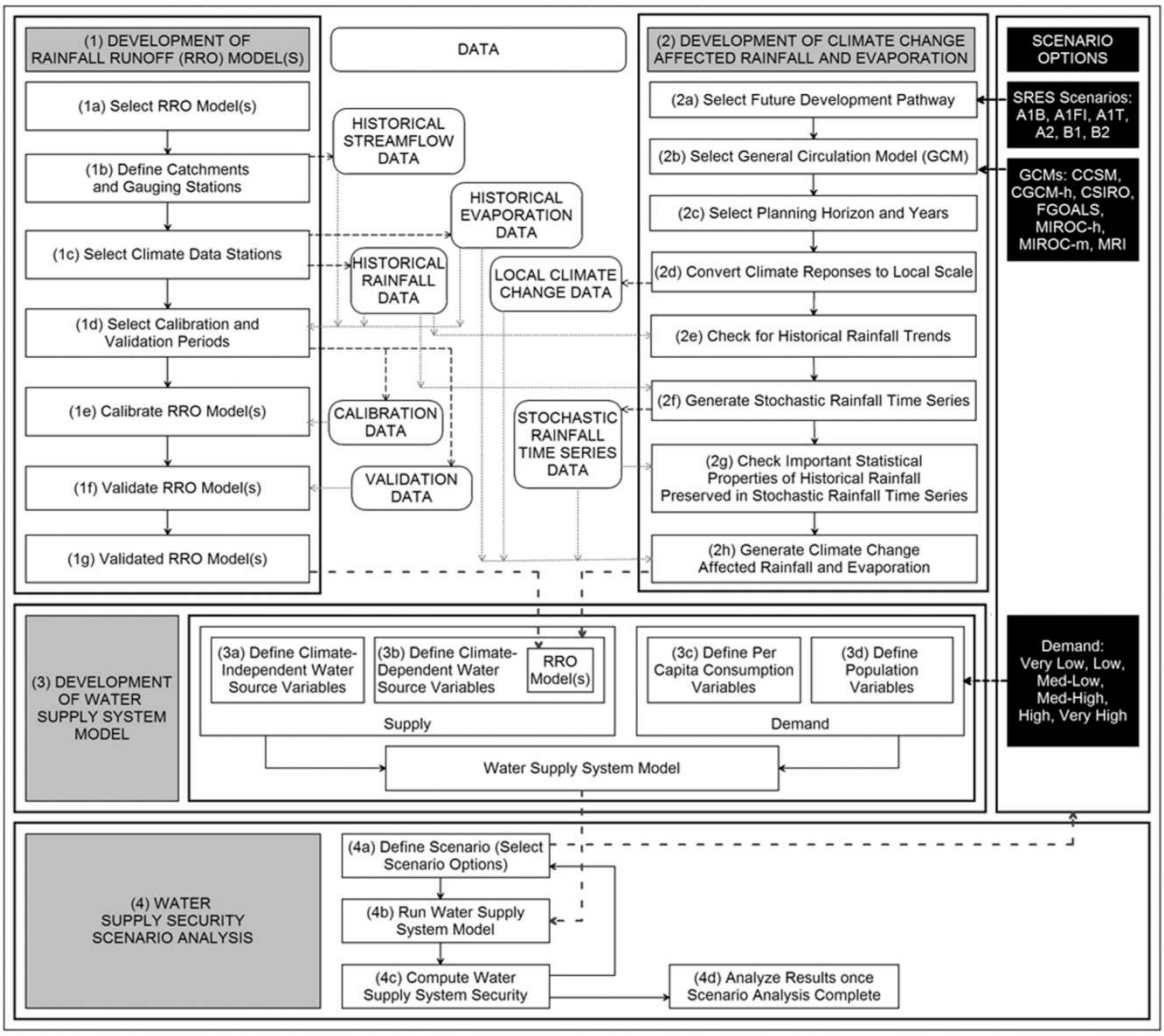

Figure 2. Flowchart of the methodology followed for the Adelaide southern water supply system case study.

evaporation (Figure 2). For clarity, data that were used in the case study for both the RRO models and the development of climate change affected rainfall and evaporation are highlighted in Figure 2. The validated RRO models from Step 1 and the climate change affected rainfall and evaporation from Step 2 were then applied in the development of the water supply system model for the southern Adelaide system (Figure 2). Specifically, the RRO model and the climate change affected rainfall and evaporation were used to determine supply from the climate-dependent water sources, namely the three reservoirs: Myponga, Mount Bold, and Happy Valley (Step 3, Figure 2). The supply component also incorporated the climate-independent water source of the River Murray (as explained above, see also section 3.3.1.1), while demand was a combination of per capita consumption and population (Step 3, Figure 2). Finally, in Step 4, water supply security was assessed for various uncertain water supply scenarios in a systematic fashion, investigating uncertainties in future development pathways, GCMs, and demand (Figure 2). Steps 3 and 4 are very important because as illustrated in section 1, studies have examined the relative magnitudes of uncertainty associated with climate change impacts on runoff, but there is a need to extend this to water supply systems, for which there are additional uncertainties (e.g., demand) and additional complexities (e.g., storages).

[18] The four major steps of the flowchart are discussed in more detail in the following sections, while justification for the scenario options considered in this paper (delineated by the black boxes in Figure 2), is provided in section 3.4. While the following discussion focuses on Adelaide's southern water supply system, the methodology presented in Figure 2 could also be readily applied to other water supply systems. However, some alterations may be required. For example, in the case study, stochastic rainfall time series were generated for a historical record and then

Table 1. Gauging Station Data for Each Catchment

Catchment	Catchment Area (km^2)	Gauging Station Identification	Gauging Station Area (Percentage of Catchment Area) (%)	Gauging Station Data Period Available	Data Record Completeness (Percentage of Data Period Available) (%)
Myponga	124	A5020502	61	Oct. 1979–Feb. 2011	98.8
Mount Bold	388	A5030504	83	May 1973–Jan. 2011	100
		A5030506	9	Apr. 1973–Dec. 2010	97.1
		A5031001	59	Jul. 2002–Jul. 2011	99.2
		A5030537	4	Apr. 1993–Mar. 1996; Jul. 2002–Jul. 2011	98.1
Clarendon Weir	54	A5030502	49	Apr. 1969–Dec. 2010	100

perturbed for climate change, while in other cases, calibrating a weather generator on a climate change perturbed record (for example, see *Kilsby et al*. [2007]), or conditioning the parameters of a weather generator using GCM output to directly incorporate the climate change signal, may be more appropriate. In addition, the focus in this case study is on the impacts of climate change on supply; however, climate change impacts on demand could also be incorporated. For example, *Groves et al*. [2008] found outdoor water demand was projected to increase by 10% in southern California by 2040 due to the impact of climate change.

3.1. Development of RRO Model(s)

3.1.1. Select RRO Model(s)

[19] The WC1 model was selected to determine runoff in this case study (Step 1a, Figure 2) because it has been used previously throughout the Mount Lofty Ranges [*Alcorn*, 2006; *Savadamuthu*, 2003; *Teoh*, 2002] and because it was developed based on experience with South Australian RRO calibration in the Mount Lofty Ranges and other parts of the state (see www.waterselect.com.au). WC1 is a 10-parameter, conceptual RRO model that employs a three-bucket concept, in which the three storage components (or buckets) of the model are (1) interception store, (2) soil moisture store, and (3) groundwater store. Surface, interflow, and groundwater flow potentially contribute to surface runoff. Further details of the WC1 model can be found in the WaterCress user manual, available from www.waterselect.com.au. Both daily rainfall and monthly evaporation are required for WC1 to compute runoff.

3.1.2. Define Catchments and Gauging Stations

[20] Daily flow data from gauging stations A5020502, A5030504, A5030506, and A5030502 (Figure 1) were selected for this case study (Step 1b, Figure 2) because large areas of the Myponga, Mount Bold, and Clarendon Weir catchments contribute flow at these stations and because the data sets span three to four decades and are relatively complete (Table 1). Furthermore, a catchment model of increased complexity was also defined for the Mount Bold catchment to assess the impact of model complexity on model performance. For the complex model, which contains four RRO models (one for each subcatchment), a further two suitable gauging stations for the Mount Bold catchment (A5031001 and A5030537, see Figure 1) were selected (Table 1).

[21] For each of the six gauging stations, streamflow data were sourced from the Government of South Australia's surface water archive (www.waterconnect.sa.gov.au/SWA). Long and complete records were available for A5030502 and A5030504, long but incomplete records were available for A5030506 and A5020502, while relatively shorter and incomplete records were available for A5030537 and A5031001 (Table 1). For records that contained missing streamflow data at the very beginning or very end of the data periods, the data were excluded, while if the missing data were in the middle of the data set, they were estimated using regression analysis with nearby flow gauges. Flow records downstream of the MBO pipeline were also adjusted to take into account volumes supplied from the River Murray. Furthermore, an assessment of the rainfall and streamflow records for the Myponga catchment illustrated that from about the late 1990s, there was a marked decrease in large streamflow events but no decreasing trend in rainfall. A5020502 data were predominantly tagged as good quality, so errors in gauging seem unlikely to have caused this trend. The altered flow regime is more likely due to an increase in small farm dams and an intensification of dairying, viticulture, and olive horticulture that has occurred in the catchment over time. Consequently, calibration and validation were only carried out for Myponga catchment from January 1999 to December 2010.

3.1.3. Select Climate Data Stations

[22] The Bureau of Meteorology (BoM) stations Myponga Reservoir (23738), Hahndorf (23720), and Cherry Gardens (23709) were selected as suitable climate data stations (Step 1c, Figure 2) to represent Myponga, Mount Bold, and Clarendon Weir catchments, respectively. These stations were selected because they are part of the patched point data set (PPD) [*Jeffrey et al*., 2001], a data set comprising approximately 4600 locations around Australia and spanning from 1890 to the current day. The PPD is based on observed BoM daily meteorological records that have been enhanced by high-quality, rigorously tested data infilling (when data are missing) and deaccumulation of any records that represented rainfall over multiple days, rather than a single day [*Charles et al*., 2008].

3.1.3.1. Rainfall

[23] A number of advantages exist in using the PPD for rainfall data in this study. First, the data from each site span identical time periods with interstation correlations being upheld. Second, the data cover a long timeframe so that the existing long-term variability in rainfall experienced in Adelaide is incorporated, while third, the rainfall data are a continuous time series, which is a necessary input requirement for the modeling and analysis tools used in this study. Finally, rainfall data in the original BoM data

sets for these stations span a significant time period and are relatively complete (Table 2), ensuring that the potential errors occurring through the infilling process are minimized because the use of observed data is maximized. For example, the stations selected have greater than 90 years of rainfall records and are between 89% and 98% complete (Table 2).

[24] The climate data stations were also selected because of their location within each catchment (Figure 1), which is an important consideration in attempting to obtain an accurate representation of rainfall for a particular area because rainfall displays the largest spatial variability among meteorological variables [*Srikanthan and McMahon*, 2001]. In this case study, the average annual rainfall for each catchment was estimated using ArcGIS. First, all BoM stations that occurred in the PPD and that were within 15 km of the three catchments were selected. The average annual rainfalls for all stations were then spatially interpolated using the inverse distance-weighted tool and with the resulting interpolation classified into seven categories (isoheytal areas) using the Natural Breaks (Jenks) method. The average of the bounding rainfall values for each of the isoheytal areas was taken as the average rainfall for each respective area (Figure 1). These average values were then weighted by area to calculate an average annual rainfall for each of the catchments (Table 2). The resulting differences between these values and the average annual rainfall amounts for each respective climate data station were then used to create a rainfall scaling factor (Table 2), by which all daily rainfall amounts in the historical data sets were multiplied.

3.1.3.2. Evaporation

[25] Evaporation (which is treated as an equivalent to actual evapotranspiration in WC1) was calculated by multiplying recorded daily evaporation by the pan factor for soil (which is one of the RRO parameters to be calibrated). Recorded daily evaporation was converted from monthly Pan A evaporation inputs, which in this case study were sourced from averaging values in the PPD between 1975 and 2004 (Table 3). While the PPD contain daily evaporation values from 1889 onward, Class A evaporation pans were only installed in Australia during the 1960s [*Rayner*, 2005], so values in the PPD pre-1970 were interpolated from long-term averages and were thus not included. Furthermore, to develop the climate change scenarios for evaporation later in this study, evaporation data based on the 30 years from 1975 to 2004 are required (see section 3.2.3), so this 30 year period was selected.

3.1.4. Select Calibration and Validation Periods

[26] Approximately 60%–70% of the available data were used for calibration and 30%–40% for validation (Step 1e, Figure 2), ensuring that at least 5 years of data were used in calibration and at least 3 years were used in validation (Table 4). The calibration and validation periods for Myponga, Woodside, Hahndorf, and Bridgewater were very short, which could potentially limit the RRO models in accurately capturing the catchments' RRO behavior, particularly if these time periods do not contain particular extreme events, such as droughts. Calibration and validation periods began in January and were multiples of 12 months, so as not to bias the RRO models' calibrated parameters toward a particular month's flow properties.

Table 2. Rainfall Station Data for Each Catchment

Catchment	Subcatchment	Climate Data Station (BoM Identification Number)	BoM Record Length	BoM Data Set Completeness (%)	Average Annual Rainfall for Climate Data Station (mm/yr)	Average Annual Rainfall for Catchment (mm/yr)		Rainfall Scaling Factor	
						Calibration and Validation	Whole Catchment	Calibration and Validation	Whole Catchment
Myponga		Myponga Reservoir (23738)	1914–2010	89	752	736	728	0.9785	0.9677
Mount Bold (simple)		Hahndorf (23720)	1884–2010	95	849	919	914	1.0828	1.0770
Mount Bold (complex)	Woodside	Hahndorf (23720)	1884–2010	95	849	906	906	1.0671	1.0671
	Hahndorf	Hahndorf (23720)	1884–2010	95	849	856	856	1.0085	1.0085
	Bridgewater	Hahndorf (23720)	1884–2010	95	849	990	990	1.1659	1.1659
	Echunga (& Mount Bold Reservoir)	Hahndorf (23720)	1884–2010	95	849	842	841	0.9918	0.9911
Clarendon Weir		Cherry Gardens (23709)	1899–2010	98	929	943	859	1.0150	0.925

Table 3. Average Monthly Evaporation for Climate Data Stations

Rainfall Station	Average Evaporation (mm/month)											
	Jan.	Feb.	Mar.	Apr.	May	Jun.	Jul.	Aug.	Sep.	Oct.	Nov.	Dec.
Myponga Reservoir	219	188	151	96	62	45	50	67	90	130	165	199
Hahndorf	233	201	162	102	66	47	52	72	95	139	179	213
Cherry Gardens	217	188	149	92	57	39	44	61	84	124	161	195

[27] Adelaide also suffered a severe drought from 2003 to 2009, so data from this time period alone possibly suffered from a dry rainfall bias. While it is important to understand water supply security during dry periods, it is also critical to accurately simulate runoff during wet periods as this runoff can replenish storages and potentially be used to buffer droughts. Furthermore, RRO models calibrated only on dry periods may not be able to accurately simulate the response to wet periods, so this was avoided where possible. However, it could not be helped when calibrating Woodside, Hahndorf, and Bridgewater catchments (Table 4) because of the need to use overlapping data from identical periods, a result of the Bridgewater gauging station (A5030504) being downstream of both the Woodside and Hahndorf gauging stations (A5031001 and A5030537, respectively) (Figure 1).

3.1.5. Calibrate RRO Model(s)

[28] A genetic algorithm (GA) was chosen over classical methods of optimization to calibrate the WC1 models (Step 1f, Figure 2), because genetic algorithms have shown to be successful in optimizing RRO models [*Wang*, 1991]. Upper and lower limits for each parameter for WC1 were defined to restrict the search space of the GA and ensure the physical plausibility of the parameter values. The bounds for WC1 parameters were based on limits defined in the WaterCress user manual (see www.waterselect.com.au), which were similar to those used in the Mount Lofty Ranges, studies by *Teoh* [2002] and *Savadamuthu* [2003].

[29] Initial GA parameter trials examined populations of 100–400, generations of 100–300, and values of 0.6–0.9 for the probability of crossover, with final GA parameter selection being 200 for population, 150 for maximum number of generations, and 0.7 for probability of crossover. The probability of mutation was taken as 0.1—the inverse of the number of model parameters. In order to check whether parameter equifinality [*Beven*, 2006] is a potential problem, each calibration run was repeated 10 times from different starting positions in parameter space. First, there was little change in the calibration errors for the 10 trials. Similarly, the calibrated RRO parameters were reasonably stable over the 10 calibration runs, and the flows were not sensitive to these slight changes in parameters.

Table 4. Calibration and Validation Periods for Catchments and Subcatchments

Catchment or Subcatchment		Calibration Period	Validation Period
Myponga		Jan. 1999–Dec. 2006	Jan. 2007–Dec. 2010
Mount Bold (simple)		Jan. 1974–Dec.1999	Jan. 2000–Dec. 2010
Mount Bold (complex)	Woodside	Jan. 2003–Dec. 2007	Jan. 2008–Dec. 2010
	Hahndorf	Jan. 2003–Dec. 2007	Jan. 2008–Dec. 2010
	Bridgewater	Jan. 2003–Dec. 2007	Jan. 2008–Dec. 2010
	Echunga	Jan. 1975–Dec.1999	Jan. 2000–Dec. 2010
Clarendon Weir		Jan. 1970–Dec.1997	Jan. 1998–Dec. 2009

[30] The root-mean-square error (RMSE) of the monthly flows was selected as the performance criterion; such that RMSE was minimized in the optimization process (an RMSE equal to zero indicates a perfect fit). RMSE is biased toward minimizing error in high flows but was selected as the objective because, as mentioned in section 3.1.4, when studying water supply security, accurately simulating runoff from the large rainfall events is likely to be more important than simulating runoff from the more frequent low rainfall events, because of the ability of reservoirs to store water. If the amount of runoff from wet periods was underestimated or overestimated, the amount of water available in the storages could be quite different from reality, and would thus affect the estimated supply security during dry periods when demand exceeded runoff. Hence, high flows have the potential to have a much bigger impact on water supply security than low flows and, as such, minimizing errors in these high flows is critical. A monthly time step was chosen over a daily time step for assessing model performance because the storage of the reservoirs was likely to buffer any daily errors obtained in runoff. The average annual flows for the observed and modeled data sets and the monthly Nash-Sutcliffe (NS) were also calculated following optimization. A minimal difference between the annual observed and modeled flows and an NS value approaching one were sought. However, *Jain and Sudheer* [2008] point out that a high value of NS can be achieved for a model with a poor fit. Consequently, although more subjective than the use of statistical measures of goodness-of-fit, plots of simulated and observed hydrographs were also inspected following optimization. *Refsgaard and Storm* [1996] note that the visual inspection of plots is an efficient means of assimilating information as well as providing a good overall insight into a model's capabilities. To compare the simple and complex Mount Bold catchment models, an additional criterion was required that could penalize model complexity as well as error. This is based on the principle that for a given level of accuracy a more parsimonious model is preferable [*Bozdogan*, 1987]. The application of the principle of parsimony in hydrological modeling is discussed by *Wagener et al.* [2004], but, in brief, complexity control is advantageous as it reduces parameter equifinality by identifying the simplest model that explains the observed data [*Schoups et al.*, 2008]. The Akaike information criterion (AIC) [*Akaike*, 1973] based on monthly flows was used for this purpose.

3.1.6. Validate RRO Model(s)

[31] Model validation (Step 1f, Figure 2) was necessary to check that the RRO parameters optimized during calibration also performed well on independent data. A model was to be rejected as being not behavioral (i.e., not consistent with observations) [*Beven*, 2006] for this case study if (1) the modeled hydrographs were judged to not adequately match the observed hydrographs based on visual inspection, (2) NS was < 0.50 [*Moriasi et al.*, 2007], and/or (3) the RMSE was more than half the standard deviation of the observed flows [*Singh et al.*, 2004]. Validation periods for

Table 5. Root-Mean-Squared Error (RMSE), Nash-Sutcliffe (NS), Ratio of RMSE to Standard Deviation (SD), and Average Observed and Modeled Flows for the Calibration and Validation Periods of the WC1 Models for the Myponga, Mount Bold (Simple), Mount Bold (Complex), and Clarendon Weir Catchments

		Accuracy Criteria for Calibration					Accuracy Criteria for Validation				
Catchment or Subcatchment		RMSE (ML/month)	NS	RMSE/SD	Average Observed Flow (GL/yr)	Average Modeled Flow (GL/yr)	RMSE (ML/month)	NS	RMSE/SD	Average Observed Flow (GL/yr)	Average Modeled Flow (GL/yr)
Myponga		228	0.92	0.28	7.5	7.9	315	0.80	0.44	5.2	3.2
Mount Bold (simple)		1775	0.95	0.22	51.9	51.6	1996	0.88	0.35	41.4	41.2
Mount Bold (complex)	Woodside	798	0.90	0.31	16.9	15.8	888	0.94	0.24	20.6	17.4
	Hahndorf	122	0.74	0.51	1.9	1.6	105	0.88	0.34	2.1	1.8
	Bridgewater	1277	0.75	0.50	19.8	16.8	919	0.81	0.43	16.9	18.2
	Echunga	203	0.89	0.34	3.4	3.3	148	0.87	0.35	2.6	2.6
Clarendon Weir		134	0.94	0.25	3.9	3.9	138	0.87	0.36	3.0	3.5

the case study were as defined in section 3.1.5, while the validation performance evaluation measures were the same as those defined above for calibration.

3.1.7. Validated RRO Model(s)

[32] To have confidence in using the optimized WC1 model parameters to estimate runoff for the case study, it was necessary to analyze whether the RRO models produced results within the range of accuracy identified in section 3.1.6 for the validation data. All RRO models developed for this case study had an $NS > 0.50$, while the RMSE values for most catchments were considered low, as they were less than 50% of their respective standard deviations, except for the calibration periods of the Hahndorf and Bridgewater subcatchments, for which they were slightly greater than 50% (Table 5). However, this was considered obsolete, because based on the NS efficiency values (Table 5) and AIC values (1515 for the complex model compared to 1480 for the simple model), it was decided the simple Mount Bold model should be used rather than the complex one. An assessment of the modeled monthly hydrographs indicated that the WC1 models recreated the observed flow hydrographs reasonably well. The WC1 model parameter values (Table 6) were similar to those obtained in previous calibration studies on nearby catchments [*Alcorn*, 2006; *Teoh*, 2002], indicating that the model parameters obtained were reasonable. Thus, the calibrated RRO models were considered valid (Step 1g, Figure 2) and could be applied to the case study with confidence.

3.2. Development of Climate Change Affected Rainfall and Evaporation Data

3.2.1. Select Future Development Pathway and GCM

[33] The first step in developing the climate change affected rainfall and evaporation data was to select the SRES scenario to represent a future development pathway (Step 2a, Figure 2). A GCM was then selected (Step 2b, Figure 2) to translate the future emission pathway to regional climate responses. The scenario options selected for SRES scenarios and GCMs for the case study are discussed in section 3.4.1.

3.2.2. Select Planning Horizon and Years

[34] A planning horizon and the years for which to progressively analyze system security for the case study must be selected (Step 2c, Figure 2) to ensure that future critical points in time for water supply security will be recognized. For the case study, a 40 year period from 2010 to 2050 was selected, with 2010, 2020, 2030, 2040, and 2050 identified as regular but discrete years to analyze.

3.2.3. Convert Climate Responses to Local Scale

[35] The constant scaling or delta change approach was used in the case study to obtain local rainfall and evaporation responses (Step 2d, Figure 2). The constant scaling approach meant that for each month and for each climate site, the historical baseline climate was scaled by a factor representing the change projected in that month for the closest GCM grid point.

[36] Specifically, monthly factors for rainfall and areal potential evapotranspiration (equivalent to Pan A Evaporation and calculated according to the method described in *Morton* [1983]), were obtained from the Australian Commonwealth Scientific and Industrial Research Organization's (CSIRO) OzClim (www.csiro.au/ozclim/). Ozclim is a tool developed for the scientific research community and policy makers that provides data on a 25 km grid over Australia. Change factors for each grid point are developed by (1) using linear regression to obtain the local change in the value of a climate variable (e.g., rainfall) per degree of global warming for a particular GCM, and (2) multiplying

Table 6. Parameter Values for the WC1 RRO Models for Each of the Catchments

	WC1 Model Parameter									
Catchment or Subcatchment	Median Soil Moisture (mm)	Catchment Distribution (mm)	Interception Store (mm)	Ground Water Discharge	Soil moisture discharge	Pan factor for soil	Fraction Groundwater Loss	Store Reduction Coefficient	Groundwater Recharge	Creek Loss (mm)
Myponga	160	59.4	8.1	0.0015	0.00015	0.94	0.49	0.90	0.45	0.01
Mount Bold	186	60.0	9.3	0.0015	0.00012	0.84	0.49	1.39	0.15	0.00
Clarendon Weir	195	59.5	8.0	0.0015	0.00015	0.99	0.20	0.85	0.30	0.01

this result by the degree of global warming associated with an SRES scenario. These change factors can then be applied to the baseline climatology of the climate variable (defined from 1975 to 2004), to produce future climate projections. For this case study, the change factors for rainfall and evaporation were extracted for 2020, 2030, 2040, and 2050.

[37] The delta change approach is a simple downscaling approach and has a number of limitations that include (1) the mean, maxima, and minima are the only data properties that are different between the scaled and baseline climate; (2) the spatial pattern of the present climate is assumed for the future; (3) the approach, without modification, cannot simulate changes in the occurrence of rainfall, nor changes to the size of extreme events; and (4) values for a single grid cell may contain gross biases [*Wilby and Fowler*, 2011]. However, the constant scaling approach was selected to downscale GCM data because (1) simple downscaling approaches can accurately simulate flow [*Fowler et al*., 2007] and (2) the constant scaling approach can be applied easily using multiple GCMs and SRES scenarios [*Mpelasoka and Chiew*, 2009], which was important in this case study in order to analyze uncertainties associated with these factors.

3.2.4. Check for Historical Rainfall Trends

[38] It was important that the historical rainfall time series were checked for trends before generating the stochastic rainfall time series because the stochastic rainfall generator used in this case study—stochastic climate library (SCL) (section 3.2.5), assumes that the input data (i.e., the historical rainfall) have already been checked for stationarity. Consequently, the rainfall data were run through TREND (www.toolkit.net.au/trend) (Step 1d, Figure 2), a tool developed by the Cooperative Research Centre (CRC) for Catchment Hydrology, which enables statistical testing for trend, change, and randomness in time series data [*Chiew and Siriwardena*, 2005]. As the distribution of rainfall is unknown, only the nonparametric tests were used. The Mann-Kendall and Spearman's Rho tests were used to test for a trend; the distribution-free Cumulative Sum (CUSUM) was used to test for a step jump in the mean; while the rank-sum test was used to check for a difference in median between two sections of the data set. In this case study, rainfall from May 1974 to April 2004 was elected as the baseline data from which to derive future climate change scenarios because 1975 to 2004 is the OzClim baseline (see section 3.2.3), and the River Murray license year runs from 1 May to 30 April (see section 2). Consequently, rainfall data from the three sites spanning this time period were analyzed in TREND. For each of the three rainfall stations, none of the aforementioned tests returned a significant result (indicating that there were no trends or step jumps in the nominated time series), apart from the Mann-Kendall test for Hahndorf. However, the significance level of this test suggested that there was little evidence of a trend, and given the Spearman's Rho test (which also tests for a trend) did not return a significant result, it was presumed that if such a trend in the Hahndorf data set existed, it was insignificant for the purpose of this study.

3.2.5. Generate Stochastic Rainfall Time Series

[39] Generating stochastic rainfall time series for the case study (Step 2e, Figure 2) was important because urban water supply planning should include the stochasticity in precipitation [*O'Hara and Georgakakos*, 2008] and because Adelaide has such high, natural temporal rainfall variability (see section 2). Use of stochastic rainfall data ensured that (1) the results produced were not simply a reflection of the historical rainfall time series, and (2) water supply system security could be reported as a distribution to reflect the inherent variability in historical rainfall, rather than a single deterministic value. A probability-based approach is particularly useful from a water management perspective because it establishes ranges and confidence levels to help understand future levels of risk to the system. It is important to note that while this distribution will reflect historical rainfall variability, it does not necessarily reflect future rainfall variability. To correctly achieve projections of future rainfall variability would require applying a perturbed physics ensemble or weather generator to generate rainfall sequences based on climate characteristics. For example, a weather generator could be calibrated on a climate change perturbed record or its parameters could be conditioned on large-scale atmospheric predictors, weather states, or rainfall properties to directly incorporate climate change [*Wilby and Fowler*, 2011]. These methods are beyond the scope of this paper.

[40] The stochastic rainfall time series were constructed using the multisite daily rainfall model of the SCL (www.toolkit.net.au/scl), developed by the CRC for Catchment Hydrology [*Srikanthan*, 2005]. It is a multisite two-part daily model, nested in a monthly and annual model. The first part consists of rainfall occurrence, which is determined using a first-order two-state Markov chain, while the second part relates to rainfall amounts, derived using a gamma distribution [*Srikanthan*, 2005]. This daily model is then nested in a monthly and annual model in order to preserve the monthly and annual characteristics. The monthly and annual models are driven by the noise term derived from the generated daily rainfall data. The mathematical development of the monthly and annual models is provided by *Srikanthan* [2005] and *Srikanthan and Pegram* [2009]. Because of the great spatial variability of rainfall (see section 3.1.3.1), a multisite model was necessary to account for the spatial dependence between rainfall stations, while the SCL was selected because it preserves the important characteristics of rainfall at daily, monthly, and annual time scales [*Srikanthan*, 2005].

3.2.6. Check Important Statistical Properties of Historical Rainfall Preserved in Stochastic Rainfall Time Series

[41] Statistical analyses of the developed stochastic time series were necessary to ensure that the important statistical properties of the historical data were preserved in the stochastic time series (Step 2f, Figure 2). *Srikanthan et al*. [2004] provide suggested tolerances for each statistical parameter but also suggest that users make their own assessment of the quality of the data produced by SCL because certain statistics may be more important than others depending on the application. First of all, because these stochastic time series represent natural rainfall variability, measures of variability (e.g., standard deviation) must be assessed and because of the high interannual and interdecadal variability experienced by Adelaide (see section 2), preservation of interannual and interdecadal variability was

Table 7. Important Annual Statistical Properties of the Historical and Generated Rainfall Time Series

			Climate Data Station					
			Hahndorf		Cherry Gardens		Myponga	
Parameter		Unit	Historical	Generated	Historical	Generated	Historical	Generated
Mean		mm/yr	794	794	905	906	756	756
Standard deviation		mm/yr	158	159	145	146	163	163
Maximum		mm/yr	1248	1139	1335	1220	1111	1113
Minimum		mm/yr	479	487	665	619	467	444
Low rainfall sums	2-yr	mm/2yrs	1188	1204	1441	1452	1107	1087
	3-yr	mm/3yrs	1931	1938	2261	2301	1852	1771
	5-yr	mm/5yrs	3474	3452	4140	4044	3316	3197
	7-yr	mm/7yrs	4975	5003	5864	5821	4626	4663
	10-yr	mm/10yrs	7368	7375	8665	8530	6813	6920

also necessary. For this case study, the 2-, 3-, 5-, 7-, and 10-year low rainfall sums were particularly important, because the accumulation of a number of years with below-average rainfall creates water supply security concerns, rather than a single year. This is because Adelaide currently has the ability to buffer an extremely low rainfall year through reservoir storage and pumping water from the River Murray with a 5 year rolling license, whereas an accumulated dry spell of a number of years may result in reservoirs running dry and the River Murray license being fully allocated. The annual mean rainfall was also considered an important measure, so as not to overpredict or underpredict runoff. Furthermore, the coincidence of below-average rainfall years across the three rainfall sites could also impact total water supply from the reservoirs, so matching the observed annual cross correlation between rainfall sites was also important.

[42] For the case study, 1000 stochastic rainfall time series of 30 years were developed. Differences between the annual standard deviation of the historical and generated series for all sites (Table 7) were no greater than 1 mm/yr, which is well within the tolerance of 5 mm/yr suggested by *Srikanthan et al*. [2004]. Similarly, differences in the maximum and minimum annual rainfall values for all three sites (Table 7) fell within the 10% tolerance suggested by *Srikanthan et al*. [2004]. The average difference in multiyear rainfall sums was 1.5%, with all multiyear rainfall sums (Table 7) well within the 10% tolerance suggested by *Srikanthan et al*. [2004]. The mean annual rainfall amounts in the generated data for the three sites (Table 7) were within 0.02% of the historical means, while the average difference in mean monthly rainfall amounts for the three sites was 2.0%, with only the February rainfall for Hahndorf and March rainfall for Cherry Gardens, not being within the 7.5% tolerance suggested by *Srikanthan et al*. [2004]. Finally, the differences in annual cross-correlation values between the three rainfall sites ranged from 0.01 to 0.04, well within the tolerance of 0.2 suggested by *Srikanthan et al*. [2004]. Consequently, based on the similarity in statistical properties that were considered important to this case study, the generated stochastic data were considered to preserve the important characteristics of the historical rainfall and were thus appropriate for further use in this study. However, it is recognized that the time period elected to base the stochastic rainfall time series on (30 years from 1974 to 2004), is relatively short and may therefore not represent the true natural rainfall variability of the system. While longer time periods were considered to increase the representation of natural rainfall variability, the average monthly mean rainfalls of the longer data sets were considerably different to those for OzClim's 30 year baseline (see section 3.2.3) and so could not be used in this case study.

3.2.7. Generate Climate Change Affected Rainfall and Evaporation

[43] Climate change affected rainfall and evaporation were subsequently developed by applying the percentage changes obtained from OzClim to the stochastic rainfall time series and the historical evaporation data, respectively (Step 2g, Figure 2). A caveat of this methodology is that the stochastic rainfall time series and historical evaporation data are not mutually consistent, which may affect daily runoff because it is a response to both of these variables acting together. However, uncorrelated daily rainfall and evaporation are not expected to influence water supply system security because the storage of the reservoirs is likely to buffer any daily errors obtained in runoff. Furthermore, evaporation is less variable compared with rainfall; for example, for the baseline period of 1974–2005 for Kent Town, the average standard deviation of evaporation per month was approximately half of that for rainfall.

3.3. Development of Water Supply System Model

[44] The water supply system model consisted of both supply and demand components, with supply requiring the definition of climate-independent (Step 3a, Figure 2) and climate-dependent (Step 3b, Figure 2) water sources and demand requiring per capita consumption (Step 3c, Figure 2) and population (Step 3d, Figure 2) variables to be defined. Climate change affected rainfall and evaporation data from Step 2 were used to determine supply from the reservoirs (climate-dependent sources), while the validated RRO models of Step 1 were used to calculate runoff from the catchments that flowed into the reservoirs (Figure 2).

3.3.1. Water Supply System Model

[45] The continuous time series, water resources model WaterCress (available from www.waterselect.com.au), was chosen for this case study because it can not only balance supply and demand and uphold system constraints but also (1) readily incorporate multiple rainfall time series (see section 3.2.5), (2) model multiple catchment-reservoir relationships, (3) incorporate an external supply to represent the River Murray, and (4) output data to easily compute

Table 8. Monthly Mount Bold Reservoir Levels (as a Percentage of Full Capacity) That Trigger Use of River Murray Supply

Jan.	Feb.	Mar.	Apr.	May	Jun.	Jul.	Aug.	Sep.	Oct.	Nov.	Dec.
90%	90%	90%	90%	2%	2%	2%	2%	2%	2%	80%	90%

water security. Furthermore, the model is freely available and has the advantage of being developed and supported within South Australia.

3.3.1.1. Supply

[46] As mentioned in the introduction to section 3, both climate-dependent and climate-independent supply sources were defined for Adelaide's southern system. For Adelaide, the availability of River Murray supply is dictated by licenses, rather than by climate, and as Adelaide only takes about 1% of River Murray flow, the amount prescribed is virtually guaranteed, irrespective of climatic conditions (see section 2). Consequently, the River Murray supply was considered a climate-independent source for this case study, with its 5 year rolling Adelaide license of 650 GL converted to an annual license and then reduced by half to represent the southern system demand. Consequently, supply from the River Murray was capped at 65 GL/yr, with a year defined as being from 1 May to 30 April. Simplifying the 5 year rolling license to an annual license was necessary due to limitations of the water supply system model. This simplification is therefore considered a conservative approach because it has the potential to underestimate water supply security. The daily pumping capacity for the MBO pipeline of 447 ML/day (see www.sawater.com.au) was also defined as a constraint in the model. Furthermore, water was only pumped from the River Murray when the volume of water in Mount Bold Reservoir dropped below the levels defined in Table 8 (provided that the annual cap of 65 GL had not already been reached). These levels were calibrated in WaterCress using a trial-and-error approach in order to provide a balance between minimizing the loss of water through spillage (due to the reservoir exceeding full capacity) and maximizing water supply security.

[47] To simplify the reservoir modeling and because of the relationship between Clarendon Weir and Happy Valley Reservoir (see section 2), these two storages were treated as a single reservoir and are hereafter referred to as Happy Valley Reservoir. Water was supplied from Myponga reservoir and Happy Valley reservoir (which included water from Clarendon Weir catchment, Mount Bold catchment, and the River Murray) in equal priority and equal proportions, provided that water was available in each of the reservoirs. For Myponga, Mount Bold, and Happy Valley Reservoirs, evaporation and rainfall data were obtained from the same climate data stations as used for their respective catchments (see section 3.1.3). Minimum volumes were taken as the physical minimum operating levels as per *Crawley* [1995], and maximum volumes were as specified by SA Water (see section 2) (Table 9). The first of the two mathematical expressions provided in WaterCress were used to describe the reservoir volume-area relationships (which enabled evaporation losses from the reservoir surface to be computed):

$$SA = aV^b, \tag{1}$$

where SA is the surface area of the reservoir (hectare), V is the volume of the reservoir (ML), and a and b are parameters. For each reservoir, the resulting value for the volume-area relationship parameter a (Table 9) was determined by assuming the reservoir was at full capacity and holding the other volume-area relationship parameter b at 0.68 (the default value in WaterCress). This equation and parameter selection appeared reasonable, as when the modeled surface areas for Mount Bold reservoir were compared to measured values provided by *Crawley* [1995], there was generally less than 2% difference over a broad range of volumes.

Table 9. Properties of Mount Bold, Happy Valley, and Myponga Reservoirs

Reservoir	Minimum Volume (GL)	Maximum Volume (GL)	Volume-Area Relationship Parameters	
			a	b
Myponga	4.6	26.8	0.2729	0.68
Mount Bold	0.4	46.2	0.2073	0.68
Happy Valley	4.5	11.9	0.3066	0.68

3.3.1.2. Demand

[48] In 2008, Adelaide's total mains water consumption, with severe water restrictions in place, was approximately 166 GL (effectively 83 GL for the southern system), with water restrictions estimated to have saved 50 GL for the whole of Adelaide [*Government of South Australia*, 2009]. However, because water restrictions have now been lifted in Adelaide, demand for the southern system was modeled at the higher rate of 108 GL for 2010. This demand was assumed to be a function of individual per capita consumption and population, and both of these variables were adjusted on an annual basis over the 40 year planning horizon to constitute the demand scenario options (see section 3.4.1).

[49] Initial individual per capita consumption for the case study was based on the breakdown of demand between sectors in Adelaide for 2008, such that 63% was accounted for by the residential sector (with 40% of this demand attributed to outdoor use and 60% attributed to in-house use), while the remaining 37% was split between primary production, industrial, commercial and public purposes, and other [*Government of South Australia*, 2009]. Thus, total annual demands for the southern system in 2010 were assumed to be 40.8 GL for residential indoor use, 27.2 GL for residential outdoor demand, and 40.0 GL for nonresidential demand. Due to Adelaide's high natural intra-annual rainfall variability, outdoor demand in Adelaide also varies with time of year. Consequently, outdoor residential demand was varied using the percentages of exhouse usage estimated by *Barton* [2005] for Adelaide (Table 10).

[50] Adelaide's population in 2010 was about 1.2 million people, so assuming the southern system demand is approximately half of Adelaide's demand (see section 2), the initial population for the southern system was assumed to be approximately 600,000 people. Australia's average household size in 2001 was 2.6 people, while in 2026, this is projected to decrease to between 2.2 and 2.3 people, a

Table 10. Monthly Outdoor Water Use as a Percentage of Total Annual Outdoor Water Use [*Barton*, 2005]

Jan.	Feb.	Mar.	Apr.	May	Jun.	Jul.	Aug.	Sep.	Oct.	Nov.	Dec.
22.9%	18.8%	14.2%	6.4%	3.0%	0.0%	0.1%	0.7%	1.4%	4.9%	10.7%	17.0%

reflection of the increase in single-person households [*Australian Bureau of Statistics*, 2008]. For simplicity in the modeling, average household size was held at a constant 2.3 people throughout the planning period.

3.4. Water Supply Security Scenario Analysis

3.4.1. Define Scenario (Select Scenario Options)

[51] For the water supply security scenario analysis, scenario options were selected (Step 4a, Figure 2) in accordance with the objectives of the paper. Sixteen scenario options were defined to (1) assess the relative magnitude of the impacts of major sources of uncertainty and (2) identify critical points in the future for water supply security for Adelaide's southern water supply system. Average, best, and worst cases were defined to project a likely scenario and establish likely bounds of water supply security for Adelaide's southern water supply system.

3.4.1.1. Scenarios to Assess the Relative Magnitudes of Major Sources of Uncertainty and Identify Critical Points in the Future for Water Supply Security for Adelaide's Southern Water Supply System

[52] Different SRES scenarios, GCMs, and demands were considered as scenario options in the case study (Figure 2). The six SRES scenarios of A1B, A1FI, A1T, A2, B1, and B2 were selected (Figure 2) to cover the full range of potential future development pathways defined by the IPCC. The A1B scenario explores the situation of rapid economic growth and introduction of new and efficient technologies, a peak in global population at about 2050 and a balance across all energy sources, while A1FI and A1T are based on the same assumptions except in terms of technological advancement; A1FI assumes intense fossil fuel use while A1T assumes a non fossil fuel-directed future [*Intergovernmental Panel on Climate Change*, 2007]. A2 assumes a future with high population growth, slow economic growth, and gradual technological development; B1 reflects the same population outcomes as the A1 family but with quicker changes in economic structures to enable a service and information economy; while B2 represents intermediate population and economic growth with a focus on local sustainable solutions [*Intergovernmental Panel on Climate Change*, 2007].

[53] In selecting GCMs for this case study, CSIRO's Climate Futures Framework (CFF) [*Clarke et al*., 2011] was applied, in which plausible climates simulated by GCMs for different SRES scenarios are classified into a small set of representative climate futures (RCFs) defined by, and represented by, a matrix of two climate variables [*Whetton et al*., 2012]. Consequently, a smaller subset of models can be selected that covers the identified RCFs to reduce computational effort but still address the uncertainty in GCM projections. Skill-based GCM assessments are another method used to define smaller subsets of GCMs, but these suffer from (1) the assumption that a good estimation of past climate correlates with a good estimation of future climate, and (2) the lack of a robust method [*Whetton et al*., 2012], and community-agreed metric [*Perkins and Pitman*, 2009], to use when attempting to identify "best performing" models.

[54] Before constructing the RCFs and in consultation with a CSIRO climate scientist, five GCMs were removed from the 24 available CGMs in the CFF (23 CMIP GCMs and CSIRO's Mk3.5 model) because they did not simulate the El Niño-Southern Oscillation (ENSO) phenomenon (L. Webb, personal communication), which was critical because (1) Adelaide's climate is influenced by ENSO interannual variability and (2) natural climate variability is important for this case study. The five GCMs excluded based on their poor simulation of ENSO were INM-CM3.0, PCM, GISS-EH [*Irving et al*., 2011], GISS-AOM, and GISS-ER [*Irving et al*., 2011; *van Oldenborgh et al*., 2005].

[55] The two indices used to categorize the models into RCFs for this case study were annual change in rainfall and annual change in temperature. Temperature was used as a surrogate for evaporation because (1) there exists a 90% correlation between temperature and potential evaporation for Australia [*Whetton et al*., 2012] and (2) evaporation data were only available for eight of the GCMs, while temperature data were available for all 19 models.

[56] Using these models and indices, six RCFs were defined for the Adelaide and Mount Lofty Ranges region for the A1B scenario in 2050, ranging from "warmer with little precipitation change" to "hotter and much drier." However, only five RCFs from this matrix were represented by the seven GCMs in OzClim that (1) were not eliminated based on poor ENSO simulation and (2) had both rainfall and evaporation data available. Maintaining physically consistent combinations of rainfall and evaporation data was necessary in order to maximize the robustness of the impact assessment [*Clarke et al*., 2011]. The GCMs in OzClim were CCSM3 (hereinafter CCSM), CGCM3.1(T63) (hereinafter CGCM-h), CSIRO-MK3.5 (hereinafter CSIRO), FGOALS-g1.0 (hereinafter FGOALS), MIROC3.2(hires) (hereinafter MIROC-h), MIROC3.2(medres) (hereinafter MIROC-m), and MRI-CGCM2.3.2 (hereinafter MRI). These seven GCMs did not represent the "warmer and much drier" RCF but they still represented the most and least severe RCF. Furthermore, while three of these models fell within the same RCF, they were all included in the case study, because the RCF matrix only examined annual changes to the variables, while monthly changes are analyzed in the case study, which are potentially dissimilar between models.

[57] Six demand options were investigated to cover a broad range of potential future demand scenarios (Figure 2), constituted from two per capita consumption projections and three population projections (Table 11). The first individual per capita consumption case (labeled Reduction, Table 11) included a reduction in per capita consumption due to the effects of permanent water conservation measures, savings due to government incentives and increasing water price, and increases in the use of water-efficient technologies. By 2050, total water savings due to demand management strategies for Adelaide are expected to be 48 L/capita/day (Lcd) for households and 21 Lcd for other demands [*Government of South Australia*, 2009]. *Water for Good*

Table 11. Demand Scenario Options

Demand Scenario	Per Capita Consumption	Population
Very low	Reduction	Small
Low	Constant	Small
Medium low	Reduction	Medium
Medium high	Constant	Medium
High	Reduction	Large
Very high	Constant	Large

does not differentiate the 48 Lcd savings between in-house and ex-house use; however, the preceding water security plan for Adelaide, *Waterproofing Adelaide: A Thirst for Change 2005–2025* [*Government of South Australia*, 2005], provides an estimate of the breakdown to 2025. For example, in-house measures such as low-flow showerheads, water-efficient washing machines, and dual-flush toilets are projected to account for about 37% of household savings by 2025, while permanent water conservation measures, urban consolidation, more efficient practices, and low water use vegetation are expected to contribute the remaining 63% of household savings [*Government of South Australia*, 2005]. Consequently, annual linear (i.e., noncompounded) percentage decreases were applied to per capita consumption over the 40 year planning horizon to account for demand management savings; residential indoor use was reduced by 0.237% per annum, residential outdoor demand was reduced by 0.606% per annum, while nonresidential demand was reduced by 0.281% per annum. The second case (labeled "constant," Table 11) reflected the possibility that no savings in individual per capita consumption would be made over the planning horizon, such that individual per capita consumptions remained constant over the planning horizon at 187 Lcd for residential indoor demand, 124 Lcd for residential outdoor demand, and 183 Lcd for nonresidential demand. The impacts of climate change on demand have not been investigated in this study because future projections are not available for Adelaide. Furthermore, while demand is affected by weather and climate factors [*House-Peters and Chang*, 2011], it is also a response to the complex interaction of multiple variables, including economic and social factors (e.g., water pricing); consequently, projecting the impacts of climate change on demand is not as straightforward as simply correlating demand to climate variables. However, the constant variation defined above can be considered a very conservative approach to demand projection and thus does not only reflect the possibility of "no savings" but could represent the possibility of making some savings (which is highly likely) in combination with increasing demand due to climate change.

[58] Taking into account fertility, mortality, net interstate migration, and net overseas migration rates, the Australian Bureau of Statistics' (ABS) median population projection (from 72 population projections) for Adelaide in 2050 is approximately 1.56 million people [*Australian Bureau of Statistics*, 2008]. Therefore, the first population case (labeled "medium," Table 11) applied a linear (i.e., noncompounded) percentage increase of 0.736% per year to the southern system population. Two additional population options (labeled "small" and "large," Table 11) were also defined to investigate futures with small and large populations. Consequently, the 5th and 95th percentile values of the 72 population projections made by the ABS for Adelaide were used, corresponding to annual linear percentage changes of −0.680% (small) and 1.579% (large), respectively. The resulting demand scenarios formulated from combinations of the two per capita consumption cases and the three options for population are labeled very low, low, medium-low, medium-high, high, and very high (Table 11).

[59] A "base case," from which to compare the scenario options, was defined as a combination of the A1B SRES scenario, the FGOALS GCM, and the medium-low demand scenario (base case, Table 12). As no likelihoods have been assigned to the SRES scenarios [*Intergovernmental Panel on Climate Change*, 2007], the A1B SRES scenario was selected for the base case as it represents a median GHG emissions future compared to the other SRES scenarios.

Table 12. Scenario Options Defined for the Case Study of Adelaide's Southern Water Supply System

		Scenario ID																	
Scenario Options		Base Case	1	2	3	4	5	6	7	8	9	10	11	12	13	14	15	16	Best Case	Worst Case
SRES Scenario	A1B	x						x	x	x	x	x	x	x	x	x	x	x		
	A1FI		x																	x
	A1T			x																
	A2				x															
	B1					x													x	
	B2						x													
GCM	FGOALS	x		x	x	x	x	x						x	x	x	x	x		
	CCSM							x												
	CGCM-h								x										x	
	CSIRO									x										x
	MIROC-h										x									
	MIROC-m											x								
	MRI												x							
Demand	Medium High	x		x	x	x	x	x	x	x	x	x	x							
	Very Low													x					x	
	Low														x					
	Medium Low															x				
	High																x			
	Very High																	x		x

FGOALS was selected for the base case because the percentage of models supporting an RCF may be considered as providing an indication of relative likelihood [*Whetton et al*., 2012], and out of the seven selected GCMs, it was the only GCM that represented the RCF supporting the highest percentage of GCMs. Furthermore, FGOALS represented a "warmer and drier" future climate, which is a middle of the range projection. The medium-low demand scenario was selected because the per capita consumption rate with water savings is projected for Adelaide, while a medium population is more likely to occur than either the small or large population projections. The remaining 16 scenarios used to test the magnitude of uncertainty sources are summarized in Table 12, with scenarios 1–5 used to compare across the SRES scenarios, scenarios 6–11 used to compare GCM selection, while scenarios 12–16 are used to compare different demand projections. In each of these scenarios, there is only one change made to the base case, so that uncertainty due to a particular source can be isolated.

[60] While an almost infinite number of possible scenario combinations could have been explored, it was appropriate to limit the scenarios to those listed in Table 12 as these scenarios ensured that the major sources of uncertainty were examined while keeping computational effort reasonable, and thus the first objective of the paper could be met. The impacts on water supply security of other sources of uncertainty, such as the downscaling model, GCM initial conditions, RRO model, and RRO model parameters were not examined in the case study for reasons discussed below.

[61] A caveat of this study is that rainfall and evaporation data sets derived from different downscaling methods are not available and thus the impact of the downscaling model on supply reliability could not be tested as a source of uncertainty. However, in previous studies of the impact of climate change on runoff, downscaling models were shown to contribute less uncertainty than GCMs [*Boé et al*., 2009; *Chen et al*., 2011a, 2011b; *Mpelasoka and Chiew*, 2009; *Wilby and Harris*, 2006], less uncertainty than SRES scenarios [*Chen et al*., 2011a, 2011b], and less uncertainty than GCM initial conditions [*Chen et al*., 2011b] (see section 1). Direct comparisons of downscaling approaches are also difficult to achieve because they use different spatial domains, predictor variables, predictands, and assessment criteria [*Fowler et al*., 2007]. GCM initial conditions were not examined in the case study because (1) the authors did not run the GCMs and (2) the data sourced from OzClim did not include multiple ensemble runs.

[62] Different RRO models and their parameters were also not tested in the case study because *Chiew et al*. [2009a] illustrated that RRO models exhibited less uncertainty in determining the impacts of climate change on runoff than GCMs; *Chen et al*. [2011b] illustrated that in estimating runoff under climate change impacts, hydrological models and hydrological model parameters contributed less uncertainty than GCMs, GCM initial conditions, and GHG emissions scenarios; while *Wilby and Harris* [2006] showed hydrological models and their parameters contributed less uncertainty in estimating runoff under climate change impacts than GCMs (see section 1). However, *Wilby and Harris* [2006] did show that hydrological models and their parameters contributed more uncertainty to estimating runoff under climate change impacts than SRES scenarios, so this study is limited in that it only assesses one RRO model and one set of RRO model parameters.

[63] It should be noted that the relatively insensitive responses of runoff to the downscaling model and the choice of RRO model and parameters, compared to other sources of uncertainty, cannot necessarily be generalized to other cases. However, a water supply manager with limited resources for impact assessments must make some assumptions as to the importance of uncertainty sources based on previous case studies to ensure effort is directed toward the greatest expected sources of uncertainty.

3.4.1.2. Scenarios to Project Ranges of Water Supply Security for Adelaide's Southern Water Supply System

[64] To project the likely range of the impact of climate change on water supply security for Adelaide's southern water supply system (and thus address the third objective of this paper), best and worst cases were defined, with scenario options only selected from those detailed in section 3.4.1.1. For the best case, the very low demand scenario was selected, while for the worst case, the very high demand scenario was selected (Table 12). However, it was not so clear which SRES scenario and GCM would be associated with the lowest and highest water supply securities. Consequently, the SRES scenarios and GCMs for the best and worst cases were selected after the base case and scenarios 1–11 (Table 12) were run and analyzed. Following this analysis (section 4.1), B1 was found to return the highest water supply security and thus was selected for the best case (Table 12), while choosing A1FI resulted in the lowest water supply security at the end of the planning horizon, so it was selected for the worst case (Table 12). Similarly for the GCMs, CGCM-h was selected for the best case because it returned the highest reliability in 2050, while CSIRO was selected for the worst case as it corresponded to the smallest reliability for all years (Table 12). The results for these best and worst cases were discussed in reference to those obtained for an "average" case, which for this case study was defined as scenario 6 (Table 12). The average case was different to the base case, because the base case was composed of a combination of the most likely projections, or when there was no understanding of their likelihood of occurrence, median projections were used (e.g., for population growth). Consequently, while the A1B scenario and medium-low demand scenarios were appropriate to use for both the base case and average case (see Figures 3, 6, and 7), CCSM provided reliabilities that were closer to representing the average for the GCM scenarios than FGOALS, which was used for the base case (see Figures 4 and 5).

3.4.2. Run Water Supply System Model and Compute Water Supply System Security

[65] The scenarios listed in Table 12 were run through the WaterCress model (Step 4b, Figure 2) for each of the 1000 stochastic rainfall time series for 2020, 2030, 2040, and 2050. Water supply system security, represented by reliability calculated on a daily time step for the case study, was then determined for each scenario (Step 4c, Figure 2). Reliability was selected to represent water supply system security for the case study because it provides information as to the proportion of time spent in failure, an important factor in understanding water supply security.

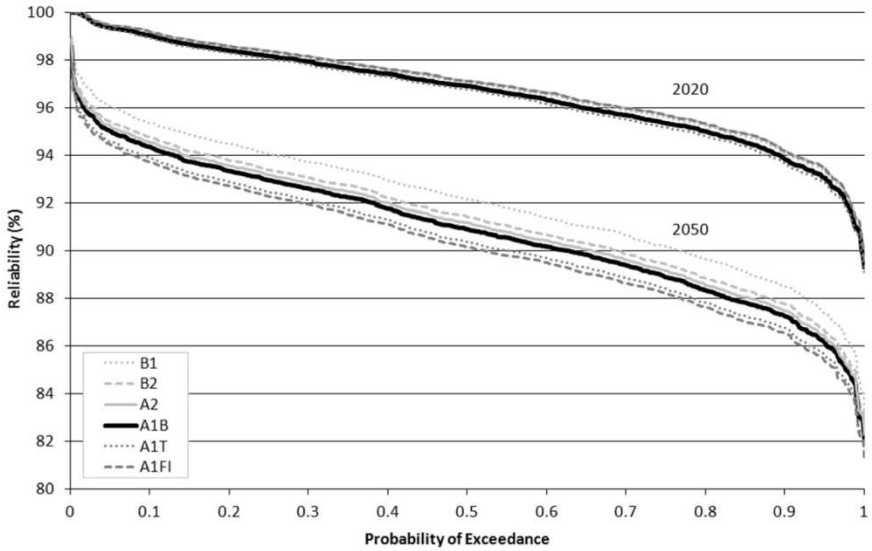

Figure 3. The cdf of reliability (based on 1000 stochastic rainfall time series) of Adelaide's southern water supply system for different SRES scenarios for 2020 and 2050.

[66] Reliability for each of the future years is defined as

$$R_{yi} = \frac{T_{syi}}{T_{tyi}}, \tag{2}$$

where R_{yi} is the reliability for stochastic time series i ($i = 1 - 1000$) for year y ($y = 2010$, 2020, 2030, 2040, or 2050), T_{syi} is the total number of days that available supply exceeds demand for stochastic time series i and year y, and T_{tyi} is the total number of days for stochastic time series i and year y. For each year and for each of the 1000 stochastic rainfall time series (developed in Step 2e of Figure 2), the model was run and reliability was computed (Equation (2)), such that for each scenario, 1000 different reliabilities were calculated. Consequently, reliability could be presented as a probability (based on the 1000 stochastic rainfall time series), rather than a deterministic value. This meant that uncertainties in natural rainfall variability, expressed by the probabilities of reliability for each scenario, could be analyzed and compared to the uncertainties in selecting SRES scenarios, GCMs, and demand.

[67] From a planning perspective, it is also important to understand how reliability changes through time so that

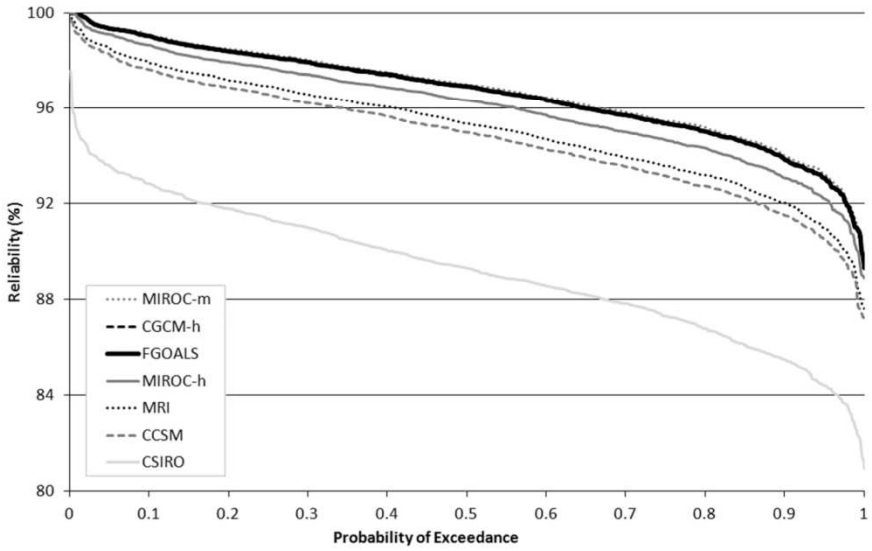

Figure 4. The cdf of reliability (based on 1000 stochastic rainfall time series) of Adelaide's southern water supply system for different GCMs for 2020.

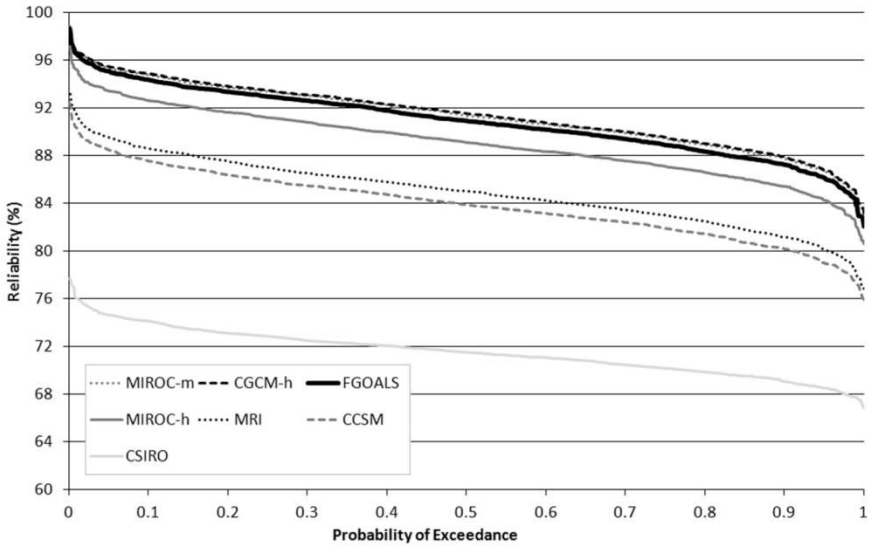

Figure 5. The cdf of reliability (based on 1000 stochastic rainfall time series) of Adelaide's southern water supply system for different GCMs for 2050.

additional supply or demand management schemes can be sequenced to come on line when they are required to raise reliability to an acceptable level (see section 1). Consequently, changes in reliability between years over the planning horizon were also analyzed by linear interpolation.

4. Results and Discussion

[68] The analysis of reliability in section 4.1 addresses the first objective of this paper, which is to understand the relative magnitudes of major sources of uncertainty when analyzing the impacts of climate change on water supply security. It is important to note that the cumulative distribution functions (cdfs) presented herein purely reflect the stochastic nature of the natural rainfall variability, rather than any other systematic uncertainty. Changes in reliability over the planning horizon are then analyzed in section 4.2 in order to illustrate future critical points in time for water supply security and thereby address the second objective of the paper. Finally, section 4.3 examines the best and worst cases to understand water supply security ranges projected for Adelaide's southern system, thus satisfying the third

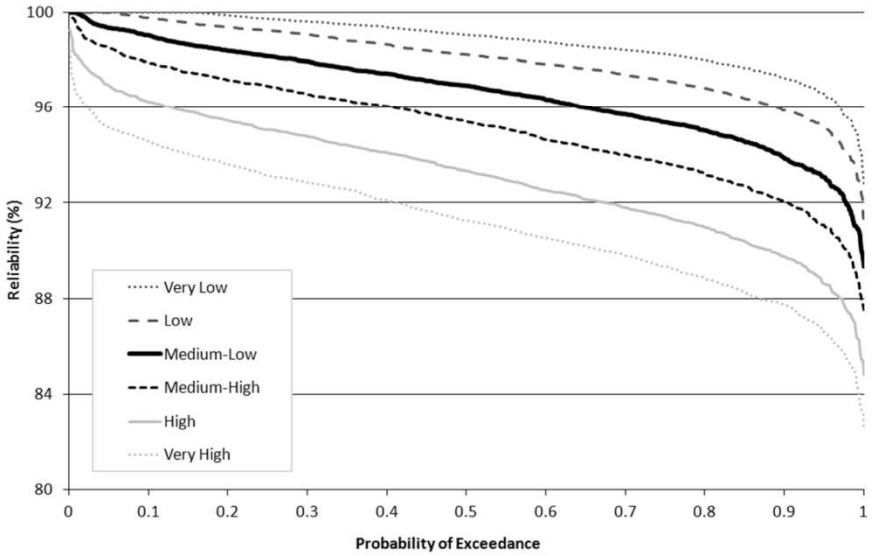

Figure 6. The cdf of reliability (based on 1000 stochastic rainfall time series) of Adelaide's southern water supply system for different demands for 2020.

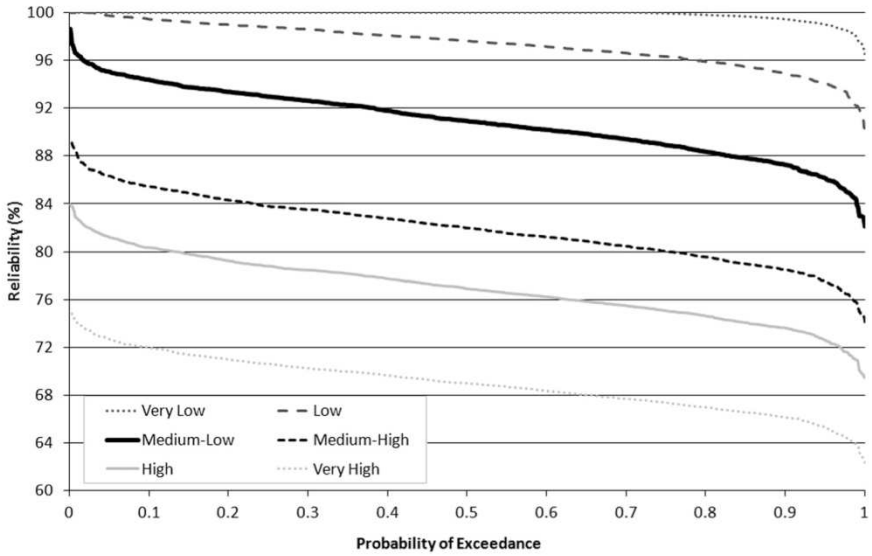

Figure 7. The cdf of reliability (based on 1000 stochastic rainfall time series) of Adelaide's southern water supply system for different demands for 2050.

objective of the paper. The base case and scenarios 1–16 (Table 12) are analyzed in sections 4.1 and 4.2, while the average, best, and worst cases are analyzed in section 4.3.

4.1. Relative Magnitudes of Sources of Uncertainty

[69] In this section, the cdfs of the 1000 stochastic rainfall time series are illustrated for each of the 16 scenarios (Table 12) for 2020 and 2050 (Figures 3–7); for 2030 and 2040, median reliability values are illustrated in Figures 8–10 and 0.05 and 0.95 probabilities of exceedance values summarized in Table 13; while the cdf for natural rainfall variability for 2010 is illustrated in Figure 11. Cdfs of natural rainfall variability for the 16 scenarios for 2030 and 2040 are not illustrated, as the patterns were similar to those for 2020 and 2050 and the differences could be well illustrated in Table 13. Furthermore, the following discussion focuses on the median or 50th percentile values representing natural rainfall variability because the patterns between the scenarios are similar for all percentiles.

[70] The cdfs of reliability based on the 1000 stochastic rainfall time series of Adelaide's southern water supply system for different SRES scenarios for 2020 and 2050 are shown in Figure 3. For the base case, the difference in median reliability across the SRES scenarios was 0.4% in 2020, which by 2050 had increased progressively to 2.0% (Figure 3 and Table 14). The order of SRES scenarios in terms of impact on reliability changed depending on the future year (Figure 3 and Table 13). By 2050, A1B returned greater reliabilities than A1FI and A1T, but smaller reliabilities than A2, B2, and B1 (Figure 3). While it was expected that B1 and B2 would produce more favorable reliabilities due to their more moderate development pathways (see section 3.4.1.1), it was not intuitive that A1T would produce the lowest reliabilities for 2020 and 2030, and the second lowest reliabilities in 2040 and 2050, because it represents the least fossil-fuel intensive pathway of the A1 family (see section 3.4.1.1). However, this can be explained by examining the impacts of the development pathways in terms of changes to precipitation (sourced from OzClim for the FGOALS GCM) up until the end of the 21st century. A1FI has a greater impact on precipitation than A1T from 2040 onward, while A1B has a greater impact on precipitation than A1T from 2080 onward. Consequently, although by the end of the 21st century the impact on water supply security of A1FI and A1B should be greater than that of A1T, it did not occur for this case study due to the timeframe only extending to 2050.

Table 13. Probability of Exceedance Summary for Reliability for Years 2030 and 2040 for Each of the 16 Scenarios Detailed in Table 12

	Year	2030		2040	
Uncertainty Source	Probability of Exceedance	0.05	0.95	0.05	0.95
SRES scenario	B1	98.5	91.0	96.8	88.3
	B2	98.3	90.5	96.4	87.8
	A2	98.4	90.8	96.4	87.8
	A1B	98.3	90.5	96.2	87.6
	A1T	98.0	90.2	95.7	86.8
	A1FI	98.3	90.6	95.7	86.9
GCM	MIROC-m	98.3	90.7	96.4	87.9
	FGOALS	98.3	90.5	96.2	87.6
	CGCM-h	98.2	90.4	95.9	87.3
	MIROC-h	97.5	89.3	94.7	85.9
	MRI	96.0	87.4	92.6	83.2
	CCSM	95.3	86.3	91.4	81.9
	CSIRO	87.1	78.1	79.7	72.3
Demand	Very Low	100.0	97.5	100.0	98.2
	Low	100.0	94.8	99.7	94.0
	Medium-Low	98.3	90.5	96.2	87.6
	Medium-High	94.9	86.2	90.3	81.3
	High	91.5	82.4	85.4	76.5
	Very High	87.2	78.3	78.8	70.7

Table 14. Range in Median Reliability Caused by Uncertainty in SRES Scenario, GCM and Demand for 2020, 2030, 2040 and 2050 for Each of the 16 Scenarios in Table 12

	Uncertainty Source		
Year	SRES Scenario	GCM	Demand
2020	0.4	7.7	7.8
2030	0.6	12.5	16.8
2040	1.4	16.6	25.2
2050	2.0	20.0	31.0

[71] The cdfs of reliability (representing stochastic uncertainty in rainfall) of Adelaide's southern water supply system for different GCMs for 2020 and 2050 are illustrated in Figures 4 and 5, respectively. The difference in reliability across the GCMs was approximately 20 times that for the SRES scenarios in 2020, decreasing progressively to 10 times by 2050 (Figures 4 and 5). The lowest median reliability in 2050 was 71.5% under CSIRO (Figure 5). This was expected because the CSIRO GCM resulted in the greatest overall decrease in annual rainfall (23% reduction by 2050) compared to the other GCMs. Lower rainfall translated to Mount Bold storage levels being lower for longer periods, thus requiring water to be pumped from the River Murray for more days of the year, such that the annual River Murray license was used up earlier in the year and there were, therefore, more days of failure. MIROC-m and CGCM-h resulted in the greatest median reliabilities of 91.3% and 91.5% in 2050, respectively, which was expected considering these two GCMs resulted in very slight annual rainfall increases of 0.7% and 0.5% by 2050, respectively. Interestingly though, FGOALS with a 5.3% annual reduction in rainfall by 2050 only resulted in a slightly smaller median reliability of 90.9%, even though a similar reduction in annual rainfall was exhibited by CCSM (6.6% reduction by 2050), which returned reliabilities approximately 7% smaller than FGOALS (Figure 5). CCSM actually projected a smaller decrease in annual rainfall than MIROC-h (7.3%) and MRI (7.4%) but still returned a lower reliability. Furthermore, the similarity in annual rainfall reduction between MIROC-h and MRI was not translated into reliability with an approximate 4% difference between the two by 2050. These differences in the reliability patterns appear to be the result of differences in rainfall distribution over the year. Furthermore, these results illustrate both the complexity of studying the impacts of climate change on Adelaide's water supply security and the importance of considering seasonal variations for climate change scenarios.

[72] The cdfs of reliability based on natural rainfall variability of Adelaide's southern water supply system for different demand scenarios for 2020 and 2050 are shown in Figures 6 and 7, respectively. In a similar way to the SRES scenarios and GCMs, the range of water supply security increased with time across demand scenarios, so by 2050 reliability ranged from 69.0% for the very high demand scenario to 100% for the very low scenario (Figure 7). Thus, the range in median AAR of 31.0% across the demand scenarios was more than one and a half times that obtained across the seven GCMs and more than 15 times that observed for the six SRES scenarios. The changes in reliability for each of the demand scenarios were to be expected, such that an increasing demand (due to a greater population and/or less water savings) resulted in a lower reliability (Figures 6 and 7).

[73] The six cdfs of natural climate variability (Figures 3–7) illustrate that reliability noticeably changed depending upon the particular stochastic rainfall time series. For example, for the base case, the difference between the minimum and maximum reliabilities was 10.7% in 2020, 12.9% in 2030, 15.5% in 2040, and 16.5% in 2050. This meant that demand uncertainty was always greater and SRES uncertainty always smaller than uncertainty due to natural rainfall variability, but compared to GCM uncertainty it was dependent on the future year; for 2020 and 2030, inherent natural rainfall variability created more uncertainty than GCMs, for 2040 the uncertainties were almost identical, and by 2050 GCMs were the second greatest source of uncertainty (Table 14). However, the extremely low probabilities of exceedance for reliability correspond to extremely large return periods (e.g., the maximum probability of exceedance is equivalent to 1 in 1000 year event), so these events are very unlikely. While this may appear to lessen the significance of the impact of natural rainfall variability, a 1 in 1000 year event is still possible. Second, as the probability of occurrence is unknown for each of the scenarios listed in Table 12, these scenarios could also be as unlikely to occur as a 1 in 1000 year event. Furthermore, when considering all scenarios in Table 12, natural rainfall variability can only cause up to 16%–17% variability at any of the years. This is because the greatest variation occurs when reliability ranges from 78% to 95% and this does not always occur for the base case. This pattern is believed to be a function of the large River Murray supply (65 GL/yr) that is, in this case study, unaffected by natural rainfall variability. In other words, when reliability is low (<78%–95%), the River Murray dominates supply, so natural variability in reservoir supply (reflecting natural rainfall variability) is dampened out by the climate-independent River Murray supply. However, when less River Murray supply is required, greater natural rainfall variability is expressed in the reliability, through reservoir supply. At very high reliabilities, the natural rainfall variability has less effect because there are fewer failures.

4.1.1. Summary of Relative Magnitude of Uncertainty Sources

[74] For this case study, uncertainty source significance was dependent on the future year; however, demand was always the greatest source of uncertainty on water supply security and SRES scenario the least. Natural rainfall variability was second only to demand for the first half of the planning horizon, essentially equal to GCM uncertainty by 2040 and then of less importance than GCM choice by 2050. However, it is important to also remember that, while the synthetic rainfall data are believed to be representative of the historical 30-year time series they were derived from (section 3.2.6), this short time period may not reflect the real natural rainfall variability over a 100 year period. Therefore, natural rainfall variability could be underestimated in this analysis and could be an even greater source of uncertainty than determined here. These findings

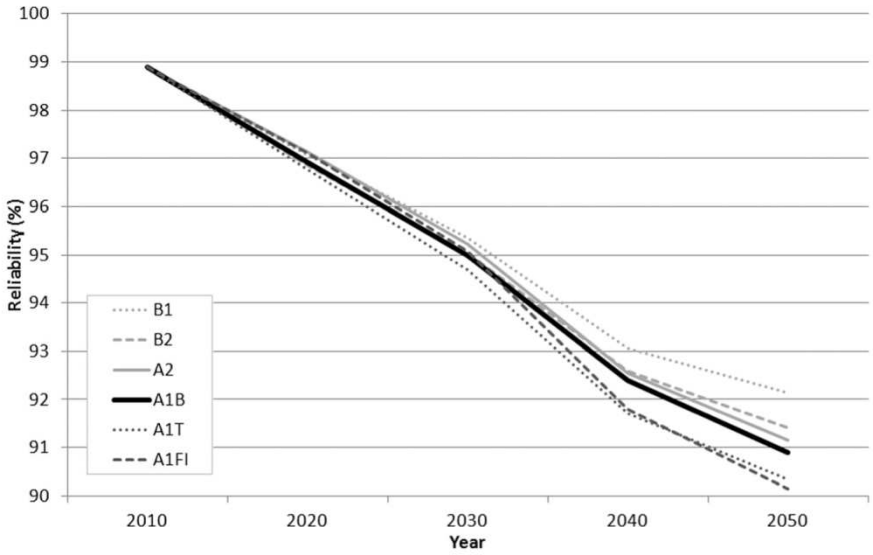

Figure 8. Change in median reliability over the planning horizon of Adelaide's southern water supply system for different SRES scenarios.

indicate that, in analyzing the uncertainties of the impact of climate change on water supply systems, demand uncertainties, and natural rainfall variability, should not be excluded, as these can be greater sources of uncertainty than those associated with climate change modeling. They also illustrate the importance of analyzing changes in reliability progressively through time, such that if a longer planning horizon is selected, more effort can be directed to characterizing uncertainty of supply security due to demand and GCMs, while a shorter time period would suggest focus be directed on natural rainfall variability, as well as demand uncertainty.

[75] In terms of management implications, demand uncertainty could be reduced in the future by the water authority if they could control per capita consumption through demand management schemes and, while outside the scope of most water authorities, climate scientists working toward improving GCMs may also be able to reduce uncertainties associated with these model outputs. Of comfort to water authorities is the knowledge that the impact of SRES scenarios, in which uncertainty is irreducible, was minor compared to the other sources of uncertainty. Similarly, the planning of supply systems under demand uncertainty and natural rainfall variability is traditional for water

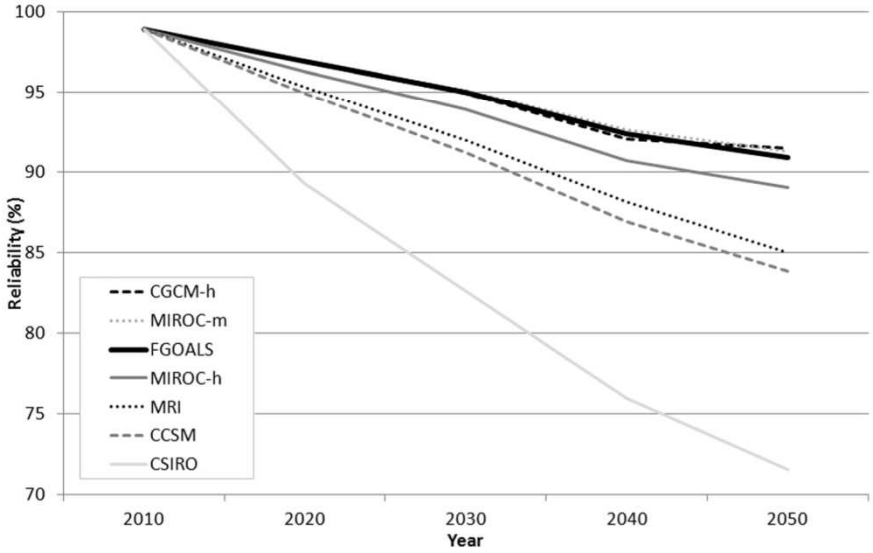

Figure 9. Change in median reliability over the planning horizon of Adelaide's southern water supply system for different GCMs.

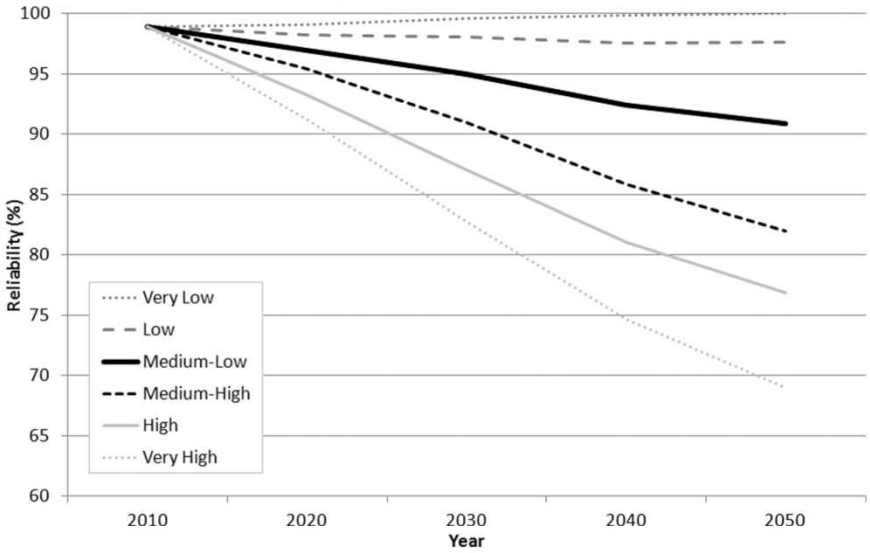

Figure 10. Change in median reliability over the planning horizon of Adelaide's southern water supply system for different demands.

authorities, so it is encouraging that these two sources were discovered to be the dominant sources of uncertainty, at least in the short term.

4.2. Identifying Critical Points in Time for Water Supply Security

[76] Changes in median reliability of Adelaide's southern water supply system for different SRES scenarios are shown in Figure 8, while changes in median reliability for different GCMs are shown in Figure 9 and changes in median reliability for different demands are shown in Figure 10. Median reliability for the base case decreased from 98.9% in 2010 to 90.9% in 2050 (Figure 8), which was expected due to population growth and the increasingly adverse impacts of climate change. However, there was a good degree of variability in the trajectories of supply reliability over the planning horizon (Figures 8–10).

[77] As mentioned in section 1, understanding these changes in reliability with time, and their associated uncertainties, is important from a planning perspective, as additional supply sources or demand management schemes could be sequenced to come online when they are required to maintain reliability at an acceptable level. However, defining what an acceptable level is for reliability is subjective. While 100% reliability is desirable, when considering other objectives such as cost, water planners may accept a lower reliability for economic gain or accept the need for temporary water restrictions or other demand management actions. For example, if water supply planners accepted reliability levels in excess of 95%, then most of the 16 scenarios analyzed would at some stage over the planning horizon require supply to be increased or demand reduced. While this would occur around 2030 for the SRES scenarios (Figure 8); for the GCM scenarios, water supply security would be threatened between 2015 and 2030 (Figure 9); while for the demand scenarios, supply augmentation or demand mitigation would be required between 2015 and 2030 or not at all (Figure 10).

[78] While the order of median reliability remained constant with time when comparing the different demand scenarios, the order of median reliability for the SRES scenarios and GCM scenarios changed slightly depending on the year (Figures 8 and 10). For example, A1FI resulted in a sharper decline in median reliability over the planning horizon than the other SRES scenarios, but this decline only accelerated after 2030 (Figure 8). Hence, the order of the impact of SRES scenarios and GCMs on water supply security is dependent on the year, which again highlights the importance of considering the temporal dimension when analyzing the impacts of climate change on water supply security.

[79] Over the planning horizon, the uncertainty in median reliability increased (Figures 8–10). While reliabilities were similar at the beginning of the planning horizon, the lowest median reliability for 2050 was 69.0% for the very high demand scenario, while the greatest median reliability was 100% for the very low demand scenario (Figure 10). Furthermore, differences in median reliability caused by the different sources of epistemic uncertainty were in agreement with the order of the magnitude of uncertainty sources defined in section 4.1 (without natural rainfall variability). A number of planning options, including the addition of alternative sources or demand management schemes could reduce this window of uncertainty in terms of water supply security; however, should the very low demand scenario ensue, then there would be a level of regret (for example unnecessary economic expenditure) associated with the selected option. Consequently, the findings illustrate that continual reassessment of planning may be necessary to ensure maximum reliability with minimal regret.

4.3. Water Supply Security Ranges

[80] For the best case, Adelaide's southern supply system had slightly greater reliability in 2050 than in 2010,

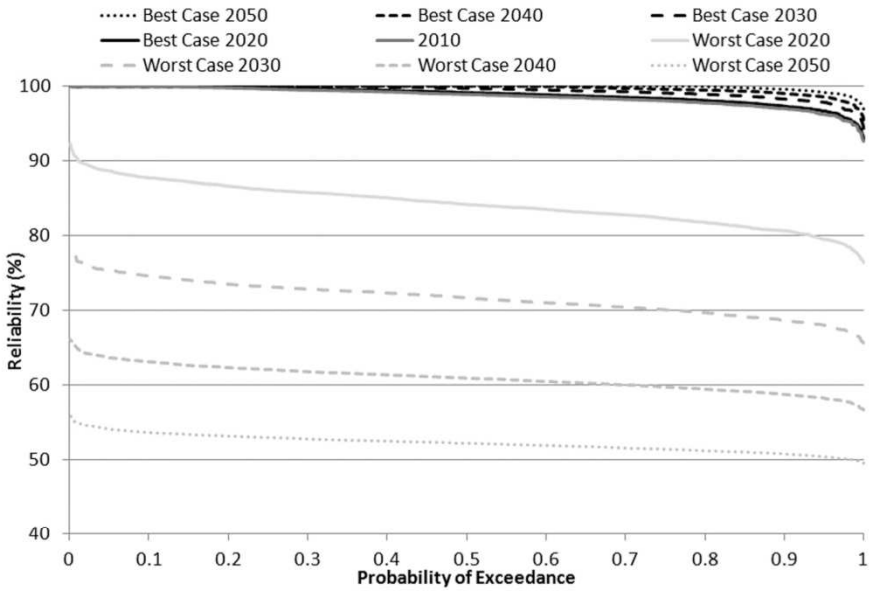

Figure 11. Cdf of reliability (based on 1000 stochastic rainfall time series) of Adelaide's southern water supply system for 2010 and for the Best and Worst Cases for 2020, 2030, 2040 and 2050.

which progressively increased with time over the planning horizon (Figure 11). While counterintuitive, this increase in reliability over time is caused by the very low demand scenario, which corresponds to a slight decrease in population and decreasing per capita consumption over the planning horizon (see section 3.4.1.1). If the best case ensued and water supply planners accepted reliability levels greater than 95%, then there is only a very slight probability that the supply system will not quite reach the target reliability in 2020 and 2030 due to natural rainfall variability, while for 2040 and 2050 it will always be met (Figure 11). In stark contrast, the worst case has reliabilities that decreased with time over the planning horizon and by 2050, for all stochastic rainfall time series, reliability was less than 56% (Figure 11). If 95% is considered the reliability threshold by the water authority and the worst case was to occur, then as early as 2020, the system would exhibit failures, regardless of natural rainfall variability. This stark contrast between the best and worst cases was expected, due to selecting SRES scenarios, GCMs, and demands that corresponded to the best and worst outcomes for reliability, respectively. As mentioned in section 4.2, the increasing uncertainty envelope with time was also expected, as projections made for the more distant future are less certain than those for the near future.

[81] The best and worst cases are both extreme cases and have low probabilities of occurrence. To place them in perspective, the average case was analyzed, which had a median reliability of 84% by 2050 (Figure 5), considerably smaller than the best case (100%), and much greater than the worst case (52%). However, while the best and worst cases are unlikely to occur, they do provide water authorities with the likely upper bound on the range of water supply security up to 2050. If some uncertainties can be reduced, which is likely in the future with projected improvements to GCM model accuracy and potential demand management actions implemented by the water authority, then the overall uncertainty envelope will also be reduced. If the uncertainties are irreducible though, then the water authority must consider adaptation options that are extremely flexible, so as not to regret adaptation responses nor jeopardize water supply security. For example, if plans were made based on findings from the Worst case to ensure maximum water supply security and should the Best case occur, there would be a relatively high level of regret (such as unnecessary economic expenditure) associated with the selected option.

[82] These results from the best and worst cases also illustrate that the multiplicative impacts of epistemic uncertainty sources on supply reliability lessen the importance of natural rainfall variability. However, these cases are first not likely to occur and second, while the stochastic time series was found to preserve the important characteristics of the historical rainfall time series (section 3.2.6), the short 30 year historical rainfall time series may not have included the entire range of possible natural rainfall events, and so natural rainfall variability may be underestimated.

5. Summary and Conclusions

[83] Previous studies that have compared the magnitude of uncertainty sources associated with climate change impacts on water resources have largely focused on runoff. However, because of the nonlinear translation of runoff to water supply (due to a number of complexities in modeling water supply systems including the incorporation of demand and storages), there is a need to understand the importance of major uncertainty sources for climate change impacts on water supply security. Understanding the major sources of uncertainty and whether they are reducible or

not will help water authorities to focus efforts toward reducing uncertainty where possible or to develop strategies to cope with the uncertainties if they are irreducible. Furthermore, from a planning perspective, it is also important to understand changes in water supply security with time, and their associated uncertainties, so that additional supply sources or demand management schemes can be sequenced to come on line when they are required to raise water supply security to an acceptable level. This paper presents a scenario-based sensitivity approach for analyzing the impacts of climate change on water supply security tailored to the case study of Adelaide's southern water supply system. The methodology developed ensured that the three objectives of this paper were met, these being that (1) relative magnitudes of major sources of uncertainty on water supply security were assessed, (2) changes in water supply security through time were traced, and (3) water supply security ranges were established. Three major sources of systematic uncertainty—SRES scenarios, GCMs, and demand—were compared in the case study, as well as stochastic natural climate variability.

[84] In the earlier half of the adopted planning horizon of 2010–2050, the level of demand created the most uncertainty in water supply security, followed by natural rainfall variability, GCM, and lastly SRES scenario. By the later stages of the planning horizon though, GCMs created more uncertainty in reliability than natural rainfall variability. This suggests that, for studies analyzing the impacts of climate change on water supply security, uncertainties other than those associated with climate change and hydrological modeling should in fact be considered as they could have as great, or greater, impacts on water supply security projections. Furthermore, in the short term, efforts by water authorities should be directed toward demand and natural rainfall variability, but that for longer-term plans, uncertainties in GCMs should be analyzed.

[85] The case study also illustrated that reliability generally decreased over the planning horizon, a result of increasing demands and decreasing rainfall under climate change. From a local policy perspective, the projected reduction in system reliability realized in this analysis of Adelaide's southern system justifies (1) the production of flexible plans to ensure the security of Adelaide's future water supply and (2) the need for current and future initiatives to supplement Adelaide's water supply as well as curb demand.

[86] Furthermore, the findings illustrate the benefits from a water management perspective of assessing reliability progressively over a planning horizon to determine when to reduce demand and/or augment supply to maintain water supply security. However, the uncertainty envelope or range of uncertainty increased with time for Adelaide's southern system, which was particularly noticeable when comparing the best and worst cases. While some of this uncertainty may be reducible (by the water authority or others), stochastic uncertainty and some epistemic uncertainty will always exist, so flexible management may therefore be necessary to strike a balance between water supply security and regret. Thus a move away from single, long-lived, and large-scale centralized water sources toward decentralized, diverse water sources at much smaller scales is necessary [*Pahl-Wostl*, 2007]. For Adelaide's southern system, this would mean that if supply were to be augmented by additional sources, local stormwater harvesting schemes or household rainwater tanks, would be preferred over centralized, larger-scale sources, such as a desalination plant. However, such climate-dependent sources have disadvantages compared with climate-independent sources (such as desalination), as climate-independent sources can guarantee supply (subject to loss of power and mechanical faults) regardless of whether it rains or not. Consequently, for Adelaide's southern system, trade-offs exist in selecting planning initiatives when attempting to maintain system reliability and minimize system regret. Future research should focus on identifying potential solutions for the southern system and the associated trade-offs.

[87] Furthermore, extending this research to examine multiple case studies and assess an increased number of uncertainty sources and scenarios would be valuable to determine whether generalized patterns and rules regarding the relative degree of uncertainty associated with particular major sources of uncertainty can be established. This would assist water planners in understanding where the greatest level(s) of effort should be focused when (1) attempting to reduce epistemic uncertainty and (2) developing tools to assist in planning for the future under great uncertainty. However, the findings of this case study clearly show that, in addition to examining demand uncertainty, natural rainfall variability must be considered in short-term plans, while in the longer-term, the focus will need to shift to consider the uncertainties of GCMs.

[88] **Acknowledgments.** This work is financed by The University of Adelaide and eWater CRC. We thank David Cresswell for his technical support of WaterCress and for adapting the program to suit the requirements of the case study. We also thank Sri Srikanthan for his assistance with SCL, Leanne Webb for running the CFF for this case study, Matthew Gibbs for his help with programming, Mark Thyer and Michael Leonard for their advice on catchment calibration, and the three anonymous reviewers who have assisted with improving the quality of this paper significantly.

References

Akaike, H. (1973), Information theory and an extension of the maximum likelihood principle, in *2nd International Symposium on Information Theory, Tsahkadsor, Armenia, USSR, September 2–8, 1971*, edited by B. Petrov and F. Csáki, pp. 267–281, Akadémiai Kiadó, Budapest.

Alcorn, M. (2006), Surface water assessment of the currency creek catchment, Report DWLBC 2006/07, 61 pp., Dep. of Water, Land and Biodiversity Conservation, Adelaide, Australia.

Australian Bureau of Statistics (2008), Population projections: Australia 2006 to 2101, Report, 96 pp., Australian Bureau of Statistics, Canberra.

Barton, A. B. (2005), Management and reuse of local water resources in residential developments in Adelaide, 199 pp., Univ. of South Australia, Adelaide, Australia.

Beven, K. (2006), A manifesto for the equifinality thesis, *J. Hydrol.*, *320*(1–2), 18–36, doi:10.1016/j.jhydrol.2005.07.007.

Boé, J., L. Terray, E. Martin, and F. Habets (2009), Projected changes in components of the hydrological cycle in French river basins during the 21st century, *Water Resour. Res.*, *45*(8), W08426, doi:10.1029/2008WR007437.

Bozdogan, H. (1987), Model selection and Akaike's Information Criterion (AIC): The general theory and its analytical extensions, *Psychometrika*, *52*(3), 345–370, doi:10.1007/bf02294361.

Charles, S. P., T. M. Heneker, and B. C. Bates (2008), Stochastically downscaled rainfall projections and modelled hydrological response for the Mount Lofty Ranges, South Australia, in *Proceedings of Water Down Under 2008*, edited by M. Lambert, T. Daniell, and M. Leonard, pp. 428–439, Engineers Australia; Casual Productions, Adelaide.

Chen, J., F. P. Brissette, and R. Leconte (2011a), Uncertainty of downscaling method in quantifying the impact of climate change on hydrology, *J. Hydrol.*, *401*(3–4), 190–202, doi:10.1016/j.jhydrol.2011.02.020.

Chen, J., F. P. Brissette, A. Poulin, and R. Leconte (2011b), Overall uncertainty study of the hydrological impacts of climate change for a Canadian watershed, *Water Resour. Res.*, *47*(12), W12509, doi:10.1029/2011WR010602.

Chiew, F. H. S., and T. A. McMahon (2002), Modelling the impacts of climate change on Australian streamflow, *Hydrol. Process.*, *16*, 1235–1245, doi:10.1002/hyp.1059.

Chiew, F. H. S., and L. Siriwardena (2005), Trend: Trend/change detection software user guide, CRC for Catchment Hydrology, Australia.

Chiew, F. H. S., D. G. C. Kirono, D. Kent, and J. Vaze (2009a), Assessment of rainfall simulations from global climate models and implications for climate change impact on runoff studies, in *18th World IMACS Congress and MODSIM09 International Congress on Modelling and Simulation*, edited by R. Anderssen, R. Braddock, and L. Newham, pp. 3907–3913, Modelling and Simulation Society of Australia and New Zealand and International Association for Mathematics and Computers in Simulation, Canberra.

Chiew, F. H. S., J. Teng, J. Vaze, and D. G. C. Kirono (2009b), Influence of global climate model selection on runoff impact assessment, *J. Hydrol.*, *379*(1–2), 172–180, doi:10.1016/j.jhydrol.2009.10.004.

Chiew, F. H. S., J. Teng, J. Vaze, D. A. Post, J. M. Perraud, D. G. C. Kirono, and N. R. Viney (2009c), Estimating climate change impact on runoff across southeast Australia: Method, results, and implications of the modeling method, *Water Resour. Res.*, *45*(10), W10414, doi:10.1029/2008WR007338.

Chiew, F. H. S., D. G. C. Kirono, D. M. Kent, A. J. Frost, S. P. Charles, B. Timbal, K. C. Nguyen, and G. Fu (2010), Comparison of runoff modelled using rainfall from different downscaling methods for historical and future climates, *J. Hydrol.*, *387*(1–2), 10–23, doi:10.1016/j.jhydrol.2010.03.025.

Clarke, J. M., P. H. Whetton, and K. J. Hennessy (2011), Providing application-specific climate projections datatsets: CSIRO's Climate Futures Framework, in *MODSIM2011, 19th International Congress on Modelling and Simulation*, edited by F. Chan, D. Marinova, and R. Anderssen, pp. 2683–2690, Modelling and Simulation Society of Australia and New Zealand, Canberra.

Crawley, P. D. (1995), *Risk and Reliability Assessment of Multiple Reservoir Water Supply Headworks Systems*, 601 pp., Univ. of Adelaide, Adelaide.

Crawley, P. D., and G. C. Dandy (1993), Optimal operation of multiple-reservoir system, *J. Water Resour. Plann. Manage.*, *119*(1), 1–17, doi:10.1061/(ASCE)0733–9496(1993)119:1(1).

Cubasch, U., G. A. Meehl, G. J. Boer, R. J. Stouffer, M. Dix, A. Noda, C. A. Senior, S. Raper, and K. S. Yap (2001), Projections of future climate change, in *Climate Change 2001: The Scientific Basis. Contribution of Working Group I to the Third Assessment Report of the Intergovernmental Panel on Climate Change*, edited by J. T. Houghton et al., p. 881, Cambridge Univ. Press, Cambridge, U. K.

Diaz-Nieto, J., and R. L. Wilby (2005), A comparison of statistical downscaling and climate change factor methods: Impacts on low flows in the River Thames, United Kingdom, *Clim. Change*, *69*(2), 245–268, doi:10.1007/s10584-005-1157-6.

Dibike, Y. B., and P. Coulibaly (2005), Hydrologic impact of climate change in the Saguenay watershed: Comparison of downscaling methods and hydrologic models, *J. Hydrol.*, *307*(1–4), 145–163, doi:10.1016/j.jhydrol.2004.10.012.

Forbes, K., S. Kienzle, C. Coburn, J. Byrne, and J. Rasmussen (2011), Simulating the hydrological response to predicted climate change on a watershed in southern Alberta, Canada, *Clim. Change*, *105*(3), 555–576, doi:10.1007/s10584-010-9890-x.

Fowler, H. J., C. G. Kilsby, and P. E. O'Connell (2003), Modeling the impacts of climatic change and variability on the reliability, resilience, and vulnerability of a water resource system, *Water Resour. Res.*, *39*(8), 11, doi:10.1029/2002WR001778.

Fowler, H. J., S. Blenkinsop, and C. Tebaldi (2007), Linking climate change modelling to impacts studies: Recent advances in downscaling techniques for hydrological modelling, *Int. J. Climatol.*, *27*(2), 1547–1578, doi:10.1002/joc.1556.

Gober, P., C. W. Kirkwood, R. C. Balling, A. W. Ellis, and S. Deitrick (2010), Water planning under climatic uncertainty in Phoenix: Why we need a new paradigm, *Ann. Assoc. Am. Geogr.*, *100*(2), 356–372, doi:10.1080/00045601003595420.

Government of South Australia (2005), *Water Proofing Adelaide—A Thirst for Change 2005–2025*, 60 pp., Gov. of South Australia, Adelaide, Australia.

Government of South Australia (2009), *Water for Good—A Plan to Ensure Our Water Future to 2050*, 190 pp, Gov. of South Australia, Adelaide, Australia.

Groves, D. G., D. Yates, and C. Tebaldi (2008), Developing and applying uncertain global climate change projections for regional water management planning, *Water Resour. Res.*, *44*(12), W12413, doi:10.1029/2008WR006964.

House-Peters, L. A., and H. Chang (2011), Urban water demand modeling: Review of concepts, methods, and organizing principles, *Water Resour. Res.*, *47*, W05401, doi:10.1029/2010WR009624.

Intergovernmental Panel on Climate Change (2000), Special report on emissions scenarios, 570 pp., Cambridge Univ. Press, U.K.

Intergovernmental Panel on Climate Change (2007), Climate change 2007: Synthesis report. Contribution of Working Groups I, II and III to the Fourth Assessment Report of the Intergovernmental Panel on Climate Change, 104 pp., IPCC, Geneva, Switzerland.

Irving, D. B., et al. (2011), Evaluating global climate models for the Pacific island region, *Clim. Res.*, *49*(3), 169–187, doi:10.3354/cr01028.

Jain, S. K., and K. P. Sudheer (2008), Fitting of hydrologic models: A close look at the Nash–Sutcliffe index, *J. Hydrol. Eng.*, *13*(10), 981–986, doi:10.1061/(asce)1084-0699(2008)13:10(981).

Jeffrey, S. J., J. O. Carter, K. B. Moodie, and A. R. Beswick (2001), Using spatial interpolation to construct a comprehensive archive of Australian climate data, *Environ. Modell. Software*, *16*(4), 309–330, doi:10.1016/S1364–8152(01)00008-1.

Kaczmarek, Z., J. Napiorkowski, and M. Strzepek (1996), Climate change impacts on the water supply system in the Warta River catchment, Poland, *Water Resour. Dev.*, *12*(2), 165–180, doi:10.1080/07900629650041939.

Kilsby, C. G., P. D. Jones, A. Burton, A. C. Ford, H. J. Fowler, C. Harpham, P. James, A. Smith, and R. L. Wilby (2007), A daily weather generator for use in climate change studies, *Environ. Modell. Software*, *22*(12), 1705–1719, doi:10.1016/j.envsoft.2007.02.005.

Lopez, A., F. Fung, M. New, G. Watts, A. Weston, and R. L. Wilby (2009), From climate model ensembles to climate change impacts and adaptation: A case study of water resource management in the southwest of England, *Water Resour. Res.*, *45*(8), W08419, doi:10.1029/2008WR007499.

Majone, B., C. I. Bovolo, A. Bellin, S. Blenkinsop, and H. J. Fowler (2012), Modeling the impacts of future climate change on water resources for the Gállego river basin (Spain), *Water Resour. Res.*, *48*(1), W01512, doi:10.1029/2011WR010985.

Manning, L. J., J. W. Hall, H. J. Fowler, C. G. Kilsby, and C. Tebaldi (2009), Using probabilistic climate change information from a multimodel ensemble for water resources assessment, *Water Resour. Res.*, *45*(11), W11411, doi:10.1029/2007WR006674.

Milly, P. C. D., J. Betancourt, M. Falkenmark, R. M. Hirsch, Z. W. Kundzewicz, D. P. Lettenmaier, and R. J. Stouffer (2008), Climate change—Stationarity is dead: Whither water management?, *Science*, *319*(5863), 573–574, doi:10.1126/science.1151915.

Moriasi, D. N., J. G. Arnold, M. W. Van Liew, R. L. Bingner, R. D. Harmel, and T. L. Veith (2007), Model evaluation guidelines for systematic quantification of accuracy in watershed simulations, *Am. Soc. Agric. Biol. Eng.*, *50*(3), 885–900.

Morton, F. I. (1983), Operational estimates of areal evapotranspiration and their significance to the science and practice of hydrology, *J. Hydrol.*, *66*(1–4), 1–76, doi:10.1016/0022–1694(83)90177-4.

Mpelasoka, F. S., and F. H. S. Chiew (2009), Influence of rainfall scenario construction methods on runoff projections, *J. Hydrometeorol.*, *10*(5), 1168–1183, doi:10.1175/2009jhm1045.1.

O'Hara, J., and K. Georgakakos (2008), Quantifying the urban water supply impacts of climate change, *Water Resour. Manage.*, *22*(10), 1477–1497, doi:10.1007/s11269-008-9238-8.

Pahl-Wostl, C. (2007), Transitions towards adaptive management of water facing climate and global change, *Water Resour. Manage.*, *21*(1), 49–62, doi:10.1007/s11269-006-9040-4.

Perkins, S. E., and A. J. Pitman (2009), Do weak AR4 models bias projections of future climate changes over Australia?, *Clim. Change*, *93*(3–4), 527–558, doi:10.1007/s10584-008-9502-1.

Randall, D. A., et al. (2007), Climate models and their evaluation, in *Climate Change 2007: The Physical Science Basis. Contribution of Working Group I to the Fourth Assessment Report of the Intergovernmental*

Panel on Climate Change, edited by S. Solomon, et al., pp. 589–662, Cambridge Univ. Press, Cambridge, U. K.

Rayner, D. (2005), Australian synthetic daily Class A pan evaporation, Report QNRM05435, 38 pp., Dep. of Nat. Resources and Mines, Queensland, Brisbane.

Refsgaard, J. C., and B. Storm (1996), Construction, calibration and validation of hydrological models, in *Distributed Hydrological Modelling*, edited by M. B. Abbott and J. C. Refsgaard, pp. 41–54., Kluwer Acad., Dordrecht, Netherlands.

Salas, J., B. Rajagopalan, L. Saito, and C. Brown (2012), Special section on climate change and water resources: Climate nonstationarity and water resources management, *J. Water Resour. Plann. Manage.*, *138*(5), 385–388, doi:10.1061/(ASCE)WR.1943–5452.0000279.

Savadamuthu, K. (2003), Surface water assessment of the Upper Finniss Catchment, Report DWLBC 2003/18, Dep. of Water, Land and Biodiversity Conservation, Adelaide, Australia.

Schoups, G., N. C. van de Giesen, and H. H. G. Savenije (2008), Model complexity control for hydrologic prediction, *Water Resour. Res.*, *44*, W00B03, doi:10.1029/2008WR006836.

Singh, J., H. V. Knapp, and M. Demissie (2004), Hydrologic modelling of the Iroquois River watershed using HSPF and SWAT, Report ISWS CR 2004-08, 24 pp., Watershed Science Section, Illinois State Water Survey, Champaign.

Srikanthan, R. (2005), Stochastic generation of daily rainfall at a number of sites, Report 05/7, CRC for Catchment Hydrology, Canberra.

Srikanthan, R., and T. A. McMahon (2001), Stochastic generation of annual, monthly and daily climate data: A review, *Hydrol. Earth Syst. Sci.*, *5*(4), 653–670.

Srikanthan, R., and G. G. S. Pegram (2009), A nested multisite daily rainfall stochastic generation model, *J. Hydrol.*, *371*(1–4), 142–153, doi:10.1016/j.jhydrol.2009.03.025.

Srikanthan, R., F. H. S. Chiew, and A. J. Frost (2004), *SCL: Stochastic Climate Library User Guide*, CRC for Catchment Hydrology, Canberra.

Teoh, K. S. (2002), *Estimating the Impact of Current Farm Dams Development on the Surface Water Resources of the Onkaparinga River Catchment*, 153 pp., The Dep. of Water, Land and Biodiversity Conservation, Adelaide, Australia.

Traynham, L., R. Palmer, and A. Polebitski (2011), Impacts of future climate conditions and forecasted population growth on water supply systems in the Puget Sound Region, *J. Water Resour. Plann. Manage.*, *137*(4), 318–326, doi:10.1061/(asce)wr.1943–5452.0000114.

van Oldenborgh, G. J., S. Philip, and M. Collins (2005), El Nino in a changing climate: A multi-model study, *Ocean Sci. Discuss.*, *2*(3), 267–298.

Vicuna, S., J. A. Dracup, J. R. Lund, L. L. Dale, and E. P. Maurer (2010), Basin-scale water system operations with uncertain future climate conditions: Methodology and case studies, *Water Resour. Res.*, *46*(4), W04505, doi:10.1029/2009WR007838.

Wagener, T., H. S. Wheater, and H. V. Gupta (2004), *Rainfall-Runoff Modelling in Gauged and Ungauged Catchments*, 306 pp., Imperial College Press, London.

Wang, Q. J. (1991), The genetic algorithm and its application to calibrating conceptual rainfall-runoff models, *Water Resour. Res.*, *27*(9), 2467–2471, doi:10.1029/91WR01305.

Whetton, P., K. Hennessy, J. Clarke, K. McInnes, and D. Kent (2012), Use of representative climate futures in impact and adaptation assessment, *Clim. Change*, 1–10, doi:10.1007/s10584-012-0471-z.

Wilby, R. L., and S. Dessai (2010), Robust adaptation to climate change, *Weather*, *65*(7), 180–185, doi:10.1002/wea.543.

Wilby, R. L., and H. J. Fowler (2011), Regional climate downscaling, in *Modelling the Impact of Climate Change on Water Resources*, edited by F. Fung, A. Lopez, and M. New, pp. 34–85, Blackwell, Oxford.

Wilby, R. L., and I. Harris (2006), A framework for assessing uncertainties in climate change impacts: Low-flow scenarios for the River Thames, UK, *Water Resour. Res.*, *42*(2), W02419, doi:10.1029/2005WR004065.

Wilby, R. L., P. G. Whitehead, A. J. Wade, D. Butterfield, R. J. Davis, and G. Watts (2006), Integrated modelling of climate change impacts on water resources and quality in a lowland catchment: River Kennet, UK, *J. Hydrol.*, *330*(1–2), 204–220, doi:10.1016/j.jhydrol.2006.04.033.

Wiley, M. W., and R. N. Palmer (2008), Estimating the impacts and uncertainty of climate change on a municipal water supply system, *J. Water Resour. Plan. Manage.*, *134*(3), 239–246, doi:10.1061/(asce)0733–9496(2008)134:3(239).

Zhu, T., M. W. Jenkins, and J. R. Lund (2005), Estimated impacts of climate warming on California water availability under twelve future climate scenarios, *J. Am. Water Resour. Assoc.*, *41*(5), 1027–1038, doi:10.1111/j.1752-1688.2005.tb03783.x.

Appendix B – Information on the climate-independent and climate-dependent water sources for the case study of Journal Paper 2

B.1 Climate-Independent Supply Sources

While it is intuitive that the desalination plant be treated as a climate-independent source, it is less so for the River Murray. However, historically Adelaide's River Murray supply has been a function of licenses, rather than climate. Furthermore, and contrary to the common principle that a license does not guarantee supply, Adelaide's supply is almost certainly guaranteed because: (1) current extraction constitutes less than one percent of total River Murray flow; (2) critical human needs, including for Adelaide, are the highest priority in allocating River Murray water; and (3) the significant storage of the River Murray system helps to dampen out temporal variability in flow that might otherwise restrict water availability for a particular time period. As WaterCress required the capacity of the desalination plant to be expressed on a daily basis, constraints of 68.5 and 137.0 Megaliters per day (ML/day) were applied for the desalination plant to represent the 25 and 50 GL/yr alternatives, respectively. The River Murray supply was constrained to 447 ML/day (the pumping capacity of the MBO pipeline), and 325 GL over 5 years. This second constraint represented the 5-year rolling license and was a necessary simplification because WaterCress could not incorporate a rolling license. However, this simplification represents a conservative approach because it has the potential to underestimate water supply security. River Murray supply was also constrained by Mount Bold Reservoir levels in an attempt to limit reservoir spill but maintain water levels for water supply security when necessary (see *Paton et al.* [2013] for further details).

B.2 Climate-Dependent Supply Sources

B.2.1 Impervious Catchments

For the impervious catchments (harvested stormwater and harvested rainwater), runoff volume was calculated in WaterCress by multiplying the effective area by the runoff depth. The effective area was equal to the total impervious area (roof area plus pavement area – Table B.1) multiplied by the connectivity.

Table B. 1: Roof and pavement areas for Adelaide's southern water supply system for household rainwater tanks and the six stormwater harvesting schemes

Catchment	Roof Area	Pavement Area
Household Rainwater Tanks	250m^2	n/a
Brownhill-Keswick	33.89 km^2	21.01 km^2
Sturt Creek	11.50 km^2	8.63 km^2
Field River	9.23 km^2	5.58 km^2
Christie Creek	6.95 km^2	4.80 km^2
Onkaparinga River	8.82 km^2	6.09 km^2
Pedler Creek	3.53 km^2	3.76 km^2

Runoff depth was calculated as:

$$RO = (R - IL) * OF \qquad (\text{for R}>\text{IL}) \qquad \text{(B.1)}$$

where RO is daily runoff depth in millimetres (mm), R is daily rainfall in mm, IL is initial loss in mm and OF is the ongoing runoff fraction. For roof runoff, an initial loss of 1mm and an ongoing fraction of 0.9 were applied, while an initial loss of 2mm and ongoing fraction of 0.85 were used for pavement runoff [*Wallbridge and Gilbert,* 2009]. The roof connectivity for household rainwater tanks and stormwater was taken as 0.5, while 0.8 was used as the pavement connectivity for the stormwater harvesting schemes [*Wallbridge and Gilbert,* 2009]. However, when rainwater tanks were considered (which had a roof connectivity of 0.5); the roof connectivity for stormwater harvesting was reduced from 0.5 to 0.3 because less roof runoff was assumed to be entering the stormwater collection network. This reduction in stormwater roof connectivity does not equal that of rainwater roof connectivity because rainwater tanks usually collect water from the rear of the roof, whereas the stormwater collection network usually takes water from the front roof section.

B.2.2 Pervious Catchments

While the modelling of impervious runoff is relatively straightforward, the estimation of runoff from pervious areas is more complicated, requiring a number of assumptions, as well as extensive calibration and validation of rainfall runoff (RRO) models. This is important because an appropriate level of confidence in the performance of an RRO model must be established in order to effectively use it for assessment purposes [*Bennett et al.,* 2013]. The following summary details the in-depth analysis applied to RRO model development for this case study, ensuring that the RRO models developed are fit for purpose. However, RRO models for Myponga, Mount Bold and Clarendon Weir catchments were developed previously by *Paton et al.* [2013]. Consequently, only catchment calibration for the pervious areas of the stormwater catchments was required, in which the method employed by *Paton et al.* [2013] for the development of the RRO models was followed. The following synopsis describes both calibration of local catchment reservoir RRO models and stormwater catchment RRO models; however, for more detail on the RRO models for the local catchment reservoirs see *Paton et al.* [2013].

For the local catchment reservoirs, daily flow data from gauging stations A5020502, A5030504, A5030506, and A5030502 were selected, as large areas of the Myponga, Mount Bold, and Clarendon Weir catchments contribute flow at these stations and because the data sets span three to four decades and are relatively complete (Table B.2) (see *Paton et al.* [2013] for further detail). Similarly, daily flow data from gauging stations A5040583, A5040549, A5031010, A5030547, A5031005, and A5030543 were selected for the stormwater catchments, as large areas of the stormwater catchments contribute flow at these stations and the records are relatively complete (Table B.2). However, as mentioned in the paper, there are four ungauged stormwater catchments - namely Grange Area, Port Road, Mile End Drain, and Willunga (Figure 3.2), which could not be calibrated. Consequently, the calibrated WC1 model parameters for Brownhill-Keswick were assumed to be appropriate for Grange Area, Port Road, and Mile End Drain, while Pedler Creek's calibrated WC1

Table B. 2: Gauging station data for the local catchment reservoir and harvested stormwater catchments

Catchment	Catchment Area (km^2)	Gauging Station Identification	Gauging Station Area (Percentage of Catchment Area) (%)	Gauging Station Data Period Available	Data Record Completeness (Percentage of Data Period Available) (%)
Myponga	124	A5020502	6	Oct. 1979-Feb. 2011	98.8
Mount Bold	388	A5030504	83	May. 1973-Jan. 2011	100.0
		A5030506	9	Apr. 1973-Dec. 2010	97.1
Clarendon Weir	54	A5030502	49	Apr. 1969-Dec. 2010	100.0
Brownhill-Keswick	70	A5040583	98	Dec'93-Jan'12	98.4
Sturt Creek	128	A5040549	92	Sep'07-Jan'12	100.0
Field River	55	A5031010	99	May'10-Jan'12	100.0
Christie Creek	38	A5030547	96	Dec'00-Jan'12	100.0
Onkaparinga River	113	A5031005	77	Jul'06-Jan'12	100.0
Pedler Creek	106	A5030543	88	Aug'00-Aug'11	99.6

model parameters were assumed to be appropriate for Willunga (Figure 3.2). For economy, the ungauged stormwater schemes were amalgamated with the Brownhill-Keswick or Pedler Creek schemes in Adelaide's southern water supply system model, such that there were a total of six modelled stormwater harvesting schemes.

Daily streamflow data for the gauging stations were sourced from the South Australian Government Department of Environment, Water, and Natural Resources' Surface Water Archive (https://www.waterconnect.sa.gov.au/SWA). For records that contained missing streamflow data at the very beginning or very end of the data periods, the data were excluded. However, if the missing data were in the middle of the data set and if nearby gauges existed, the data were estimated using regression analysis with nearby flow gauges. For the stormwater catchments, even though the data records were relatively complete (Table B.2), the data periods available were fairly limited, particularly for the Field River (21 months), and, to a lesser extent, for the Sturt Creek (53 months) and Onkaparinga River catchments (67 months) (Table B.2). Furthermore, *Wallbridge and Gilbert* [2009] found that data provided by a number of the gauging stations were suspect. However, the data had to be used for calibration and validation of the pervious catchment models, as there were no better streamflow records available.

WC1 computes runoff using the inputs of daily rainfall and monthly Pan A evaporation data. For the case study, rainfall and Pan A evaporation data were sourced from the Patched Point Dataset, which contains complete daily datasets for multiple climate variables based on Bureau of Meteorology records for about 4600 locations around Australia [*Jeffrey et al.*, 2001]. The PPD is advantageous over the original BoM records because the dataset has already undergone high-quality, rigorously-tested data infilling (when data are missing) and deaccumulation of any records that represent rainfall over multiple days, rather than a single day [*Charles et al.*, 2008]. Eight climate data stations for the case study were defined, namely Belair State Flora Nursery (23704), Cherry Gardens (23709), Clarendon (23710), Hahndorf (23720), Happy Valley Reservoir (23721), McClaren Vale (23729), Myponga Reservoir (23738), and Unley (23029). These were scaled for the relevant catchments to represent the average rainfall over the whole catchment (see *Paton et al.* [2013] for methodology applied to calculate average rainfall for the catchments).

Approximately the first 60-70% of available data was applied for calibration, while the remaining data were used for validation. Calibration and validation periods were multiples of 12 months, so as not to bias the RRO models' calibrated parameters towards a particular month's flow properties, except for the Field River stormwater catchment, which only had 21 months of flow data, so all data were used.

A genetic algorithm (GA) was applied to optimise the ten WC1 model parameters for the calibration of the three local reservoir catchments and six stormwater catchments (Table B.3). Variations of the population (P) (100-400), number of generations (G) (100-350), and probability of crossover (P_c) (0.6-0.9) were trailed, with final parameters selected as P=200, G=150, and P_c=0.7 for the local reservoir catchments and P=400, G=350, and P_c=0.7 for the stormwater catchments. A value of 0.1 was taken for the probability of mutation, as it was equal to the inverse number of model parameters. These GA parameters were selected as they generally produced robust results (in terms of consistent values of the objective function value and the 10 parameter values), regardless of the 10 random starting positions trailed, which was important due to the potential problem of parameter equifinality [*Beven*, 2006].

For the local catchment reservoirs, the root mean squared error (RMSE) of monthly flows was minimised during the optimisation procedure. RMSE was selected as the objective function for the local reservoir catchments because, even though it is biased toward matching high flows, accurately simulating high flows is very important when studying water supply systems [*Paton et al.*, 2013]. For example, if the amount of runoff from wet periods was underestimated, there could be less water available in the storages compared to reality during the next dry period (when demand exceeded runoff), which could therefore falsely reduce estimates of water supply security. Furthermore, *Bennett et al.* [2013] recommend RMSE as a good initial candidate for a performance metric because its wide usage aids communication of model performance. Monthly values were appropriate to use

Table B. 3: WC1 model parameters for the pervious catchments for the southern water supply system model

Catchment	WC1 Model Parameter									
	Median Soil Moisture (mm)	Catchment Distribution (mm)	Interception Store (mm)	Ground Water Discharge	Soil moisture discharge	Pan factor for soil	Fraction Groundwater Loss	Store Reduction Coefficient	Groundwater Recharge	Creek Loss (mm)
Myponga	160	59.4	8.1	0.0015	0.00015	0.94	0.49	0.90	0.45	0.01
Mount Bold	186	60.0	9.3	0.0015	0.00012	0.84	0.49	1.39	0.15	0.00
Clarendon Weir	195	59.5	8.0	0.0015	0.00015	0.99	0.20	0.85	0.30	0.01
Brownhill-Keswick	256	80.0	23.5	0.0015	0.00005	1.00	0.99	0.94	0.96	0.00
Sturt Creek	149	15.0	30.0	0.0015	0.00008	0.45	0.00	0.78	0.99	0.16
Field River	119	80.0	28.2	0.0015	0.00015	0.74	0.92	1.40	0.85	0.00
Christie Creek	90	78.0	21.4	0.0015	0.00005	0.79	0.99	0.98	1.00	0.00
Onkaparinga River	236	42.9	20.0	0.0009	0.00008	0.74	0.92	1.40	0.90	0.01
Pedler Creek	277	55.8	27.0	0.0015	0.00009	0.69	0.93	0.98	0.86	0.01

for the reservoir catchments because daily and weekly errors in the flows can be buffered by the large reservoir storages.

However, RMSE was not an appropriate metric for the stormwater schemes, because: (1) RMSE favours high flows and peaks and is more sensitive than other metrics to infrequent large errors due to the squaring process [*Dawson et al.*, 2007]; and (2) matching high flows was not as important for the stormwater catchments. Simulating low flows was more important for these catchments because: (1) the gauging stations recorded a number of high flows that were usually recognised as estimates only [*Wallbridge and Gilbert*, 2009]; and (2) high flow volumes could exceed the capacity of the wetland storage and be spilled out to sea, so underestimating these flows is unlikely to greatly affect stormwater yield. Consequently, a Nash-Sutcliffe (NS) coefficient of the log of weekly flows approaching one was sought for the stormwater catchments. A weekly time step was also more appropriate for assessing stormwater catchments because the wetland storages are much smaller. Furthermore, due to the extremely positively-skewed nature of the stormwater schemes' runoff (which was discovered by visually analysing the flow data), NS of the natural logarithmic-transformed weekly flows was used. Consequently this placed less emphasis on matching the few, large flows and more emphasis on simulating the more frequent, low flows [*Oudin et al.*, 2006; *Perrin et al.*, 2007].

To avoid incurring an error when attempting to return the natural logarithm of zero, the natural logarithmic-transformed flow NS equation was altered to:

$$NS_{\log} = 1 - \frac{\sum_{w=1}^{W} (\ln(Q_{observed}^{w} + 1.0) - \ln(Q_{\mathrm{mod}\,eled}^{w} + 1.0))^2}{\sum_{w=1}^{W} (\ln(Q_{observed}^{w} + 1.0) - \ln(Q_{observed}^{average} + 1.0))^2} \qquad \text{(B.2)}$$

where NS_{log} is the natural logarithmic-transformed flow Nash Sutcliffe value, w is the week, W is the total number of weeks, $Q_{observed}^{W}$ is the observed flow for week w, $Q_{\mathrm{mod}\,eled}^{w}$ is the modelled flow

for week w, and $Q_{observed}^{average}$ is the average observed weekly flow. However, *Jain and Sudheer* [2008] point out that a high value of NS can be achieved for a model with a poor fit. Consequently, and although more subjective than the use of statistical measures of goodness-of-fit, plots of simulated and observed hydrographs were also inspected following optimisation. *Refsgaard and Storm* [1996] note that the visual inspection of plots is an efficient means of assimilating information, as well as providing a good overall insight into a model's capabilities.

For all catchments, the calibrated models were validated on independent data, to check whether the model should be rejected as being not behavioural [*Beven*, 2006]. Consequently, the calibrated parameters for reservoirs were not rejected if for both calibration and validation: (1) RMSE was less than half the standard deviation [*Singh et al.*, 2004]; (2) NS was greater than 0.5 [*Moriasi et al.*, 2007]; (3) the observed and modelled flows were reasonably similar; and (4) the hydrographs of observed and modelled flows demonstrated a reasonably good fit. For the stormwater catchments (in which matching the observed and modelled flows was not as important, as discussed above), catchment parameterisations were judged adequate if NS was greater than 0.5 and if, upon visual inspection, the modelled and observed hydrographs matched the low flows. The conditions outlined for accepting the RRO models as valid were found to be satisfied for the catchments (Table B.4). However, deviations from optimal values for the stormwater schemes were expected, as limited streamflow data were available and *Wallbridge and Gilbert* [2009] determined that a number of the stormwater gauges were producing suspect data, as mentioned above. For example, the Anzac Highway Gauge, which was used to calibrate the Sturt Creek catchment, is believed to underestimate flow. This was supported by the calibration and validation findings of this case study, as modelled flow was generally 20-30% greater than observed flow.

Table B. 4: Performance criteria for the calibration and validation of pervious catchments

Catchment	RMSE/SD		NS(*) or NS_{log}		Average Observed Flow (GL/yr)		Average Modelled Flow (GL/yr)	
	Calibration	Validation	Calibration	Validation	Calibration	Validation	Calibration	Validation
Myponga	0.28	0.44	0.92*	0.80*	7.5	5.2	7.9	3.2
Mount Bold	0.22	0.35	0.95*	0.88*	51.9	41.4	51.6	41.2
Clarendon Weir	0.25	0.36	0.94*	0.87*	3.9	3.0	3.9	3.5
Brownhill-Keswick	n/a	n/a	0.86	0.83	n/a	n/a	n/a	n/a
Sturt Creek	n/a	n/a	0.81	0.74	n/a	n/a	n/a	n/a
Field River	n/a	n/a	0.80	0.53	n/a	n/a	n/a	n/a
Christie Creek	n/a	n/a	0.81	0.55	n/a	n/a	n/a	n/a
Onkaparinga River	n/a	n/a	0.97	0.84	n/a	n/a	n/a	n/a
Pedler Creek	n/a	n/a	0.91	0.91	n/a	n/a	n/a	n/a

Appendix C – Details of the development of the stochastic rainfall time series for the case study of Journal Paper 2

Similar to the development of the RRO models, climate change affected rainfall and evaporation were developed for this case study based on the methodology described by *Paton et al.* [2013]. However, *Paton et al.* [2013] only applied the methodology to three climate data sites (one for each local reservoir catchment), while a further five climate data sites were necessary to represent the climate for the stormwater and rainwater harvesting schemes in this case study. These eight sites were synonymous with the sites used for calibrating and validating the RRO models. They included Belair State Flora Nursery (23704), Cherry Gardens (23709), Clarendon (23710), Hahndorf (23720), Happy Valley Reservoir (23721), McClaren Vale (23729), Myponga Reservoir (23738), and Unley (23029).

The multi-site daily rainfall model of the Stochastic Climate Library (SCL) (www.toolkit.net.au/scl), developed by the Cooperative Research Centre (CRC) for Catchment Hydrology [*Srikanthan*, 2005] was used to develop the stochastic time series for this case study. SCL is a multi-site two part model, nested in a monthly and annual model. The first part consists of rainfall occurrence, which is determined using a first-order two-state Markov chain, while the second part relates to rainfall amounts, derived using a gamma distribution [*Srikanthan*, 2005]. Because of the great spatial variability of rainfall, a multi-site model was necessary to account for the spatial dependence between rainfall stations, while the SCL was selected because it preserves the important characteristics of rainfall at daily, monthly, and annual time scales [*Srikanthan*, 2005]. The historical 30-year baseline of 1975-2004 was used to derive the stochastic rainfall time series, as this matched the baseline climate used by OzClim when developing change factors for climate change. Consequently, 1,000 30-year stochastic time series were developed. To be confident that these time series were a good representation of the natural variability in the historical rainfall time series, important statistical comparisons between the stochastic and the historical data series were conducted. Specifically, upholding mean values, measures of variability (e.g., standard deviation), the 2-, 3-, 5-, 7-, and 10-year low rainfall sums, and the cross-correlations between sites were considered important (see *Paton et al.* [2013] for justification). An assessment of these statistics

indicated considerable similarity, so the generated stochastic data were considered to preserve the important characteristics of the historical rainfall and could thus be used with confidence for the remainder of the case study.

Appendix D – Information on the economic costs derived for the case study of Journal Paper 2

SA Water's expenditure on electricity and total consumption of electricity (as per SA Water's 2010 annual report - see www.sawater.com.au), equated to an electricity purchase price of approximately 10 cents per kilowatt hour (c/kWh). However, an indicative cost of 12 c/kWh was assumed for this case study so as to account for potential electricity price increases in South Australia. Note that all costs are in Australian dollars (A$).

D.1 Local Catchment Reservoirs

No capital costs for reservoirs were accounted for in the case study because they were already components of the southern system, as mentioned previously. No costs accounting for major upgrades to the reservoirs were necessary either, because: (1) previous major upgrades to Adelaide reservoirs have been undertaken after approximately 100 years of being constructed; and (2) in 1962 both Myponga reservoir was constructed and the Mount Bold dam level raised, while Happy Valley reservoir was upgraded in 2004. Similarly, Happy Valley WTP and Myponga WTP were already existing components of the southern system built in 1991 and 1993, respectively, so their capital costs were not included. However, assuming a plant lifetime of 50 years, both WTPs were assumed to be replaced once: Happy Valley WTP in 2041 and Myponga WTP in 2043. Mechanical assets were assumed to be replaced every seven years. In addition, $17.8 million for replacing the chlorination facility at Happy Valley WTP was included in 2012 [*Public Works Committee*, 2011a]. Other ongoing costs for the reservoirs were based on indicative costs (Robert May, United Water, personal communication, 2008) that cover the power and chemical costs of treating water and the cost of labour.

D.2 River Murray

No capital costs for the existing MBO pipeline were accounted for, while ongoing costs were attributed to power costs required to pump water from the River Murray to Mount Bold catchment and water treatment costs at Happy Valley WTP. Costs associated with repair, maintenance,

replacement and labour are considered negligible compared to power costs (Tim Kelly, SA Water, personal communication, 2008). Hence, these were not included in the analysis.

D.3 Desalination Plant

The 100 GL/yr desalination plant was estimated to have a capital cost of $1.83 billion [Government of South Australia, 2009], while $1.347 billion was estimated for a 50 GL/yr plant [SA Water, 2009]. Half of these costs were assumed for the case study, to reflect the reduced size of the desalination plants (as a result of only considering the southern system and not the whole of Adelaide). The Port Stanvac-Happy Valley (PSHV) transfer pipeline (used to transfer desalinated water to Happy Valley where it enters the mains distribution network) had a capital cost of $100 million, while the electricity required to treat 50 GL of water was taken as 250 Gigawatt hours (GWh) [*SA Water*, 2009], equating to 5 Kilowatt hours per kiloliter (kWh/kL). Furthermore, the electricity required for the delivery pipeline from the 50 GL/yr plant was 35 GWh [*SA Water*, 2009]. Assuming that energy and other ongoing resource inputs doubled when the volume of water doubled [*SA Water*, 2009], 5.7 kWh/kL was the energy intensity assumed for both plant sizes. Operational electricity was assumed to account for approximately half of the total operating costs, which equated to $68.4 million/year for the 100 GL plant and $34.2 million/year for the 50 GL plant when the plants were operating at full capacity (based on 5.7 kWh/kL and 12 c/kWh). Consequently, while true electricity costs were estimated based on the actual volume of desalinated water produced each year, other operating costs (e.g. chemical costs) were estimated at a fixed rate of $34.2 million/year for the 50 GL plant and $68.4 million/year for the 100 GL plant. The desalination plant was not replaced over the planning horizon, but RO membranes were assumed to be replaced every five years at a cost of $15.5 million and $31 million for the 50 GL and 100 GL plants, respectively. For the PSHV pipeline, electricity costs associated with pumping and the cost of pump replacement after 20 years in 2030 were accounted for. The cost of replacing the pumps was assumed to be $30 million.

D.4 Household Rainwater Tanks

Capital costs of rainwater tanks included the cost of the tank, pump, plumbing, installation, base, and delivery, which, for this case study, were estimated from a number of Adelaide rainwater tank suppliers. All rainwater tanks used in the case study were circular, made from polyethylene and above ground, such that the total capital cost for each 5.0 kL tank was $2708. All rainwater tanks installed were replaced every 30 years (at a cost of $2708/tank). Rainwater tank pumps cost $355 and were replaced every 15 years. A 5c/kL operating and maintenance cost and a fixed additional maintenance cost of $20/year [*Tam et al.*, 2010] were applied as ongoing costs. An average energy intensity of 1.5 kWh/kL was assumed for the pump [*Retamal et al.*, 2009].

D.5 Harvested Stormwater

The capital material and construction costs associated with the stormwater wetlands, aquifer storage and recovery (ASR), and water distribution network for harvested stormwater were accounted for in the case study. Land acquisition costs were not included, as the area required to capture, treat and store stormwater should be available without significant land purchases or interference with existing development [*Wallbridge and Gilbert*, 2009]. Capital costs for the wetlands and ASR were derived from *Wallbridge and Gilbert* [2009]. However, these capital costs do not account for distribution costs. Consequently, distribution costs for the case study were estimated from three ASR schemes in Adelaide for which distribution costs are available: (1) Oaklands Park; (2) Munno Para and Andrews Farm Wetlands; and (3) the Water Proofing the West Project. These schemes operate similarly to the schemes in this case study, in that water is distributed to a limited number of public purposes, such as irrigation of local reserves and parks. Costs for the distribution networks were particularly varied, so $0.41/kL/year (the average cost of the three schemes when taking into account projected yields) was applied in this case study.

Operating stormwater harvesting costs for the case study were based on operating and maintenance costs for Oaklands Park and Water Proofing the West. For Oaklands Park, operating and

maintenance costs were estimated at $350,000 per annum, which includes the cost of labour, replacement capital, maintenance, electricity for pumping, UV treatment, monitoring/licensing fees and 6% contingency [*Public Works Committee*, 2011b]. Annual operating costs for Water Proofing the West once fully operational will be approximately $5.1 to $5.6million, which incorporates the cost of labour, operation and maintenance of mechanics/electronics/controls, replacement capital, electricity consumption, landscaping/wetland plant maintenance, UV treatment, monitoring/licensing fees (including some contingency), depreciation costs and financing costs [*City of Charles Sturt*, 2010]. When taking into account the projected yields of these stormwater schemes, operational costs are estimated at $1.26/kL and $1.20/kL for Oaklands Park and Water Proofing the West, respectively. Consequently, the average of these two values ($1.23/kL) was applied in the case study.

Appendix E – Economic costs of water supply sources for the case study of Journal Paper 3

E.1 Local Catchment Reservoirs

As the local catchment reservoirs and their associated water treatment plants (WTPs) were existing features of Adelaide's southern water supply system, only ongoing costs were accounted for. These included power and chemical costs of treating water at the WTPs, the cost of labour to run the WTPs and the cost of upgrading and/or replacing infrastructure. Indicative costs (Table E.1) were used for the power and chemical costs of treating water and the cost of labour [Robert May, United Water, personal communication, 2008]. No major upgrades to the reservoirs were assumed for the planning horizon of the case study, because: (1) previous major upgrades to Adelaide reservoirs have been undertaken after approximately 100 years (yrs) of being constructed; and (2) in 1962 both Myponga reservoir was constructed and the Mount Bold dam level was raised, while Happy Valley reservoir was upgraded in 2004. However, assuming a WTP lifetime of 50 years, both WTPs were assumed to be replaced once over the planning horizon: Happy Valley WTP in 2041 and Myponga WTP in 2043. The cost of replacement was considered the same as the initial capital costs of these two WTPs. The capital cost to construct Myponga WTP was $28.39 million in 2010 net present value (www.sawater.com.au). However, the cost to build Happy Valley WTP was not reported and thus was estimated using cost information from water treatment plants built in South Australia (www.sawater.com.au) (Table E.2). Using these WTP capacities and capital costs, the sixth-tenths capacity/cost equation used to estimate the cost of a WTP [*Baruth*, 2005] was thus applied to estimate the cost of the Happy Valley WTP:

$$\left(\frac{CC_1}{CC_2}\right) = \left(\frac{Cap_1}{Cap_2}\right)^{0.6} \quad \text{(E.1)}$$

where CC_1 is the unknown capital cost of Happy Valley WTP (in $million) with capacity Cap_1 (Cap_1=850 Mega Litres per day (ML/day)), and CC_2 is the known capital cost of a water treatment plant (CC_2) with capacity Cap_2 (in ML/day). Ignoring the capital cost estimate derived using Anstey

Hill WTP (considered an outlier, possibly a result of its extremely small capacity) the capital cost for replacing Happy Valley WTP was estimated to be $162.5million in 2010 present value.

Mechanical assets were replaced every seven years, with the cost associated with this replacement estimated at 13.8% of the total capital cost for each WTP. This percentage represents the cost of mechanical and miscellaneous equipment compared with the total capital cost of a WTP [*Baruth*, 2005]. In addition, $17.8million for replacing the chlorination facility at Happy Valley WTP was included in 2012 [*Public Works Committee*, 2011a].

E.2 River Murray

The River Murray was an existing Adelaide southern system supply source, so it was not necessary to account for capital costs associated with the Murray Bridge-Onkaparinga (MBO) pipeline (used to convey water from the River Murray to the Onkaparinga River). Consequently, only ongoing costs of River Murray supply were accounted for, which included treatment costs at Happy Valley WTP (see Section E.1) and pumping costs. Costs associated with repair, maintenance, replacement and labour are considered negligible compared to power costs associated with pumping River Murray water [Tim Kelly, SA Water, personal communication, 2008], so they were not accounted for in the case study. Power costs were derived from first principles, firstly using the Darcy-Weisbach head loss equation to calculate head loss:

$$h_f = \frac{fLV^2}{2Dg} \quad \text{(E.2)}$$

where h_f is the head loss along the pipe (in metres (m)), f is the Darcy-Weisbach friction factor (f=0.02), L is the pipe length (L=40,700m) [*Crawley*, 1995], V is the average velocity of flow in the pipe (in metres per second (m/s)), D is the pipe internal diameter (1.65m) [*Crawley*, 1995], and g is the gravitational acceleration (g=9.81 metres per second squared (m/s^2)). The velocity depended on the flow of water through the pipeline, with an average velocity assumed per day based on 24-hour continuous pumping. Thus, if the maximum flow of the pipeline of 447ML/day was reached, the

Table E. 1: Indicative costs for the power and chemical costs of treating water at the WTPs and the cost of labour

Location	Power			Chemicals	Labour						
	Electricity Cost (c/kWh)	Power (kilo Watt hours per Mega Litre (kWh/ML))	Power Cost ($/ML)	Chemical Cost ($/ML)	Maintenance Staff	Operators	Plant Supervisors	Maintenance Rate ($million/yr)	Operator Rate ($/yr)	Plant Supervisor Rate ($/yr)	Labour Cost ($million/yr)
Happy Valley	12	100	12	25	7	2	1	0.08	0.12	0.20	1.00
Myponga	12	140	17	70	1	2	0	0.08	0.12	0.20	0.32

Table E. 2: Capital cost information for water treatment plants built in South Australia used to calculate the capital cost of the Happy Valley WTP

Water Treatment Plant	Capacity (Cap_2) (ML/day)	Capital Cost (CC_2) ($2010million)	Capital Cost of Happy Valley WTP (CC_1) ($2010million)
Hope Valley	273	92.31	182.5
Anstey Hill	3	52.88	1565.6*
Barossa	160	54.15	147.5
Little Para	160	59.1	161.0
Myponga	50	28.39	155.4
Morgan	200	69.65	165.9
Average			162.5

*N.B. The capital cost estimate using Anstey Hill was considered an outlier and thus was not included in the average capital cost calculation of Happy Valley WTP. The very small capacity of Anstey Hill WTP may have contributed to the very high cost associated with this plant.

head loss was approximately 100m.

The maximum power required to pump desalinated water from Murray Bridge to the Onkaparinga River was then calculated, using the pump power equation:

$$P = \frac{\gamma Q(H_f + H_s)}{\eta} \quad \text{(E.3)}$$

where P is the Pump Power (Watts), ɣ is the specific weight of water (ɣ =9789 Newtons per metre cubed (N/m^3)), Q is the flow (in metres cubed per second (m^3/s)), H_f is the head loss (m), H_s is the static loss (H_s=419m) [*Crawley*, 1995], and η is the pumping efficiency (η=0.8). The pump power was then converted to kWh, based on 24-hour operation, before being converted to a cost using the electricity purchase rate of 12 c/kWh.

E.3 Desalination

The reverse osmosis desalination plant capacities could range from 100ML/day to 500ML/day in 50ML/day increments (Table E.3). However, as it was assumed that the southern system only accounted for half of Adelaide's demand, only half of the volume of water produced by the plant was available for the southern water supply system. Consequently, only half of the costs associated with the desalination plant were attributed to the southern system. The desalination plant also required the construction of a transfer pipeline from Port Stanvac to Happy Valley, because desalinated water was combined with water from Happy Valley Reservoir prior to release into the mains distribution system [*Government of South Australia*, 2009]. Similar to the desalination plant, only half of the costs associated with the transfer pipeline were attributed to the southern system.

E.3.1 Capital Costs – Desalination Plant

The capital cost of the Adelaide desalination plant (≈274ML/day capacity) was $1.83 billion [*Government of South Australia*, 2009], or $1.73 billion not including the transfer pipeline to Happy Valley. To estimate the cost of the different desalination plant capacities (Table E.3), this information was used in a capital cost estimate equation for desalination plants reported by *Wittholz et al.* [2008]:

$$\left(\frac{CC_1}{CC_2}\right) = \left(\frac{Cap_1}{Cap_2}\right)^{0.8} \quad \text{(E.4)}$$

where CC_1 is the unknown capital cost of the desalination plant (in $billion) with capacity Cap_1 (in ML/day), and CC_2 is the known capital cost of the desalination plant (CC_2=$1.77billion) with capacity Cap_2 (Cap_2=274ML/day). As *Wittholz et al.* [2008] note, this power law rule is similar to the one commonly used in engineering for capacity/cost correlation (e.g., as was used to calculate the Happy Valley WTP capital costs – see Section E.1); however, an exponent value of 0.8, rather than 0.6, was used, as this was more suitable for desalination plants. Another method to estimate capital costs of different capacity RO desalination plants for the case study would have been to determine an equation that reflected the costs of recently constructed RO desalination plants in Australia.

Table E. 3: Capital costs for the different desalination plant capacities

Plant Capacity (ML/day)	Capital Cost (2010$Billion)
100	0.77
150	1.07
200	1.35
250	1.61
300	1.86
350	2.11
400	2.34
450	2.57
500	2.80

Table E. 4: Capital costs and current and expansion capacities of reverse osmosis desalination plants recently built in Australian cities

Australian City	Plant name	Current Capacity (ML/day)	Expansion Capacity (ML/day)	Capital Cost ($billion)* [*Tal*, 2011]
Gold Coast	Gold Coast Desalination Plant	125	167	$1.20
Perth	Southern Seawater Desalination Plant	137	274	$0.96
Sydney	Kurnell Desalination Plant	250	500	$2.40
Melbourne	Wonthaggi Desalination Plant	410	550	$3.50

*N.B. *Tal* [2011] does not cite the year these capital costs relate to

However, as demonstrated in Table E.4, desalination plants have been built in Australia with various initial capacities and planned expansion capacities. Furthermore, project and site-specific characteristics in different Australian cities presumably affect the capital costs (Table E.4), so this

method was not used to estimate the desalination plant capital costs. A direct comparison of the Adelaide Desalination Plant with the Southern Seawater Desalination Plant in Perth supports this, as the expansion to 274ML/day is projected to cost another $450million (http://www.water-technology.net), resulting in a total cost of $1.41billion, $360million less than the same capacity Adelaide desalination plant.

E.3.2 Capital Costs – Transfer Pipeline

The transfer pipeline was designed based on the potential capacity of the Port Stanvac desalination plant, with standard pipe diameters selected for each desalination capacity (Table E.5) based on a head loss of about 35 to 45 metres at full flow. This was an appropriate assumption for head loss, given that the static lift over the 12km pipeline is 140m, and the current design has a total lift of 185m (i.e. head loss of 45m) at full flow. A number of standard diameters were trialled for each desalination plant capacity until an appropriate head loss was found. The Darcy-Weisbach head loss equation (Equation E.2) was used to calculate head loss, while the average velocity of flow was calculated from the maximum flow required to meet the daily desalination plant capacity. The maximum power required to pump desalinated water from Port Stanvac to Happy Valley (Table E.5) was then calculated for each of the desalination capacities, using the pump power equation (Equation E.3).

Given that eight pumps were selected for the current pump station design (http://www.arup.com/Projects/Adelaide_Desalination_Plant_Transfer_Pipeline_System.aspx), between four and ten pumps were selected for each design to meet the calculated pump power (Table E.5). An additional stand-by pump was also allocated to each design, to allow for uninterrupted full-capacity pumping during maintenance and to ensure there was a back-up option, should one of the pumps fail.

For the transfer pipeline, total capital costs (Table E.6) comprised of supply of the Mild Steel Cement Lined (MSCL) pipe and fittings; construction of the pipeline, including tunnel boring; supply of the

Table E. 5: Design features of the transfer pipeline for each potential Port Stanvac desalination plant capacity

Desalination Plant Capacity (ML/day)	Internal Pipe Diameter (m)	Pump Power (Watts)	Number of Pumps (excluding stand-by pump)
100	0.90	2620	4
150	1.13	3679	4
200	1.20	5175	4
250	1.30	6540	6
300	1.45	7533	6
350	1.50	9064	8
400	1.60	10,227	8
450	1.75	11,011	10
500	1.75	12,779	10

pumps and pump station building; project mobilisation and site management; contingencies; engineering surveys and design; and project construction and management.

The costs of supply of the MSCL pipes (in 2010 present value) (Table E.6) were calculated based on costs for MSCL pipe reported by *Dandy and Engelhardt* [2006] and *Rawlinsons* [2007]:

$$C = 0.8687 * D + 129.23 \quad \text{(E.5)}$$

where C is the cost of supply of MSCL pipe (in $/m) and D is the diameter of the pipe (in millimetres). Cost estimates used for an Australian pipeline design by *Snowy Mountains Engineering Corporation Australia* [2007] were used to determine the cost of fittings, the cost to lay and fit the pipeline, and the cost of the pump station building (Table E.6). To minimise impact on major road and rail services,

Table E. 6: Cost breakdown for transfer pipeline for each potential Port Stanvac desalination plant capacity

Desalination Plant Capacity (ML/day)	Pipe Supply (including fittings) ($Million)	Pipe Construction ($Million)	Pump Station Building ($Million)	Pumps ($Million)	Extras ($Million)	Total ($Million)
100	11.3	7.7	7.4	9.6	20.9	56.9
150	13.8	9.8	7.6	12.2	25.1	68.4
200	14.6	10.3	7.6	15.4	27.8	75.8
250	15.7	11.3	7.7	19.2	31.3	85.2
300	17.4	12.7	7.8	21.1	34.3	93.3
350	18.0	13.0	7.9	25.3	37.2	101.4
400	19.1	14.3	8.0	27.5	39.9	108.8
450	20.9	15.4	8.1	30.3	43.3	117.9
500	20.9	15.4	8.1	33.6	45.2	123.1

the cost of several tunnel bores was also added to the pipe construction costs, reflecting the contract value of approximately $5million for tunnel boring for the current 1.575m-diameter pipeline (www.winslow.com.au). As reported by *Walski* [2012], pump costs can be estimated using the relationship estimated by *Dickson* [1978]:

$$C = 5040\ P^{0.69} \tag{E.6}$$

where C is the Cost (US$) and P is the pump power (horsepower). This equation was applied to estimate the pump costs for this case study (Table E.6), with the costs corrected for inflation and converted to Australian dollars. Finally, 10% was added to the cost for project mobilisation and site management, 30% was added for contingencies, 15% was added for engineering surveys and design,

and 3% was added for project construction and management [*GHD Fitchner*, 2007]. These costs have been listed as 'Extras' in Table E.6. The costs appear reasonable, given that the current transfer pipeline is costed at $100million and can pump up to 375ML/day (www.macdow.com.au).

E.3.3 Ongoing Costs – Desalination Plant

Ongoing costs for the desalination plant were attributed to purchasing electricity, labour, chemicals, and membrane and plant replacement. As illustrated in Table E.7, a review of a number of desalination plant operating costs illustrates that operational costs make up about a half to two-thirds of the total costs of a desalination plant. This compares well with the Adelaide desalination plant, for which ongoing costs account for approximately 58% of the total costs over the 20-year life of the project [*SA Water*, 2009]. Ongoing costs were assumed to be $130million per year (http://www.abc.net.au/news/2010-12-01/130m-annual-cost-to-run-desal-plant/2358158) for this estimation. The cost of electricity for energy consumption is reported to be the greatest contributor to ongoing costs for RO desalination plants, ranging from 48% to 70% for a number of examples documented in the literature (Table E.7). Again, calculations of the cost of energy consumption for the Adelaide desalination plant fall within this percentage range. Approximately 5.0kWh/kL of energy is estimated to be required for the desalination plant, which results in a cost of $68.4million per year, or 53% of the operating costs (assuming the plant operates at full capacity and assuming a 12 c/kWh electricity purchase price). The cost of membrane replacement was relatively constant, ranging from 7% to 10% of ongoing costs, while the labour, chemical and other cost percentages were more varied (Table E.7). There was also no correlation found between plant capacity and the percentage of operational costs apportioned to energy, labour, or membrane replacement; however, as plant capacity increased, so too did the percentage of operational costs attributed to chemicals (Table E.7). However, *GHD Fitchner* [2005] reported that the percentage of costs attributed to energy and chemicals would be greater, while the percentage of labour costs would be less, for a 500ML/day plant compared to a 50ML/day plant (Table E.7), which was expected in terms of economies of scale.

Table E. 7: Operational cost information for RO desalination plants

Reference		*Semiat* [2000]	*GHD Fitchner* [2005]	*GHD Fitchner* [2005]	*Hoang et al.* [2009]
Plant Capacity (ML/day)		-	50	500	100
Operational Costs as a Percentage of Total Costs		63	-	-	48
Percentage of Operational Costs (%)	Energy	70	50	55	48
	Chemicals	5	16	19	17
	Labour	6	15	4	21
	Membrane Replacement	8	7	7	10
	Other	-	12	15	4
	Maintenance and Parts	11	-	-	-
TOTAL		100	100	100	100

Using the cost information for the Adelaide desalination plant and the cost breakdown summarised in Table E.7, the ongoing costs for the different desalination plant capacities in the case study (when operating at maximum capacity) were derived. The operational cost as a percentage of total cost for the Adelaide desalination plant of 58% was firstly used to derive the maximum operational cost for each of the plant capacities (Table E.8) (calculations used the capital costs from Table E.3, assumed a 20-year plant life-time and discounted future ongoing costs to 2010 present value using Weitzman's gamma discounting). The cost of energy was then determined, using the 5.0kWh/kL energy intensity value for the Adelaide desalination plant. Consequently, ongoing costs attributed to energy ranged from 42% to 58% of the total ongoing costs (Table E.8). These seem reasonable, given the values reported in Table E.7 and given that for a bigger desalination plant capacity, there would be a

Table E. 8: Operational cost breakdown for the different capacity desalination plants of the case study

Plant Capacity (ML/day)		100	150	200	250	300	350	400	450	500
Operational Costs as a Percentage of Total Costs (%)						58				
Percentage of Operational Costs (%)	Energy	42	46	48	50	52	54	56	57	58
	Chemicals	16	16	17	17	18	18	19	19	20
	Labour	20	19	18	17	16	15	14	13	12
	Membrane Replacement	8	8	8	8	8	8	8	8	8
	Other	14	11	9	8	6	5	3	3	2
Annual Operational Cost (2010$Million)	Energy	25	37	50	62	75	87	100	112	125
	Chemicals	9	13	18	21	26	29	34	38	43
	Labour	12	16	19	21	23	24	25	26	26
	Membrane Replacement	5	7	8	10	11	13	14	16	17
	Other	8	9	9	9	8	8	6	6	5
Total Annual Operational Costs (2010$million)		59	82	104	124	143	162	180	198	216

greater percentage of ongoing costs apportioned to energy. The percentage cost attributed to chemicals was then estimated to be between 16% and 20%, with the cost percentage increasing for larger plant capacities (Table E.8). On the contrary, the percentage attributed to the cost of labour decreased with plant capacity, ranging between 12% and 20% of total operational costs (Table E.8). Membrane replacement costs were held at a constant 8% of operational costs for all plant capacities, while the remainder of operational costs were attributed to “other”, which could include maintenance and parts (Table E.8). Costs of labour, membrane replacement and other were

assumed to be fixed, regardless of the amount of water used per year from the desalination plant. For example, for the 250ML/day plant, the plant would cost $40million, even if no water were produced by the plant. However, chemical and energy costs depended on the amount of water supplied by the desalination plant. Energy consumption was computed based on the 5.0kWh/KL rate, resulting in a linear scaling of the energy costs with plant capacity. Similarly, the cost of chemicals was scaled linearly, for example, if 25ML of water were produced per day by the 250ML/day plant, 10% of the chemical costs would be accounted for, while 50% of the chemical costs would be accounted for if water was produced at the rate of 125ML/day.

Further to membrane replacement, the desalination plant was replaced once in 2030, given that it was assumed to have a lifetime of 20 years [*SA Water*, 2009]. Replacement was assumed to cost the same as the initial capital cost.

E.3.4 Ongoing Costs – Transfer Pipeline

The ongoing costs of the transfer pipeline were attributed to the electricity required to pump the water and the replacement of the pumps. The electricity required to pump the water was a function of the pumping power, which in turn was a function of flow (and head loss) and dependent on the volume of water supplied by the desalination plant. Consequently, the method applied to calculating the pump power (and hence pump costs) for the MBO pipeline (see Section E.2) was also applied to the transfer pipeline. The pumps were assumed to be replaced once over the planning horizon in 2030, as they were assumed to have a lifetime of 20 years, with the initial capital cost assumed for pump replacement costs. Furthermore, as per the MBO pipeline, costs associated with repair, maintenance, replacement and labour were considered negligible compared to power costs and were thus ignored in this case study.

E.4 Rainwater Tanks

All tanks were assumed to be: (1) the same size for every house in the case study; (2) round; (3) above ground and located toward the rear of the property; and (4) made from polyethylene. The

tanks were also accompanied by a fixed-speed pump, as this is the most common type of pump used in household rainwater systems [*Retamal et al.*, 2009]. All rainwater tanks were replaced every 25 years, while pumps were replaced every 10 years [*Marsden Jacob Associates*, 2009]. All houses were assumed to have a roof area of 250m^2.

E.4.1 Capital Costs

Capital costs for rainwater tanks were comprised of the tank; delivery and installation; dolomite base; pump (and for indoor use a mains switch); and plumbing. The cost of the tank, delivery, installation, and dolomite base (Table E.9) were based on costs derived from local metropolitan Adelaide tank suppliers. The cost of the pump and plumbing was dependent on the end use of harvested rainwater. For garden use only, the pump was assumed to cost $300, while if harvested rainwater was used indoors, the cost of the pump with a mains switch (to automatically switch to mains water when the rainwater tank supply was depleted) was assumed to be $800 (Table E.10). These were middle-of-the-range cost estimates based on a number of brands and sizes of pumps and mains switches available in Australia. Costs attributed to plumbing (Table E.10) were based on values used by *Marsden Jacob Associates* [2009]. Retrofitting the plumbing of an existing house to incorporate harvested rainwater supply was more expensive than plumbing a new house, while there was no plumbing cost when harvested rainwater was purely used for garden supply [*Marsden Jacob Associates*, 2009]. Furthermore, an indicative cost of $20 was added for every 10% increase in roof connectivity above 50% to account for redirecting water collected from the front roof sections to the rear of the house, where the rainwater tank was assumed to be located. Consequently, for a 5KL rainwater tank retrofitted into an existing house with 70% roof connectivity and with harvested rainwater supplying toilet and laundry end uses, the total capital cost was $3,547.

E.4.2 Ongoing Costs

Ongoing costs were associated with electricity use of the pump; tank maintenance; and replacement of the tank and pump. The electricity use of the pump was determined from the average energy

Table E. 9: Cost of tank, delivery, installation and dolomite base for different sized rainwater tanks

Tank Size (kL)	Tank Cost ($2010)	Delivery & Installation ($2010)	Dolomite Base ($2010)	Total Cost ($2010)
1.0	484	650	250	1,384
2.0	615	650	250	1,515
3.0	746	650	250	1,646
4.0	876	650	250	1,776
5.0	1007	650	250	1,907
7.0	1269	750	350	2,369
10.0	1662	750	350	2,762
15.0	2316	850	450	3,616
22.5	2615	850	450	3,915
27.0	2804	850	450	4,104

Table E. 10: Cost of pump and plumbing for different harvested rainwater end uses

Harvested Rainwater End Use	Pump Cost (2010$)	Existing house plumbing cost ($2010)	New house plumbing cost ($2010)
Garden only	300	0	0
Garden + 1 inside use	800	700	300
Garden + 2 inside uses	800	800	300
Garden + 3 inside uses	800	1000	300

intensity of the pump, which was dependent on the end use. *Retemal et al.* [2009] illustrated that the lowest energy intensities occurred when irrigation systems, washing machines, and showers and

baths were used, as these end uses allowed for a greater and more continuous flow, allowing the pump to operate at or near its Best Efficiency Point. Conversely, greater energy intensities occurred for pumps when toilets and taps were used, because the valves were only partially open (e.g., trickle top-up of the toilet cistern) and because of the lack of continuous flow (e.g., taps turned on and off) [*Retamal et al.*, 2009]. Consequently, energy intensities for the case study were based on the volume of water supplied to each end use and the energy intensities reported by *Retemal et al.* [2009], resulting in a range from 1.2kWh/kL (garden only) to 1.5kWh/kL (garden and toilet) (Table E.11). Tank maintenance was assumed to be $20 per year [*Tam et al.*, 2009; *Marsden Jacob Associates*, 2009], while the costs of replacing the tank and pump were assumed to be the same as the initial capital costs for these items.

E.5 Stormwater Schemes

E.5.1 Capital Costs

The capital material and construction costs associated with the stormwater wetlands, aquifer storage and recovery (ASR), and water distribution network for harvested stormwater were accounted for in the case study. Land acquisition costs were not included as the area required to capture, treat and store stormwater should be available without significant land purchases or interference with existing development [*Wallbridge and Gilbert*, 2009].

Material and construction costs for the stormwater wetlands and ASR schemes estimated by *Wallbridge and Gilbert* [2009] were assumed for this case study (Table E.12). The material and construction costs of the water distribution network (which was required due to the non-potable end use of stormwater), were estimated from three ASR schemes in Adelaide for which distribution costs were available (*Wallbridge and Gilbert* [2009] did not account for capital costs for the stormwater distribution network). The three ASR schemes in Adelaide were: (1) Oaklands Park; (2) Munno Para and Andrews Farm Wetlands; and (3) the Water Proofing the West Project. These schemes operate similarly to the schemes in this case study, in that water is distributed to a limited

Table E. 11: Energy intensities of the pump for different harvested rainwater end uses

Harvested Rainwater End Use	Energy Intensity (kWh/kL)
Garden only	1.20
Garden & Toilet	1.50
Garden, Toilet, & Laundry	1.45
Garden & Laundry	1.23
Garden, Laundry, & Hot Water	1.25
Garden & Hot Water	1.24
Garden, Hot Water, & Toilet	1.44
Garden, Toilet, Laundry, & Hot Water	1.41

number of public purposes, such as irrigation of local reserves and parks. However, costs for the distribution networks were particularly varied, so $410/ML/year (the average cost of the three existing ASR schemes in Adelaide when taking into account projected yields) was applied to each scheme's projected yield [*Wallbridge and Gilbert*, 2009] (Table E.12) to determine capital distribution costs (Table E.12). The total capital cost for all four stormwater schemes came to $261.2million in 2010 present value.

E.5.2 Ongoing Costs

Operating stormwater harvesting costs for the case study were based on operating and maintenance costs for Oaklands Park and Water Proofing the West. For Oaklands Park, operating and maintenance costs were estimated at $350,000 per annum, which included the cost of labour,

Table E. 12: Capital cost summary for the stormwater harvesting schemes

Stormwater Harvesting Scheme for Case Study	Stormwater Harvesting Scheme [*Wallbridge and Gilbert*, 2009]	Projected Yield (ML/year)	Material and Construction Costs (2010$million)	Water Distribution Network Costs (2010$million)	Total Capital Cost (2010$million)
Brownhill-Keswick	Brownhill-Keswick Grange Area Mile End Drain Port Road	7855	74.6	3.22	77.8
Sturt Creek	Sturt Creek	6188	86.5	2.54	89.0
Field River	Field River	2616	31.4	1.07	32.5
Pedler Creek	Pedler Creek Christie Creek Onkaparinga River Willunga	5072	59.8	2.08	61.9

replacement capital, maintenance, electricity for pumping, UV treatment, monitoring/licensing fees and 6% contingency [*Public Works Committee*, 2011b]. Annual operating costs for Water Proofing the West once fully operational is estimated to be approximately $5.1 to $5.6million, which incorporates the cost of labour, operation and maintenance of mechanics/electronics/controls, replacement capital, electricity consumption, landscaping/wetland plant maintenance, UV treatment, monitoring/licensing fees (including some contingency), depreciation costs, and financing costs [*City of Charles Sturt*, 2010]. When taking into account the projected yields of these stormwater schemes, operational costs were estimated at $1.26/kL and $1.20/kL for Oaklands Park and Water Proofing the West, respectively. Consequently, the average of these two values ($1.23/kL) was applied to all schemes in the case study.

Appendix F – GHG emissions of water supply sources for the case study of Journal Paper 3

F.1 Local Catchment Reservoirs

As the local catchment reservoirs and their associated water treatment plants (WTPs) were existing features of Adelaide's southern water supply system, only ongoing GHG emissions were accounted for, namely the energy required for treatment at the WTPs and those associated with chemical use. GHG emissions associated with the replacement of Happy Valley WTP in 2041 and Myponga WTP in 2043 (see Section E.1) could not be accounted for in the case study due to the absence of data.

The power required at Happy Valley WTP was assumed to be 100kWh/ML, while for Myponga WTP it was assumed to be 140kWh/ML (see Section E.1). While there is an absence of case-specific data for the GHG emissions associated with chemicals for Adelaide's WTPs, *Racoviceanu et al.* [2007] found that 94% of energy usage is attributable to operation, 5% is attributable to chemical manufacturing and 1% to chemical transportation, which was similar to a study by *Tarantini and Ferri* [2001] that estimated chemical manufacturing accounted for 10% of energy usage and chemical transportation was insignificant. Consequently, the power rates of 100kWh/ML and 140kWh/ML for each of the water treatment plants were assumed to account for 94% of energy, with 6% attributed to chemical manufacturing and transport. Consequently, for Happy Valley and Myponga WTP, GHG emission estimates were based on energy requirements of 106.4kWh/ML and 148.9kWhh/ML, respectively. These energy intensities were multiplied by the GHG emissions factor of 0.73kgCO_2^{-e}/kWh and the volume of water treated at each WTP to calculate the total emissions attributable to treatment energy for the local catchment reservoirs.

F.2 River Murray

The River Murray was an existing Adelaide southern system supply source, so it was not necessary to account for capital GHG emissions associated with the Murray Bridge-Onkaparinga (MBO) pipeline. Consequently, only ongoing GHG emissions of River Murray supply were accounted for, which included GHG emissions of treating the water at Happy Valley WTP (see Section F.1) and GHG emissions due to pumping. As per the estimation of costs, GHG emissions due to pumping were

derived from first principles, using the Darcy-Weisbach head loss equation and the pump power equation (see Equation E.2 and Equation E.3 in Section E.2). The pump power was then converted to kWh, based on 24-hour operation, before being converted to GHG emissions using the GHG emission rate of 0.73kgCO_2^{-e}/kWh, which is the latest full fuel cycle emission factor estimate for purchased electricity by South Australian end users [*Department of Industry Innovation Climate Change Science Research and Tertiary Education*, 2013]. For example, if the River Murray supplied 50GL/yr, the GHG emissions associated with electricity to pump River Murray water would be 1.1kgCO_2^{-e}/kL or 55,000tCO_2^{e-}/yr.

F.3 Desalination

F.3.1 Capital GHG Emissions – Desalination Plant

The capital GHG emissions for the desalination plant were attributed to the materials, electricity, and diesel used to construct the main plant and onsite power facilities. SA Water [2009] estimated quantities and resulting GHG emissions for these resources for the 50 GL/yr proposed Adelaide desalination plant and proposed that there would be minimal additional construction energy for the 100 GL/yr plant because the 50 GL/yr plant was designed for an upgrade to 100 GL/yr capacity. Consequently, an indicative 10% of capital GHG emissions was added to the GHG emissions reported by *SA Water* [2009] (Table F.1), to represent the additional buildings for process equipment that were required for the 100 GL/yr capacity plant.

Using the ongoing GHG emissions derived for desalination plants (see Section F.3.3), a 100GL/yr (≈274ML/day) plant would have operational GHG emissions of about 394,000tCO_2^{-e}/yr. Consequently, as capital GHG emissions are estimated at approximately 71,000tCO_2^{-e}/yr (Table F.1),

Table F. 1: Estimated GHG emissions for a 100GL/yr desalination plant based on values reported by *SA Water* [2009] for the Adelaide desalination plant

Resource	GHG emissions (tCO_2^{-e})
Electricity	3,289
Diesel	12,148
Concrete	20,306
Steel	23,058
Stainless Steel	1,760
Aluminium	431
Copper	1,181
Significant Plastics	1,071
Minor and Unknown GHG emissions	8,017
Total	71,262

capital GHG emissions would equate to about 0.9% of total GHG emissions over the plant's lifetime (assuming a lifetime of 20 years [*SA Water*, 2009]). This percentage is smaller than that reported by *GHD Fitchner* [2005], as they estimated that 5% of total GHG emissions were attributable to materials and the construction phase for an RO plant. However, the 5% estimate by *GHD Fitchner* [2005] was for desalination plants in Sydney, so the value for Adelaide of 0.9% was used to estimate the capital GHG emissions for each desalination capacity in the case study (Table F.2). For ongoing GHG emission calculations of the desalination plant, see Section F.3.3.

F.3.2 Capital GHG Emissions – Transfer Pipeline

Capital GHG emissions associated with materials for the mild steel cement lined (MSCL) pipeline and construction of the pipeline were accounted for; however, GHG emissions associated with the

Table F. 2: Capital GHG emissions for the different desalination plant capacities

Plant Capacity (ML/day)	Capital GHG emissions (tCO_2^{e-})
100	22,147
150	33,221
200	44,295
250	55,369
300	66,442
350	77,516
400	88,590
450	99,664
500	110,737

materials for the pumps were considered insignificant and thus were excluded from the inventory based on the fact that for the Murrumbidgee to Googong MSCL pipeline (12km, 1.0m diameter), the materials and transport of the pumps only constituted 35 tCO_2^{-e} or 0.1% of total capital GHG emissions [*ACTEW Corporation*, 2009].

For the GHG emissions associated with the cement and steel of the pipeline, nominal diameters were assumed with the cement and steel thicknesses detailed in Table F.3 to estimate the volume of cement and steel for each pipeline design (Table F.3). Assuming a density of 2,300kg/m^3 for cement and 7,850kg/m^3 for steel, and applying the emission factors of 3.5GJ/t for cement and 32GJ/t for steel [*Investor Group on Climate Change*, 2007], the resulting GHG emissions for the cement and steel of the pipeline were derived (Table F.3).

Table F. 3: Pipe diameter, cement and steel thickness and volumes of materials and resulting GHG emissions for the 12km MSCL transfer pipeline designed for the different desalination plant capacities

Plant Capacity (ML/day)	Internal Pipe Diameter (m)	Cement thickness (mm)	Mild steel thickness (mm)	Cement Volume (m^3)	Mild steel volume (m^3)	GHG emissions for steel and cement (tCO_2^{e-})	Total GHG emissions including diesel and vegetation clearance (tCO_2^{e-})
100	0.90	19	8.0	285	658	15,607	23,107
150	1.13	25	9.5	424	1,084	23,378	30,878
200	1.20	25	10.0	475	1,155	26,081	33,581
250	1.30	25	11.0	564	1,249	30,787	38,287
300	1.45	25	11.0	627	1,390	34,187	41,687
350	1.50	25	13.0	766	1,437	41,365	48,865
400	1.60	25	13.0	815	1,532	44,015	51,515
450	1.75	25	13.0	889	1,673	47,991	55,491
500	1.75	25	13.0	889	1,673	47,991	55,491

For the construction of the Adelaide desalination plant transfer pipeline, *SA Water* [2009] estimated that 1650kL of diesel would be required, resulting in GHG emissions of 4,698tCO_2^{e-}. In addition to diesel and steel, other major GHG emissions were expected to be from vegetation clearance and concrete, which were expected to contribute 1,932tCO_2^{e-} and 954tCO_2^{e-}, respectively [*SA Water*, 2009]. Consequently, an additional 7,500tCO_2^{e-} were added to the GHG emissions for steel and cement to account for other GHG emissions involved in the construction of the pipeline. Due to insufficient data, these GHG emissions were not scaled for the different sized pipelines.

F.3.3 Ongoing GHG Emissions – Desalination Plant

GHG emissions of the operating desalination plant were based on GHG emissions associated with electricity required for treatment; chemicals; membrane and plant replacement; and diesel. Assuming the plant was running at full capacity, the electricity required for power was assumed to be 5.0kWh/KL (see Section E.3). GHG emissions for chemicals, membranes and diesel were based on those for the proposed 50GL/year Adelaide desalination plant, which were estimated to be 26,771 tonnesCO_2^{e-}/yr, 1,773 tonnesCO_2^{e-}/yr and 41 tonnesCO_2^{e-}/yr, respectively [*SA Water*, 2009]. The GHG emissions of these three components were relatively small compared with those associated with power, which contributed to 92.7% of the ongoing GHG emissions (Table F.4). The percentage breakdowns are very similar to other published percentage breakdowns (Table F.4) and were consequently applied to all desalination plant capacities in the case study to determine total ongoing GHG emissions (Table F.5).

The GHG emissions associated with membrane replacement were applied every five years (Table F.4) and were independent of the amount of water the desalination plant produced. Furthermore, the GHG emissions associated with plant replacement were accounted for once in 2030 and were estimated to be the same as the initial capital GHG emissions (see Table F.2, Section F.3.1). However, in the case study, GHG emissions associated with power and chemicals depended on the amount of water supplied by the desalination plant. Energy consumption was computed based on the 5.0kWh/KL rate, resulting in a linear scaling of GHG emissions for power with volume of water supplied. Similarly, the GHG emissions associated with chemicals were scaled linearly, for example, if 25ML of water were produced per day by the 250ML/day plant, 10% of the chemical GHG emissions would be accounted for, while 50% of the chemical GHG emissions would be accounted for if water was produced at the rate of 125ML/day.

While accredited green power has been assigned to power the Adelaide Desalination Plant, in this case study renewable energy was not assumed to run the desalination plant. This was appropriate

Table F. 4: Ongoing GHG emission breakdown for the major desalination operating processes

GHG emissions (% of Total Ongoing GHG emissions)				Source
Power	Chemicals	Membranes	Other	
92.7	6.8	0.5	*negligible*	[*SA Water*, 2009]
92.1	7.0	<0.1		[*Biswas*, 2009]
95.0	4.0	1.0		[*Mrayed and Leslie*, 2009]

Table F. 5: GHG emissions attributed to power, chemicals, and membranes for each desalination plant capacity (assuming the plant operated at full capacity)

Desalination Plant Capacity (ML/day)	Power (tCO_2^{e-}/yr)	Chemicals (tCO_2^{e-}/yr)	Membranes (tCO_2^{e-}/5yrs)	Total (tCO_2^{e-}/yr)
100	133,316	9,779	3,595	143,815
150	199,974	14,669	5,393	215,722
200	266,633	19,559	7,191	287,629
250	333,291	24,449	8,988	359,537
300	399,949	29,338	10,786	431,444
350	466,607	34,228	12,584	503,352
400	533,265	39,118	14,381	575,259
450	599,923	44,007	16,179	647,166
500	666,581	48,897	17,977	719,074

because (1) the renewable energy for the desalination plant is being sourced from South Australia's electricity grid, so technically renewable energy is not directly powering the desalination plant; (2) SA Water have elected to purchase renewable energy to cover the electricity requirements of the

desalination plant but have not chosen to do so for other water sources, thus creating bias for one water source over another from a GHG emissions point of view; and (3) by using the same factors, the unit GHG emissions derived in this case study for each water source truly reflect the electricity required to power the water sources, rather than reflecting the source of electricity for each water source. Consequently, the same GHG emission rate of 0.73kgCO_2^{-e}/kWh was applied to all water sources for the purposes of this case study, including the desalination plant.

F.3.4 Ongoing GHG Emissions – Transfer Pipeline

The operating GHG emissions for the transfer pipeline were attributed to the electricity required to power the transfer of water. The power required to pump the water was estimated using first principles, as illustrated in Section F.2. The power requirements were then multiplied by the electricity GHG emission factor of 0.73kgCO_2^{-e}/kWh and assuming 24-hour continuous pumping. The maximum annual GHG emissions associated with pumping water from Port Stanvac to Happy Valley for each desalination plant capacity are reported in Table F.6. GHG emissions associated with pump replacement were excluded for this case study, as they were negligible compared with GHG emissions associated with pumping: the materials for pumps were estimated to be in the order of 35tCO_2^{-e} (see Section F.3.2), equating to 0.04-0.21% of the maximum annual GHG emissions required for pumping (Table F.6). Maintenance for the pipeline was also assumed to have negligible GHG emissions and was thus not included in estimating GHG emissions for this case study.

F.4 Rainwater Tanks

F.4.1 Capital GHG Emissions

Capital GHG emissions were attributed to the rainwater tank, pump, pipes, fixtures, and installation of materials to site. The transport of the rainwater tank system to site was not accounted for, as this was expected to vary considerably for each house. When greater than 50% roof connectivity was selected, capital GHG emissions for indicative lengths of PVC pipe to connect the extra roof area were also accounted for. However, there was no differentiation in capital GHG emissions when

Table F. 6: Maximum pump power and maximum annual GHG Emissions for the transfer pipeline

Desalination Plant Capacity (ML/day)	Maximum Pump Power (Watts)	Maximum Annual GHG emissions (tCO_2^{e-})
100	2620	16,765
150	3679	23,541
200	5175	33,116
250	6540	41,851
300	7533	48,205
350	9064	58,000
400	10,227	65,445
450	11,011	70,461
500	12,779	81,774

water was used for different end uses because there was insufficient data to accurately determine the materials required to plumb in different end uses. This was also difficult to estimate given that house layouts vary considerably.

The rainwater tanks in this case study were assumed to be made from high density polyethylene (HDPE). To estimate the GHG emissions associated with using HDPE for the tanks, the volume of HDPE for each tank (Table F.7) was first estimated for each tank size using middle-of-the-range diameters sourced from a number of rainwater tank suppliers in Adelaide (Table F.7), their corresponding heights (Table F.7) and assuming that the thickness of the base was 10mm and the thickness of the sides and tops were either 5mm (1.0-7.5kL tank) or 7.5mm (10.0-27.0kL). These values were then converted to GHG emissions (Table F.7) assuming a density of 950kg/m^3, an embodied energy factor of 75.2MJ/kg (20.9kWh/kg) [*Piratla et al.*, 2012] and the GHG electricity

Table F. 7: Diameter, height, volume of HDPE and GHG emissions for different sized rainwater tanks

Size (kL)	Diameter (m)	Height (m)	Volume of HDPE for single tank (m^3)	GHG emissions for single tank ($kgCO_2^{e-}$)	Total GHG emissions for southern system in 2010 (tCO_2^e)
1.0	0.93	1.72	0.035	512	133,150
2.0	1.30	2.00	0.061	880	229,045
3.0	1.50	2.00	0.074	1067	277,608
4.0	1.83	1.75	0.090	1300	338,411
5.0	1.84	2.15	0.102	1478	384,665
7.0	2.00	2.42	0.123	1784	464,308
10.0	2.55	2.35	0.243	3513	914,418
15.0	2.50	3.10	0.282	4091	1,064,695
22.5	3.70	2.50	0.426	6171	1,606,188
27.0	3.85	3.10	0.508	7360	1,915,500

conversion rate of $0.73kgCO_2^{e-}/kWh$. The resulting GHG emissions for the southern system in 2010 (Table F.7) were therefore estimated by multiplying these GHG emissions by the number of houses in 2010 (260,261 houses).

Parkes et al. [2010] concluded that there is a lack of good quality data for estimating the embodied energy for components of rainwater tank systems. However, they report that a generic electro-mechanical pump for rainwater harvesting once installed has GHG emissions of $184kgCO_2^{e-}$. Furthermore, they estimated that excluding the tank and pump, all other initial rainwater tank components (e.g. pipes and fixtures) once installed contributed another $143kgCO_2^{-e}$. The applicability of these data to this case study is questionable, considering the study is from the United Kingdom

and applies to a single household with a header tank, rather than a direct feed (as is assumed for this case study). However, in lieu of any other data regarding embodied energy estimates for components of household rainwater tank systems, these data were used with 327kgCO_2^{e-} being added to the capital GHG emissions of the rainwater tanks in Table F.7.

To estimate the GHG emissions associated with redirecting more roof runoff into the rainwater tank, indicative lengths of PVC pipe were assumed, with a diameter of 90mm and wall thickness of 1.9mm. Similar to estimating the GHG emissions from using HDPE for the rainwater tanks, the volume of PVC was thus estimated, and then converted to GHG emissions assuming a density of 1390kg/m^3, an embodied energy factor of 74.9MJ/kg (20.8kWh/kg) [*Piratla et al.*, 2012] and the GHG electricity conversion rate of 0.73kgCO_2^{e-}/kWh (Table F.8). While for larger tanks these additional GHG emissions only constituted a small proportion of the capital GHG emissions (e.g. 0.4%-1.5% for the 27.0kL tank), for the smaller tanks they added considerably to the capital GHG emissions (e.g. 5.1%-17.8% for the 1.0kL tank).

F.4.2 Ongoing GHG Emissions

Ongoing GHG emissions for rainwater tanks were attributed to electricity use of the pump and replacement of the tank and pumps. However, no replacement GHG emissions associated with pipes nor fixtures were accounted for, as these were assumed to have a lifetime greater than the planning horizon. Similarly, no GHG emissions associated with maintenance were accounted for due to a lack of data. The electricity use of the pump was determined from the average energy intensity of the pump (Table F.9), which, as explained in Section E.4.2, was dependent on the end use (a decision variable in the case study). To transfer these values to GHG emissions, the energy intensities were multiplied by the volume of rainwater supplied and the GHG emission rate of 0.73kgCO_2^{-e}/kWh. For example, if 50kL was supplied to the garden and laundry in a year, the annual GHG emissions associated with pumping would be about 45kgCO_2^{e-} per household and about 11,700tCO_2^{e-} for the whole of the southern system in 2010. As the rainwater tanks were assumed to have a lifetime of 25

Table F. 8: Length, volume of, and GHG emissions associated with the PVC pipe for the different roof connectivities

Roof Connectivity	Length (m)	Volume (m^3)	GHG emissions for single tank ($kgCO_2^{e-}$)	Total GHG emissions for southern system in 2010 (tCO_2^{e})
0.6	2.5	0.0013	28	7,223
0.7	5.0	0.0026	56	14,447
0.8	7.5	0.0039	83	21,670
0.9	10.0	0.0053	111	28,894

Table F. 9: Energy intensities of the pump for different harvested rainwater end uses

Harvested Rainwater End Use	Energy Intensity (kWh/kL)
Garden only	1.20
Garden & Toilet	1.50
Garden, Toilet, & Laundry	1.45
Garden & Laundry	1.23
Garden, Laundry, & Hot Water	1.25
Garden & Hot Water	1.24
Garden, Hot Water, & Toilet	1.44
Garden, Toilet, Laundry, & Hot Water	1.41

years, replacement GHG emissions for the tanks were accounted for and were assumed to be the same as the initial capital GHG emissions (see Section F.4.1). Similarly, $184kgCO_2^{e-}$ was accounted for when the pump was replaced every 10 years (see Section F.4.1).

F.5 Stormwater Schemes

F.5.1 Capital GHG Emissions

The capital material and construction GHG emissions for the stormwater schemes were attributed to the materials and construction of the wetland, Aquifer Storage and Recovery (ASR) wells, and the distribution network. The GHG emissions associated with pumps were not considered, given that GHG emissions for pumps of large pipelines were found to be negligible compared to other capital GHG emissions and the operating GHG emissions of pumps (see Section F.3.4).

For the wetlands and ASR wells, GHG emissions were attributed to the concrete and steel used in their construction and the excavation of soil required to create the wetlands and wells. The amount of concrete and steel used in a wetland's outlet structure was estimated from data supplied in supplementary material by *Moore and Hunt* [2013]. Specifically, values for the mass of concrete and mass of steel per square metre (1.90kg/m^2 and 0.02kg/m^2, respectively) were derived by dividing the mass of concrete and steel estimated by *Moore and Hunt* [2013] for their case study wetland by its area. For this case study, these rates were then applied to the total wetland area for the stormwater schemes and converted to GHG emissions using the emission factors of 1.3GJ/t and 32GJ/t for concrete (30MPa) and steel, respectively (Table F.10) [*Investor Group on Climate Change*, 2007]. In the study by *Moore and Hunt* [2013], GHG emissions associated with the PET plastic trays used to package wetland seedlings were also accounted for; however, these were found to constitute less than 2% of the wetland material GHG emissions, so they were neglected.

The volume of concrete used for the ASR wells was calculated by multiplying the number of wells for each stormwater harvesting scheme (Table F.11) [*Wallbridge and Gilbert*, 2009] by the volume of concrete used in each well, which was estimated by assuming a well height of 150m, an outside diameter of 500mm, and a wall thickness of 50mm. Using the emission factor for concrete (30MPa) of 3.2GJ/m^3 [*Investor Group on Climate Change*, 2007], the GHG emissions for the concrete used for the wells was subsequently estimated (Table F.11).

Table F. 10: Wetland area, mass of concrete and steel estimated for each wetland, and corresponding GHG emissions

Stormwater Scheme	Total Wetland Area (ha)	Mass of Concrete (kg)	Mass of Steel (kg)	GHG Emissions (tCO_2^{e-})
Brownhill-Keswick	49.72	944,051	10,070	265
Sturt Creek	50.4	956,962	10,208	268
Field River	25.26	479,620	5,116	135
Pedler Creek	40.03	760,063	8,107	213

Table F. 11: Materials and construction GHG emissions for the ASR wells

Stormwater Scheme	Number of wells	Volume of Concrete (m^3)	Material GHG Emissions (tCO_2^{e-})
Brownhill-Keswick	73	409	213
Sturt Creek	80	448	233
Field River	5	28	15
Pedler Creek	30	168	87

For excavation energy (Table F.12), the volumes of the wetlands and ASR wells were multiplied by the assumed density of soil of 1250kg/m^3, and the energy required for excavation of 0.1MJ/kg [*Alcorn*, 2003]. This energy was then multiplied by the emissions associated with the diesel used in excavation, which was estimated at 69.2kgCO_2^{-e}/GJ [*Department of Industry Innovation Climate Change Science Research and Tertiary Education*, 2013], to obtain the final estimates of GHG emissions for wetland construction (Table F.12). The relatively greater number of GHG emissions associated with construction (Table F.12) compared with those associated with materials (Tables F.10 and F.11) for the wetlands was expected, considering *Moore and Hunt* [2013] found that construction of stormwater wetlands accounted for the majority of capital GHG emissions.

Table F. 12: Wetland and ASR construction GHG emissions for each stormwater scheme

Stormwater Scheme	Total Wetland & ASR Well Volume (m^3)	Total Energy for Excavation (GJ)	Construction GHG Emissions for Wetland (tCO_2^{e-})
Brownhill-Keswick	729,430	91,179	6,310
Sturt Creek	739,686	92,461	6,398
Field River	365,927	45,741	3,165
Pedler Creek	573,464	71,683	4,960

For the distribution network, pipes were assumed to be made from high density polyethylene (HDPE), have a pressure rating of 600kPa, an outside diameter of 280mm, and a wall thickness of 10.8mm. The length of pipeline required for the distribution of harvested stormwater to non-potable industrial and commercial users (Table F.13) was estimated from a number of similar stormwater schemes in Adelaide. Specifically, the following equation was derived to estimate pipe length based on the potential yield of the schemes:

$$L = 18.108 * Y^{0.5681} \quad \text{(F.1)}$$

where L is the length of pipeline (in km) and Y is the potential yield of the stormwater scheme (in GL/yr). Consequently, the volume of HDPE for each of the stormwater scheme distribution networks was estimated and converted to GHG emissions (Table F.13) by multiplying the volume of HDPE by its density (950kg/m^3), an embodied energy factor of 75.2MJ/kg (20.9kWh/kg) [*Piratla et al.*, 2012] and the GHG electricity conversion rate of 0.73kgCO_2^{e-}/kWh. *Piratla et al.* [2012] estimated that GHG emissions of 2,830.4kgCO_2^{e-} were incurred for installation of a 152.4m-long, 200mm-diameter section of pipe buried 1.22m below the surface. This value converts to an average 18.6kgCO_2^{e-}/m of pipe installed. Considering the pipelines for the stormwater distribution in this case study were almost a third larger in diameter than that reported by *Piratla et al.* [2012], an indicative value for

Table F. 13: Estimated length of pipelines for the stormwater schemes' distribution network, the corresponding volume of HDPE required and the resulting GHG emissions associated with the HDPE and installation of the pipeline

Stormwater Scheme	Length of Pipeline (km)	Volume of HDPE (m^3)	GHG Emissions for HDPE (tCO_2^{e-})	GHG Emissions for Pipe Installation (tCO_2^{e-})
Brownhill-Keswick	58.5	529.8	7,675	1,522
Sturt Creek	51.0	461.7	6,688	1,326
Field River	31.3	283.1	4,101	813
Pedler Creek	45.5	412.3	5,973	1,184

installation of 26kgCO_2^{e-}/m was applied to this case study to estimate GHG emissions for the distribution network installation (Table F.13).

Total capital GHG emissions for the stormwater harvesting schemes are summarised in Table F.14.

F.5.2 Ongoing GHG Emissions

Ongoing GHG emissions for the stormwater harvesting schemes were based on operating GHG emissions, namely those associated with pumping the stormwater. The wetlands, wells and distribution network were assumed to have lifetimes greater than the planning horizon of 40 years considered in this case study, so no GHG emissions associated with replacement were attributed to stormwater harvesting. GHG emissions for pump replacement were also ignored, as these were assumed to be negligible compared with those associated with the electricity required to pump the harvested stormwater.

Dandy et al. [2013] estimated that the GHG emissions associated with pumping for a stormwater harvesting scheme (the scheme included a wetland, ASR and distribution to open spaces for irrigation) were approximately 554MWh for 0.88GL of stormwater. This translates to a rate of 0.63kWh/kL or 0.50kgCO_2^{e-}/kL using the electricity emissions factor of 0.73kgCO_2^{e-}/kWh, which was applied to the yield of the stormwater harvesting schemes in this case study to estimate ongoing

Table F. 14: Summary of capital GHG emissions for the stormwater harvesting schemes

Stormwater Scheme	Capital GHG Emissions (tCO_2^{e-})			
	Wetland and Well Materials	Wetland and Well Excavation	Distribution Network	Total
Brownhill-Keswick	478	6,310	9,197	15,985
Sturt Creek	501	6,398	8,014	14,913
Field River	150	3,165	4,914	8,229
Pedler Creek	300	4,960	7,158	12,418

GHG emissions. For example, if the Brownhill-Keswick scheme produced its maximum yield of 7.9GL/yr, annual operating GHG emissions for the Brownhill-Keswick scheme would be 3,950tCO_2^{e-}.

Appendix G – Boxplots illustrating results from the post-optimisation robustness assessment for the case study of Journal Paper 3

Figures G.1 to G.4 contained in this appendix have three sections – the top section compares across the GCMs, the middle section across the SRES scenarios and the bottom section across the demands. Within each section, the six or seven different scenario options are illustrated, and within each of these, there are six columns that represent each of the six solutions from the post-optimisation robustness assessment (consecutively from Solution 1 in the furthest left column through to Solution 6 in the furthest right column).

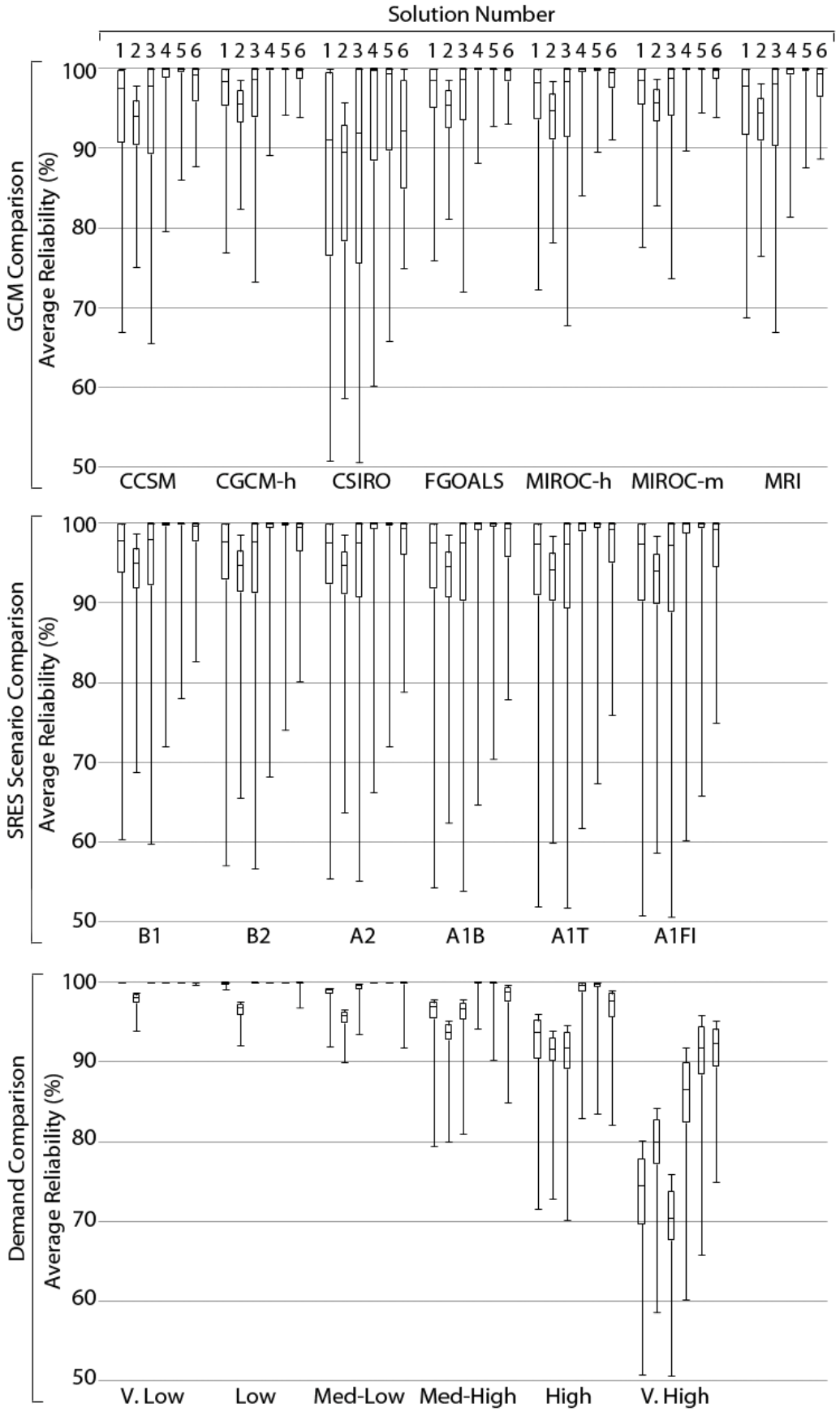

Figure G. 1: Boxplot of average reliability comparing the different GCMs (top section), different SRES scenarios (middle section), and different demands (bottom section).

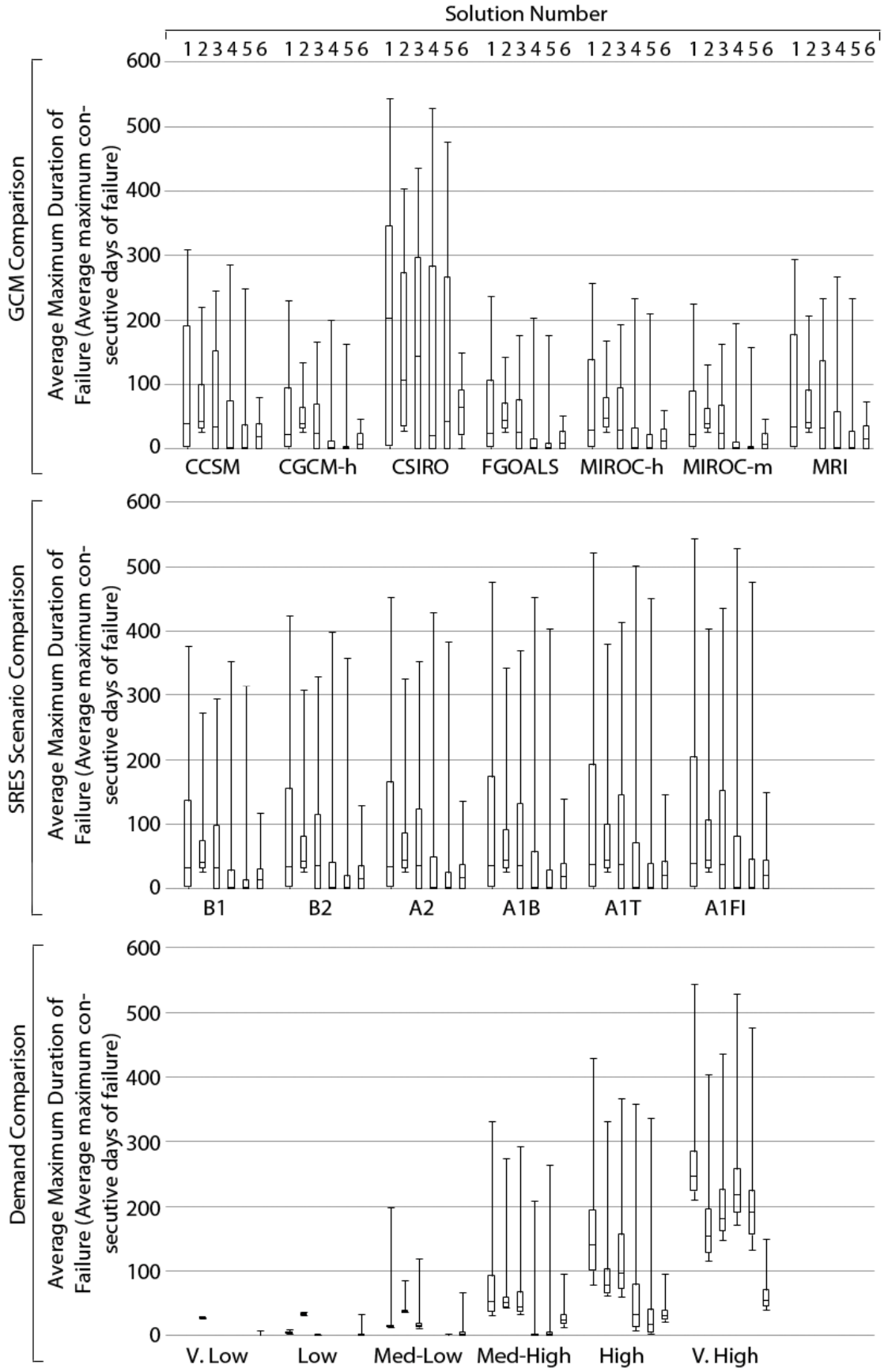

Figure G. 2: Boxplot of average maximum duration of failure comparing the different GCMs (top section), different SRES scenarios (middle section), and different demands (bottom section).

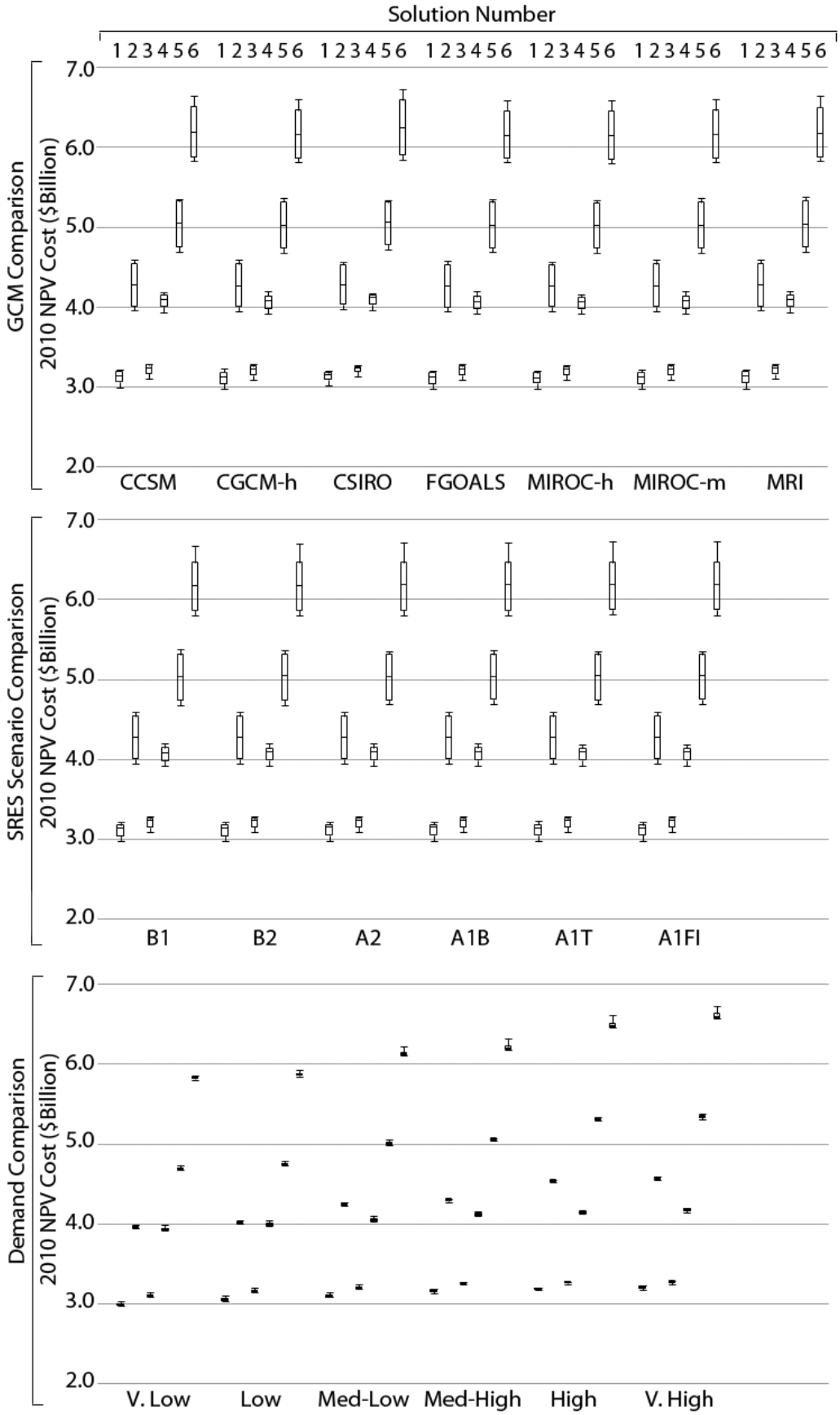

Figure G. 3: Boxplot of 2010 NPV total system cost comparing the different GCMs (top section), different SRES scenarios (middle section), and different demands (bottom section).

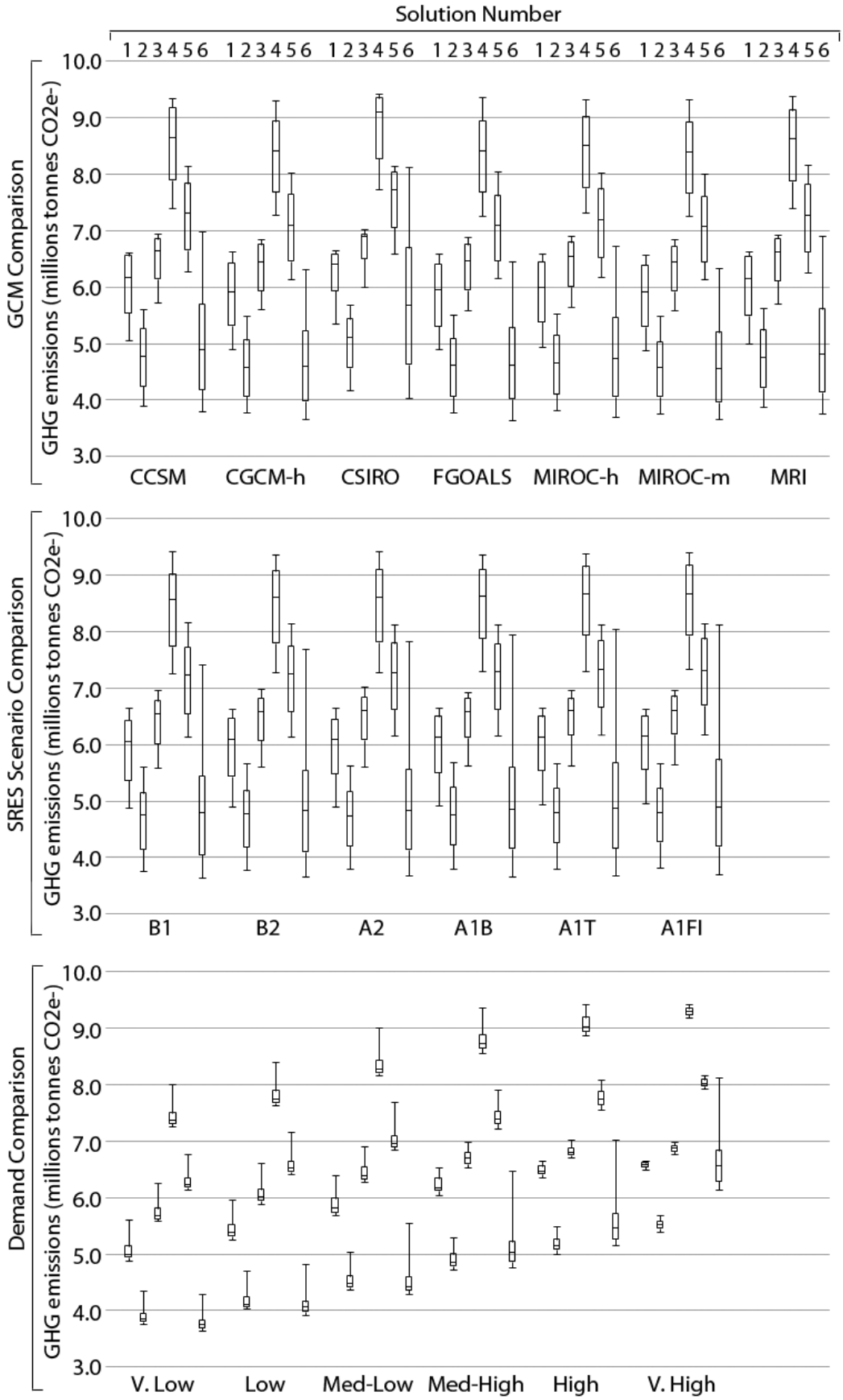

Figure G. 4: Boxplot of total system GHG emissions comparing the different GCMs (top section), different SRES scenarios (middle section), and different demands (bottom section).

References

ACTEW Corporation (2009), Appendix N: Greenhouse Gas Assessment, in *Murrumbidgee to Googong Water Transfer Project - Environmental Impact Statement*, Canberra.

Akaike, H. (1973), Information theory and an extension of the maximum likelihood principle, in 2nd International Symposium on Information Theory, Tsahkadsor, Armenia, USSR, September 2-8, 1971, edited by B. Petrov and F. Csáki, pp. 267-281, Akadémiai Kiadó, Budapest.

Alcorn, A. (2003), Embodied Energy and CO2 Coefficients for NZ Building Materials, 31 pp, Centre for Building Performance Research, Victoria University of Wellington, Wellington, New Zealand.

Alcorn, M. (2006), Surface Water Assessment of the Currency Creek Catchment *Rep. DWLBC 2006/07*, 61 pp, Department of Water, Land and Biodiversity Conservation, Adelaide.

Alcubilla, R., Lund, J. (2006), Derived Willingness to-Pay for Household Water Use with Price and Probabilistic Supply, *Journal of Water Resources Planning and Management*, *132*(6), 424-433, doi:10.1061/(ASCE)0733-9496(2006)132:6(424).

Australian Bureau of Statistics (2008), Population Projections: Australia 2006 to 2101 *Rep. 3222.0*, 96 pp, Australian Bureau of Statistics, Canberra.

Australian Energy Market Operator (2014), South Australian Fuel and Technology Report, 50 pp, Australian Energy Market Operator, Adelaide.

Barjoveanu, G., I. Comandaru, G. Rodriguez-Garcia, A. Hospido, and C. Teodosiu (2014), Evaluation of water services system through LCA. A case study for Iasi City, Romania, *Int J Life Cycle Assess*, *19*(2), 449-462, doi: 10.1007/s11367-013-0635-8.

Barton, A. B. (2005), Management and Reuse of Local Water Resources in Residential Developments in Adelaide, 199 pp, University of South Australia, Adelaide.

Baruth, E. (2005), *Water Treatment Plant Design*, 4th ed., 896 pp., McGraw-Hill Professional, New York.

Beh, E. H. Y., G. C. Dandy, H. R. Maier, and F. L. Paton (2014), Optimal sequencing of water supply options at the regional scale incorporating alternative water supply sources and multiple objectives, *Environ. Modell. Softw.*, *53*(0), 137-153, doi:10.1016/j.envsoft.2013.11.004.

Bennett, N. D., B. F. W. Croke, G. Guariso, J. H. A. Guillaume, S. H. Hamilton, A. J. Jakeman, S. Marsili-Libelli, L. T. H. Newham, J. P. Norton, C. Perrin, S. A. Pierce, B. Robson, R. Seppelt, A. A. Voinov, B. D. Fath, and V. Andreassian (2013), Characterising performance of environmental models, *Environ. Modell. Softw.*, *40*(0), 1-20, doi:10.1016/j.envsoft.2012.09.011.

Beven, K. (2006), A manifesto for the equifinality thesis, *J. Hydrol.*, *320*(1–2), 18-36, doi:10.1016/j.jhydrol.2005.07.007.

Biswas, A. (1976), Systems Approach to Water Management, in *Systems Approach to Water Management*, edited by A. Biswas, pp. 1-15, McGraw-Hill Inc., New York.

Biswas, W. K. (2009), Life Cycle Assessment of Seawater Desalinization in Western Australia, *World Academy of Science, Engineering & Technology* (32), 369-375.

Boé, J., L. Terray, E. Martin, and F. Habets (2009), Projected changes in components of the hydrological cycle in French river basins during the 21st century, Water Resour. Res., 45(8), W08426, doi:10.1029/2008WR007437.

Bozdogan, H. (1987), Model selection and Akaike's Information Criterion (AIC): The general theory and its analytical extensions, *Psychometrika*, *52*(3), 345-370, doi:10.1007/bf02294361.

Cai, X. M., D. C. McKinney, and L. S. Lasdon (2002), A framework for sustainability analysis in water resources management and application to the Syr Darya Basin, *Water Resour. Res.*, *38*(6), doi:10.1029/2001wr000214.

Canadian Government (2011), National Inventory Report 1990-2009, Greenhouse Gas Sources and Sinks in Canada – The Canadian Government's Submission to the UN Framework Convention on Climate Change, Part 3, *Rep. En81-4/2009E-PDF,* 105 pp, Environment Canada, Quebec.

Charles, S. P., T. M. Heneker, and B. C. Bates (2008), Stochastically downscaled rainfall projections and modelled hydrological response for the Mount Lofty Ranges, South Australia, in *Proceedings of Water Down Under 2008*, edited by M. Lambert, T. Daniell, and M. Leonard, pp. 428–439, Engineers Australia; Casual Productions, Adelaide.

Chen, J., F. P. Brissette, and R. Leconte (2011a), Uncertainty of downscaling method in quantifying the impact of climate change on hydrology, *J. Hydrol.*, *401*(3–4), 190-202, doi:10.1016/j.jhydrol.2011.02.020.

Chen, J., F. P. Brissette, A. Poulin, and R. Leconte (2011b), Overall uncertainty study of the hydrological impacts of climate change for a Canadian watershed, *Water Resour. Res.*, *47*(12), W12509, doi:10.1029/2011wr010602.

Chiew, F. H. S., and T. A. McMahon (2002), Modelling the impacts of climate change on Australian streamflow, *Hydrological Processes*, *16*, 1235-1245, doi:10.1002/hyp.1059.

Chiew, F. H. S., and L. Siriwardena (2005), Trend: Trend/Change Detection Software User Guide, CRC for Catchment Hydrology, Australia.

Chiew, F. H. S., D. G. C. Kirono, D. Kent, and J. Vaze (2009a), Assessment of rainfall simulations from global climate models and implications for climate change impact on runoff studies, in *18th World IMACS Congress and MODSIM09 International Congress on Modelling and Simulation*, edited by R. Anderssen, R. Braddock, and L. Newham, pp. 3907–3913, Modelling and Simulation Society of Australia and New Zealand and International Association for Mathematics and Computers in Simulation, Canberra.

Chiew, F. H. S., J. Teng, J. Vaze, and D. G. C. Kirono (2009b), Influence of global climate model selection on runoff impact assessment, *J. Hydrol.*, *379*(1-2), 172-180, doi:10.1016/j.jhydrol.2009.10.004.

Chiew, F. H. S., J. Teng, J. Vaze, D. A. Post, J. M. Perraud, D. G. C. Kirono, and N. R. Viney (2009c), Estimating climate change impact on runoff across southeast Australia: Method, results, and implications of the modeling method, *Water Resour. Res.*, *45*(10), W10414, doi:10.1029/2008wr007338.

Chiew, F. H. S., D. G. C. Kirono, D. M. Kent, A. J. Frost, S. P. Charles, B. Timbal, K. C. Nguyen, and G. Fu (2010), Comparison of runoff modelled using rainfall from different downscaling methods for historical and future climates, *J. Hydrol.*, *387*(1-2), 10-23, doi:10.1016/j.jhydrol.2010.03.025.

Chong, J., J. Herriman, S. White, and D. Campbell (2009a), Review of Water Restrictions Volume 2 - Appendices, 31 pp, Institute for Sustainable Futures, ACIL Tasman Pty Ltd, Sydney.

Chong, J., J. Herriman, S. White, and D. Campbell (2009b), Review of Water Restrictions Volume 1 - Review and Analysis, 31 pp, Institute for Sustainable Futures, ACIL Tasman Pty Ltd, Sydney.

Chung, G., K. Lansey, and G. Bayraksan (2009), Reliable water supply system design under uncertainty, *Environ. Modell. Softw.*, *24*(4), 449-462, doi:10.1016/j.envsoft.2008.08.007.

Chung, G., K. Lansey, P. Blowers, P. Brooks, W. Ela, S. Stewart, and P. Wilson (2008), A general water supply planning model: Evaluation of decentralized treatment, *Environ. Modell. Softw.*, *23*(7), 893-905, doi:10.1016/j.envsoft.2007.10.002.

City of Charles Sturt (2010), *Prudential Review: Water Proofing the West - Stage 1 Project*, 18 pp, Adelaide.

Clarke, J.M., P.H. Whetton, and K.J. Hennessy (2011), Providing application-specific climate projections datatsets: CSIRO's Climate Futures Framework, in *MODSIM2011, 19th International Congress on Modelling and Simulation*, edited by F. Chan, D. Marinova, and R. Anderssen, pp. 2683–2690, Modelling and Simulation Society of Australia and New Zealand, Canberra.

Coombes, P. J., and G. Kuczera (2003), Analysis of the performance of rainwater tanks in Australian capital cities, paper presented at 28th International Hydrology and Water Resources Symposium: About Water; Symposium Proceedings, Institute of Engineers, Australia, Wollongong, NSW, Australia, 10-14 November 2003.

Crawley, P. D. (1995), Risk and reliability assessment of multiple reservoir water supply headworks systems, 601 pp, University of Adelaide, Adelaide.

Crawley, P. D., and G. C. Dandy (1993), Optimal operation of multiple-reservoir system, *Journal of Water Resources Planning and Management*, *119*(1), 1-17, doi:10.1061/(ASCE)0733-9496(1993)119:1(1).

Cubasch, U., G. A. Meehl, G. J. Boer, R. J. Stouffer, M. Dix, A. Noda, C. A. Senior, S. Raper, and K. S. Yap (2001), Projections of Future Climate Change, in *Climate Change 2001: The Scientific Basis. Contribution of Working Group I to the Third Assessment Report of the Intergovernmental Panel on Climate Change*, edited by J. T. Houghton, Y. Ding, D. J. Griggs, M. Noguer, P. J. van der Linden, X. Dai, K. Maskell and C. A. Johnson, p. 881, Cambridge University Press, Cambridge, United Kingdom and New York, NY, USA.

Dandy, G.C. (1992), Assessing the Economic Cost of Restrictions on Outdoor Water Use, *Water Resour. Res.*, *28*(7) 1759-1766, doi: 10.1029/92WR00691.

Dandy, G. C., A. Ganji, J. Kandulu, D. Hatton MacDonald, A. Marchi, H. R. Maier, A. Mankad, and C. E. Schmidt (2013), Managed Aquifer Recharge and Stormwater Use Options: Net Benefits Report, 180 pp, Goyder Institute for Water Research - Marsuo Project Final Report, Adelaide.

Dandy, G. C., and M. O. Engelhardt (2006), Multi-objective trade-offs between cost and reliability in the replacement of water mains, *Journal of Water Resources Planning and Management*, *132*(2), 79-88, doi:10.1061/(ASCE)0733-9496(2006)132:2(79).

Dawson, C. W., R. J. Abrahart, and L. M. See (2007), HydroTest: A web-based toolbox of evaluation metrics for the standardised assessment of hydrological forecasts, *Environ. Modell. Softw.*, *22*(7), 1034-1052, doi:10.1016/j.envsoft.2006.06.008.

Deb, K., A. Pratap, S. Agarwal, and T. Meyarivan (2002), A fast and elitist multiobjective genetic algorithm: NSGA-II, *IEEE Transactions on Evolutionary Computing*, *6*(2), 182-197, doi:10.1109/4235.996017.

Department of Industry Innovation Climate Change Science Research and Tertiary Education (2013), Australian National Greenhouse Accounts, 84 pp, Department of Industry, Innovation, Climate Change, Science, Research and Tertiary Education; Australian Government, Canberra, Australia.

Diaz-Nieto, J., and R. L. Wilby (2005), A comparison of statistical downscaling and climate change factor methods: impacts on low flows in the River Thames, United Kingdom, *Clim. Change*, *69*(2), 245-268, doi:10.1007/s10584-005-1157-6.

Dibike, Y. B., and P. Coulibaly (2005), Hydrologic impact of climate change in the Saguenay watershed: comparison of downscaling methods and hydrologic models, *J. Hydrol.*, *307*(1–4), 145-163, doi:10.1016/j.jhydrol.2004.10.012.

Dickson, R. D. (1978), Estimating water system costs, in *Water Treatment Plant Design for the practicing engineer*, edited by R. L. Sanks, Ann Arbor Science Publishers, Ann Arbor, Michigan.

Dolnicar, S., and A. I. Schäfer (2009), Desalinated versus recycled water: Public perceptions and profiles of the accepters, *J. Environ. Manage.*, *90*(2), 888-900, doi:10.1016/j.jenvman.2008.02.003.

Erlanger, P., and B. Neal (2005), Framework for Urban Water Resource Planning, p. 32, Water Services Association of Australia Inc., Melbourne.

Forbes, K., S. Kienzle, C. Coburn, J. Byrne, and J. Rasmussen (2011), Simulating the hydrological response to predicted climate change on a watershed in southern Alberta, Canada, *Clim. Change*, *105*(3), 555-576, doi:10.1007/s10584-010-9890-x.

Foster, V., and D. Bedrosyan (2014), Understanding CO2 Emissions from the Global Energy Sector, *Rep. 85126*, 4 pp, Live Wire, The World Bank Open Knowledge Repository, Washington.

Fowler, H. J., C. G. Kilsby, and P. E. O'Connell (2003), Modeling the impacts of climatic change and variability on the reliability, resilience, and vulnerability of a water resource system, *Water Resour. Res.*, *39*(8), 11, doi:10.1029/2002wr001778.

Fowler, H. J., S. Blenkinsop, and C. Tebaldi (2007), Linking climate change modelling to impacts studies: recent advances in downscaling techniques for hydrological modelling, *International Journal of Climatology*, *27*(2), 1547-1578, doi:10.1002/joc.1556.

GHD Fitchner (2005), *Planning for Desalination,* 47 pp, GHD Fitchner & Sydney Water, Sydney, Australia.

GHD Fitchner (2007), Direct Connection Pipeline - Burdekin to South East Queensland*,* 103 pp, Department of Natural Resources and Water, Queensland Government, Brisbane, Queensland.

Gober, P., C. W. Kirkwood, R. C. Balling, A. W. Ellis, and S. Deitrick (2010), Water Planning Under Climatic Uncertainty in Phoenix: Why We Need a New Paradigm, *Annals of the Association of American Geographers*, *100*(2), 356-372, doi:10.1080/00045601003595420.

Government of South Australia (2005), Water Proofing Adelaide - A thirst for change 2005 - 2025, 60 pp, Government of South Australia, Adelaide.

Government of South Australia (2009), Water for Good - A plan to ensure our water future to 2050, 190 pp, Government of South Australia, Adelaide.

Griffin, R. C., and J. W. Mjelde (2000), Valuing Water Supply Reliability, *Am. J. Agr. Econ.*, *82*(2), 414-426.

Groves, D. G., R. J. Davis, J. Wilkinson, and R. J. Lempert (2008a), Planning for Climate Change in the Inland Empire: Southern California, *Water Resources IMPACT*, *10*(4), 14-17.

Groves, D. G., and R. J. Lempert (2007), A new analytic method for finding policy-relevant scenarios, *Global Environmental Change*, *17*(1), 73-85, doi:10.1016/j.gloenvcha.2006.11.006.

Groves, D. G., R. J. Lempert, D. Knopman, and S. Berry (2008b), Preparing for an Uncertain Future Climate in the Inland Empire: Identifying Robust Water-Management Strategies, 84 pp, Environment, Energy, and Economic Development Program within RAND Infrastructure, Safety, and Environment. RAND Corporation, Santa Monica, CA.

Groves, D. G., D. Yates, and C. Tebaldi (2008c), Developing and applying uncertain global climate change projections for regional water management planning, *Water Resour. Res.*, *44*(12), W12413, doi:10.1029/2008wr006964.

Hall, M. R., J. West, B. Sherman, J. Lane, and D. de Haas (2011), Long-Term Trends and Opportunities for Managing Regional Water Supply and Wastewater Greenhouse Gas Emissions, *Environ. Sci. Technol.*, *45*(12), 5434-5440, doi:10.1021/es103939a.

Hashimoto, T., D. P. Loucks, and J. R. Stedinger (1982a), Robustness of Water Resources Systems, *Water Resour. Res.*, *18*(1), 21-26, doi:10.1029/WR018i001p00021.

Hashimoto, T., J. R. Stedinger, and D. P. Loucks (1982b), Reliability, Resiliency, and Vulnerability Criteria for Water-Resource System Performance Evaluation, *Water Resour. Res.*, *18*(1), 14-20, doi:10.1029/WR018i001p00014.

Hensher, D., N. Shore, and K. Train (2006), Water Supply Security and Willingness to Pay to Avoid Drought Restrictions*, *Economic Record*, *82*(256), 56-66, doi: 10.1111/j.1475-4932.2006.00293.x.

Herstein, L.M., and Y.R. Filion (2011), Life-cycle assessment of common water main materials in water distribution networks. *J. Hydroinform.*, *13*(3), 346–357, doi:10.2166/hydro.2010.127.

Herstein, L., Y. Filion, and K. Hall (2009), Evaluating Environmental Impact in Water Distribution System Design, *Journal of Infrastructure Systems*, *15*(3), 241-250, doi: 10.1061/(ASCE)1076-0342(2009)15:3(241).

Herstein, L. M., Y. R. Filion, and K. R. Hall (2011), Evaluating the Environmental Impacts of Water Distribution Systems by Using EIO-LCA-Based Multiobjective Optimization, *J. Water Resour. Plan. Manage.-ASCE*, *137*(2), 162-172, doi: 10.1061/(asce)wr.1943-5452.0000101.

Hoang, M., B. Bolto, C. Haskard, O. Barron, S. Gray, and G. Leslie (2009), Desalination in Australia, 21 pp, CSIRO, Melbourne.

House-Peters, L. A., and H. Chang (2011), Urban water demand modeling: Review of concepts, methods, and organizing principles, *Water Resour. Res., 47*, W05401, doi:10.1029/2010WR009624.

Intergovernmental Panel on Climate Change (2000), Special Report on Emissions Scenarios, 570 pp, Cambridge University Press, UK.

Intergovernmental Panel on Climate Change (2007), Climate Change 2007: Synthesis Report. Contribution of Working Groups I, II and III to the Fourth Assessment Report of the Intergovernmental Panel on Climate Change, 104 pp, IPCC, Geneva, Switzerland.

Investor Group on Climate Change (2007), Potential Earnings Impacts from Climate Change: Construction Materials, 29 pp, Investor Group on Climate Change, Goldman Sachs JBWere, and Monash Sustainability Enterprises, Melbourne.

Irving, D. B., S. E. Perkins, J. R. Brown, A. Sen Gupta, A. F. Moise, B. F. Murphy, L. C. Muir, R. A. Colman, S. B. Power, F. P. Delage, and J. N. Brown (2011), Evaluating global climate models for the Pacific island region, *Clim. Res.*, *49*(3), 169-187, doi:10.3354/cr01028.

Jain, S. K., and K. P. Sudheer (2008), Fitting of Hydrologic Models: A Close Look at the Nash–Sutcliffe Index, *Journal of Hydrologic Engineering*, *13*(10), 981-986, doi:10.1061/(asce)1084-0699(2008)13:10(981).

Jeffrey, S. J., J. O. Carter, K. B. Moodie, and A. R. Beswick (2001), Using spatial interpolation to construct a comprehensive archive of Australian climate data, *Environ. Modell. Softw.*, *16*(4), 309-330, doi:10.1016/S1364-8152(01)00008-1.

Kaczmarek, Z., J. Napiorkowski, and M. Strzepek (1996), Climate change impacts on the water supply system in the Warta River catchment, Poland, *Water Resources Development*, *12*(2), 165-180, doi:10.1080/07900629650041939.

Kasprzyk, J., P. Reed, B. Kirsch, and G. Characklis (2009), Managing population and drought risks using many-objective water portfolio planning under uncertainty, *Water Resour. Res.*, *45*(12), W12401, doi:10.1029/2009wr008121.

Kasprzyk, J., P. Reed, G. Characklis, and B. Kirsch (2012), Many-objective de Novo water supply portfolio planning under deep uncertainty, *Environmental Modelling and Software*, *34*(0), 87-104, doi:10.1016/j.envsoft.2011.04.003.

Kasprzyk, J., S. Nataraj, P. Reed, and R. Lempert (2013), Many objective robust decision making for complex environmental systems undergoing change, *Environ. Modell. Softw.*, *42*(0), 55-71, doi:10.1016/j.envsoft.2012.12.007.

Keedwell, E., and S. T. Khu (2006), A novel evolutionary meta-heuristic for the multi-objective optimization of real-world water distribution networks, *Engineering Optimization*, *38*(3), 319-336, doi:10.1080/03052150500476308.

Kilsby, C. G., P. D. Jones, A. Burton, A. C. Ford, H. J. Fowler, C. Harpham, P. James, A. Smith, and R. L. Wilby (2007), A daily weather generator for use in climate change studies, *Environ. Modell. Softw.*, *22*(12), 1705-1719, doi:10.1016/j.envsoft.2007.02.005.

Korteling, B., S. Dessai, and Z. Kapelan (2013), Using Information-Gap Decision Theory for Water Resources Planning Under Severe Uncertainty, *Water Resour. Manag.*, *27*(4), 1149-1172, doi:10.1007/s11269-012-0164-4.

Lempert, R. J., and D. G. Groves (2010), Identifying and evaluating robust adaptive policy responses to climate change for water management agencies in the American west, *Technological Forecasting and Social Change*, *77*(6), 960-974, doi:10.1016/j.techfore.2010.04.007.

Lopez, A., F. Fung, M. New, G. Watts, A. Weston, and R. L. Wilby (2009), From climate model ensembles to climate change impacts and adaptation: A case study of water resource management in the southwest of England, *Water Resour. Res.*, *45*(8), W08419, doi:10.1029/2008wr007499.

Lundie, S., G. M. Peters, and P. C. Beavis (2004), Life Cycle Assessment for sustainable metropolitan water systems planning, *Environ. Sci. Technol.*, *38*(13), 3465-3473, doi: 10.1021/es034206m.

Maheepala, S., and C. Perera (2003), Climate change and reliability of urban water supply, *Water Science and Technology*, *47*(9), 101-108.

Maier, H. R., F. L. Paton, G. C. Dandy, and J. Connor (2013), Impact of drought on Adelaide's water supply system: Past, present and future, in *Drought in Arid and Semi-Arid Environments: A Multi-Disciplinary and Cross-Country Perspective*, edited by K. Schwabe, J. Albiac, J. Connor, R. Hassan and L. Meza-Gonzalez, pp. 41-62, Springer, Dordrecht.

Majone, B., C. I. Bovolo, A. Bellin, S. Blenkinsop, and H. J. Fowler (2012), Modeling the impacts of future climate change on water resources for the Gállego river basin (Spain), *Water Resour. Res.*, *48*(1), W01512, doi:10.1029/2011wr010985.

Makropoulos, C. K., K. Natsis, S. Liu, K. Mittas, and D. Butler (2008), Decision support for sustainable option selection in integrated urban water management, *Environ. Modell. Softw.*, *23*(12), 1448-1460, doi:10.1016/j.envsoft.2008.04.010.

Manning, L. J., J. W. Hall, H. J. Fowler, C. G. Kilsby, and C. Tebaldi (2009), Using probabilistic climate change information from a multimodel ensemble for water resources assessment, *Water Resour. Res.*, *45*(11), W11411, doi:10.1029/2007WR006674.

Marsden Jacob Associates (2009), The cost effectiveness of rainwater tanks in Perth, 21 pp, Water Corporation and the Department of Water, Perth, Western Australia.

Martine, G. (2007), State of the World Population 2007 - Unleashing the potential of urban growth, United Nations Population Fund (UNFPA), New York.

Matrosov, E. S., A. M. Woods, and J. J. Harou (2013), Robust Decision Making and Info-Gap Decision Theory for water resource system planning, *J. Hydrol.*, *494*(0), 43-58, doi:10.1016/j.jhydrol.2013.03.006.

Miller, L., A. Ramaswami, and R. Ranjan (2013), Contribution of Water and Wastewater Infrastructures to Urban Energy Metabolism and Greenhouse Gas Emissions in Cities in India, *Journal of Environmental Engineering*, *139*(5), 738-745, doi:10.1061/(ASCE)EE.1943-7870.0000661.

Milly, P. C. D., J. Betancourt, M. Falkenmark, R. M. Hirsch, Z. W. Kundzewicz, D. P. Lettenmaier, and R. J. Stouffer (2008), Climate change - Stationarity is dead: Whither water management?, *Science*, *319*(5863), 573-574, doi:10.1126/science.1151915.

Mitchell, V. G., D. T. McCarthy, A. Deletic, and T. D. Fletcher (2008a), Urban stormwater harvesting - sensitivity of a storage behaviour model, *Environ. Modell. Softw.*, *23*(6), 782-793, doi:10.1016/j.envsoft.2007.09.006.

Mitchell, V. G., N. Siriwardene, H. Duncan, and M. Rahilly (2008b), Investigating the impact of temporal and spatial lumping on rainwater tank system modelling, in *Proceedings of Water Down Under 2008*, edited by M. Lambert, T. Daniell, and M. Leonard, pp.54-65, Engineers Australia; Casual Productions, Adelaide.

Moody, P., and C. Brown (2013), Robustness indicators for evaluation under climate change: Application to the upper Great Lakes, *Water Resour. Res., 49*, 3576–3588, doi:10.1002/wrcr.20228.

Moore, T. L. C., and W. F. Hunt (2013), Predicting the carbon footprint of urban stormwater infrastructure, *Ecological Engineering*, *58*(0), 44-51, doi:10.1016/j.ecoleng.2013.06.021.

Moriasi, D. N., J. G. Arnold, M. W. Van Liew, R. L. Bingner, R. D. Harmel, and T. L. Veith (2007), Model evaluation guidelines for systematic quantification of accuracy in watershed simulations, *American Society of Agricultural and Biological Engineers*, *50*(3), 885–900.

Mortazavi, M., G. Kuczera, and L. Cui (2012), Multiobjective optimisation of urban water resources: Moving toward more practical solutions, *Water Resour. Res.*, *48*(3), W03514, doi: dx.doi.org/10.1029/2011wr010866.

Morton, F. I. (1983), Operational estimates of areal evapotranspiration and their significance to the science and practice of hydrology, *J. Hydrol.*, *66*(1–4), 1-76, doi:10.1016/0022-1694(83)90177-4.

Mpelasoka, F. S., and F. H. S. Chiew (2009), Influence of Rainfall Scenario Construction Methods on Runoff Projections, *Journal of Hydrometeorology*, *10*(5), 1168-1183, doi:10.1175/2009jhm1045.1.

Mrayed, S., and G. Leslie (2009), Examination of Greenhouse footprint for both Desalination and Water recycling processes, paper presented at Australian Water Association (AWA) Ozwater' 09 Conference, Australian Water Association, Melbourne, Australia.

National Research Council (2009), Informing Decisions in a Changing Climate. Panel on Strategies and Methods for Climate-Related Decision Support, Committee on the Human Dimensions of Global Change. Division of Behavioral and Social Sciences and Education, 188 pp, The National Academies Press, Washington, D.C.

Nicklow, J., P. Reed, D. Savic, T. Dessalegne, L. Harrell, A. Chan-Hilton, M. Karamouz, B. Minsker, A. Ostfeld, A. Singh, and E. Zechman (2010), State of the Art for Genetic Algorithms and Beyond in Water Resources Planning and Management, *Journal of Water Resources Planning and Management*, *136*(4), 412-432, doi:10.1061/(ASCE)WR.1943-5452.0000053.

O'Hara, J., and K. Georgakakos (2008), Quantifying the Urban Water Supply Impacts of Climate Change, *Water Resour. Manag.*, *22*(10), 1477-1497, doi:10.1007/s11269-008-9238-8.

Oudin, L., V. Andréassian, T. Mathevet, C. Perrin, and C. Michel (2006), Dynamic averaging of rainfall-runoff model simulations from complementary model parameterizations, *Water Resour. Res.*, *42*(7), W07410, doi:10.1029/2005wr004636.

Pahl-Wostl, C. (2007), Transitions towards adaptive management of water facing climate and global change, *Water Resour. Manag.*, *21*(1), 49-62, doi:10.1007/s11269-006-9040-4.

Parkes, C., H. Kershaw, J. Hart, R. Sibille, and Z. Grant (2010), Energy and carbon implications of rainwater harvesting and greywater recycling, *Rep. SC090018*, 93 pp, Environment Agency, Bristol.

Paton, F. L., H. R. Maier, and G. C. Dandy (2013), Relative magnitudes of sources of uncertainty in assessing climate change impacts on water supply security for the southern Adelaide water supply system, *Water Resour. Res.*, *49*(3), 1643-1667, doi:10.1002/wrcr.20153.

Perkins, S. E., and A. J. Pitman (2009), Do weak AR4 models bias projections of future climate changes over Australia?, *Clim. Change*, *93*(3-4), 527-558, doi:10.1007/s10584-008-9502-1.

Perrin, C., L. Oudin, V. Andreassian, C. Rojas-Serna, C. Michel, and T. Mathevet (2007), Impact of limited streamflow data on the efficiency and the parameters of rainfall—runoff models, *Hydrological Sciences Journal*, *52*(1), 131-151, doi:10.1623/hysj.52.1.131.

Piratla, K., S. Ariaratnam, and A. Cohen (2012), Estimation of Emissions from the Life Cycle of a Potable Water Pipeline Project, *Journal of Management in Engineering*, *28*(1), 22-30, doi:10.1061/(ASCE)ME.1943-5479.0000069.

Public Works Committee (2011a), Happy Valley Water Treatment Plant (WTP) Chlorination Facility Upgrade, 30 pp, House of Assembly, Parliament of South Australia, First Session, Fifty-Second Parliament, Adelaide.

Public Works Committee (2011b), Oaklands Park Stormwater Harvesting & Reuse Scheme, 18 pp, House of Assembly, Parliament of South Australia, First Session, Fifty-Second Parliament, Adelaide.

Racoviceanu, A., B. Karney, C. Kennedy, and A. Colombo (2007), Life-Cycle Energy Use and Greenhouse Gas Emissions Inventory for Water Treatment Systems, *Journal of Infrastructure Systems*, *13*(4), 261-270, doi:10.1061/(ASCE)1076-0342(2007)13:4(261).

Rambaud, S. C., and M. J. M. Torrecillas (2005), Some considerations on the social discount rate, *Environ. Sci. Policy*, 8(4), 343-355, doi:10.1016/j.envsci.2005.04.003.

Randall, D. A., et al. (2007), Climate Models and Their Evaluation, in *Climate Change 2007: The Physical Science Basis. Contribution of Working Group I to the Fourth Assessment Report of the Intergovernmental Panel on Climate Change*, edited by S. Solomon, D. Qin, M. Manning, Z. Chen, M. Marquis, K. B. Averyt, M. Tignor and H. L. Miller, pp. 589-662, Cambridge University Press, Cambridge, UK and New York, NY, USA.

Rawlinsons (2007), Detailed Prices, in *Australian Construction Handbook*, edited by Rawlinsons Construction Cost Consultants and Quantity Surveyors, p. 916, Rawlhouse Publishing Pty Ltd, Perth, Western Australia.

Rayner, D. (2005), Australian synthetic daily Class A pan evaporation, *Rep. QNRM05435*, 38 pp, Department of Natural Resources and Mines, Queensland, Brisbane.

Reed, P., B. S. Minsker, and D. E. Goldberg (2003), Simplifying multiobjective optimization: An automated design methodology for the nondominated sorted genetic algorithm-II, *Water Resour. Res.*, *39*(7), 1196, doi:10.1029/2002wr001483.

Reed, P., D. Hadka, J. Herman, J. Kasprzyk, and J. Kollat (2013), Evolutionary multiobjective optimization in water resources: The past, present, and future, *Advances in Water Resources*, *51*, 438-456, doi:10.1016/j.advwatres.2012.01.005.

Refsgaard, J. C., and B. Storm (1996), Construction, Calibration and Validation of Hydrological Models, in *Distributed Hydrological Modelling*, edited by M. B. Abbott and J. C. Refsgaard, pp. 41-54., Kluwer Academic Publishers, Dordrecht.

Retamal, M., J. Glassmire, K. Abeysuriya, A. Turner, and S. White (2009), The Water-Energy Nexus: Investigation into the Energy Implications of Household Rainwater Systems, 71 pp, Institute for Sustainable Futures, University of Technology, Sydney.

Roshani, E., S. P. MacLeod, and Y. R. Filion (2012), Evaluating the Impact of Climate Change Mitigation Strategies on the Optimal Design and Expansion of the Amherstview, Ontario, Water Network: Canadian Case Study, *J. Water Resour. Plan. Manage.-ASCE*, *138*(2), 100-110, doi:10.1061/(asce)wr.1943-5452.0000158.

Rothausen, S. G. S. A., and D. Conway (2011), Greenhouse-gas emissions from energy use in the water sector, *Nature Clim. Change*, *1*(4), 210-219, doi:10.1038/nclimate1147.

SA Water (2009), Proposed Adelaide Desalination Plant, Environmental Impact Statement - Response Document, 170 pp, Adelaide.

Sahely, H. R., C. A. Kennedy, and B. J. Adams (2005), Developing sustainability criteria for urban infrastructure systems, *Can. J. Civ. Eng.*, *32*(1), 72-85, doi:10.1139/l04-072.

Sahely, H. R., and C. A. Kennedy (2007), Water use model for quantifying environmental and economic sustainability indicators, *J. Water Resour. Plan. Manage.-ASCE*, *133*(6), 550-559, doi: 10.1061/(asce)0733-9496(2007)133:6(550).

Salas, J., B. Rajagopalan, L. Saito, and C. Brown (2012), Special Section on Climate Change and Water Resources: Climate Nonstationarity and Water Resources Management, *Journal of Water Resources Planning and Management*, *138*(5), 385-388, doi:10.1061/(ASCE)WR.1943-5452.0000279.

Savadamuthu, K. (2003), Surface Water Assessment of the Upper Finniss Catchment *Rep. DWLBC 2003/18*, Department of Water, Land and Biodiversity Conservation, Adelaide.

Schoups, G., N. C. van de Giesen, and H. H. G. Savenije (2008), Model complexity control for hydrologic prediction, *Water Resour. Res.*, *44*, W00B03, doi:10.1029/2008wr006836.

Semiat, R. (2000), Present and Future, *Water Int.*, *25*(1), 54-65, doi:10.1080/02508060008686797.

Singh, J., H. V. Knapp, and M. Demissie (2004), Hydrologic modelling of the Iroquois River watershed using HSPF and SWAT *Rep. ISWS CR 2004-08*, 24 pp, Watershed science section, Illinois State Water Survey, Champaign.

Slagstad, H., and H. Brattebø (2014), Life cycle assessment of the water and wastewater system in Trondheim, Norway – A case study, *Urban Water Journal*, *11*(4), 323-334, doi:10.1080/1573062x.2013.795232.

Snowy Mountains Engineering Corporation Australia (2007), Integrated Water Supply Options for north east NSW and south east Queensland, 72 pp, National Water Commission.

Srikanthan, R. (2005), Stochastic generation of daily rainfall at a number of sites, *Rep. 05/7*, CRC for Catchment Hydrology, Canberra.

Srikanthan, R., and G. G. S. Pegram (2009), A nested multisite daily rainfall stochastic generation model, *J. Hydrol.*, *371*(1-4), 142-153, doi:10.1016/j.jhydrol.2009.03.025.

Srikanthan, R., and T. A. McMahon (2001), Stochastic generation of annual, monthly and daily climate data: A review, *Hydrology and Earth System Sciences*, *5*(4), 653-670, doi:10.5194/hess-5-653-2001.

Srikanthan, R., F. H. S. Chiew, and A. J. Frost (2004), SCL: Stochastic Climate Library User Guide, CRC for Catchment Hydrology, Canberra.

Stokes, J., and A. Horvath (2006), Life cycle energy assessment of alternative water supply systems, *Int. J. Life Cycle Assess.*, *11*(5), 335-343, doi: 10.1065/lca2005.06.214.

Stokes, J. R., and A. Horvath (2009), Energy and Air Emission Effects of Water Supply, *Environ. Sci. Technol.*, *43*(8), 2680-2687, doi:10.1021/es801802h.

Stokes, C. S., Simpson, A. R., and Maier H. R. (2014) The cost–greenhouse gas emission nexus for water distribution systems including the consideration of energy generating infrastructure: an integrated conceptual optimization framework and review of literature, *Earth Perspectives*, 1:9, doi:10.1186/2194-6434-1-9.

Tal, A. (2011), The Desalination Debate—Lessons Learned Thus Far, *Environment: Science and Policy for Sustainable Development*, *53*(5), 34-48, doi:10.1080/00139157.2011.604009.

Tam, V. W. Y., L. Tam, and S. X. Zeng (2010), Cost effectiveness and tradeoff on the use of rainwater tank: An empirical study in Australian residential decision-making, *Resources, Conservation and Recycling*, *54*(3), 178-186, doi:10.1016/j.resconrec.2009.07.014.

Tarantini, M., and F. Ferri (2001), LCA of drinking and wastewater treatment systems of Bologna City: Final Results, in *4th Inter-Regional Conference on Environmental Water: Competitive use and conservation strategies for water and natural resources*, Fotaleza, Brazil.

Teoh, K. S. (2002), Estimating the Impact of Current Farm Dams Development on the Surface Water Resources of the Onkaparinga River Catchment *Rep. DWLBC 2002/22*, 153 pp, The Department of Water, Land and Biodiversity Conservation, Adelaide.

Towler, E., B. Raucher, B. Rajagopalan, A. Rodriguez, D. Yates, and R. Summers (2012), Incorporating Climate Uncertainty in a Cost Assessment for New Municipal Source Water, *Journal of Water Resources Planning and Management*, *138*(5), 396-402, doi:10.1061/(ASCE)WR.1943-5452.0000150.

Traynham, L., R. Palmer, and A. Polebitski (2011), Impacts of Future Climate Conditions and Forecasted Population Growth on Water Supply Systems in the Puget Sound Region, *Journal of Water Resources Planning and Management*, *137*(4), 318-326, doi:10.1061/(asce)wr.1943-5452.0000114.

van Oldenborgh, G. J., S. Philip, and M. Collins (2005), El Nino in a changing climate: a multi-model study, *Ocean Science Discussions*, *1*, 81-95, doi:10.5194/os-1-81-2005.

Vicuna, S., J. A. Dracup, J. R. Lund, L. L. Dale, and E. P. Maurer (2010), Basin-scale water system operations with uncertain future climate conditions: Methodology and case studies, *Water Resour. Res.*, *46*(4), W04505, doi:10.1029/2009WR007838.

Wade Miller, G. (2006), Integrated concepts in water reuse: managing global water needs, *Desalination*, *187*(1–3), 65-75, doi:10.1016/j.desal.2005.04.068.

Wagener, T., H. S. Wheater, and H. V. Gupta (2004), *Rainfall-Runoff Modelling in Gauged and Ungauged Catchments*, 306 pp., Imperial College Press, London.

Wallbridge and Gilbert (2009), Urban Stormwater Harvesting Option Study, 93pp, Wallbridge and Gilbert, Adelaide.

Walski, T. (2012), Planning-Level Capital Cost Estimates for Pumping, *Journal of Water Resources Planning and Management*, *138*(3), 307-310, doi:10.1061/(ASCE)WR.1943-5452.0000167.

Wang, Q. J. (1991), The Genetic Algorithm and Its Application to Calibrating Conceptual Rainfall-Runoff Models, *Water Resour. Res.*, *27*(9), 2467-2471, doi:10.1029/91wr01305.

Weitzman, M. L. (2001), Gamma discounting, *American Economic Review*, *91*(1), 260-271, doi:10.1257/aer.91.1.260.

Whetton, P., K. Hennessy, J. Clarke, K. McInnes, and D. Kent (2012), Use of Representative Climate Futures in impact and adaptation assessment, *Clim. Change*, 1-10, doi:10.1007/s10584-012-0471-z.

Wilby, R. L., and H. J. Fowler (2011), Regional Climate Downscaling, in *Modelling the Impact of Climate Change on Water Resources*, edited by F. Fung, A. Lopez and M. New, pp. 34-85, Blackwell Publishing Ltd, Oxford.

Wilby, R. L., and I. Harris (2006), A framework for assessing uncertainties in climate change impacts: Low-flow scenarios for the River Thames, UK, *Water Resour. Res.*, *42*(2), W02419, doi:10.1029/2005wr004065.

Wilby, R. L., and S. Dessai (2010), Robust adaptation to climate change, *Weather*, *65*(7), 180-185, doi:10.1002/wea.543.

Wilby, R. L., P. G. Whitehead, A. J. Wade, D. Butterfield, R. J. Davis, and G. Watts (2006), Integrated modelling of climate change impacts on water resources and quality in a lowland catchment: River Kennet, UK, *J. Hydrol.*, *330*(1-2), 204-220, doi:10.1016/j.jhydrol.2006.04.033.

Wiley, M. W., and R. N. Palmer (2008), Estimating the impacts and uncertainty of climate change on a municipal water supply system, *J. Water Resour. Plan. Manage.-ASCE*, *134*(3), 239-246, doi:10.1061/(asce)0733-9496(2008)134:3(239).

Wittholz, M. K., B. K. O'Neill, C. B. Colby, and D. Lewis (2008), Estimating the cost of desalination plants using a cost database, *Desalination*, *229*(1-3), 10-20, doi:10.1016/j.desal.2007.07.023.

Wong, H. Y., and J. Rosenhead (2000), A Rigorous Definition of Robustness Analysis, *The Journal of the Operational Research Society*, *51*(2), 176-182, doi:10.2307/254258.

Wu, W., A. Simpson, and H. Maier (2009), Single-Objective versus Multi-Objective Optimization of Water Distribution Systems Accounting for Greenhouse Gas Emissions by Carbon Pricing, *Journal of Water Resources Planning and Management,* doi:10.1061/(ASCE)WR.1943-5452.0000072.

Wu, W., A. Simpson, and H. Maier (2010), Accounting for Greenhouse Gas Emissions in Multiobjective Genetic Algorithm Optimization of Water Distribution Systems, *J. Water Resour. Plan. Manage.-ASCE*, *136*(2), 146-155, doi:10.1061/(asce)wr.1943-5452.0000020.

Wu, W., H. Maier, and A. Simpson (2013), Multiobjective optimization of water distribution systems accounting for economic cost, hydraulic reliability, and greenhouse gas emissions, *Water Resour. Res.*, *49*(3), 1211-1225, doi:10.1002/wrcr.20120.

Wu, W., A. Simpson, H. Maier, and A. Marchi (2012), Incorporation of Variable-Speed Pumping in Multiobjective Genetic Algorithm Optimization of the Design of Water Transmission Systems, *Journal of Water Resources Planning and Management*, *138*(5), 543-552, doi: doi:10.1061/(ASCE)WR.1943-5452.0000195.

Zhu, T., M. W. Jenkins, and J. R. Lund (2005), Estimated impacts of climate warming on California water availability under twelve future climate scenarios, *JAWRA Journal of the American Water Resources Association*, *41*(5), 1027-1038, doi:10.1111/j.1752-1688.2005.tb03783.x.

Zongxue, X., K. Jinno, A. Kawamura, S. Takesaki, and K. Ito (1998), Performance Risk Analysis for Fukuoka Water Supply System, *Water Resour. Manag.*, *12*(1), 13-30, doi:10.1023/a:1007951806144.